VOLUME 52, NO. 1 | **2019**

MERCK

ALDRICHIMICA ACTA

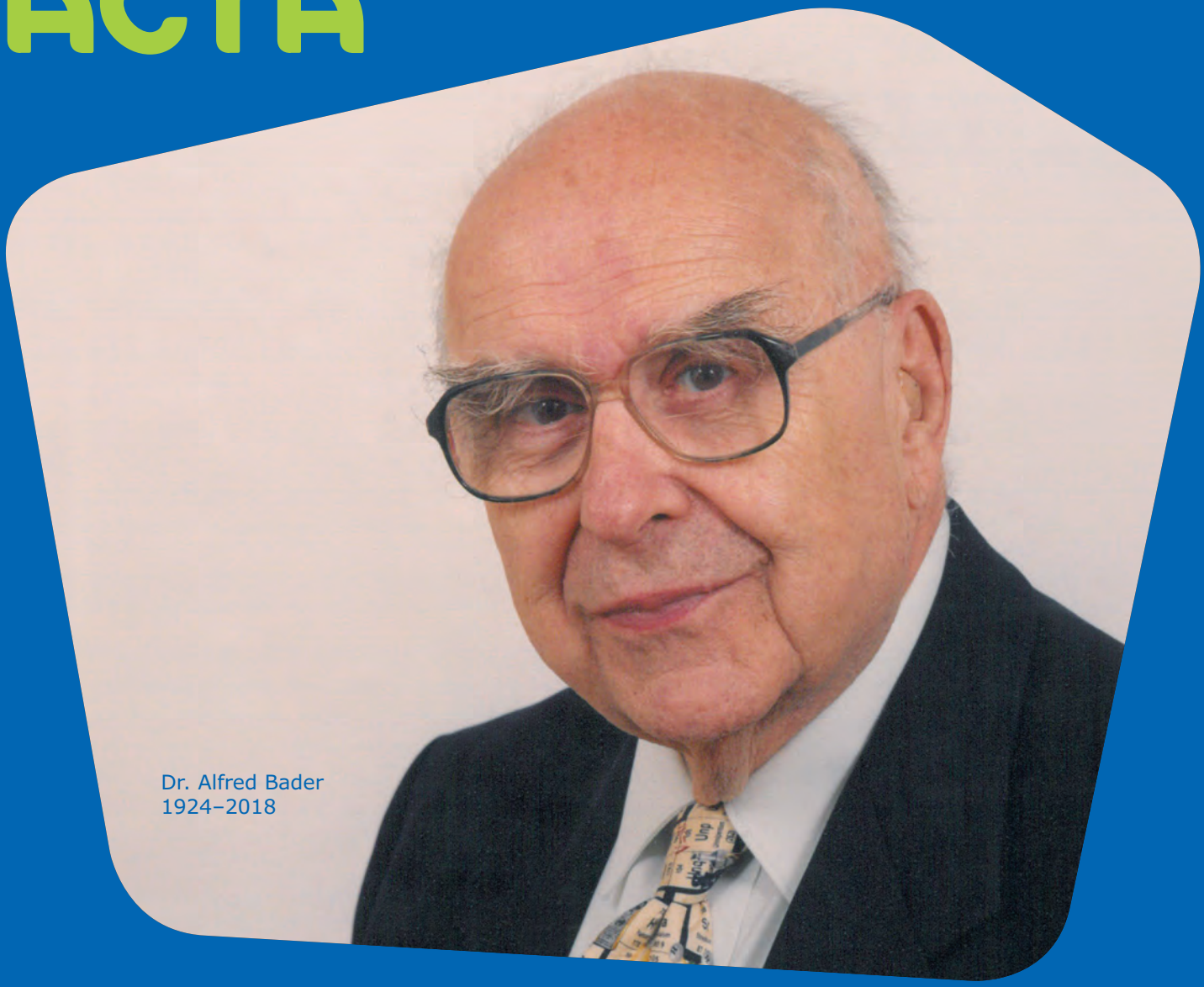

Dr. Alfred Bader
1924–2018

Remembering Dr. Alfred R. Bader (1924–2018)

Phenothiazines, Dihydrophenazines, and Phenoxazines: Sustainable Alternatives to Precious-Metal-Based Photoredox Catalysts

Titanium Salalen Catalysts for the Asymmetric Epoxidation of Terminal (and Other Unactivated) Olefins with Hydrogen Peroxide

Remembering Dr. Alfred Bader

Alfred Bader, a pioneer in the field of chemistry and co-founder of Aldrich Chemical Company, now a part of the Life Science business of Merck KGaA, Darmstadt, Germany, passed away on December 23, 2018, at the age of 94.

Scientists from around the world grew up using Aldrich Chemical products in their labs, referencing the Aldrich Catalog and Handbook, and appreciating the oft-used request to "Please Bother Us."— a request for customers to call at any time with any question or idea. Bader's commitment to his customers and to the broader scientific community could be felt in all aspects of his work.

Bader's remarkable story began in 1938, when at age 14, he fled his native Vienna during the rise of Nazism. He would eventually complete a chemistry degree at Queen's University in Kingston, Ontario, and later a Ph.D. in organic chemistry at Harvard. Bader was an entrepreneur at heart. He began his career in 1950 working as a chemist for the Pittsburgh Plate Glass Company in Milwaukee. A year later, he and Jack Eisendrath founded Aldrich Chemical Company, which would eventually grow to become one of the largest chemical companies in the world. Aldrich later merged with Sigma International, Ltd., to form Sigma-Aldrich Corporation. Bader became president of Sigma-Aldrich Corp. and then served on its board until 1992, when he left to focus on philanthropic efforts.

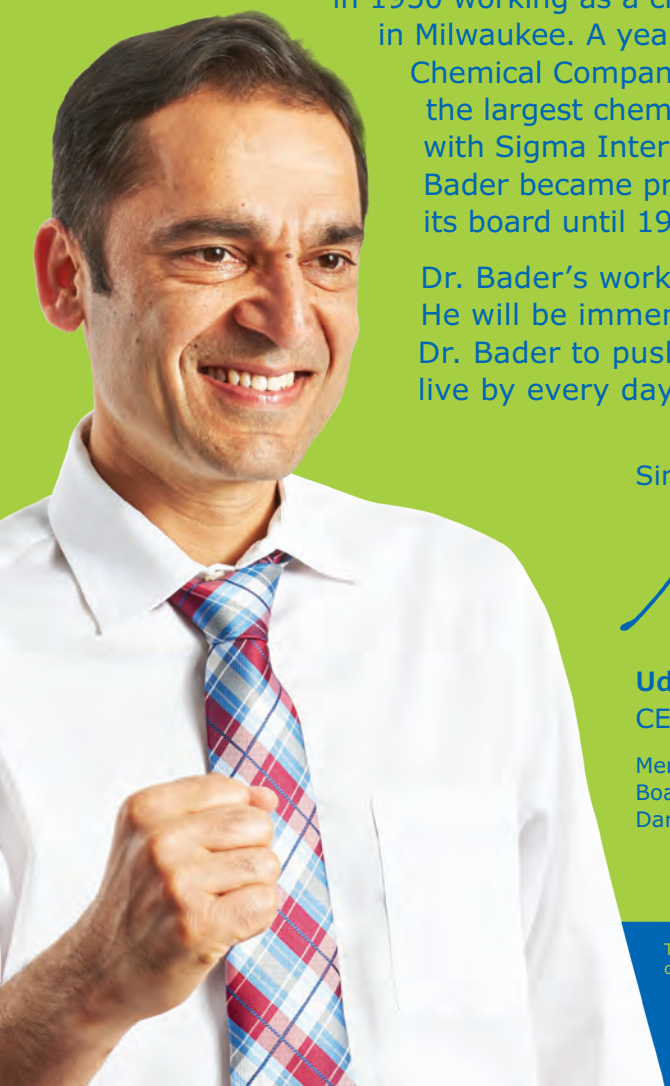

Dr. Bader's work and legacy have left a lasting impact on science. He will be immensely missed. Passion and curiosity drove Dr. Bader to push the boundaries of chemistry, something we live by every day.

Sincerely yours,

Udit Batra, Ph.D.
CEO, Life Science

Member of the Executive Board, Merck KGaA, Darmstadt, Germany

ALDRICHIMICA ACTA
VOL. 52, NO. 1 • 2019

Merck KGaA
Frankfurter Strasse 250
64293 Darmstadt, Germany
Phone +49 6151 72 0

To Place Orders / Customer Service
Contact your local office or visit
SigmaAldrich.com/order

Technical Service
Contact your local office or visit
SigmaAldrich.com/techinfo

General Correspondence
Editor: Sharbil J. Firsan, Ph.D.
Sharbil.Firsan@milliporesigma.com

Subscriptions
Request your FREE subscription to the *Aldrichimica Acta* at **SigmaAldrich.com/acta**

The entire *Aldrichimica Acta* archive is available at **SigmaAldrich.com/acta**

Aldrichimica Acta (ISSN 0002-5100) is a publication of Merck KGaA.

"PLEASE BOTHER US."

Dear Fellow Chemists,

Professor Garret M. Miyake of the Department of Chemistry at Colorado State University kindly suggested that we offer PhenO_1Naph_Biph (**901111**) and PhenN_2Naph (**901112**) as sustainable alternatives to precious-metal-based photoredox catalysts, such as the Ir- and Ru-based ones. These organic photoredox catalysts act as strong excited-state reductants, and have proven effective in controlling atom-transfer radical polymerizations (ATRPs).[1] They have also proven very valuable in small-molecule organic synthesis by efficiently catalyzing carbon–carbon and carbon–heteroatom bond formations,[2] and enabling transformations not previously accessible with precious-metal catalysts.[3]

(1) Theriot, J. C.; Lim, C.-H.; Yang, H.; Ryan, M. D.; Musgrave, C. B.; Miyake, G. M. *Science* **2016**, *352*, 1082. (2) Du, Y.; Pearson, R. M.; Lim, C.-H.; Sartor, S. M.; Ryan, M. D.; Yang, H.; Damrauer, N. H.; Miyake, G. M. *Chem.—Eur. J.* **2017**, *23*, 10962. (3) For a fuller discussion of the chemistry of these and other organic photoredox catalysts, see Professor Miyake's review in this issue (pp 7–21).

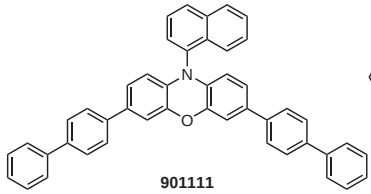

901111
PhenO_1Naph_Biph

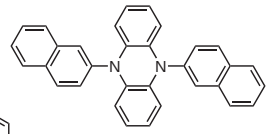

901112
PhenN_2Naph

901111	PhenO_1Naph_Biph, ≥97%	100 mg
901112	PhenN_2Naph, ≥97%	100 mg

We welcome your product ideas. Do you need a product that is not featured on our website? Ask us! For more than 60 years, your research needs and suggestions have shaped our product offering. Email your suggestion to **techserv@sial.com**.

Udit Batra, Ph.D.
CEO, Life Science

TABLE OF CONTENTS

ABOUT OUR COVER

Dr. Alfred Robert Bader—co-founder of Aldrich Chemical Co. and Sigma-Aldrich Corp. (today a part of the Life Science business of Merck KGaA, Darmstadt, Germany) and one of the most influential men in the chemical industry* since the mid-twentieth century—passed away peacefully on December 23, 2018, at the age of 94.

Dr. Bader founded and launched the *Aldrichimica Acta* in 1968. For about the first 24 years of its existence, the *Acta* cover featured paintings from Dr. Bader's private collection, and he often wrote the "About Our Cover" commentary about the featured painting. A Harvard chemistry graduate, Alfred was also a renowned art connoisseur and avid art collector, who acquired the nickname *The Chemist Collector*. Until the end, Dr. Bader was a most enthusiastic supporter of, and advocate for, the *Acta*: He believed strongly in its value, eagerly anticipated each issue, requested copies of each, and distributed them to his visitors. He promoted the *Acta* wherever he went and whenever he could. He will be missed.

Alfred perusing his favorite publication (April 2014).

* *To find out more about Dr. Bader's enduring legacy to chemistry and the art world, visit* ***SigmaAldrich.com/Acta***

Remembering Dr. Alfred R. Bader (1924–2018)[1,2]

Dr. S. J. Firsan

Sharbil J. Firsan

MilliporeSigma
6000 N. Teutonia Avenue
Milwaukee, WI 53209, USA
Email: Sharbil.Firsan@milliporesigma.com

Outline

1. Introduction

Dr. Alfred Robert Bader—co-founder of Aldrich Chemical Co. and Sigma-Aldrich Corp. (today a part of the Life Science business of Merck KGaA, Darmstadt, Germany)—passed away peacefully on December 23, 2018, at the age of 94. He is survived by his wife, Isabel, his two sons, David and Daniel, and several grandchildren.[3]

When I began writing this personal account as a tribute to Alfred, whom I had the honor of knowing and working with for more than 20 years, I approached the task with a good deal of concern about how to properly cover in just a few pages a life so rich in accomplishments. With this in mind, this piece constitutes a look through a narrow window at a man who was very closely associated with, and has heavily impacted, the business and science of chemistry for over a half century.[4] A more complete picture of a man as influential and complex as Alfred was awaits a future biographer.[5,6]

I first saw and heard Alfred while still in graduate school at the University of Illinois in Urbana-Champaign. Sometime in the early 1980s, Alfred came to the UI to give a lecture on the intersection of art and chemistry and on playing detective with unattributed or misattributed works of art by using various scientific techniques. It was an engaging lecture, and while it was not about Aldrich Chemical Co., it still indirectly served as a powerful advertisement for the relatively young company.

Dr. Bader as the Guest Speaker at the ACS Milwaukee Section Meeting (September 2001).

Although Alfred no longer had official ties to the company, he still liked to meet new employees whom he perceived could have some impact on the business—after all, he was still the largest individual shareholder and had a vested interest in how well the company was performing. In my case, I met Alfred not long after I joined Aldrich in January of 1996 at one of the regular meetings of the ACS Milwaukee Section. Alfred cared a great deal about the *Aldrichimica Acta* throughout his life and liked to see it in capable hands. Therefore, when he found out that, among other things, I had responsibility for the *Acta*, he naturally took a keen interest in me. Thus, began our professional and personal relationship that continued almost until his death.

The *Acta* was but one of our mutual interests. With Alfred having a strong interest in Middle Eastern affairs and I being originally from Lebanon, he was naturally curious to hear my perspective on current happenings in the region. Whenever we met, Alfred would often initiate a conversation about the Middle East. He was especially proud that his ancestors were from the region and that his last name meant "full-moon-faced". He would

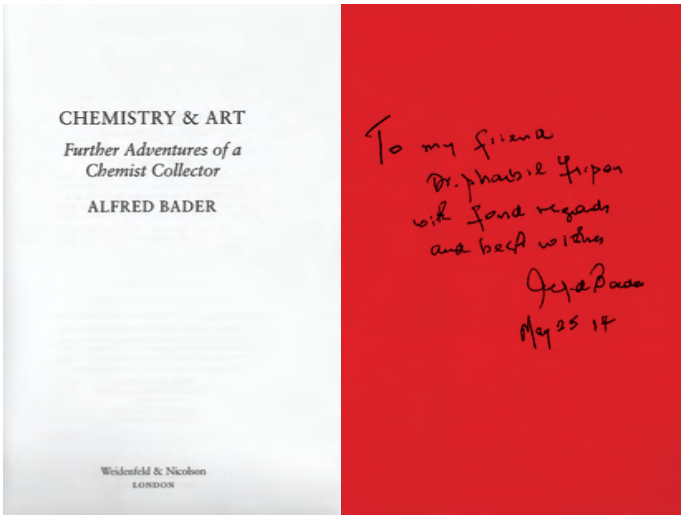

often tell me fondly and proudly about his paternal grandfather—born in Moravia of the Czech Republic and a graduate of the prestigious French civil engineering school, L'École des Ponts et Chaussées in Paris—who had worked with Ferdinand Marie de Lesseps on the construction of the Suez Canal in the mid-1800s.[7] In subsequent years, I would meet with Alfred mostly at his request a few times a year.[8] As I pointed out in my editorial in early 2009 on the occasion of his 85th birthday,[9] Alfred had primarily four pursuits in life that he was passionate about (what he called his **ABC**s): **A**rt (the appreciation and collection of), **B**ible (the study and teaching of), **C**hemistry (the science and business of), and, later in life, **P**hilanthropy. One other lesser known, but nonetheless very early interest he had, was collecting stamps.

2. If at First You Don't Succeed, …

My interactions with Alfred followed mostly from my responsibilities at Aldrich, and revolved principally around two of Alfred's four pursuits, **C**hemistry and **A**rt: **C**hemistry in terms of suggestions for review articles and new products, and **A**rt in terms of paintings that Alfred owned and that he passionately wanted used on the covers of the *Aldrichimica Acta*. In this second regard, Alfred was anything if not persistent. He pushed very hard, *and often*, to have paintings in his collection[10] be featured on the cover. His persistence paid off, as we eventually featured a painting that Alfred owned[11] on the cover of the second issue of the *Acta* of 2001, after a hiatus of about 10 years. Thereafter, we featured one of his paintings every now and then.[12]

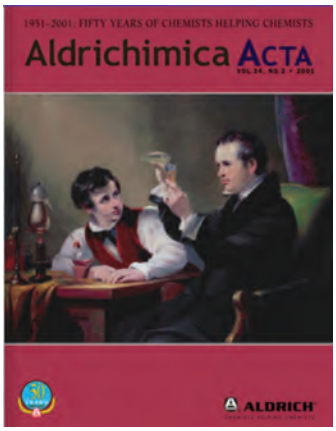

First of the Paintings in Alfred's Collection to Be Featured on the Cover of the *Aldrichimica Acta* After a 10-Year Hiatus.

3. The Business of Chemistry

Whatever the final verdict on Alfred's lifetime achievements may be, one undisputable fact is the central and critical roles he played in starting, building, and running a robust chemical company—Aldrich and then Sigma-Aldrich, now a part of the Life Science business of Merck KGaA, Darmstadt, Germany—that is still a world leader in the chemistry and life science businesses. In the process, Alfred has (i) helped countless researchers around the world by facilitating and accelerating their research, and thus contributed significantly to the tremendous scientific advances that we have all witnessed over the past half century; and (ii) provided steady employment and a good standard of living for thousands of individuals, their families, and their communities.

3.1. Adversity Stokes the Drive

This accomplishment, however, did not come easily to the young Austrian immigrant, who had fled Vienna as a teenager after the Nazis marched into the city and just before Europe plunged into World War II, and who had to overcome major obstacles along the way. While Alfred grew up in the home of his well-off paternal aunt in Vienna,[13] he suddenly found himself moving around from country to country and place to place as a refugee, sometimes regarded with suspicion as an "enemy" alien by the host country, and having to shine shoes and wash clothes in order to survive.[14] However, Alfred had what it takes to overcome adversity and to succeed: intelligence, drive, persistence, passion, and a business acumen that came naturally to him.

3.2. The Consummate Salesman

Throughout his life, Alfred was a tireless salesman and negotiator. Armed with a first-rate knowledge of chemistry, he crisscrossed North America and Europe in search of new products to list and sell, of business partners, and of customers for the young company he co-founded and ran for decades. Most valuable was his connection to, appreciation of, and repeat visits to chemistry academics who proved to be a tremendous innovation asset for the company. They helped Alfred keep his pulse on what areas were being actively researched and, thus, in need of reagents, starting materials, solvents, and laboratory equipment. *Alfred loved selling.* Whenever I happened to meet him soon after he had sold a painting, large or small, or a copy of one of his books, I would find him beaming. Of course, at that point it was not for the money he made on the sale, but for the sheer joy of making the sale.

3.3. Continued Involvement

Alfred never lost his strong interest in the goings-on at the company to his last days. He frequently explained this to me and others by saying that the company was his "baby" and that he could not let go of it. For this reason, he was not content with the official statements and reports that the company put out, and liked to learn as many additional details as he could. He would often write to, or call, officers of the company to get more information, and would make an effort to attend as many of the company functions that were open to him as he could.

3.4. The Perpetual Entrepreneur

If you were a centimillionaire[15] in your sixties, seventies, or eighties, how would you live your life? Would you aim to enjoy a quiet, carefree retirement? Not Alfred! Until he no longer physically could, he continued to maintain a regular work schedule at his gallery, to travel and give several lectures a year, to do philanthropic work, correspond with an astonishing variety of professionals and, perhaps most importantly for the business of chemistry, to help chemistry startups by investing in them, with mixed results—some succeeding, some failing.[16] Labeling Alfred as a workaholic would not have been an exaggeration.

Alfred Perusing His Favorite Publication (April 2014).

4. Alfred, the Person

Alfred Challenging the Author's Older Son in a Game of Chess (May 2014). Needless to Say That Alfred Quickly Won That Game and Many Others.

What, then, was Alfred like in person? If you had the opportunity to meet him, the first thing that would strike you about Alfred would be his modesty that was manifested in the clothes he wore, the car he drove, the house he lived in, and in the unassuming manner he carried himself with people of all walks of life.[9] He was consistently soft-spoken, polite, and considerate.

4.1. The Philanthropist

Alfred was a generous donor and was liberal in showing his gratitude to the institutions that helped him as a young refugee. He was also interested in establishing a lasting legacy and in contributing to institutions of higher learning and scientific societies. That he did, abundantly, as his donations to universities (in Canada, in particular Queen's University, and in Britain, the U.S., and the Czech Republic) and chemical societies (ACS, RSC, Czech, and Canadian) attest to. In addition to endowing chairs in chemistry, and setting up scholarships,[17] fellowships, and many other types of assistance to able and/or needy young professionals, Alfred has also contributed generously and consistently to a number of humanitarian efforts around the world.[18] As generous as Alfred was towards universities, scientific societies, and humanitarian organizations, he was exacting with money on a personal level throughout his life to a point that used to astonish his acquaintances and colleagues.

4.2. A Religious Man

Alfred taught, and was deeply interested all his life in, the (Hebrew) Bible and its teachings (the **B** part of his **ABC**). Born to a devout Catholic mother, who could not raise him because she had fallen on hard times, he was raised by his paternal aunt, who instilled in him the love of Judaism. He thus sought all his life to live as much as possible as a committed [his word] and devout Jew, albeit one who was not comfortable with the labels orthodox, conservative, or reformist.[19] Despite that, he still had to be converted to Judaism, *as an adult*, in a ritual ceremony before his first marriage.[20]

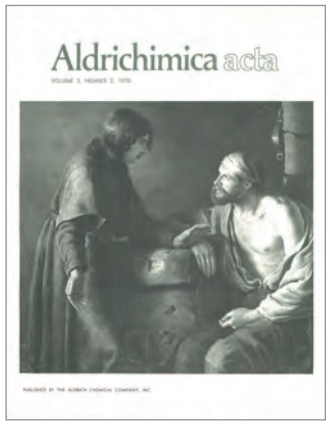

Alfred's Favorite Painting, *Joseph and the Baker* by a Rembrandt Student, Was Featured on the Cover of AA **1970**, *3* (2). The Painting Is Now in the Private Collection of David Bader.

4.3. Contrary to Prevailing Wisdom

With regard to diet and exercise, and as far as this author knows, Alfred did not participate in any kind of sport or fitness program most of his life. He also was not particularly mindful of how healthy or unhealthy the foods he ate were. (A lifestyle that reminds me of that of a nonagenarian friend of Alfred, the late Professor H. C. Brown.) Nonetheless, he was in amazingly good health most of his life. Even at 86 years of age, when many of his younger and more physically fit colleagues had passed away, he still had a sharp intellect, good hearing, good eyesight, and still drove his car to and from work. However, as can be expected and as Alfred got older, his recollection of events and their relative importance gradually started to blur, as I discovered when I was researching my article on the history of Aldrich when Alfred was about 77 years old.[4a]

5. Farewell

In all the years I dealt with Alfred, I came to expect a phone call from him on a fairly regular basis, often bright and early in the morning, when he would, among other things, comment favorably

The Author and His Family Enjoying Sunday Brunch with Alfred and Isabel at the Astor Hotel in Milwaukee (August 2007).

or, more often, unfavorably on something he saw in a recent issue of the *Aldrichimica Acta* or in one of our other publications such as the catalog/handbook. After I wrote my 2001 piece about the history of the company on the occasion of the 50th anniversary of Aldrich,[4a] he called and gave me a glowing review of the piece. With Alfred's departure, the *Acta* has lost another staunch and longtime supporter and believer in its mission and value.[21] Until almost the end, Alfred promoted the *Acta* wherever he went and whenever he could.

Farewell, Alfred! Farewell, Friend! Your kindness, humility, and friendship will be missed forever. I offer my sincere condolences to Alfred's widow, Isabel, his two sons, David and Daniel, and their families.

6. References and Notes

(1) The information, views, and opinions expressed in this article are the sole responsibility of the author and do not necessarily reflect those of Merck KGaA, Darmstadt, Germany, its affiliates, or its officers.

(2) I wish to thank my colleagues, Ms. Rachel Bloom Baglin and Dr. Ben Glasspoole, for a critical reading of, and insightful comments on, early drafts of this article.

3) Dr. Bader's obituary and selected related information can be found at: (a) The Goodman-Bensman Whitefish Bay Funeral Home web site at https://www.goodmanbensman.com/obit/dr-alfred-bader/ (accessed Jan 17, 2019). (b) Glauber, B. *The Milwaukee Journal Sentinel* [Online], December 24, 2018. https://www.jsonline.com/story/news/2018/12/24/alfred-bader-chemical-magnate-milwaukee-philanthropist-dies-94/2407962002/. (c) Wang, L. *Chem. Eng. News* [Online], December 25, 2018. https://cen.acs.org/people/obituaries/Alfred-Bader-dies-age-94/96/web/2018/12. (d) Bader Philanthropies, Inc., web site. https://www.bader.org/honoring-life-legacy-dr-alfred-bader/ (accessed Jan 17, 2019).

(4) (a) Firsan, S. J. *Aldrichimica Acta* **2001**, *34*, 35. (b) Alfred Bader. *Wikipedia–The Free Encyclopedia*; Wikimedia Foundation, Inc. https://en.wikipedia.org/wiki/Alfred_Bader (accessed Jan 18, 2019).

(5) Alfred has authored two, relatively short and candid autobiographies. (See reference 6.) However, several topics from his life and work are not adequately covered in them.

(6) (a) Bader, A. *Adventures of a Chemist Collector*; Weidenfeld & Nicolson: London, U.K., 1995. (b) Bader, A. *Chemistry & Art: Further Adventures of a Chemist Collector*; Weidenfeld & Nicolson: London, U.K., 2008.

(7) Reference 6a, p 10.

(8) I last saw Alfred on February 1, 2015, when I visited him at The Eastcastle Place Health and Rehabilitation Center, where he had settled permanently following a series of strokes and consequent falls that began on July 16, 2010, during one of his customary stays at his second home in Bexhill, England. After that visit, Alfred had become too frail, tired easily, and could not receive visitors, except very close family members.

(9) Firsan, S. J. "Please Call Me Alfred." *Aldrichimica Acta* **2009**, *42* (1), IFC.

(10) In 1992, Alfred opened an art gallery, Alfred Bader Fine Arts, at a suite in the historic Astor Hotel on Milwaukee's East Side. (See reference 6a, page 180, last paragraph.)

(11) This famous painting, *Prussian Blue* by Thomas Phillips (London, 1816), was featured on the cover of *Aldrichimica Acta*, Vol. *34*, No. 2, 2001, and is now owned by Alfred's son, Daniel Bader.

(12) In this regard, it is worth noting that Alfred rarely liked paintings featured on the *Acta* cover that were not from his collection. This, in spite of the fact that *Acta* readers, internal and external, enjoyed them a great deal and that many of the paintings he wanted featured (typically dark portraits of dignified old men and women in stoic poses, albeit by renowned artists) no longer appealed to the growing younger generations of readers.

(13) Reference 6a, pp 11–12

(14) Reference 6a, pp 26–30.

(15) Alfred's own description of his wealth during an undated meeting with the author.

(16) (a) Materia Will Build Plant in Singapore. *Chem. Eng. News* **2011**, *89* (12), March 21, p 23. (b) See also reference 6b, pp 16–18.

(17) For an example, see the announcement: Alfred and Isabel Bader Scholars. *Chem. Eng. News* **2010**, *88* (19), May 10, p 47.

(18) For some examples, see reference 6b, Chapter 18.

(19) Reference 6a, pp 66–67.

(20) Reference 6a, p 66, 4th paragraph.

(21) The other was Dr. Jai P. Nagarkatti, former Chairman, CEO, and President of Sigma-Aldrich Corp. See Firsan, S. J. *Aldrichimica Acta* **2010**, *43*, (3) 63.

About the Author

Sharbil J. Firsan is the longtime editor of the *Aldrichimica Acta,* and has been with Sigma-Aldrich Corp.—now a part of the Life Science business of Merck KGaA, Darmstadt, Germany—for over 23 years. He was born and raised in Lebanon, and completed his undergraduate studies at the American University of Beirut. After obtaining his Ph.D. degree in organic chemistry from the University of Illinois at Urbana–Champaign, he did a year of postdoctoral work at the University of Oregon, and then moved to Oklahoma State University to become Research Associate and then Visiting Assistant Professor. With his wife and two sons, Sharbil enjoys reading, outdoor activities, gardening, and travel. The two accomplishments he is most proud of are his two sons, Paul and Patrick.

Phenothiazines, Dihydrophenazines, and Phenoxazines: Sustainable Alternatives to Precious-Metal-Based Photoredox Catalysts


Mr. D. A. Corbin


Dr. C.-H. Lim


Prof. G. M. Miyake

Daniel A. Corbin, Chern-Hooi Lim, and Garret M. Miyake*

Department of Chemistry
Colorado State University
Fort Collins, CO 80523, USA
Email: garret.miyake@colostate.edu

Keywords. phenothiazines; dihydrophenazines; phenoxazines; organic photoredox catalysis; O-ATRP; strong excited-state reductant; light-driven polymerization; precious-metal-free; oxidative quenching.

Abstract. The application of photoredox catalysis to atom-transfer radical polymerization (ATRP) has resulted in the development of strongly reducing organic photoredox catalysts (PCs) that are some of the most reducing catalysts known. The objectives of this review are to highlight these PCs with regard to their development and applications in polymer and organic synthesis, as well illuminate aspects of these PCs that remain to be studied further.

Outline

1. Introduction

Photoredox catalysis has gained increasing attention because it provides chemists with the ability to perform challenging transformations by harnessing the reactivity of excited state photoredox catalysts (PCs) under mild reaction conditions. This ability is particularly important in synthetic organic chemistry, where photoinduced electron transfer (PET), between a PC and either a donor (reductive quenching) or acceptor (oxidative quenching), and energy transfer have facilitated previously challenging reactions and enabled a myriad of novel transformations.[1–7] Among the best known PCs are those containing precious metals such as ruthenium and iridium.[2,4] However, these PCs present an issue with regards to sustainability,[8] as Ru and Ir are among the rarest metals on earth. To this end, several organic PC families have been reported as alternatives—including anthracenes,[9–11] benzophenones,[12–14] acridiniums,[15–17] xanthene dyes,[18–20] perylene diimides,[21] and many more[3]—that are capable of mediating various synthetic transformations. However, most organic PCs operate through a reductive quenching pathway, and strongly reducing organic PCs are less common.

Given the wide range of transformations to which photoredox catalysis has been applied, it is not surprising that it has also

found use in polymer synthesis.[22] For example, in the free radical polymerization of methacrylates reported in 2011, $Ru(bpy)_3^{2+}$ operated as a PC through a reductive quenching mechanism requiring the use of a sacrificial electron donor.[23] Notably, the controlled radical polymerization of methyl methacrylate (MMA) in the presence of *fac*-[Ir(ppy)$_3$] (**1**) under visible light irradiation was reported a year later.[24] Operating by an atom-transfer radical polymerization (ATRP) mechanism, control in this class of reactions is achieved by reversible deactivation, most commonly with a bromide chain end group, which can be iteratively removed and reinstalled on the polymer chain via reduction and oxidation, respectively. As this process minimizes the number of reactive radicals in solution at any given time, it reduces bimolecular radical termination processes,[25] thus enabling control over the polymerization as evidenced by (1) linear first-order kinetics, (2) linear growth of polymer molecular weight (MW) as a function of monomer conversion, (3) relatively low- to low-molecular-weight dispersity ($Đ$ < 1.2 and $Đ$ < 1.1, respectively), and (4) achievement of initiator efficiency (I^* = $M_{n[theoretical]}/M_{n[experimental]}$; M_n = number average molecular weight) near 100%. Notably, this system efficiently polymerized MMA employing low catalyst loadings (as little as 50 ppm of **1**) while maintaining good control over the polymerization, something that has been challenging even in the traditional ATRP.[26] Moreover, temporal control over the polymerization was demonstrated by cycling the light source on and off, showing that the polymerization could be started and stopped without loss of the bromide end-group functionality.[24]

Despite these achievements, concerns regarding the sustainability of this PC remained, motivating the development of an ATRP method employing organic PCs, or organocatalyzed ATRP (O-ATRP), instead. Furthermore, the purification of polymers presents challenges, and trace contamination by metal residues could impede application of these materials in biomedical devices, electronic applications, and multistep syntheses.[27] Thus, shortly after the seminal paper by Fors and Hawker,[24] O-ATRP was demonstrated in two concurrent reports, polymerizing MMA using perylene (**2**)[28] or 10-phenylphenothiazine (**3**).[29] Of these two catalysts, the superior capability of **3** to mediate a controlled polymerization was evidenced in its ability to synthesize polymers with lower dispersity ($Đ$) compared to **2**. This difference was attributed to **3**'s significantly stronger excited state reduction potential [$E^0(^2PC^{\bullet+}/^3PC^*)$ = –0.6 V for **2**,[30] $E^0(^2PC^{\bullet+}/^1PC^*)$ = –2.1 V for **3**,[29] both vs SCE]. However, **2** could operate using visible light irradiation, whereas **3** required the use of UV light, raising concerns for potential side reactions that might result from UV absorption by the organic molecules in solution.[4] Thus, the development of strongly reducing and visible-light-absorbing organic PCs has been pursued, yielding a variety of PCs based on the phenothiazine (PhenS), dihydrophenazine (PhenN), and phenoxazine (PhenO) scaffolds (**Figures 1 and 2**).

To date, a number of reviews have been published detailing the applications of photoredox catalysis in organic and polymer synthesis.[1–4,22,31,32] However, due to their relatively recent development, reviews of PCs based on PhenS, PhenN, and PhenO are relatively few.[3,30,33] Therefore, this review will focus on these PCs, highlighting their development, reactions, and mechanisms in hope of demonstrating their broad utility in synthetic organic and polymer chemistry. Moreover, this review will discuss future research directions regarding these PCs in the hope of accelerating their development, improvement, and utilization in the coming years.

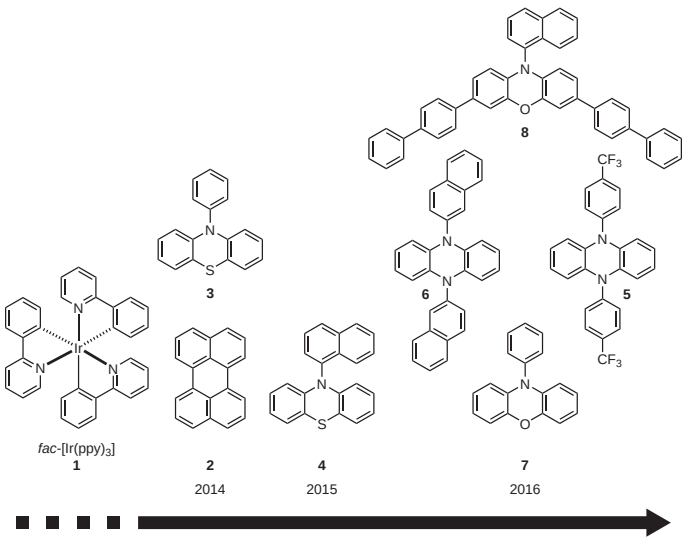

Figure 1. Examples Highlighting the Evolution of Strongly Reducing Organic PCs Based on PhenS, PhenN, and PhenO.

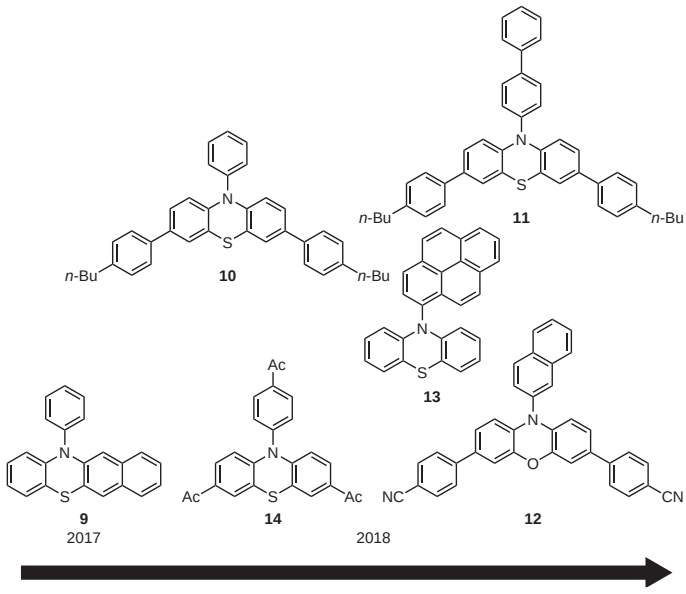

Figure 2. Further Examples Highlighting the Evolution of Strongly Reducing Organic PCs Based on PhenS, PhenN, and PhenO.

2. Development of Strongly Reducing Organic Photoredox Catalysts

While their application scope has since grown, the original motivation for using PhenS, PhenN, and PhenO as strongly reducing organic PCs came from O-ATRP. Inspired by the seminal report on photoredox catalyzed ATRP using **1**,[24] this method was developed as a metal-free variant of ATRP to eliminate metal contamination of polymer products for metal-sensitive applications. Originally, it made use of either **2**[28] or **3**[29] to polymerize methacrylates in a controlled fashion, but differences between these two organic PCs as well as the drawbacks of each soon became apparent, prompting the development of strongly reducing organic PCs that are capable of establishing a high degree of control over polymerizations by using a visible light source so as to avoid possible side reactions caused by UV light.[34]

In the proposed mechanism, the PC operates through oxidative quenching (**Scheme 1**),[28,29] in which the photoexcited PC reduces an electron acceptor to generate the PC radical cation ($^2PC^{\bullet+}$), followed by oxidation of an electron donor by $^2PC^{\bullet+}$ to regenerate the ground state catalyst. In the case of O-ATRP, the acceptor is typically an alkyl bromide initiator or a bromide-capped polymer chain-end, whereas the donor is the propagating radical formed by activation of the C–Br bond. With this mechanism in mind, several desirable characteristics were targeted in the search for new O-ATRP catalysts:[34] (i) Strong visible-light absorption (high molar absorptivity); (ii) long-lived excited state; (iii) sufficiently negative excited state reduction potential [$E^0(^2PC^{\bullet+}/PC^*)$, singlet or triplet excited state] for the reduction of common alkyl bromide ATRP initiators [E^0(C–Br/C–Br$^{\bullet-}$) = –0.6 to –0.8 V vs SCE[35]]; (iv) sufficiently oxidizing $^2PC^{\bullet+}$ [$E^0_{ox} = E^0(^2PC^{\bullet+}/^1PC)$] for oxidation of the propagating radical [E^0(C–Br/C–Br$^{\bullet-}$) = –0.6 to –0.8 V vs SCE]; (v) redox reversibility, i.e., a stable $^2PC^{\bullet+}$ that does not partake in degradative side reactions; (vi) low reorganization energy for the transition from PC* to $^2PC^{\bullet+}$ to ^1PC; and (vii) photoinduced charge-transfer excited states resulting from spatially separated singly occupied molecular orbitals (SOMOs).

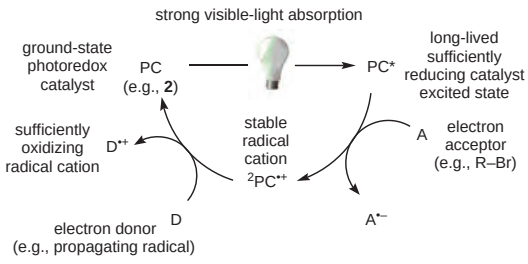

Scheme 1. A General, Oxidative Quenching Mechanism by Which Strongly Reducing PCs Operate. First, an Electron Is Donated by the Excited State PC (PC*) to an Acceptor (A), Followed by Extraction of an Electron from an Electron Donor (D) to Regenerate the Ground State PC. *(Ref. 28,29)*

Following these design principles and with guidance from computational methods, two new families of PCs with favorable properties for O-ATRP were discovered: *N,N*-diaryldihydrophenazines (PhenN's) (e.g., **5** and **6**)[34] and *N*-arylphenoxazines (PhenO's) (e.g., **7** and **8**).[36] PhenN's improved upon previous generations of PCs by accessing more reducing triplet excited states [computationally predicted $E^0(^2PC^{\bullet+}/^3PC^*)$ < –2.0 V vs SCE] while maintaining visible light absorption.[34] In turn, polymerizations with PhenN's produced polymers with dispersities (*Đ*) as low as 1.10 (for PC **5**), although with consistently moderate initiator efficiencies, presumably due to side reactions of the PCs with propagating radicals. A major conclusion in this report was that PhenN PCs bearing electron-withdrawing groups (EWGs) or an extended π system on the *N*-aryl substituents appeared to consistently outperform other PCs, prompting an investigation into the cause of these observed differences.

As all of the PCs investigated in this study were sufficiently reducing (as PC*) and oxidizing (as $^2PC^{\bullet+}$) to mediate O-ATRP, density functional theory (DFT) calculations were used to elucidate the differences in their electronic structure that might influence PC performance.[34] These calculations revealed that all of the PC triplet excited states studied featured low-lying SOMOs localized on the PhenN core, whereas the nature of the high-lying SOMOs was dependent on the functionality on the *N*-aryl substituents. Specifically, PCs bearing electronically neutral or donating groups exhibited population of high-lying SOMOs on the PhenN core. In contrast, PCs bearing EWGs or extended π systems on the *N*-aryl substituents showed high-lying SOMOs localized onto the *N*-aryl group, suggesting photoinduced intramolecular charge transfer (CT). With these properties in mind, PC **6** was computationally predicted to contain spatially separated SOMOs and, experimentally, **6** exhibited enhanced performance in O-ATRP, producing polymers with *Đ* as low as 1.03.

More recently, 10-phenylphenoxazine (**7**) was also predicted and demonstrated to have favorable properties for use as an O-ATRP catalyst.[36] While **3** and **7** differ only by their chalcogenide, the difference in size between O and S was hypothesized to have significant impacts on the comparative performance of these PCs, as the ground state structure of **3** is noticeably bent while the ground state structure of **7** is more planar, and computations predict that the radical cation of both compounds is nearly planar. As such, owing to the smaller size of O and more planar core structure, DFT calculations predicted PhenO's would have lower reorganization energies than PhenS when transitioning from the triplet excited state to the radical cation and back to the ground state. As these PCs have been proposed to operate via an outer-sphere electron-transfer mechanism, this lower penalty for structural reorganization was hypothesized to result in enhanced PC performance due to more favorable electron-transfer processes.

To investigate whether photoinduced intramolecular CT might also be accessible in PhenO's, derivatives possessing different *N*-aryl substituents were synthesized and investigated in

O-ATRP.[36] Computations predicted that PhenO's possessing either a 1- or 2-naphthyl substitution at the *N*-aryl position could access photoinduced CT excited states, and experimentally these PCs were observed to produce, under UV irradiation, polymers with $Đ$ < 1.3. While these studies were useful in determining structural influences on PC properties, and these PCs were successful in O-ATRP, neither **7** nor the *N*-naphthylphenoxazines absorb light in the visible spectrum. Therefore, structural modifications of 1-naphthylphenoxazine were undertaken to red-shift its absorption while maintaining a strong excited state reduction potential as well as CT character. Thus, **8** was introduced, bearing biphenyl core-substituents that effectively red-shifted the absorption into the visible range as well as increased the molar extinction coefficient to 26,600 $M^{-1}cm^{-1}$ (**Table 1**).[35,36] It should be noted that although the wavelength of maximum absorption of **8** is still in the UV range (λ_{max} = 388 nm), its absorption tails significantly into the visible range, resulting nonetheless in strong visible light absorption. Gratifyingly, the use of **8** in the polymerization of MMA under white light irradiation resulted in polymers possessing relatively low $Đ$'s ($Đ$ = 1.13) and achieving nearly quantitative I*. With regards to PhenS's, similar efforts have been made to red-shift their absorption. For example, *N*-phenylbenzo[*b*]phenothiazine (**9**) has been reported, which featured a nearly 50 nm red-shifted absorption relative to **3**, allowing it to absorb in the visible region.[37] Additionally, methods to synthesize visible-light-absorbing PhenS derivatives by substitution of the PhenS core with 4-*n*-butylphenyl groups (PCs **10** and **11**) have been reported.[38,39]

The tunability of PhenO-based PCs has also been demonstrated,[35] as synthetic variations have been systematically made to tune PC absorption, CT in the excited state, and redox properties. While the former two have already been discussed in the context of various PCs, of more interest is the latter, which expanded on previous findings[34] and yielded a library of PhenO PCs with DFT-predicted $E^0(^2PC^{\bullet+}/^3PC^*)$ values spanning −1.42 V (for PC **12**) to −2.11 V (for PC **7**) and $E^0(^2PC^{\bullet+}/^1PC)$ spanning 0.30 V to 0.62 V (all vs SCE, Table 1).[35,36] Additionally, some work has also been reported on synthetically tuning the PhenN[34,40–42] and PhenS[38,39,43–45] core structures. In particular, Matyjaszewski and co-workers investigated the influence of a number of *N*-aryl substituents on PC properties and reactivity in O-ATRP for a variety of PhenS-based PCs, such as **4**.[43]

Finally, in an effort to improve PC recyclability, which remains one of the limitations of these PCs, a variant of **3** attached to a polymer support was developed that could be repeatedly added and removed from reaction mixtures simply with a set of tweezers.[46] As a result, the PC could be used in multiple polymerizations (up to 6 times) without any observable loss in performance, thus providing a means of catalyst recycling.

Table 1 Tunable Properties of PhenO's through Facile Synthetic Modifications of the Core Structure *(Ref. 35,36)*

PC	**7**	**8**	**12**
$E^0(^2PC^{\bullet+}/^3PC^*)$[a]	−2.11 (−2.48)[d]	−1.70 (−1.80)[d]	−1.42 (−1.75)[d]
$E^0(^2PC^{\bullet+}/^1PC)$[a]	0.58 (0.68)[e]	0.42 (0.65)[e]	0.62 (0.69)[e]
$\lambda_{max,abs}$[b]	324 nm	388 nm	411 nm
$\varepsilon_{max,abs}$[c]	7,700 $M^{-1}cm^{-1}$	26,600 $M^{-1}cm^{-1}$	22,300 $M^{-1}cm^{-1}$

[a] DFT-predicted redox potentials reported in V vs SCE. [b] Maximum absorption wavelengths. [c] Molar absorptivities at λ_{max}. [d] Values in parentheses are experimental $E^0(^2PC^{\bullet+}/^1PC^*)$ values (V vs SCE), where the lowest excited singlet energies were estimated from the maximum wavelength of emission. [e] Values in parentheses are experimental $E_{1/2}$ values (V vs SCE) determined using cyclic voltammetry.

3. Applications in Polymerization Reactions

3.1. O-ATRP

Broadly speaking, O-ATRP occurs by a mechanism similar to that of traditional ATRP, in that a catalyst mediates an equilibrium between "active" ($P_n^{\bullet}$) and "dormant" (P_nBr) polymer chains, repeatedly activating and deactivating polymers by reversible removal and addition of a halide end group, often a bromide (**Scheme 2**). Key to this process is that deactivation is favored over activation and propagation, thus maintaining a low concentration of reactive radicals in solution to minimize bimolecular coupling and other termination reactions.[25] In thermally driven ATRP, activation occurs via an inner sphere electron-transfer (ISET) mechanism, in which the halide is transferred from the polymer chain-end (or alkyl halide initiator) to the catalyst species at the same time as electron transfer. By contrast, activation in O-ATRP occurs through an outer sphere electron-transfer (OSET) mechanism, where an excited state PC (PC*) directly reduces an alkyl bromide (either an initiator or a polymer chain-end) to generate Br^-, $^2PC^{\bullet+}$, and an active, propagating radical. $^2PC^{\bullet+}$ may subsequently associate with Br^- to form the ion pair $^2PC^{\bullet+}Br^-$.[40] Upon deactivation, $^2PC^{\bullet+}Br^-$ oxidizes the radical chain-end and reinstalls the bromide to re-form the dormant polymer species and regenerate the ground state PC. While specific mechanistic details are still under investigation and may vary between individual PCs, the current understanding of this mechanism will be discussed in greater detail in a later section (see Section 5).

In initial reports on O-ATRP using either **2**[28] or **3**[29] in the presence of the initiator ethyl α-bromophenylacetate (EBP), the viability of the method was demonstrated through polymerization of MMA (**eq 1**).[28,29] With the potential of this method established, the homo-polymerizations of several methacrylates were demonstrated, including benzyl methacrylate,[29,34,36] *tert*-

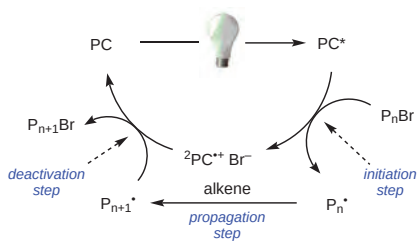

Scheme 2. Proposed O-ATRP Mechanism. *(Ref. 40)*

butyl methacrylate,[29] isobutyl methacrylate,[36] isodecyl methacrylate,[36] trimethylsilylhydroxyethyl methacrylate,[34] 2,2,2-trifluoroethyl methacrylate,[34] and di(ethylene glycol) methacrylate (**Figure 3**).[34] Notably, the polymerization of 2-(dimethylamino)ethyl methacrylate to produce polymers with relatively low *Đ*'s was unsuccessful using **1**, but was realized with PhenS catalysts.[29] In subsequent reports, the monomer scope of these PCs was expanded to methacrylates bearing long alkyl chains,[37,47] extended aromatic groups,[45] and heterocyclic functionalities.[45]

In addition to these more traditional monomers, the polymerizations of biomass-derived methacrylate monomers using PC **3** have also been reported, demonstrating that both homo- and co-polymers of these monomers could be achieved via O-ATRP.[48] The polymerization of acrylonitrile by O-ATRP using **3** and other PhenS catalysts, albeit with relatively high *Đ* (*Đ* = 1.42) compared to traditional ATRP (*Đ* = 1.04), has also been reported.[49,50] While methacrylic acid has been polymerized using **3**,[51] control over this polymerization was not evaluated, necessitating further future studies. Very interestingly, the polymerization of methacrylates with pendant furan-protected maleimides using **5** has also been reported.[52] This report not only provides a strategy for post-polymerization modification, but also demonstrates that these PCs tolerate a wide array of functionalities. However, despite various efforts, the monomer scope of O-ATRP beyond methacrylates remains largely unestablished and, as such, an important future direction of O-ATRP is to define the monomer scope and capabilities of this polymerization platform.

In all ATRP methods, the choice of initiator can also play an influential role in controlling a given polymerization. Thus, various initiators have been investigated for use with all three PC families (see eq 1), especially traditional alkyl bromides such as EBP,[29,34,36,49] diethyl 2-bromo-2-methyl malonate (DBMM),[36] methyl α-bromoisobutyrate (MBiB),[34,36,43] ethyl α-bromoisobutyrate (EBiB),[29] methyl 2-bromopropionate (MBP),[34,36] and 2-bromopropionitrile (BPN).[34,49] In addition, several alkyl chloride initiators have been investigated with PhenS catalysts, though with less success.[43] Although these PCs are capable of activating alkyl chlorides due to their strong excited state reduction potentials, they seem to be inefficient at deactivating the propagating radicals in conjunction with chloride initiators, resulting in less control during polymerizations. Perhaps the most interesting development in O-ATRP initiators thus far has been the introduction of aromatic sulfonyl halides by Chen and co-workers.[39] In their report, nearly 20 sulfonyl bromides were investigated in polymerizations mediated by **11**, achieving *Đ*'s as low as 1.21 in the polymerization of MMA, and in polymerizations of several other methacrylates and acrylates with varying levels of control. Of particular note is that this new initiating system allows for the post-polymerization modification of polystyrene (PS) via O-ATRP, as sulfonyl chlorides can be installed on the aromatic rings of PS to initiate an O-ATRP for *grafting-from* brush synthesis (see Section 3.3).

One drawback of general photoredox catalysis is the difficulty of scaling photochemical reactions,[53,54] as reactions in batch reactors must be performed on a small scale to ensure uniform irradiation throughout the reaction vessel. To overcome this obstacle, flow reactors have been implemented, in which a reaction mixture is pumped through a transparent, narrow tube wrapped around a light source to achieve both uniform irradiation as well as facile scalability.[53] In an effort to extend these benefits to O-ATRP, the polymerizations of various methacrylates using PCs **5**, **6**, and **8** were undertaken in a flow setup, resulting in the ability to synthesize the polymers on a gram scale while maintaining relatively low *Đ*.[48] Moreover, due to the improved irradiation conditions offered by continuous flow, enhanced PC performance was observed, allowing for a tenfold reduction in catalyst loading without significant loss of performance.

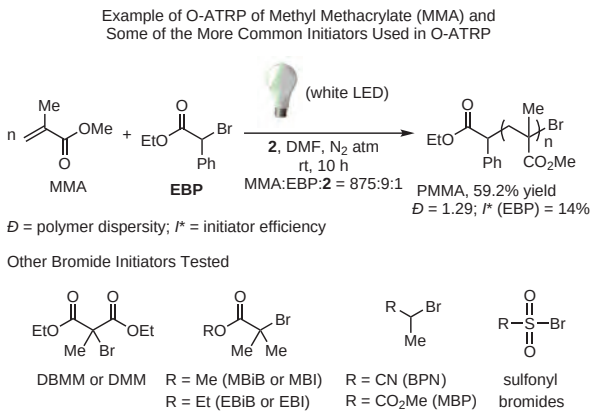

eq 1 *(Ref. 28,29,34,36,39,43,49)*

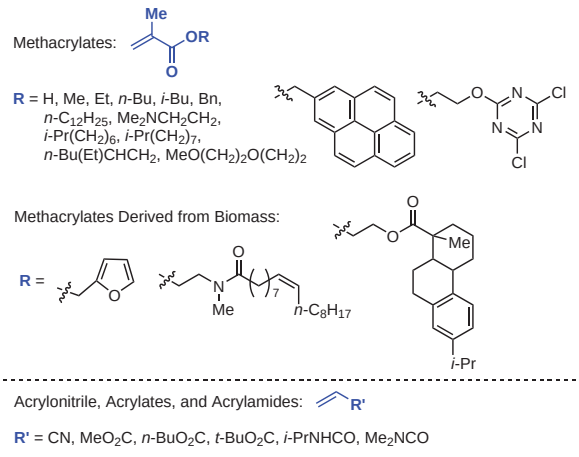

Figure 3. Monomers Successfully Polymerized via O-ATRP by Using PhenS, PhenN, and PhenO Photoredox Catalysts. *(Ref. 29,34,36,45,47–49,51)*

3.2. PET-RAFT

Although the primary application of PhenS, PhenN, and PhenO catalysts has been in O-ATRP, some applications of these PCs to PET-RAFT (photo-induced electron/energy transfer-reversible addition fragmentation chain-transfer) polymerizations have been reported.[55–59] Much like traditional RAFT, PET-RAFT makes use of a chain-transfer agent (CTA), often a thiocarbonylthio compound, to mediate a controlled radical polymerization (**Scheme 3**).[55–58] However, where traditional RAFT commonly utilizes thermal initiators, PET-RAFT makes use of a PC to mediate this process,[55–58] minimizing the formation of dead chains from the reaction of initiator radicals with active polymers.[59] Similar to what is seen in O-ATRP, PC* activates a dormant polymer-CTA bond, generating a radical that can engage in polymerization

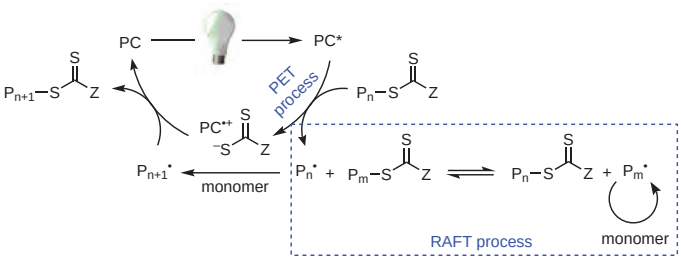

For example: Z = PhS or *n*-BuS; P_n = $MeCHCO_2H$ or $MeC(CN)(CH_2)_2CO_2H$

Scheme 3. Xu and Boyer's Proposed Mechanism of PET-RAFT. *(Ref. 55–58)*

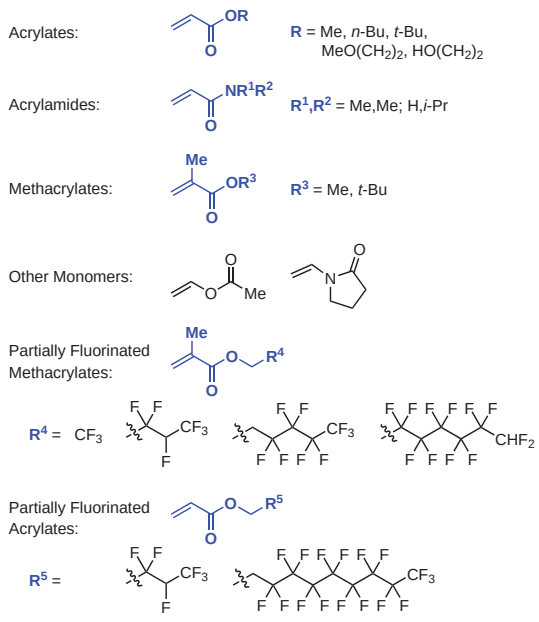

Figure 4. Monomers Polymerized via PET-RAFT by Using PhenN and PhenS Catalysts. *(Ref. 38,46,59)*

($P_n^{\bullet}$), $^2PC^{\bullet+}$, and the respective thiocarbonylthiolate (in the case of a thiocarbonylthio CTA). The active $P_n^{\bullet}$ radical can either propagate or undergo reversible deactivation by one of two pathways: in the first, the radical reacts with $^2PC^{\bullet+}$ to undergo oxidation and reinstallation of the CTA end group. In the second, the active radical can undergo chain-transfer with another CTA-capped polymer, resulting in the deactivation of one chain and the activation of another chain (Scheme 3).

Although originally reported using iridium PC **1**,[60] PET-RAFT was later expanded to PhenS, when **3** was employed to polymerize *N*-isopropylacrylamide, *N,N*-dimethylacrylamide, *tert*-butyl acrylate, and ethylene glycol methyl ether acrylate (**Figure 4**) with relatively low to low *Đ*'s and temporal control.[59] This monomer scope was recently extended to various other acrylates and methacrylates while also introducing a method for catalyst recycling by using a polymer-supported PC that is based on **3**.[46] Finally, the ability of PhenS catalysts to polymerize partially fluorinated monomers has also been demonstrated, producing a variety of partially fluorinated polymers with generally low *Đ*'s.[38]

To demonstrate the utility of PET-RAFT in materials manufacturing, existing polymer-based gels were homogeneously modified in an example of living additive manufacturing.[61] Since the gels consisted of polymer networks with trithiocarbonate iniferters embedded in the polymer backbone, chain extensions could be achieved upon irradiation by infiltrating the gels with *N*-isopropylacrylamide and **3**. Importantly, since this method involved modification of the existing polymer network, the resulting material was homogeneous in nature in contrast to the heterogeneous materials obtained by simply growing one material on another using previous methods.

Moreover, as these PCs have displayed the ability to mediate polymerizations both via O-ATRP and PET-RAFT, some work has combined these two reaction manifolds into a stepwise synthesis of copolymers of acrylates and methacrylates using **5**.[62] Capitalizing on the strengths (and weaknesses) of both methods, a multifunctional initiator bearing a trithiocarbonate moiety and an alkyl bromide moiety was synthesized, in which the former functional group would only react during PET-RAFT and the latter during O-ATRP. Thus, the polymerization of methyl acrylate was achieved via PET-RAFT, followed by the polymerization of methyl methacrylate via O-ATRP, resulting in a block copolymer that otherwise would have been challenging to prepare by either method alone.

3.3. Complex Polymer Architectures

One of the hallmarks of a controlled polymerization is the ability to synthesize complex polymer architectures.[63–65] For the methods described above, this ability has been demonstrated at various levels, through the synthesis of linear block-copolymers,[29,34,36,45,62,66] brushes,[39,67] and even star[68] polymers (**Figure 5**). For example, all three original reports on O-ATRP mediated by PhenS, PhenN, and PhenO catalysts showed that PMMA synthesized with these PCs could be isolated and used as a macroinitiator for the synthesis

of various block copolymers.[29,34,36] Moreover, a report by Xu et al. made use of **5** to synthesize block copolymers of *N*-isopropylacrylamide and *tert*-butyl methacrylate, albeit with poor control over *Đ*.[69] Notably, in addition to chain-extending polymers synthesized via O-ATRP, polymers synthesized by other methods can be synthetically modified for use as O-ATRP macroinitiators. Thus, block copolymers containing poly(3-hexylthiophene)[45] and poly(ethylene glycol)[66] have also been realized, demonstrating the ability of these PCs to tolerate a wide range of functional groups.

Expanding on this notion of modifying existing polymers, several methods have been reported for synthesizing brush polymers from existing linear homopolymers. One approach that has already been discussed to some extent is that in which sulfonyl halides were installed on the phenyl groups of polystyrene to enable grafting of poly(methyl acrylate) chains.[39] Furthermore, fluorinated polymers with chloride-functionalized backbones have been modified using PC **3** to synthesize macromolecules with interesting dielectric properties for electronics applications (**eq 2**).[67,70] Capitalizing on the presence of a chloride moiety in poly(vinylidene fluoride-*co*-chlorotrifluoroethylene) [P(VDF-*co*-CTFE)],[71] grafting of various acrylates and methacrylates onto P(VDF-*co*-CTFE) was achieved while also avoiding metal contamination that occurs in traditional ATRP methods.[70] The impact of this reduced metal contamination was also evaluated and will be discussed further in a later section (see Section 3.4).[67] Finally, the ability of these PCs to synthesize star polymers in the presence of multifunctional initiators was investigated, yielding a range of complex star architectures with up to 8 arms that are composed of either homo- or block-copolymers.[68]

Thus, a variety of polymeric architectures have become accessible by using PhenS, PhenN, and PhenO photoredox catalysts. In particular, something that should be emphasized is the number of methods using these PCs to modify existing polymer structures and yield increasingly complex architectures. While a single method to polymerize any monomer is ideal, the reality is that most methods have associated strengths and weaknesses. However, the ability of PhenS, PhenN, and PhenO photoredox catalysts to tolerate various functional groups allows methods with complementary strengths to be combined, whether it be in a one-pot synthesis[62] or in a multiple–step synthetic sequence, giving rise to polymer architectures that might not be possible by any of these methods alone.

3.4. Avoiding Metal Contamination for Sensitive Applications

Often cited as one of the major advantages of O-ATRP,[28,29,34,36] is the use of PhenS's, PhenN's, and PhenO's for the synthesis of polymers without the metal contamination associated with traditional ATRP. Although significant advances have been made toward reducing catalyst loadings[72–74] and purifying polymers synthesized by traditional ATRP,[75–78] even trace metal contamination remains problematic in polymers for electronics applications.[67,70,71] In particular, grafting insulators, such as PMMA, to poly(vinylidene fluoride)-based polymers (PVDF) has shown promise to yield materials suitable for high-pulse capacitors, whereas residual metal ions from traditional ATRP can result in significant dielectric loss.[79] As this loss has been attributed to ion migration under an applied electric field, using an organic PC to mediate the grafting process can eliminate this issue, since any catalyst remaining in the polymer should be in the ground state and would thus not be influenced by an applied field.

In this regard, the method developed for the modification of P(VDF-*co*-CTFE) using **3** (see eq 2) was shown to be capable of activating the C–Cl bond toward hydrogenation[71] as well as O-ATRP.[70] In a later report, the impact of employing an organic PC versus a traditional copper catalyst was evaluated, demonstrating that polymers prepared via O-ATRP exhibited a far reduced ion mobility compared to polymers prepared using traditional ATRP.[67] Moreover, when comparing the materials properties of these two samples, the former exhibited both enhanced discharge energy density and discharge efficiency over a range of applied electric fields, suggesting that **3** can yield these desirable materials with reduced impact on their performance.

In addition to electronics applications, biological applications of polymers have also been cited as potentially metal-sensitive to warrant the investigation of PhenS's,[66] PhenN's,[34] and PhenO's.[36] To this end, the ability of **3** to synthesize amphiphilic

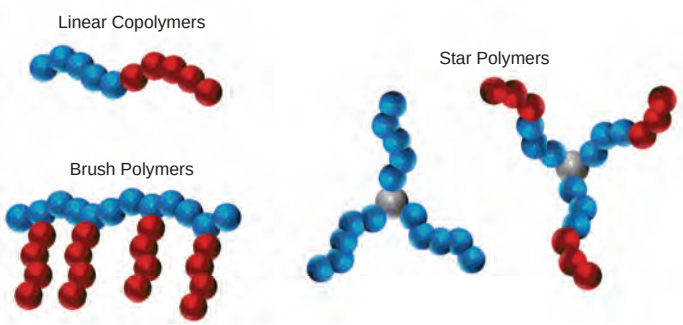

Figure 5. Polymer Architectures Synthesized Using PhenS, PhenN, and PhenO Photoredox Catalysts.

General Approach for the Modification of P(VDF-*co*-CTFE) by Reduction with PhenS Catalysts

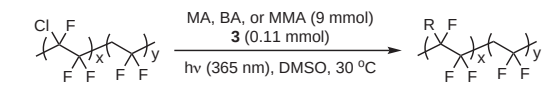

poly(vinylidene fluoride-*co*-chlorotrifluoroethylene) [P(VDF-*co*-CTFE)]

VDF:CTFE = 94:6
1.00 g

R = H, PMA, PBA, PMMA

P(VDF-*co*-CTFE)-*g*-PMA
or P(VDF-*co*-CTFE)-*g*-PBA
or P(VDF-*co*-CTFE)-*g*-PMMA

MA = methyl acrylate; BA = *n*-butyl acrylate; MMA = methyl methacrylate

eq 2 *(Ref. 67,70)*

diblock copolymers was investigated,[66] as these materials have attracted attention for drug and gene delivery.[80,81] By modifying poly(ethylene glycol) for use as an ATRP macroinitiator, copolymers of ethylene glycol and glycidyl methacrylate could be obtained, albeit with *Đ* values well above 1.5. It should be noted, however, that organic PCs for biologically relevant polymers may be unnecessary, as copper is vital to human life and copper dietary supplements have even been used to mediate traditional ATRP.[82] Moreover, while these PCs have been shown to be biologically active molecules,[83–90] their toxicity in humans has not been investigated and should warrant further study.

3.5. Surface Modifications

Surface-initiated polymerizations represent a versatile approach for the production of hybrid organic–inorganic materials with interesting surface properties.[91] In particular, surface-initiated ATRP (SI-ATRP) has emerged as an important technique capable of yielding such materials with precisely controlled architectures.[92] However, until recently, the production of patterned surfaces by SI-ATRP remained a challenge, requiring the use of advanced lithographic and printing methods. To overcome this challenge, a method was developed that capitalizes on the spatiotemporal control achieved in O-ATRP and allows the use of binary photomasks to produce patterned polymer coatings on functionalized silicon surfaces in a single step (**eq 3**).[92] Notably, features at even the micron scale could be produced reliably, demonstrating the high level of precision obtainable by this method.

In addition to the modification of flat surfaces, SI-ATRP photocatalyzed by **3** has also been reported using functionalized silica nanoparticles, which were simultaneously used to investigate parameters influencing PC control in the grafting process.[93,94] For example, the effects of various initiating moieties were investigated for both small (16 nm) and large (120 nm) silica nanoparticles, revealing that 2-bromo-2-phenylacetate based tetherable initiators exhibited superior performance to those with 2-bromoisobutyrate moieties.[93] Moreover, this work was extended to determine the impact of the tetherable initiator spacer length on the grafted polymer properties. Thus, it was determined that for O-ATRP, increasing the initiator spacer length results in both lower *Đ* polymer chains and higher grafting density (number of chains per unit of area).[93]

Other work in this area has focused on surfaces of other materials, including iron(III) oxide nanoparticles[95] and europium-doped hydroxyapatite,[96] capitalizing on the ability of these PCs to yield controlled polymer grafts without introduction of unwanted metal ions. Moreover, surface grafting of methacrylic acid onto a silicon wafer has also been achieved,[51] demonstrating compatibility between this monomer and **3**. As controlling the polymerization of methacrylic acid has historically been challenging for ATRP,[97] future work should undoubtedly include investigation of the ability of PhenS's, PhenN's, and PhenO's to yield well-defined poly(methacrylic acid).

3.6. Post-Polymerization Modifications

In addition to the ability to synthesize well-defined polymers for various applications, the ability to alter polymers post-polymerization is also desirable. One such example that has already been discussed is the one in which polystyrene was modified to enable grafting of methyl acrylate chains from the aromatic pendants.[39] In another example, researchers reported on the ability of **3** to remove chloride, bromide, and trithiocarbonate end-groups from various polymers, enhancing their long-term stability by removing these reactive functionalities.[98] Moreover, this method was extended to dehalogenate tethered initiators on functionalized silicon surfaces, allowing for patterns to be prepared on functionalized surfaces prior to use in SI-ATRP. Thus, the utility of these PCs has been demonstrated in a diverse range of polymer-based applications, including polymer synthesis and modification.

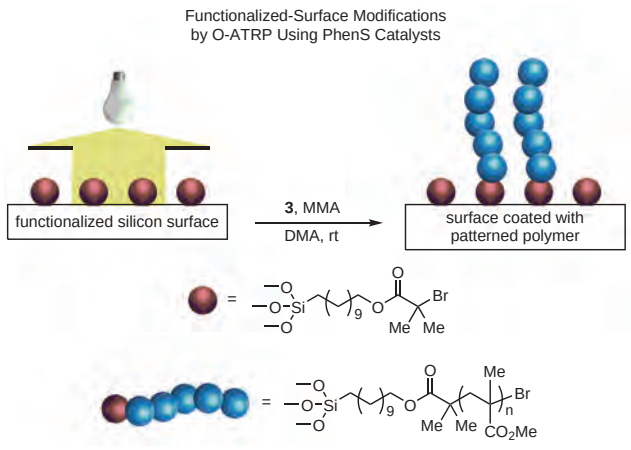

eq 3 *(Ref. 92)*

4. Applications in Small-Molecule Transformations

Although the primary application thus far of these strongly reducing organic PCs has been in polymer synthesis, several reports have emerged on their application in small-molecule transformations, demonstrating their broader utility as catalysts for diverse chemical reactions.

4.1. Carbon–Carbon Bond Formations

PhenS catalysts have been reported as PCs in the dehalogenation of various organic molecules (**eq 4**).[44] Much like the activation of alkyl halides in O-ATRP, the dehalogenation of organic halides—including aromatic iodides, aromatic and alkyl bromides, and aromatic chlorides—was demonstrated using PC **3**.[99] While these reactions were originally limited to dehalogenations followed by hydrogenations, the ability of **3** to mediate a radical cyclization provided evidence for a radical mechanism. Thus, this reactivity was later exploited to form C–C bonds with several substrates using PCs **3** and **14**.[44] In addition, by tuning PC reduction potentials [$E^0(^2PC^{\bullet+}/^1PC^*)$ = –2.1 V and –1.5 V vs SCE for **3**

and **14**, respectively], selectivity for certain halides over others was achieved. For example, using PC **14**, iodo functionalities in multi-halide substrates could be targeted. In contrast, and as PC **3** is more reducing, both iodo and bromo functionalities could be targeted while leaving chloro and fluoro groups intact.

Interestingly, the ability of PhenS catalysts to activate carbon–halogen bonds was also extended to fluorides. Using PC **3** and cyclohexanethiol (CySH) as co-catalyst, C–F bonds in various trifluoromethylarenes were activated for reaction with unactivated alkenes, allowing for the alkylation of several substrates under mild conditions (**eq 5**).[100] Although this activation approaches the thermodynamic limit of PC **3**'s reducing ability [–2.07 V vs SCE for 1,3-bis(trifluoromethyl)-benzene; $E^0(^2PC^{\bullet+}/^1PC^*)$ = –2.1 V vs SCE for **3**], quenching of PC* by 1,3-bis(trifluoromethyl)benzene was demonstrated using Stern–Volmer analysis. Thus, it was proposed that such substrates could be activated to form a radical species capable of mesolytic cleavage of a C–F bond, which would then lead to reaction with alkenes to effect the desired transformations.

Finally, the trifluoromethylation of several aromatic and olefinic compounds has been reported using PC **6** under visible light irradiation of F_3C–I (**eq 6**),[101] as PC **6**'s excited state is sufficiently reducing to directly reduce CF_3I and generate $CF_3^{\bullet}$ for the trifluoromethylation reaction. While such transformations were previously accessible by photoredox catalysis, they required the use of polypyridyl Ru and Ir PCs such as *fac*-[Ir(ppy)$_3$] (**1**),[102–106] as few PCs possess the excited state reduction potentials necessary to mediate these reactions. However, due to the strongly reducing excited states accessible by PhenS's, PhenN's, and PhenO's, transformations such as these have become accessible without the need for these precious metal PCs,[101] demonstrating the potential of these organic PCs as sustainable alternatives to precious metal catalysts.

4.2. Other Coupling Reactions

In addition to the C–C bond formations described above, methodologies for C–N and C–S cross-couplings have also been reported using these strongly reducing organic PCs. For example, through the use of a dual photoredox/nickel catalytic system, the coupling of various primary and secondary amines with aryl bromides was achieved in the presence of PCs **6** or **8** (**eq 7**).[101] Furthermore, using PC **8** at 10 times less catalyst loading than the Ir PC used in the seminal report by Oderinde, Johannes, and co-workers,[107] a similar approach was employed to couple thiols to aryl bromides, yielding a range of products in moderate-to-high yields (**eq 8**).[101] It should be noted that, while similar C–S coupling reactions were reported using aryl iodides with an Ir PC,[107] aryl bromide coupling partners were ineffective in this system. Thus, this reaction (eq 8) represents an example in which these organic PCs have enabled transformations previously inaccessible using precious metals.

Dehalogenation Selectivity Determined by the Reduction Potential of the Photoredox Catalyst

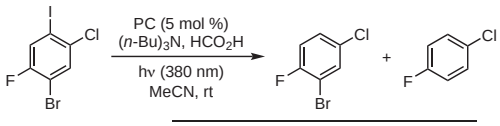

PC	Rxn Time	Yield	Yield
14	5 h	96%	4%
3	48 h	5%	90%

eq 4 *(Ref. 44)*

PhenS-Catalyzed Defluorination and C–C coupling of Trifluoromethylated Substrates with Alkenes

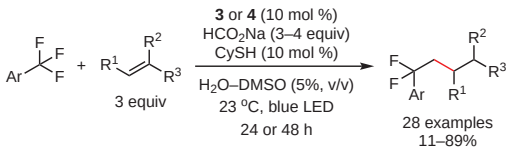

Ar = mono- and disubstituted benzene, 2-Pyr; R^1 = H, Me
R^2, R^3 = H, alkyl, terminally functionalized alkyl, cycloalkyl, cycloalkenyl, heterocycloalkyl

eq 5 *(Ref. 100)*

Trifluoroalkylation of Alkenes Catalyzed by Organic Photoredox Catalysts

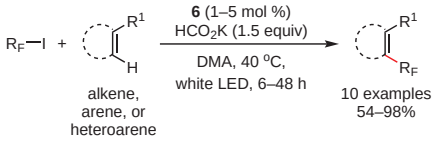

R_F = CF_3, CF_3CF_2; R^1 = H, Me, MeO

For alkenes, the major substitution product was the trans isomer

In the absence of HCO_2K, the reaction of F_3C–I with alkenes led to addition products:

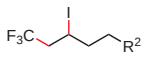

R^2 = Ph, *n*-Bu, *n*-Oct, *n*-$C_7H_{14}OH$
42–49%

eq 6 *(Ref. 101)*

Cross-Coupling of Amines with Aryl Bromides by Dual Organic Photoredox–Nickel Catalysis

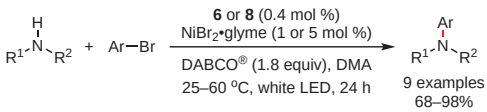

Ar = 4-XC_6H_4 (X = H, Ph, MeO, CF_3), 2-Np, 2-Pyr
R^1 = H; R^2 = *n*-Pr, Ph, (furan-2-yl)CH_2
NR^1R^2 = pyrrolidinyl, morpholin-4-yl

eq 7 *(Ref. 101)*

4.3. Selective Decarboxylative Olefinations

In another example of reactivity enabled by these strongly reducing PCs, PhenN's were employed in visible-light-mediated decarboxylative olefinations to yield terminal alkenes (**eq 9**).[108] The use of **5** in conjunction with a copper catalyst enabled these transformations to be performed with high selectivity (as preventing isomerization to an internal alkene had previously been challenging), under mild conditions and without the use of precious-metal catalysts. Furthermore, this method was demonstrated for a range of activated aliphatic acids, including some derived from biomass feedstocks—showing that the reaction tolerates a variety of functional groups within the substrates.

4.4. Photocatalytic Phosgene Generation for Organic Synthesis

PC **8** can generate fluorophosgene photocatalytically in situ for the synthesis of carbonates, carbamates, and urea derivatives (**Scheme 4**).[109] While the ability of phosgene derivatives to perform such transformations was previously understood, such syntheses required special equipment for handling phosgene due to its severe toxicity.[110,111] Alternatives to this class of reagents do exist, but they tend to be far less effective,[111] requiring one to choose between an effective synthesis and the safety of the associated reagents. As such, the ability of this method to generate a phosgene derivative in situ using photocatalysis is highly attractive, since the phosgene reacts quickly once generated, minimizing the risk of exposure and thus the safety concerns surrounding this reagent.

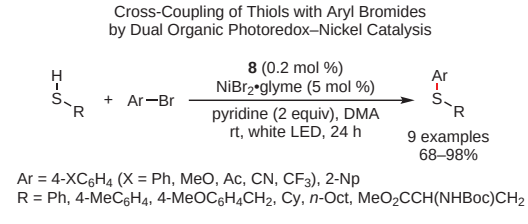

eq 8 *(Ref. 101)*

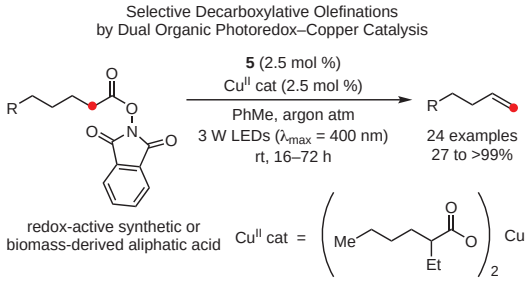

eq 9 *(Ref. 108)*

5. Mechanistic Insights Guiding Catalyst Development

Since PCs based on PhenS, PhenN, and PhenO were originally developed for use in O-ATRP, mechanistic work surrounding these PCs has primarily focused on their function in O-ATRP. Thus, mechanistic discussions in this section will be made in the context of this method, although the implications of these discoveries likely extend beyond O-ATRP.

5.1. Photoexcitation, Activation, and Deactivation in O-ATRP

As with any photoredox-catalyzed reaction, the absorption of light is the first important step to the operation of the PC. In the context of O-ATRP, visible-light absorption is preferred over absorption of UV light, as the latter has the potential to initiate undesirable side reactions. To achieve this property, synthetic modifications have been reported for various catalyst families, allowing for the design of strongly reducing but also visible-light absorbing PCs (see Section 2). Since the intensity of a light source can often be tuned with ease, this external stimulus can also be manipulated to influence light absorption by the PC (and thereby the reaction it mediates). This principle was demonstrated by polymerizing MMA in the presence of **8** under various irradiation conditions, where the emission intensity of the light source was modulated.[111,112] As a result of decreasing light intensity, molecular-weight growth during polymerization became less controlled and $Đ$ increased, indicating a loss of control over the polymerization. This result is consistent with a decrease in deactivation efficiency, as decreased light intensity yields less PC* and thereby less $PC^{\bullet+}Br^-$ to deactivate reactive radicals in solution. Significantly, the performance of **8** appeared to be influenced to a lesser extent than that of **2**, suggesting that tolerance to varying reaction conditions can be designed into these PCs.

Once a PC is photoexcited, the lifetime of the desired excited state must be long enough to allow energy or electron transfer to occur with the substrate.[5–7] In the case of PhenO's and PhenN's, activation has been proposed to occur from ^{3}PC*. As such, the lifetime of ^{3}PC* has been measured for some of the PCs in these families, including **6** (4.3 ± 0.5 μs) and **8** (480 ± 50 μs).[101] Interestingly, these lifetimes are competitive with,

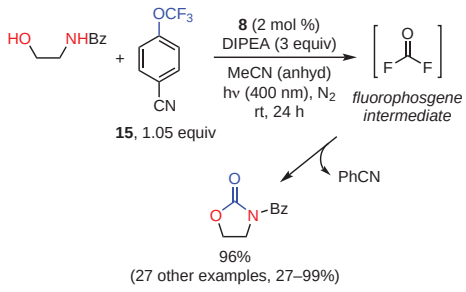

Scheme 4. Photocatalytic Generation of Fluorophosgene in Situ for the Synthesis of Carbonates, Carbamates, and Urea Derivatives. *(Ref. 109)*

or even exceed, those of traditional precious-metal-containing PCs (e.g., 1.9 μs for **1**),[113,114] although only **8** has a comparable quantum yield for the triplet excited state (Φ_t = 2% for **6** and Φ_t = 90% for **8**).[101]

However, whether these PCs operate predominately via the ^{1}PC* or ^{3}PC* excited state remains to be determined. Recently, an investigation of electron transfer between photoexcited PhenN's and methyl 2-bromopropionate (MBP) was presented, suggesting ^{1}PC* may be the most important excited state in regards to catalysis for this family of PCs.[115] Similarly, mechanistic investigations related to the dehalogenation of aryl halides have suggested that **3** can operate efficiently from ^{1}PC*.[99] On the other hand, others have argued that these PCs likely operate predominately from ^{3}PC* in O-ATRP, as these states tend to be much longer-lived than ^{1}PC*.[116] Thus, further studies are required regarding which excited state species of the PC is most pertinent to catalysis, something that may prove to be case-specific.

Regardless of the nature of the excited state, the importance of photoexcitation has been demonstrated with **3**.[43] For example, upon irradiation, **3** activates methyl 2-bromoisobutyrate (MBiB) with a rate constant k_{act} = 5.8 x 10^8 M^{-1} s^{-1}, whereas in the absence of irradiation k_{act} = 1.0 x 10^{-14} M^{-1} s^{-1}, demonstrating that ground state **3** is essentially incapable of performing the necessary reduction for activation. Moreover, a comparison of the activation of various initiators suggests similar trends are observable as in traditional ATRP, such as ethyl α-bromophenylacetate (EBP) (k_{act} = 2.0 x 10^{10} M^{-1} s^{-1}) being a faster acting initiator than MBiB, while MCiB (the chloride analogue of MBiB) is a slower acting initiator (k_{act} = 1.5 x 10^6 M^{-1} s^{-1}) than MBiB.

With regard to deactivation, initial reports proposed this step may occur via bimolecular reaction between ^{2}PC$^{\bullet+}$Br$^-$ and the propagating radical, requiring ^{2}PC$^{\bullet+}$ to pre-associate with Br$^-$ prior to deactivation.[28,29,34,36,40] Alternatively, other work has suggested that this process may in fact proceed via a termolecular mechanism.[43] Using derived activation parameters, the rates of various deactivation pathways were calculated according to Marcus theory and compared to the rate of termination for evaluation of their viability. Based on these calculations, a termolecular deactivation was predicted to be more viable than other pathways involving ISET, OSET, and dissociative ET. However, these calculations did not explicitly account for the entropic penalty associated with a three-body collision, which makes termolecular reactions unfavorable,[117] especially considering the species involved are at very low concentrations in O-ATRP. Alternatively, the influence of ion pairing on deactivation in O-ATRP has been reported, supporting a bimolecular mechanism in which PC$^{\bullet+}$ and Br$^-$ form an ion pair prior to deactivation.[40]

5.2. Intramolecular Charge Transfer in the Excited State

During early investigations of PhenN's, it was observed that PCs bearing *N*-aryl substituents with EWGs or extended π systems exhibited noticeably better performance in O-ATRP (especially in regards to producing polymers possessing lower *Đ*'s) than those bearing electron-donating or electron-neutral *N*-aryl substituents.[34] Through the aid of computational chemistry, it was discovered that the electronic properties of these substituents could influence electron density distribution in the ^{3}PC* excited state, giving rise to intramolecular charge transfer (CT) from the PhenN core to the *N*-aryl substituent containing EWGs or extended conjugation. Computationally, this property can be observed by the presence of spatially separated SOMOs in ^{3}PC* (**Figure 6**), as well as by visualizing the shift in electron density upon photoexcitation using electrostatic-potential-mapped electron density diagrams (**Scheme 5**, Part (a)).[40] Experimentally, the effects of CT can be observed (i) visually through the solvatochromism of these PCs, (Scheme 5, Part (b)) and (ii) by using fluorescence spectroscopy for quantitative analysis.[35,40] Notably, this intramolecular CT is analogous to the metal-to-ligand CT,[30] which is observed in many successful metal-based PCs.[118]

After the correlation of these CT properties and their influence on the performance of the PC, several studies have

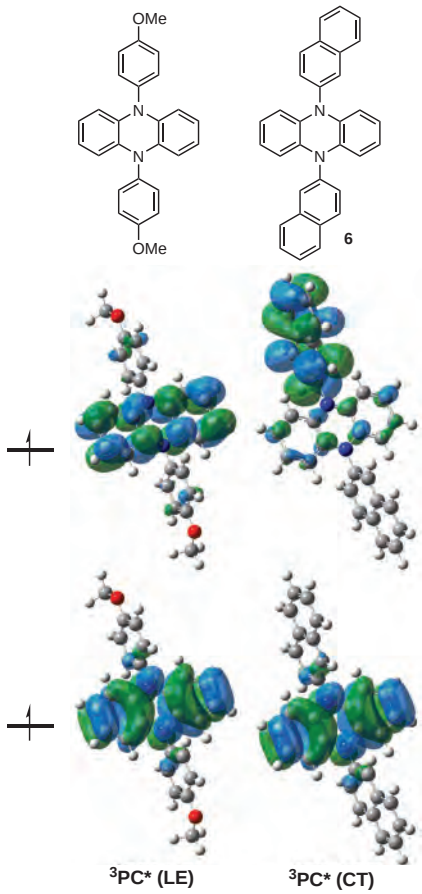

Figure 6. PhenN's Computed to Have Spatially Separated SOMOs (Right) Were Observed to Perform Better as O-ATRP Catalysts than Those That Possessed Localized SOMOs. *(Ref. 40)*

been reported on ways to manipulate CT in favor of improving polymerization control in O-ATRP. For example, following the discovery that PCs with CT character could operate in a range of solvents (whereas non-CT PCs could not), solvent optimization was performed under O-ATRP conditions for a wide range of PCs, including **5** and **6**.[41] As result, it was discovered that switching the solvent from *N,N*-dimethylacetamide (DMA) to ethyl acetate (EtOAc) can yield improved control over the polymerization of MMA, as observed through more linear growth of polymer molecular weight and lower *Đ* (1.08 in EtOAc vs 1.17 in DMA for PC **5**). In addition, a recent investigation into the photophysical properties of PCs with and without CT character has suggested that a CT excited state with perpendicular geometry and appropriate energy (e.g., PC **8**) can aid intersystem crossing (ISC) to the ^{3}PC*,[119] allowing for PCs with favorable photophysical properties to be targeted synthetically. Notably, these findings can be used to explain the observed differences in performance between CT and non-CT PCs, as improved ISC would yield a larger concentration of the active catalytic species in O-ATRP (assuming the PC operates via the ^{3}PC* excited state and not the ^{1}PC*).

5.3. Excimer Formation and Reactivity

The possibility of these PCs forming excimers has also been investigated as a means of understanding their reactivity in thermodynamically challenging reductions.[109] In an attempt to prepare carbonates, carbamates, and urea derivatives, it was observed that PC **8** was capable of reducing 4-(trifluoromethoxy)-benzonitrile (**15**), which was surprising given that this PC should not be thermodynamically capable of reducing this substrate [$E^*_{red}(^2PC^{\bullet+}/^3PC^*) = -1.7$ V whereas $E^0_{red}(\mathbf{15}/\mathbf{15}^{\bullet-}) = -2.1$ V, both vs SCE]. To explain this observation, it was proposed that PC **8** might form excimers under reaction relevant concentrations, leading to the formation of a PC radical anion and radical cation upon photoexcitation. In the absence of an electron donor, these species likely undergo a comproportionation reaction to generate two ground state PC molecules. However, upon addition of an electron donor such as an amine, it was proposed that the PC radical cation could be quenched, resulting in a longer-lived radical anion capable of reducing a substrate. Supporting these hypotheses, quenching of the radical cation upon addition of an amine was observed using transient absorption spectroscopy, and the $E^0_{red}(^1PC/^2PC^{\bullet-})$ of the radical anion of **8** was measured to be about −2.5 V vs SCE, which is sufficient to reduce **15**.[109] Thus, excimers of these PCs may offer a means of enhancing their reducing power to access more challenging transformations in the future.

6. Conclusion and Outlook

Until recently, few PCs with strongly reducing excited states existed, especially organic PCs. Thus, PhenS's, PhenN's, and PhenO's represent a unique subset of molecules that are capable of performing challenging reductions catalytically without the use of precious metals. Capitalizing on their strong excited state reduction potentials, these PC families have been widely applied to the synthesis of polymers with controlled molecular weights, low dispersities, and complex architectures. Furthermore, their ability to operate via several mechanisms

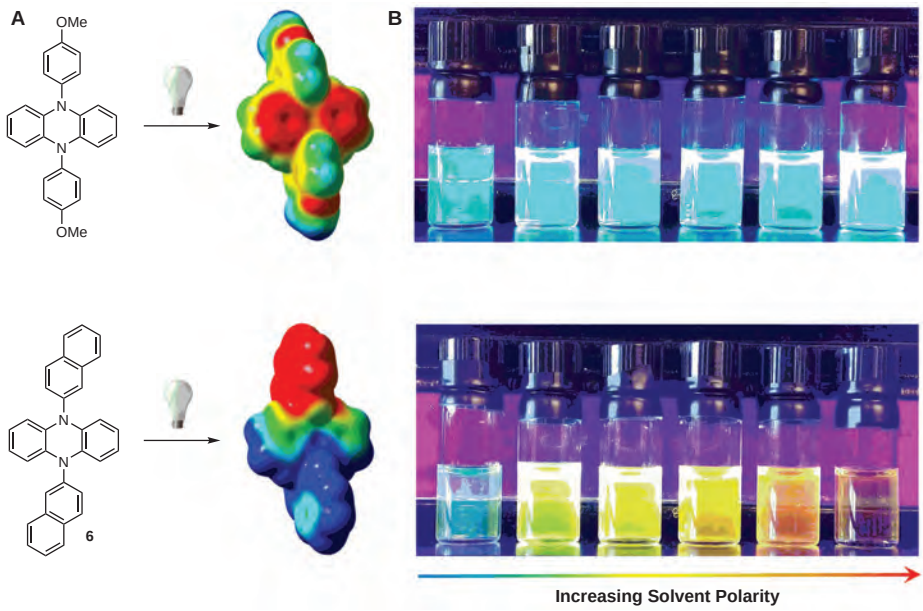

Scheme 5. Comparison of PhenN's without (Top) and with (Bottom) CT Excited States. (A) Computed Electrostatic-Potential-Mapped Electron-Density Diagrams Portraying the Distribution of Electron Density within PCs upon Photoexcitation to an Excited State, with Red Signifying Larger Populations of Electron Density. (B) Charge Transfer PCs Exhibit Large Solvatochromic Shifts in Their Emissions in Solvents of Different Polarity, While Non-CT PCs Do Not. Solvents of Increasing Polarity from Left to Right: 1-Hexene, Benzene, Dioxane, THF, Pyridine, and DMF. *(Ref. 35,40)*

(e.g., O-ATRP and PET-RAFT) has also been demonstrated. Moreover, the ability of these PC families to mediate a variety of small-molecule transformations has been reported, the scope of which will undoubtedly expand in coming years. To promote this expansion, future investigations focusing on the mechanisms of these PCs in a range of applications will be crucial, allowing for their design principles to be refined to target desired, selective transformations. Moreover, these PCs have a unique potential to increase the long-term sustainability of transformations currently mediated by precious metal catalysts. However, the sustainability of these PCs is currently hindered by the fact that all of the PCs discussed herein to date are synthesized via palladium-catalyzed transformations. Thus, future efforts should also include the development of more sustainable PC syntheses that are not dependent on precious metals.

7. Acknowledgments

The authors are thankful for financial support from Colorado State University, the American Chemical Society Petroleum Research Fund, and the National Institute of General Medical Sciences of the National Institutes of Health (Award Number R35GM119702). D. A. Corbin is grateful for financial support from a CSU Chemistry Graduate Fellowship and Professor Louis S. Hegedus Fellowship. C.-H. Lim is grateful for an NIH F32 Postdoctoral Fellowship (F32GM122392). The content is solely the responsibility of the authors and does not necessarily represent the official views of the National Institutes of Health.

8. References

(1) Narayanam, J. M. R.; Stephenson, C. R. J. *Chem. Soc. Rev.* **2011**, *40*, 102.
(2) Prier, C. K.; Rankic, D. A.; MacMillan, D. W. C. *Chem. Rev.* **2013**, *113*, 5322.
(3) Romero, N. A.; Nicewicz, D. A. *Chem. Rev.* **2016**, *116*, 10075.
(4) Shaw, M. H.; Twilton, J.; MacMillan, D. W. C. *J. Org. Chem.* **2016**, *81*, 6898.
(5) Blum, T. R.; Miller, Z. D.; Bates, D. M.; Guzei, I. A.; Yoon, T. P. *Science* **2016**, *354*, 1391.
(6) Lu, Z.; Yoon, T. P. *Angew. Chem., Int. Ed.* **2012**, *51*, 10329.
(7) Welin, E. R.; Le, C.; Arias-Rotondo, D. M.; McCusker, J. K.; MacMillan, D. W. C. *Science* **2017**, *355*, 380.
(8) Ludwig, J. R.; Schindler, C. S. *Chem* **2017**, *2*, 313.
(9) Nakamura, M.; Dohno, R.; Majima, T. *J. Org. Chem.* **1998**, *63*, 6258.
(10) Hintz, S.; Mattay, J.; van Eldik, R.; Fu, W.-F. *Eur. J. Org. Chem.* **1998**, *1998*, 1583.
(11) Pandey, G.; Laha, R. *Angew. Chem., Int. Ed.* **2015**, *54*, 14875.
(12) Manfrotto, C.; Mella, M.; Freccero, M.; Fagnoni, M.; Albini, A. *J. Org. Chem.* **1999**, *64*, 5024.
(13) Dondi, D.; Protti, S.; Albini, A.; Carpio, S. M.; Fagnoni, M. *Green Chem.* **2009**, *11*, 1653.
(14) Xia, J.-B.; Zhu, C.; Chen, C. *J. Am. Chem. Soc.* **2013**, *135*, 17494.
(15) Kotani, H.; Ohkubo, K.; Fukuzumi, S. *J. Am. Chem. Soc.* **2004**, *126*, 15999.
(16) Ohkubo, K.; Mizushima, K.; Iwata, R.; Souma, K.; Suzuki, N.; Fukuzumi, S. *Chem. Commun.* **2010**, *46*, 601.
(17) Xiang, M.; Meng, Q.-Y.; Li, J.-X.; Zheng, Y.-W.; Ye, C.; Li, Z.-J.; Chen, B.; Tung, C.-H.; Wu, L.-Z. *Chem.—Eur. J.* **2015**, *21*, 18080.
(18) Keshari, T.; Yadav, V. K.; Srivastava, V. P.; Yadav, L. D. S. *Green Chem.* **2014**, *16*, 3986.
(19) Yang, W.; Yang, S.; Li, P.; Wang, L. *Chem. Commun.* **2015**, *51*, 7520.
(20) Meyer, A. U.; Jäger, S.; Hari, D. P.; König, B. *Adv. Synth. Catal.* **2015**, *357*, 2050.
(21) Ghosh, I.; Ghosh, T.; Bardagi, J. I.; König, B. *Science* **2014**, *346*, 725.
(22) Corrigan, N.; Shanmugam, S.; Xu, J.; Boyer, C. *Chem. Soc. Rev.* **2016**, *45*, 6165.
(23) Zhang, G.; Song, I. Y.; Ahn, K. H.; Park, T.; Choi, W. *Macromolecules* **2011**, *44*, 7594.
(24) Fors, B. P.; Hawker, C. J. *Angew. Chem., Int. Ed.* **2012**, *51*, 8850.
(25) Matyjaszewski, K. *Macromolecules* **2012**, *45*, 4015.
(26) Krys, P.; Matyjaszewski, K. *Eur. Polym. J.* **2017**, *89*, 482.
(27) Shanmugam, S.; Boyer, C. *Science* **2016**, *352*, 1053.
(28) Miyake, G. M.; Theriot, J. C. *Macromolecules* **2014**, *47*, 8255.
(29) Treat, N. J.; Sprafke, H.; Kramer, J. W.; Clark, P. G.; Barton, B. E.; de Alaniz, J. R.; Fors, B. P.; Hawker, C. J. *J. Am. Chem. Soc.* **2014**, *136*, 16096.
(30) Theriot, J. C.; McCarthy, B. G.; Lim, C. H.; Miyake, G. M. *Macromol. Rapid Commun.* **2017**, *38*, 1700040.
(31) Pitre, S. P.; McTiernan, C. D.; Scaiano, J. C. *Acc. Chem. Res.* **2016**, *49*, 1320.
(32) Majek, M.; von Wangelin, A. J. *Acc. Chem. Res.* **2016**, *49*, 2316.
(33) Discekici, E. H.; Anastasaki, A.; de Alaniz, J. R.; Hawker, C. J. *Macromolecules* **2018**, *51*, 7421.
(34) Theriot, J. C.; Lim, C.-H.; Yang, H.; Ryan, M. D.; Musgrave, C. B.; Miyake, G. M. *Science* **2016**, *352*, 1082.
(35) McCarthy, B. G.; Pearson, R. M.; Lim, C.-H.; Sartor, S. M.; Damrauer, N. H.; Miyake, G. M. *J. Am. Chem. Soc.* **2018**, *140*, 5088.
(36) Pearson, R. M.; Lim, C.-H.; McCarthy, B. G.; Musgrave, C. B.; Miyake, G. M. *J. Am. Chem. Soc.* **2016**, *138*, 11399.
(37) Dadashi-Silab, S.; Pan, X.; Matyjaszewski, K. *Chem.—Eur. J.* **2017**, *23*, 5972.
(38) Gong, H.; Zhao, Y.; Shen, X.; Lin, J.; Chen, M. *Angew. Chem., Int. Ed.* **2018**, *57*, 333.
(39) Zhao, Y.; Gong, H.; Jiang, K.; Yan, S.; Lin, J.; Chen, M. *Macromolecules* **2018**, *51*, 938.
(40) Lim, C.-H.; Ryan, M. D.; McCarthy, B. G.; Theriot, J. C.; Sartor, S. M.; Damrauer, N. H.; Musgrave, C. B.; Miyake, G. M. *J. Am. Chem. Soc.* **2017**, *139*, 348.
(41) Ryan, M. D.; Theriot, J. C.; Lim, C.-H.; Yang, H.; Lockwood, A. G.; Garrison, N. G.; Lincoln, S. R.; Musgrave, C. B.; Miyake, G. M. *J. Polym. Sci., Part A: Polym. Chem.* **2017**, *55*, 3017.
(42) Singh, V. K.; Yu, C.; Badgujar, S.; Kim, Y.; Kwon, Y.; Kim, D.; Lee, J.; Akhter, T.; Thangavel, G.; Park, L. S.; Lee, J.; Nandajan, P. C.; Wannemacher, R.; Milian-Medina, B.; Luer, L.; Kim, K. S.; Gierschner, J.; Kwon, M. S. *Nat. Catal.* **2018**, *1*, 794.

(43) Pan, X.; Fang, C.; Fantin, M.; Malhotra, N.; So, W. Y.; Pateanu, L. A.; Isse, A. A.; Gennaro, A.; Liu, P.; Matyjaszewski, K. *J. Am. Chem. Soc.* **2016**, *138*, 2411.
(44) Poelma, S. O.; Burnett, G. L.; Discekici, E. H.; Mattson, K. M.; Treat, N. J.; Luo, Y.; Hudson, Z. M.; Shankel, S. L.; Clark, P. G.; Kramer, J. W.; Hawker, C. J.; de Alaniz, J. R. *J. Org. Chem.* **2016**, *81*, 7155.
(45) Nguyen, T. H.; Nguyen, L.-T. T.; Nguyen, V. Q.; Phan, L. N. T.; Zhang, G.; Yokozawa, T.; Phung, D. T. T.; Nguyen, H. T. *Polym. Chem*. **2018**, *9*, 2484.
(46) Chen, M.; Deng, S.; Gu, Y.; Lin, J.; MacLeod, M. J.; Johnson, J. A. *J. Am. Chem. Soc.* **2017**, *139*, 2257.
(47) Wang, J.; Yuan, L.; Wang, Z.; Rahman, M. A.; Huang, Y.; Zhu, T.; Wang, R.; Cheng, J.; Wang, C.; Chu, F.; Tang, C. *Macromolecules* **2016**, *49*, 7709.
(48) Ramsey, B. L.; Pearson, R. M.; Beck, L. R.; Miyake, G. M. *Macromolecules* **2017**, *50*, 2668.
(49) Pan, X.; Lamson, M.; Yan, J.; Matyjaszewski, K. *ACS Macro Lett.* **2015**, *4*, 192.
(50) Matyjaszewski, K.; Jo, S. M.; Paik, H.; Gaynor, S. G. *Macromolecules* **1997**, *30*, 6398.
(51) Ramakers, G.; Krivcov, A.; Trouillet, V.; Welle, A.; Mobius, H.; Junkers, T. *Macromol. Rapid Commun.* **2017**, *38*, 1700423.
(52) Discekici, E. H.; St. Amant, A. H.; Nguyen, S. N.; Lee, I.-H.; Hawker, C. J.; de Alaniz, J. R. *J. Am. Chem. Soc.* **2018**, *140*, 5009.
(53) Hook, B. D. A.; Dohle, W.; Hirst, P. R.; Pickworth, M.; Berry, M. B.; Booker-Milburn, K. I. *J. Org. Chem.* **2005**, *70*, 7558.
(54) Lu, H.; Schmidt, M. A.; Jensen, K. F. *Lab Chip* **2001**, *1*, 22.
(55) Shanmugam, S.; Xu, J.; Boyer, C. *J. Am. Chem. Soc.* **2015**, *137*, 9174.
(56) Xu, J.; Jung, K.; Boyer, C. *Macromolecules* **2014**, *47*, 4217.
(57) Shanmugam, S.; Xu, J.; Boyer, C. *Macromolecules* **2014**, *47*, 4930.
(58) Xu, J.; Shanmugam, S.; Duong, H. T.; Boyer, C. *Polym. Chem.* **2015**, *6*, 5615.
(59) Chen, M.; MacLeod, M. J.; Johnson, J. A. *ACS Macro Lett.* **2015**, *4*, 566.
(60) Xu, J.; Jung, K.; Atme, A.; Shanmugam, S.; Boyer, C. *J. Am. Chem. Soc.* **2014**, *136*, 5508.
(61) Chen, M.; Gu, Y.; Singh, A.; Zhong, M.; Jordan, A. M.; Biswas, S.; Korley, L. T. J.; Balazs, A. C.; Johnson, J. A. *ACS Cent. Sci.* **2017**, *3*, 124.
(62) Theriot, J. C.; Miyake, G. M.; Boyer, C. A. *ACS Macro. Lett.* **2018**, *7*, 662.
(63) Quirk, R. P.; Lee, B. *Polym. Int.* **1992**, *27*, 359.
(64) Grubbs, R. B.; Grubbs, R. H. *Macromolecules* **2017**, *50*, 6979.
(65) Hawker, C. J.; Wooley, K. L. *Science* **2005**, *309*, 1200.
(66) Kim, Y. A.; Park, G. S.; Son, K. *Polym. Int.* **2018**, *67*, 127.
(67) Tan, S.; Xiong, J.; Zhao, Y.; Liu, J.; Zhang, Z. *J. Mater. Chem. C* **2018**, *6*, 4131.
(68) Buss, B. L.; Beck, L. R.; Miyake, G. M. *Polym. Chem.* **2018**, *9*, 1658.
(69) Xu, Y.; Li, G.; Hu, Y.; Wang, Y. *Macromol. Chem. Phys.* **2018**, *219*, 1800192.
(70) Hu, X.; Zhang, Y.; Cui, G.; Zhu, N.; Guo, K. *Macromol. Rapid Commun.* **2017**, *38*, 1700399.
(71) Tan, S. B.; Zhao, Y. F.; Zhang, W. W.; Gao, P.; Zhu, W. W.; Xhang, Z. C. *Polym. Chem.* **2018**, *9*, 221.
(72) Matyjaszewski, K.; Jakubowski, W.; Min, K.; Tang, W.; Huang, J.; Braunecker, W. A.; Tsarevsky, N. V. *Proc. Natl. Acad. Sci. U. S. A.* **2006**, *103*, 15309.
(73) Jakubowski, W.; Min, K.; Matyjaszewski, K. *Macromolecules* **2006**, *39*, 39.
(74) Konkolewicz, D.; Wang, Y.; Zhong, M.; Krys, P.; Isse, A. A.; Gennaro, A.; Matyjaszewski, K. *Macromolecules* **2013**, *46*, 8749.
(75) Matyjaszewski, K.; Pintauer, T.; Gaynor, S. *Macromolecules* **2000**, *33*, 1476.
(76) Zhang, H.; Abeln, C. H.; Fijten, M. W. M.; Schubert, U. S. *e-Polym.* **2006**, *6*, 90.
(77) Faucher, S.; Okrutny, P.; Zhu, S. *Macromolecules* **2006**, *39*, 3.
(78) Canturk, F.; Karagoz, B.; Bicak, N. *J. Polym. Sci., Part A: Polym. Chem.* **2011**, *49*, 3536.
(79) Yang, L.; Allahyarov, E.; Guan, F.; Zhu, L. *Macromolecules* **2013**, *46*, 9698.
(80) Ranger, M.; Jones, M.-C.; Yessine, M.-A.; Leroux, J.-C. *J. Polym. Sci., Part A: Polym. Chem.* **2001**, *39*, 3861.
(81) Siegwart, D. J.; Oh, J. K.; Matyjaszewski, K. *Prog. Polym. Sci.* **2012**, *37*, 18.
(82) Nikolaou, V.; Anastasaki, A.; Alsubaie, F.; Simula, A.; Fox, D. J.; Haddleton, D. M. *Polym. Chem.* **2015**, *6*, 3581.
(83) Gilman, H.; Shirley, D. A. *J. Am. Chem. Soc.* **1944**, *66*, 888.
(84) Massie, S. P. *Chem. Rev.* **1954**, *54*, 797.
(85) Shirley, D. A.; Lehto, E. A. *J. Am. Chem. Soc.* **1957**, *79*, 3481.
(86) Dietrich, L. E. P.; Teal, T. K.; Price-Whelan, A.; Newman, D. K. *Science* **2008**, *321*, 1203.
(87) Price-Whelan, A.; Dietrich, L. E. P.; Newman, D. K. *Nat. Chem. Biol.* **2006**, *2*, 71.
(88) Palmer, B. D.; Rewcastle, G. W.; Atwell, G. J.; Baguley, B. C.; Denny, W. A. *J. Med. Chem.* **1988**, *31*, 707.
(89) Laursen, J. B.; Nielsen, J. *Chem. Rev.* **2004**, *104*, 1663.
(90) Mavrodi, D. V.; Blankenfeldt, W.; Thomashow, L. S. *Annu. Rev. Phytopathol.* **2006**, *44*, 417.
(91) Barbey, R.; Lavanant, L.; Paripovic, D.; Schüwer, N.; Sugnaux, C.; Tugulu, S.; Klok, H.-A. *Chem. Rev.* **2009**, *109*, 5437.
(92) Discekici, E. H.; Pester, C. W.; Treat, N. J.; Lawrence, J.; Mattson, K. M.; Narupai, B.; Toumayan, E. P.; Luo, Y.; McGrath, A. J.; Clark, P. G.; de Alaniz, J. R.; Hawker, C. J. *ACS Macro Lett.* **2016**, *5*, 258.
(93) Yan, J.; Pan, X.; Wang, Z.; Zhang, J.; Matyjaszewski, K. *Macromol*ecules **2016**, *49*, 9283.
(94) Yan, J.; Pan, X.; Schmitt, M.; Wang, Z.; Bockstaller, M. R.; Matyjaszewski, K. *ACS Macro Lett.* **2016**, *5*, 661.
(95) Wang, X.; You, N.; Lan, F.; Fu, P.; Cui, Z.; Pang, X.; Liu, M.; Zhao, Q. *RSC Adv.* **2017**, *7*, 7789.
(96) Zeng, G.; Liu, M.; Heng, C.; Huang, Q.; Mao, L.; Huang, H.; Hui, J.; Deng, F.; Zhang, X.; Wei, Y. *Appl. Surf. Sci.* **2017**, *399*, 499.
(97) Fantin, M.; Isse, A. A.; Venzo, A.; Gennaro, A.; Matyjaszewski, K. *J. Am. Chem. Soc.* **2016**, *138*, 7216.
(98) Mattson, K. M.; Pester, C. W.; Gutekunst, W. R.; Hsueh, A. T.;

Discekici, E. H.; Luo, Y.; Schmidt, B. V. K. J.; McGrath, A. J.; Clark, P. G.; Hawker, C. J. *Macromolecules* **2016**, *49*, 8162.
(99) Discekici, E. H.; Treat, N. J.; Poelma, S. O.; Mattson, K. M.; Hudson, Z. M.; Luo, Y.; Hawker, C. J.; de Alaniz, J. R. *Chem. Commun.* **2015**, *51*, 11705.
(100) Wang, H.; Jui, N. T. *J. Am. Chem. Soc.* **2018**, *140*, 163.
(101) Du, Y.; Pearson, R. M.; Lim, C.-H.; Sartor, S. M.; Ryan, M. D.; Yang, H.; Damrauer, N. H.; Miyake, G. M. *Chem.—Eur. J.* **2017**, *23*, 10962.
(102) Pham, P. V.; Nagib, D. A.; MacMillan, D. W. C. *Angew. Chem., Int. Ed.* **2011**, *50*, 6119.
(103) Nguyen, J. D.; Tucker, J. W.; Konieczynska, M. D.; Stephenson, C. R. J. *J. Am. Chem. Soc.* **2011**, *133*, 4160.
(104) Iqbal, N.; Choi, S.; Ko, E.; Cho, E. J. *Tetrahedron Lett.* **2012**, *53*, 2005.
(105) Wallentin, C.-J.; Nguyen, J. D.; Finkbeiner, P.; Stephenson, C. R. J. *J. Am. Chem. Soc.* **2012**, *134*, 8875.
(106) Koike, T.; Akita, M. *Top. Catal.* **2014**, *57*, 967.
(107) Oderinde, M. S.; Frenette, M.; Robbins, D. W.; Aquila, B.; Johannes, J. W. *J. Am. Chem. Soc.* **2016**, *138*, 1760.
(108) Tlahuext-Aca, A.; Candish, L.; Garza-Sanchez, R. A.; Glorius, F. *ACS Catal.* **2018**, *8*, 1715.
(109) Petzold, D.; Nitschke, P.; Brandl, F.; Scheidler, V.; Dick, B.; Gschwind, R. M.; König, B. *Chem.—Eur. J.* **2019**, *25*, 361.
(110) Schneider, W.; Diller, W. Phosgene. In *Ullmann's Encyclopedia of Industrial Chemistry,* 5th ed.; Elvers, B., Hawkins, S., Schulz, G., Eds.; VCH: Weinheim, 1991; Vol. A 19, pp 411–420.
(111) Ryan, M. D.; Pearson, R. M.; French, T. A.; Miyake, G. M. *Macromolecules* **2017**, *50*, 4616.
(112) Cotarca, L.; Geller, T.; Répási, J. *Org. Process Res. Dev.* **2017**, *21*, 1439.
(113) Flamigni, L.; Barbieri, A.; Sabatini, C.; Ventura, B.; Barigelletti, F. Photochemistry and Photophysics of Coordination Compounds: Iridium. In *Photochemistry and Photophysics of Coordination Compounds II*; Balzani, V., Campagna, S., Eds.; Topics in Current Chemistry Series, Vol. 281; Springer: Berlin, Heidelberg, 2007; pp 143–203.
(114) King, K. A.; Spellane, P. J.; Watts, R. J. *J. Am. Chem. Soc.* **1985**, *107*, 1431.
(115) Koyama, D.; Dale, H. J. A.; Orr-Ewing, A. J. *J. Am. Chem. Soc.* **2018**, *140*, 1285.
(116) Jockusch, S.; Yagci, Y. *Polym. Chem.* **2016**, *7*, 6039.
(117) Espenson, J. H. *Chemical Kinetics and Reaction Mechanisms*, 2nd ed.; McGraw-Hill Series in Advanced Chemistry; McGraw-Hill: New York, NY, 2002.
(118) Arias-Rotondo, D. M.; McCusker, J. K. *Chem. Soc. Rev.* **2016**, *45*, 5803.
(119) Sartor, S. M.; McCarthy, B. G.; Pearson, R. M.; Miyake, G. M.; Damrauer, N. H. *J. Am. Chem. Soc.* **2018**, *140*, 4778.

Trademarks. DABCO® (Evonik Degussa GmbH).

About the Authors

Daniel A. Corbin received his B.S. degree in chemistry in May of 2017 from James Madison University, where he performed research with Professor Brycelyn Boardman synthesizing and investigating metallopolymers with potential as hybrid photovoltaic materials. In the fall of 2017, he moved to Colorado State University in Fort Collins to pursue a doctoral degree under the direction of Professor Garret Miyake. Currently, his research is focused on developing a better understanding of photocatalysts that are used in the organocatalyzed atom-transfer radical polymerization (O-ATRP) in order to improve their performance and expand the boundaries of O-ATRP.

Chern-Hooi Lim is a postdoctoral researcher in the group of Professor Garret Miyake in the Chemistry Department at Colorado State University. He earned his Ph.D. degree in December of 2015 with Professor Charles Musgrave in the Chemical and Biological Engineering Department at the University of Colorado, Boulder. His research interests include computation-driven design of organic photoredox catalysts, photoredox- and nickel-catalyzed cross-coupling reactions, and mechanistic studies on photoredox-catalyzed reactions.

Garret M. Miyake performed his undergraduate studies at Pacific University and earned his Ph.D. degree from Colorado State University under the direction of Professor Eugene Y.-X. Chen. He was a Camille and Henry Dreyfus Environmental Chemistry Postdoctoral Fellow at the California Institute of Technology with Professor Robert H. Grubbs. The Miyake group's current research interests focus on photoredox catalysis, organocatalyzed atom-transfer radical polymerizations, the synthesis of block copolymers and their self-assembly into photonic crystals, and polymeric composite materials. He has received a Cottrell Scholar Award, a Sloan Research Fellowship, and the 2017 ACS Division of Polymer Chemistry Mark Young Scholar Award.

MERCK

Illuminated synthesis

From discovery to scale-up:
Photoreactors and catalysts to deliver consistency and reproducibility to your research.

Chemists have long struggled with reproducibility in photoredox catalysis. Both varied reaction setups and individual reactions performed with the same setup can be tricky. Our new labware seeks to alleviate these issues by providing photoreactors for each stage of reaction development while ensuring high levels of consistency across reactions and between runs.

When combined with our broad portfolio of iridium and ruthenium catalysts and acridinium-based photocatalysts, these tools free synthetic chemists to focus on their next breakthrough.

To view our complete portfolio offering, visit **SigmaAldrich.com/photocatalysis**

2018-18261 02/2019

Sigma-Aldrich®
Lab & Production Materials

Titanium Salalen Catalysts for the Asymmetric Epoxidation of Terminal (and Other Unactivated) Olefins with Hydrogen Peroxide


Prof. A. Berkessel

Albrecht Berkessel

Department of Chemistry
University of Cologne
Greinstraße 4
50939 Cologne, Germany
Email: berkessel@uni-koeln.de

Keywords. salalen; titanium; asymmetric epoxidation; hydrogen peroxide; catalysis; oxidation; asymmetric synthesis; epoxides; metal catalysis; natural product synthesis.

Abstract. The epoxidation of terminal, unconjugated olefins with high stereoselectivity has been a long-standing problem in asymmetric catalysis. In this review, we describe the development of titanium salalen catalysts which provide a practical solution to this problem. This type of epoxidation catalyst employs aqueous hydrogen peroxide as terminal oxidant, which makes this method even more attractive from a preparative point of view. The best salalen ligands for this purpose are derived from *cis*-DACH as the chiral building block, and the one such ligand incorporating two 3-(pentafluorophenyl)-salicylic aldehyde moieties (**9c**, "Berkessel ligand") currently affords the most effective and selective titanium catalyst in this regard. In addition to several examples of the recent use of titanium salalen epoxidation in natural product synthesis, practical hints for catalyst preparation and application are presented. Structural and mechanistic aspects of titanium salalens are briefly addressed as well.

Outline

1. Introduction

"If carbonyl compounds have been said to be 'virtually the backbone of organic synthesis', the epoxides correspond to at least 'one of the main muscles'."[1] This famous 1983 statement by Dieter Seebach highlights the fundamental importance of epoxides as building blocks in organic synthesis.[2] At that time, the development of methodology for the preparation of enantiomerically pure epoxides had just taken an enormous leap forward with the discovery of the stoichiometric Sharpless epoxidation of allylic alcohols (SE) in 1980.[3] The catalytic SE followed in 1987,[4a] and served as one of the cornerstones for the conferment of the Nobel Prize in chemistry to K. Barry Sharpless in 2001.[4b] In 1990, Jacobsen[5a] and Katsuki[6] reported independently the first efficient, asymmetric epoxidation of unfunctionalized *E* and *Z* alkenes catalyzed by manganese–

salen complexes such as **1** and **2** (**Figure 1**). More recent developments in the field of metal-based catalytic asymmetric epoxidation include iron complexes of N4-tetradentate ligands such as **3**, as reported by Costas;[7] or bishydroxamic acid ligands such as **4** in combination with vanadium, molybdenum, zirconium, or hafnium, as reported by Yamamoto.[8] In the area of organocatalytic epoxidations, numerous chiral ketone catalysts have been developed,[9] as exemplified by the highly practical Shi catalyst, **5**, first disclosed in 1996, and which is based on readily available D-fructose.[9]

Despite the vigorous development of the field of catalytic asymmetric epoxidation over two decades, one class of olefins had remained largely recalcitrant to efficient catalytic asymmetric epoxidation: terminal, unconjugated olefins ("α-olefins").

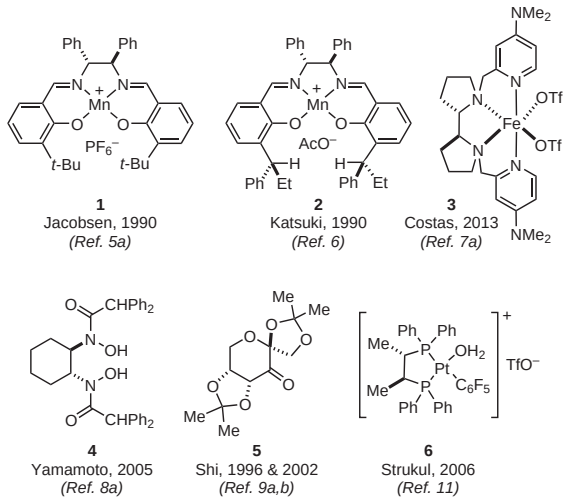

Figure 1. A Selection of Metal Complexes, Ligands, and a Chiral Ketone That Have Been Used in Recent Developments of the Catalytic Asymmetric Epoxidation of Olefins.

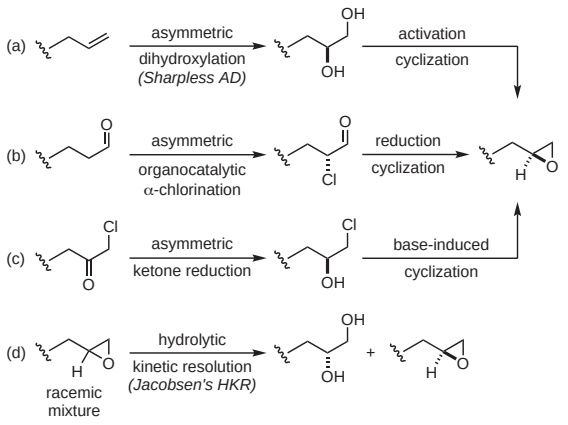

Scheme 1. Examples of Indirect Methods for the Preparation of Enantiopure Terminal Epoxides. *(Ref. 13–16)*

In 2000, Eric N. Jacobsen stated: "Perhaps most significant, no useful methods exist for the direct, enantioselective synthesis of terminal epoxides, arguably the most useful subset of these compounds from a synthetic standpoint."[10] For vinylcyclohexane, an α-branched terminal olefin, Shi reported in 2002 a 71% ee for the corresponding epoxide by utilizing a modified chiral ketone catalyst,[9b] and up to 85% ee was reported by Yamamoto in 2006 by employing a molybdenum catalyst.[8b] For α-unbranched terminal olefins such as 1-octene, only Strukul's pentafluorophenylplatinum epoxidation catalyst **6** (Figure 1) had achieved, in 2006, ca. 80% ee, with good yields, and using hydrogen peroxide as oxidant.[11] With this exception, no preparatively relevant method for the direct (i.e., one-step) catalytic transformation of terminal olefins into highly enantioenriched epoxides existed.[12] As a consequence, several "workarounds" were developed for this class of alkenes (**Scheme 1**).[13–16]

A typical two-step procedure consists of the application of the Sharpless dihydroxylation as the stereoselective step, followed by one of the established 1,2-diol-to-epoxide dehydrations (Scheme 1, Part (a)).[13] Alternatively, instead of α-olefins, aldehydes can be used as starting materials that are subjected to asymmetric organocatalytic α-chlorination, followed by reduction/ring closure (Scheme 1, Part (b)).[14] A related procedure involves the enantioselective reduction of α-haloketones to the alcohols, followed by ring closure (Scheme 1, Part (c)).[15] For terminal epoxides that are available as racemates in larger quantities, Jacobsen's hydrolytic kinetic resolution (HKR) is a frequently applied and highly efficient method for obtaining virtually enantiopure terminal epoxides (Scheme 1, Part (d)).[10,16]

2. Discovery of Titanium Salalen Catalyzed Epoxidation with H_2O_2

The situation changed significantly when, in 2005, Katsuki and co-workers reported their most remarkable discovery, namely that the dimeric titanium di-μ-oxo salalen[17] complex **7** is an efficient catalyst for the asymmetric epoxidation of various types of unactivated olefins—including terminal unconjugated 1-octene.[18] A Meerwein–Ponndorf–Verley reduction of the corresponding salen ligand upon treatment with Ti(O*i*-Pr)$_4$ led to salalen complex **7** (**Scheme 2**, Part (a)).[18] Two years later, Katsuki's group disclosed improved reaction conditions that allow the highly enantioselective epoxidation of various terminal and *(Z)*-1,2-disubstituted olefins (Scheme 2, Part (b)).[19] Besides the high yields and enantiomeric excesses, the use of cheap, readily available and environmentally benign aqueous hydrogen peroxide (typically 30%) as the terminal oxidant is another advantage of this new epoxidation method.[20] On the other hand, its drawback and obstacle to broad application in synthesis is the relatively demanding multistep synthesis of catalyst **7**.

3. Further Development of Titanium Salalen Epoxidation Catalysis

After their seminal discovery in 2005, Katsuki and co-workers mostly focused on titanium salan[17] complexes, which were then

developed within a few years into highly efficient and readily accessible catalysts for the asymmetric epoxidation of *conjugated* olefins with hydrogen peroxide.[21] In contrast, we were mostly interested in the development of practical methodology for the asymmetric epoxidation of *unactivated*, *unconjugated* olefins with hydrogen peroxide, and, therefore, set out to simplify and further improve the original titanium salalen motif. Our earlier work had dealt with the use of salalen complexes for modeling metallo enzymes, and had afforded, inter alia, catalytically active peroxidase models.[22] Methodology for the synthesis of salalen ligands was thus well established in our laboratory, and it was now applied to the titanium systems. In 2007, we presented a series of significantly simplified salalen ligands, derived from *trans*-DACH (DACH = 1,2-diaminocyclohexane).[23] The corresponding titanium complexes have principally the same structure as complex **7**, i.e., they are di-μ-oxo dimers, composed of homochiral halves with cis-β configuration, arranged in the dimer in an anti fashion.[18,19,23] (See also Section 6.) While the epoxidaton of conjugated olefins such as 1,2-dihydronaphthalene or indene proceeded with quite satisfactory yields and enantioselectivities (**eq 1**),[23] the results—in particular the low conversions—for unconjugated olefins were disappointing (1-octene: 6% yield, 60% ee; vinylcyclohexane: 14% yield, 84% ee). We suspected that a competing oxidative catalyst degradation accounted for the low yields when low-reactivity olefin substrates were employed—an assumption that was later corroborated by an in-depth mass spectroscopic study using isotopically labeled ligand **8**.[24]

Our development of simple yet active and selective salalen ligands took a big leap forward in 2013 with the introduction of *cis*-DACH as chiral building block. The *cis*-DACH-derived ligands such as **9a** and **9b** proved highly stable toward oxidative degradation and, for the first time, allowed the efficient and highly enantioselective epoxidation of a variety of unactivated olefins with structurally simple ligands, using hydrogen peroxide as terminal oxidant (**eq 2**).[25,26] Aiming at even higher catalyst stability and activity, we subsequently investigated the effect of introducing fluorine and trifluoromethyl substituents in the salicylic aldehyde moieties of the ligands. This study led to the identification of the current "champion", *cis*-salalen ligand **9c**, which is derived from *cis*-DACH and 3-(pentafluorophenyl)-salicylic aldehyde.[26,27] The corresponding Ti-**9c** complex allowed the highly enantioselective and high-yielding epoxidation of a variety of unactivated olefins.

As a rule of thumb, terminal and *(Z)*-1,2-disubstituted olefins are epoxidized at comparable rates and with high

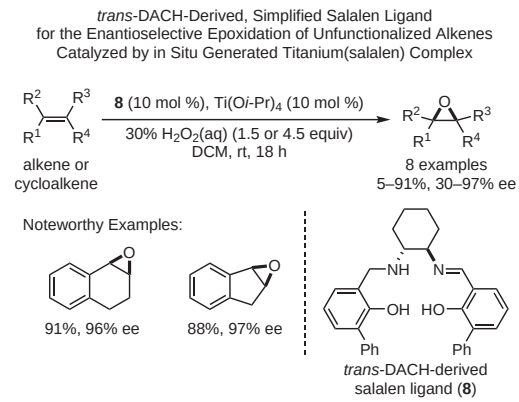

eq 1 *(Ref. 23)*

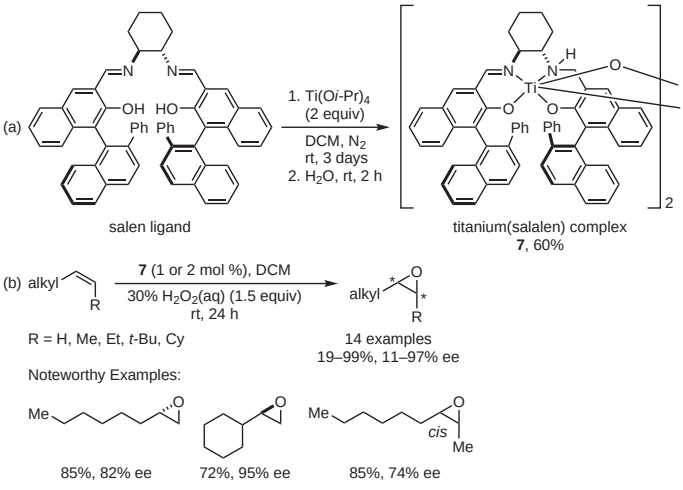

Scheme 2. (a) Last Step in the Preparation of Dimeric Titanium Di-μ-oxo Salalen Catalyst **7**. (b) Asymmetric Epoxidation of Unactivated Terminal and (*Z*)-1,2-Disubstituted Olefins with Hydrogen Peroxide as the Terminal Oxidant. *(Ref. 18,19)*

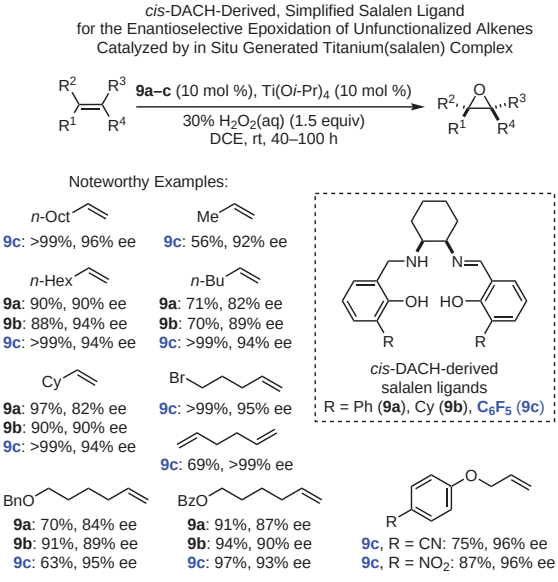

eq 2 *(Ref. 25,26)*

enantioselectivity [typically ee's for terminal olefins > ee's for *(Z)*-1,2-disubstituted ones]. Moreover, *(E)*-1,2-disubstituted substrates are epoxidized more slowly, and with low ee's. 2,2-Disubstituted and trisubstituted olefins are converted at best sluggishly and with low enantioselectivities. This reactivity pattern allows, for example, the selective epoxidation of terminal carbon–carbon double bonds in the presence of trisubstituted ones, as exemplified by substrate **10** (**Figure 2**).[28] The catalyst-induced stereoselectivity overrides the intrinsic diastereoselectivity, as shown for substrate **11**: By choosing the proper catalyst enantiomer, both epoxide diastereomers can be prepared with equal selectivity.[28]

3.1. Additive Effects

In the course of our studies, we noticed that both acidic and basic additives can significantly accelerate the epoxidation.[26] From a broader screening of acids and bases as co-catalysts, pentafluorobenzoic acid, tetra-*n*-butylammonium hydrogensulfate (TBAHS), and 2,6-di-*tert*-butylpyridine emerged as the most beneficial additives. While the transformations listed in eq 2 typically required 40–45 h for completion, the reaction time could be reduced to a more convenient 10 h—with reduction of the catalyst loading to 0.5 mol % and no loss in enantioselectivity—by employing one of these co-catalysts (**eq 3**).[26]

Katsuki's titanium salalen catalyst **7** (Scheme 2) was based on (*S*,*S*)-*trans*-DACH and two (a*R*)-binaphthyl salicylic aldehyde moieties, i.e., a total of three chiral building blocks.[18,19] After our discovery of the beneficial effect of *cis*-DACH, we became also interested in studying the combination of Katsuki's binaphthyl salicylic aldehyde motif with our novel diamine building block, and with the 3-phenyl- and 3-cyclohexylsalicylic aldehydes that had proven effective in our ligands **9a** and **9b**, respectively.[29] The structures of the resulting ligands **12**–**14** are displayed in **Figure 3**, and their corresponding titanium complexes were tested in the asymmetric epoxidation of 1-octene and vinyl cyclohexane.[29] In the series **12a**–**12d** (most closely related to Katsuki's complex **7**), up to 94% ee's were obtained for both olefins (with ligand **12c**), but only low conversions and yields were achieved, even after 100 h of reaction time. With ligands **13a**–**13d**, higher conversions and ee's up to 89% were observed. In contrast, ligands **14a**–**14d** gave high conversions and ee's of up to 94% (ligand **14d**) in relatively short reaction times (30–72 h). We could show that, with ligand **14d**, the epoxidation of 1-octene can even be performed in the absence of solvent and with only 0.5 mol % catalyst loading (72%, 96% ee).[29] With the related ligand **14b**, 78% epoxide yield and 92% ee could be achieved at a catalyst loading as low as 0.1 mol %.[29]

4. Applications of the Titanium Salalen Catalyzed Epoxidation in Natural Product Synthesis

The methodology described herein has recently found application in natural product synthesis. In 2017, Costa, Vilarrasa, and co-workers reported a formal total synthesis of the macrolide amphidinolide E, in which the preparation of building block **15**—that ends up as the C10–C17 motif in amphidinolide E—was based on the twofold application of a titanium salalen

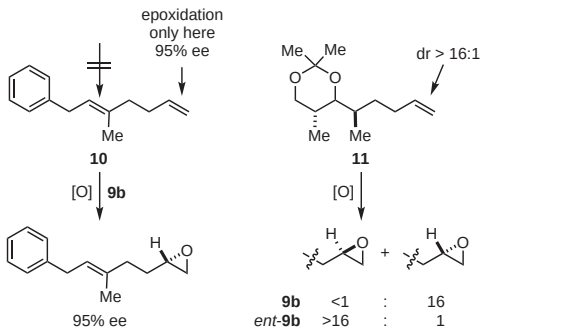

Figure 2. Regio- and Diastereoselective Epoxidations, Exemplified by the Conversion of Olefins **10** and **11**. *(Ref. 28)*

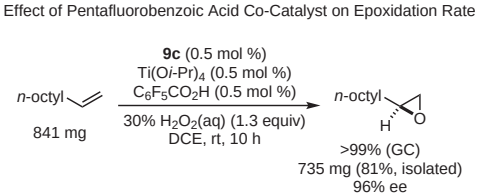

eq 3 *(Ref. 26)*

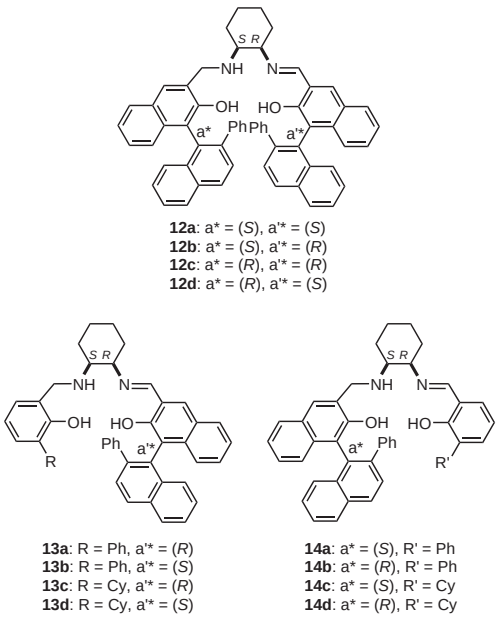

Figure 3. Salalen Ligands Derived from *cis*-DACH and Incorporating Binaphthyl Salicylic Aldehyde Motifs. *(Ref. 29)*

catalyzed asymmetric epoxidation (**Scheme 3**).[30] In the first step, *O*-TBDPS protected 4-penten-1-ol (**16**) was converted into epoxide **17** in 90% yield and 92% ee by using **9b** (see eq 2) as ligand. Epoxide opening with allylGrignard reagent and CuCl gave homoallylic alcohol **18** (88%), which was subjected to epoxidation by employing ligand **14d** (see Figure 3). The resulting hydroxy epoxide **19** isomerized instantaneously to tetrahydrofuran derivative **20**. Swern oxidation of **20** provided the desired building block, **15**.

In 2018, Stadler, Kalesse, and collaborators reported the structure elucidation of the rickiols, novel 20-, 22-, and 24-membered macrolides from the ascomycete *Hypoxylon rickii*, and the total synthesis of 24-membered-ring rickiol E3 (**Scheme 4**).[31] The total synthesis involved early on a titanium salalen catalyzed epoxidation of *O*-benzyl protected 8-nonenol (**21**) to epoxide **22** using ligand **9c** (see eq 2). Linchpin coupling of propylene oxide and epoxide **22** to 2-TBS-1,3-dithiane led to intermediate **23**, which was converted into the "southern fragment" (**24**) of rickiol E3. In this regard, a comparison was made with "workaround d" (see Scheme 1, Part (d)), i.e., the nonstereoselective epoxidation of starting olefin **21** with mCPBA followed by Jacobsen's HKR. In this two-step approach, epoxide **22** was obtained in lower yield (42%) but with virtually identical ee (95%).[31]

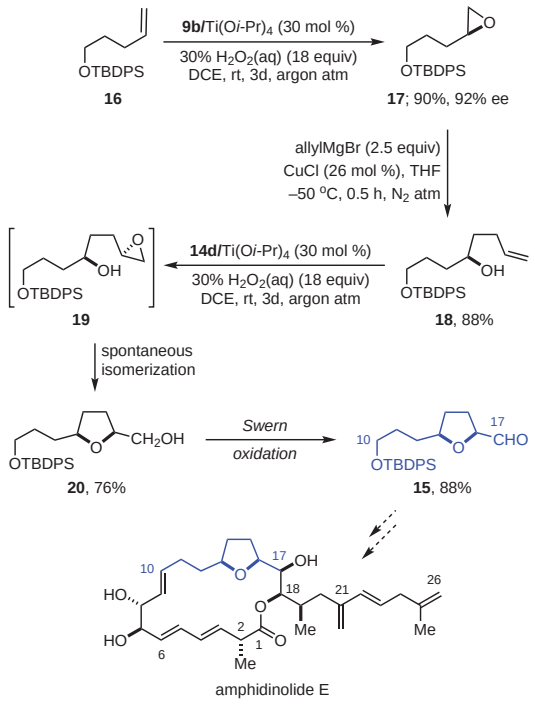

Scheme 3. Formal Total Synthesis of Amphidinolide E by Costa and Vilarrasa Involving Two Titanium Salalen Catalyzed Epoxidations Leading to Key Intermediate **15**. *(Ref. 30)*

5. Accessing the Salalen Ligands, the Titanium Salalen Catalysts, and the Related Epoxidation

5.1. Salalen Ligands Based on *trans*-DACH

Salalen ligands derived from *trans*-DACH (**25**) have routinely been synthesized in our laboratory by a versatile and practical two-step procedure (**Scheme 5**).[23,24] The first step consists of reductive N-monoalkylation of the diamine, **25**, with a salicylic aldehyde, **26**, in the presence of $NaBH_3CN$ or $NaBH_4$. The monoalkylated product is then condensed with a second

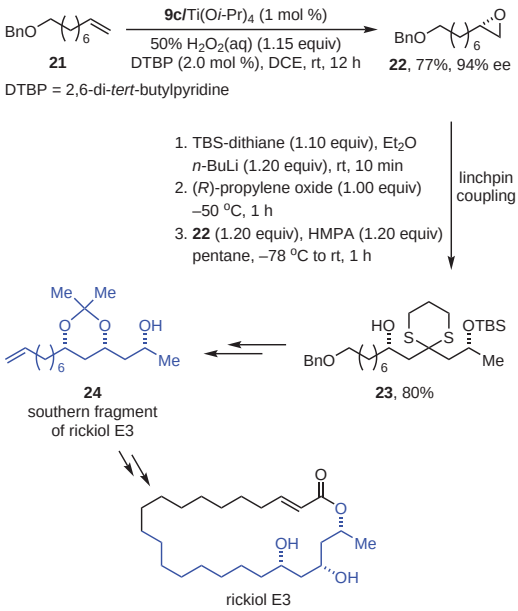

Scheme 4. The Titanium Salalen Catalyzed Epoxidation as the First Step in Stadler and Kalesse's Total Synthesis of Rickiol E3. *(Ref. 31)*

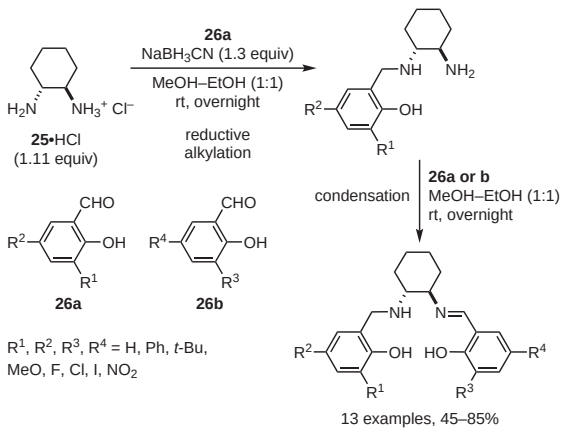

Scheme 5. Synthesis of Salalen Ligands Derived from *trans*-DACH. *(Ref. 23,24)*

equivalent of salicylic aldehyde (same or different) to generate the salalen ligand. Typically, it was sufficient to employ the mono-HCl salt of *trans*-DACH (**25**•HCl) to achieve exclusive monoalkylation of the diamine component.[23,24]

5.2. Salalen Ligands Based on *cis*-DACH

We had reported in 2010 that *cis*-DACH can be desymmetrized in an operationally simple fashion by enantiotopos-differentiating mono-*N*-Alloc protection using diallyl carbonate as the acylating agent in the presence of commercially available *Candida antarctica* lipase B (CAL-B, **Scheme 6**).[32] With enantiopure mono-Alloc *cis*-DACH (**27**) in hand, both enantiomers of the salalen ligands derived from *cis*-DACH were easily prepared, as shown in Scheme 6 for **9c** and its enantiomer *ent*-**9c**.[25,26] Typically, *cis*-DACH salalen ligands such as **9c** are obtained, after a final recrystallization from methanol or ethanol, as analytically pure yellow crystalline materials.

5.3. Titanium Salalen Catalysts

Mixing the salalen ligands derived from either *trans*- or *cis*-DACH with equimolar amounts of Ti(O*i*-Pr)$_4$ in a solvent such as dichloromethane (DCM) and exposing the mixture to traces of moisture (e.g., by simply opening the flask or using nonanhydrous DCM) result in complete conversion into the dimeric di-μ-oxo titanium complexes (**Scheme 7**). The procedure can be run in air, and no inert atmosphere is required. Simple evaporation of the solvent in vacuo is typically sufficient to induce crystallization, whereupon the catalytically active titanium complexes can be collected by filtration in air. A final recrystallization from methanol or ethanol affords analytically pure dimeric di-μ-oxo titanium complexes. These crystalline, yellow to orange materials such as the Berkessel-Katsuki catalyst (**31**) are bench-stable catalysts, and can be stored under air and at room temperature in brown glass containers indefinitely.

As an alternative to the isolation and use of the di-μ-oxo dimers, we have established the so-called "in situ/vac" procedure, for the in situ preparation of the active titanium complexes. For this purpose, equimolar amounts of the ligand and Ti(O*i*-Pr)$_4$ are dissolved in dichloromethane and exposed to traces of water, as described in the preceding paragraph. The solvent is then removed completely, and the remaining yellow to orange solid is dried thoroughly under reduced pressure at room temperature. This "vac" step ensures removal of the isopropyl alcohol byproduct, for which we had earlier observed an inhibitory effect on the subsequent epoxidation reaction.[25] After drying, the solid complex is taken up in the solvent of

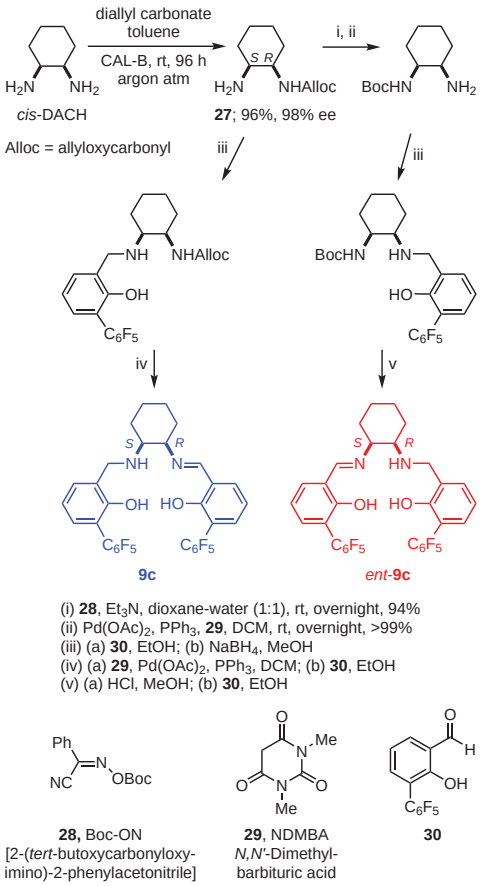

Scheme 6. Synthesis of Both Enantiomers of the Salalen Ligand **9c** from *cis*-DACH. *(Ref. 25,26,32)*

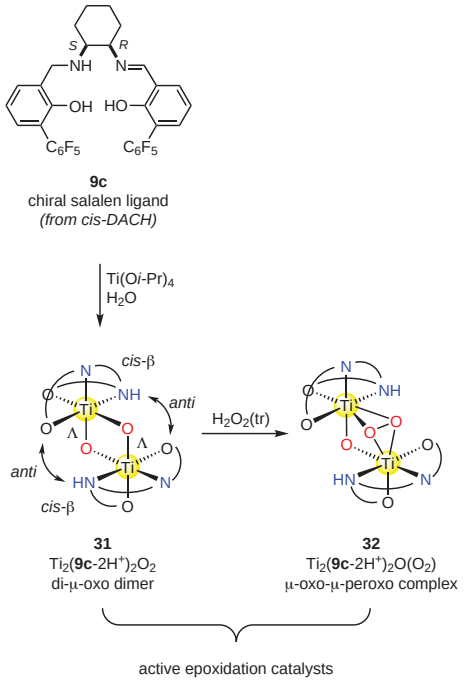

Scheme 7. Self-assembly of the Titanium Di-μ-oxo Dimer **31** and Its Further Conversion into the μ-Oxo-μ-peroxo Dimer **32**. *(Ref. 23,25,26,29)*

choice for the epoxidation. In our hands, the "in situ/vac" generated catalysts performed epoxidations in a manner that was equivalent to that of the "isolated" catalysts.

5.4. Practical Considerations for the Titanium Salalen Catalyzed Epoxidations

Due to the better solubility of hydrogen peroxide in them, dichloromethane and in particular 1,2-dichloroethane have typically been employed as solvents for the epoxidations, while acetonitrile and ethyl acetate are viable alternatives. The epoxidations are started by addition of aqueous hydrogen peroxide, typically in one portion, to the solution of catalyst and olefin (and additive if required) in the solvent of choice. In a typical experiment, a 4–6 M solution of the olefin in 0.3–0.5 mL of solvent is prepared and 0.5 mol % of the catalytically active dimer is added. Under "in situ/vac" conditions, the latter is first prepared from 1 mol % each of the ligand and Ti(O*i*-Pr)$_4$. Typically, 1.3–1.5 equivalents of 30% or 50% aqueous H_2O_2 are used, with the latter concentration typically providing higher reaction rates. Vigorous stirring is recommended to ensure efficient mixing of the (typically) biphasic reaction mixture. No inert atmosphere is required, and the epoxidations are typically run at room temperature. Note, however, that increasing the reaction temperature above rt may well have a beneficial effect on *both* rate *and* enantioselectivity. Once reaction monitoring indicates completion, the reaction mixture is passed through a short bed of anhydrous $MgSO_4$–MnO_2 (10:1) mixture, to remove water and to disproportionate excess H_2O_2. The filtrate can then be worked up further in the usual way, ideally by distillation, and workup by column chromatography is possible as well. Under these conditions, the catalyst could be recovered intact in many instances, albeit in the form of the μ-oxo-μ-peroxo dimer. The latter are catalytically just as active as the di-μ-oxo dimers, bench stable, and can therefore be re-used without loss of activity. In our hands, 3–4 runs with the recycled catalyst were possible without significant loss of activity.

As mentioned in Section 3 and eq 3, co-catalysts such as pentafluorobenzoic acid, tetra-*n*-butylammonium hydrogen-sulfate (TBAHS), or 2,6-di-*tert*-butylpyridine (typically employed at the same loading as the catalyst) significantly accelerate the epoxidation.[26] While typical reaction times in the absence of additives are on the order of 40 h at rt (vide supra for temperature effects), the additives allow reduction of the reaction time to ca. 10 h and simultaneous reduction of the catalyst loading by 50%. When exploring epoxidation conditions for a new alkene substrate, testing of the acid/base additives mentioned is strongly recommended.

6. Structural and Mechanistic Aspects of Titanium Salalen Catalysts

All of the salalen ligands investigated by us (trans and cis) coordinate to the titanium ion in a pseudo-octahedral *cis*-β fashion (Scheme 7).[23,25,26,29] The sense of chirality at the metal center is dictated by the ligand: For example, the sense of chirality at the metal center is Λ in the complex with enantiomeric ligand **9c**. This astonishing act of molecular self-assembly is completed by *anti*-selective dimerization of the complex to the di-μ-oxo dimer (e.g., **31**). Upon exposure to hydrogen peroxide, even in very low concentrations, the di-μ-oxo dimer is converted into the μ-oxo-μ-peroxo complex (e.g., **32**) (Scheme 7).[26]

While the μ-oxo-μ-peroxo complex **32** itself does not transfer oxygen to olefins, salalen dimers **31** and **32** show virtually the same activity under the catalytic epoxidation conditions, i.e., in the presence of aqueous hydrogen peroxide. This behavior is in line with earlier observations by Katsuki and co-workers on a titanium di-μ-oxo and μ-oxo-μ-peroxo pair derived from a *salan* ligand,[21c] and we share Katsuki's conclusion that the μ-oxo-μ-peroxo complex serves as a reservoir species that needs to be activated further for oxygen transfer to occur.[21c] The mechanistic details of this activation process for *cis*-DACH derived titanium salalen complexes are currently under investigation in our laboratory.[33]

7. Conclusion

For the synthetic organic chemist, titanium salalen catalysts efficiently close a gap in synthetic methodology, namely the one-step, high-yield, and highly enantioselective epoxidation of unactivated olefins—in particular, terminal, unconjugated ones. As an additional benefit, this type of epoxidation uses aqueous hydrogen peroxide, a readily available, safe, and environmentally benign terminal oxidant. Reported first in 2005 for *trans*-DACH derived complexes by Katsuki and co-workers,[18] our research efforts have since furnished the novel class of *cis*-DACH derived salalen ligands, in particular bis(pentafluorophenyl)salalen ligand **9c**, which exhibits outstanding stability, catalytic activity, and stereoselectivity.

8. References and Notes

(1) Seebach, D.; Weidmann, B.; Wilder, L. In *Modern Synthetic Methods: Transition Metals in Organic Synthesis*; Scheffold, R., Ed.; Otto Salle Verlag: Frankfurt, 1983; Vol. 3, p 324.

(2) (a) Berkessel, A.; Engler, H.; Leuther, T. M. Epoxidation of Alkenes. In *Science of Synthesis: Catalytic Oxidation in Organic Synthesis*; Muñiz, K., Ed.; Thieme: Stuttgart, 2018; Chapter 5, Section 5.1, pp 245–307. (b) Vilotijevic, I.; Jamison, T. F. *Angew. Chem., Int. Ed.* **2009**, *48*, 5250. (c) He, J.; Ling, J.; Chiu, P. *Chem. Rev.* **2014**, *114*, 8037.

(3) Katsuki, T.; Sharpless, K. B. *J. Am. Chem. Soc.* **1980**, *102*, 5974.

(4) (a) Gao, Y.; Hanson, R. M.; Klunder, J. M.; Ko, S. Y.; Masamune, H.; Sharpless, K. B. *J. Am. Chem. Soc.* **1987**, *109*, 5765. (b) The Nobel Prize in Chemistry 2001: William S. Knowles, Ryoji Noyori, and K. Barry Sharpless; NobelPrize.org; Nobel Media AB 2018; https://www.nobelprize.org/prizes/chemistry/2001/press-release/ (accessed Dec 11, 2018).

(5) (a) Zhang, W.; Loebach, J. L.; Wilson, S. R.; Jacobsen, E. N. *J. Am. Chem. Soc.* **1990**, *112*, 2801. (b) For the 1,2-diaminocyclohexane-derived catalyst, see Jacobsen, E. N.; Zhang, W.; Muci, A. R.; Ecker, J. R.; Deng, L. *J. Am. Chem. Soc.* **1991**, *113*, 7063.

(6) Irie, R.; Noda, K.; Ito, Y.; Matsumoto, N.; Katsuki, T. *Tetrahedron Lett.* **1990**, *31*, 7345.

(7) (a) Cussó, O.; Garcia-Bosch, I.; Ribas, X.; Lloret-Fillol, J.; Costas, M. *J. Am. Chem. Soc.* **2013**, *135*, 14871. (b) Olivo, G.; Cussó, O.; Borrell, M.; Costas, M. *J. Biol. Inorg. Chem.* **2017**, *22*, 425.

(8) (a) Zhang, W.; Basak, A.; Kosugi, Y.; Hoshino, Y.; Yamamoto, H. *Angew. Chem., Int. Ed.* **2005**, *44*, 4389. (b) Barlan, A. U.; Basak, A.; Yamamoto, H. *Angew. Chem., Int. Ed.* **2006**, *45*, 5849. (c) Zhang, W.; Yamamoto, H. *J. Am. Chem. Soc.* **2007**, *129*, 286. (d) Li, Z.; Yamamoto, H. *Acc. Chem. Res.* **2013**, *46*, 506.

(9) (a) Tu, Y.; Wang, Z.-X.; Shi, Y. *J. Am. Chem. Soc.* **1996**, *118*, 9806. (b) Tian, H.; She, X.; Yu, H.; Shu, L.; Shi, Y. *J. Org. Chem.* **2002**, *67*, 2435. (c) Shi, Y. *Acc. Chem. Res.* **2004**, *37*, 488.

(10) Jacobsen, E. N. *Acc. Chem. Res.* **2000**, *33*, 421.

(11) Colladon, M.; Scarso, A.; Sgarbossa, P.; Michelin, R. A.; Strukul, A. *J. Am. Chem. Soc.* **2006**, *128*, 14006.

(12) Another exception may be seen in the application of mono-oxygenases and peroxidases: Bühler, B.; Bühler, K.; Hollmann, F. Oxyfunctionalization of C–C Multiple Bonds. In *Enzyme Catalysis in Organic Synthesis*, 3rd ed.; Drauz, K., Gröger, H., May, O., Eds.; Wiley-VCH: Weinheim, 2012; Volume 3, Part VII, Chapter 31, pp 1269–1324.

(13) Kolb, H. C.; Sharpless, K. B. *Tetrahedron* **1992**, *48*, 10515.

(14) (a) Winter, P.; Swatschek, J.; Willot, M.; Radtke, L.; Olbrisch, T.; Schäfer, A.; Christmann, M. *Chem. Commun.* **2011**, *47*, 12200. (b) Halland, N.; Braunton, A.; Bachmann, S.; Marigo, M.; Jørgensen, K. A. *J. Am. Chem. Soc.* **2004**, *126*, 4790. (c) Brochu, M. P.; Brown, S. P.; MacMillan, D. W. C. *J. Am. Chem. Soc.* **2004**, *126*, 4108.

(15) Berkessel, A.; Rollmann, C.; Chamouleau, F.; Labs, S.; May, O.; Gröger, H. *Adv. Synth. Catal.* **2007**, *349*, 2697.

(16) (a) Tokunaga, M.; Larrow, J. F.; Kakiuchi, F.; Jacobsen, E. N. *Science* **1997**, *277*, 936. (b) Schaus, S. E.; Brandes, B. D.; Larrow, J. F.; Tokunaga, M.; Hansen, K. B.; Gould, A. E.; Furrow, M. E.; Jacobsen, E. N. *J. Am. Chem. Soc.* **2002**, *124*, 1307.

(17) In salalen ligands, one C=N double bond of the salen motif is reduced to a C–N single bond. In salan ligands, both C=N double bonds are reduced to C–N single bonds.

(18) Matsumoto, K.; Sawada, Y.; Saito, B.; Sakai, K.; Katsuki, T. *Angew. Chem., Int. Ed.* **2005**, *44*, 4935.

(19) Sawada, Y.; Matsumoto, K.; Katsuki, T. *Angew. Chem., Int. Ed.* **2007**, *46*, 4559.

(20) (a) Bryliakov, K. P. *Chem. Rev.* **2017**, *117*, 11406. (b) Wang, C.; Yamamoto, H. *Chem.—Asian J.* **2015**, *10*, 2056.

(21) (a) Sawada, Y.; Matsumoto, K.; Kondo, S.; Watanabe, H.; Ozawa, T.; Suzuki, K.; Saito, B.; Katsuki, T. *Angew. Chem., Int. Ed.* **2006**, *45*, 3478. (b) Shimada, Y.; Kondo, S.; Ohara, Y.; Matsumoto, K.; Katsuki, T. *Synlett* **2007**, 2445. (c) Kondo, S.; Saruhashi, K.; Seki, K.; Matsubara, K.; Miyaji, K.; Kubo, T.; Matsumoto, K.; Katsuki, T. *Angew. Chem., Int. Ed.* **2008**, *47*, 10195. (d) Matsumoto, K.; Sawada, Y.; Katsuki, T. *Pure Appl. Chem.* **2008**, *80*, 1071.

(22) (a) Berkessel, A.; Bats, J. W.; Schwarz, C. *Angew. Chem., Int. Ed. Engl.* **1990**, *29*, 106. (b) Schwenkreis, T.; Berkessel, A. *Tetrahedron Lett.* **1993**, *34*, 4785. (c) Berkessel, A.; Bolte, M.; Griesinger, C.; Huttner, G.; Neumann, T.; Schiemenz, B.; Schwalbe, H.; Schwenkreis, T. *Angew. Chem., Int. Ed. Engl.* **1993**, *32*, 1777. (d) Berkessel, A.; Bolte, M.; Schwenkreis, T. *Chem. Commun.* **1995**, 535. (e) Berkessel, A.; Frauenkron, M.; Schwenkreis, T.; Steinmetz, A.; Baum, G.; Fenske, D. *J. Mol. Catal. A: Chem.* **1996**, *113*, 321. (f) Berkessel, A.; Frauenkron, M.; Schwenkreis, T.; Steinmetz, A. *J. Mol. Catal. A: Chem.* **1997**, *117*, 339.

(23) Berkessel, A.; Brandenburg, M.; Leitterstorf, E.; Frey, J.; Lex, J.; Schäfer, M. *Adv. Synth. Catal.* **2007**, *349*, 2385.

(24) Berkessel, A.; Brandenburg, M.; Schäfer, M. *Adv. Synth. Catal.* **2008**, *350*, 1287.

(25) Berkessel, A.; Günther, T.; Wang, Q.; Neudörfl, J.-M. *Angew. Chem., Int. Ed.* **2013**, *52*, 8467.

(26) Lansing, M.; Engler, H.; Leuther, T. M.; Neudörfl, J.-M.; Berkessel, A. *ChemCatChem* **2016**, *8*, 3706.

(27) Note that the trans diastereomer of ligand **9c** is less effective/selective: with 1-octene as substrate, 74% of the epoxide was obtained with 84% ee (reference 26). As documented in references 23 and 25, we have also discovered ligand substitution patterns that render the corresponding titanium complexes catalytically inactive. These findings are mechanistically revealing, but are not discussed in this review.

(28) Lansing, M.; Krüger, S.; Berkessel, A.; Christmann, M. Cologne University, Cologne, Germany, and The Free University of Berlin, Berlin, Germany. Unpublished work, 2018.

(29) Wang, Q.; Neudörfl, J.-M.; Berkessel, A. *Chem.—Eur. J.* **2015**, *21*, 247.

(30) Bosch, L.; Mola, L.; Petit, E.; Saladrigas, M.; Esteban, J.; Costa, A. M.; Vilarrasa, J. *J. Org. Chem.* **2017**, *82*, 11021.

(31) Surup, F.; Kuhnert, E.; Böhm, A.; Pendzialek, T.; Solga, D.; Wiebach, V.; Engler, H.; Berkessel, A.; Stadler, M.; Kalesse, M. *Chem.—Eur. J.* **2018**, *24*, 2200.

(32) Berkessel, A.; Ong, M.-C.; Nachi, M.; Neudörfl, J.-M. *ChemCatChem* **2010**, *2*, 1215.

(33) For a mechanistic study on titanium catalysts based on *trans*-DACH-derived ligands, see Talsi, E. P.; Rybalova, T. V.; Bryliakov, K. P. *J. Mol. Catal. A: Chem.* **2016**, *421*, 131.

About the Author

Albrecht Berkessel was born in 1955 in Saarlouis, and obtained his Diploma in 1982 at the University of Saarbrücken. For his Ph.D. studies, he moved to the laboratory of Professor Waldemar Adam at the University of Würzburg. In 1985, he obtained his Ph.D. degree (*summa cum laude*) for mechanistic studies on the photochemistry of divinyl ethers. The same year, he joined the research group of Professor Ronald Breslow at Columbia University, New York, as a Lynen Fellow (Alexander von Humboldt Foundation) to work on functionalized cyclodextrins as enzyme models and on the mechanism of biotin action. In 1986, he returned to Germany to start independent research on the mechanisms of nickel enzymes from methanogenic archaea. His "Habilitation" at the Goethe University of Frankfurt/Main, in association with Professor Gerhard Quinkert, was completed in 1990, and he was then appointed "Privatdozent". In 1992, he

became Associate Professor at the University of Heidelberg. Since 1997, he has been Full Professor of Organic Chemistry at the University of Cologne. His current research interests center around mechanistic and preparative aspects of metal-based catalysis, organocatalysis, biocatalysis, and biological/medicinal chemistry.

Professor Berkessel has held visiting professorships at the University of Wisconsin, Madison; the Research School of Chemistry of the Australian National University, Canberra; the National University of Singapore; Chuo University, Tokyo; and, recently, a Distinguished Visiting Professorship at Kyoto University, Japan. His awards include the Young Faculty Award of the Fonds der Chemischen Industrie, and the Award in Chemistry of the Göttingen Academy of Sciences. Professor Berkessel is the recipient of the Horst-Pracejus-Preis 2019 of the German Chemical Society. He has published more than 200 research papers and is one of the two authors of the Wiley-VCH bestseller *Asymmetric Organocatalysis* (2005).

MERCK

Turn research into reality

Your Trusted Partner for Bench to Bulk Chemicals

Whether you work in academia, pharmaceuticals or diagnostics, we are here with support and solutions for **every stage of product development**.

From research reagents to production materials, each of our chemicals comes with a **guarantee of quality, reliability and timely delivery, so your breakthroughs feel closer than ever.**

We manufacture our products in state-of-the-art facilities, monitor all processes and suppliers to ensure excellent quality, and offer more validation data than any other brand.

Discover more benefits from bench to bulk:
SigmaAldrich.com/bulk

The life science business of Merck operates as MilliporeSigma in the U.S. and Canada.

Sigma-Aldrich®
Lab & Production Materials

Page intentially blank

Page intentially blank

VOLUME 52, NO. 2 | **2019**

MERCK

ALDRICHIMICA ACTA

Accelerating the Discovery of Next-Generation Small-Molecule Protein Degraders

Coumarin-Based Hybrids as Fluorescent Probes for Highly Selective Chemosensing and Biological Target Imaging

DEAR READER:

Over the past few months, alarmist headlines such as **"Chinese Scientist Claims to Use CRISPR to Make First Genetically Edited Babies[1]"** and **"Is the CRISPR baby controversy the start of a terrifying new chapter in gene editing?[2]"** have appeared with some frequency in mainstream media worldwide.

As scientists, researchers, and innovators of gene-editing technology, we have a responsibility to seek out the best minds in bioethics to educate us, guide us and help us navigate this uncharted territory.

This is why Merck KGaA, Darmstadt, Germany established a **Bioethics Advisory Panel,** which includes leading external experts representing law, ethics, medicine and science from the US, Europe, Africa and Asia. The panel meets annually to explore, discuss and provide a wider worldview of the impact of our technologies, research and therapies on human health, agriculture and even all living beings. Thus far, with the panel's help, we have published clear guidelines for our business on fertility treatments, stem cell research, clinical trials and off-label use, among other important topics.

Most recently, in collaboration with our Gene Editing & Novel Modalities team, the panel provided a clear statement of our **position** on gene editing. This led to a published paper, **Ethical Considerations in the Manufacture, Sale and Distribution of Genome Editing Technologies,** in *The American Journal of Bioethics.*

As we continue to explore and innovate in this exciting area of science, we will continue to ask the tough questions and seek the answers necessary to advance gene-editing ethically and responsibly for our customers and mankind.

[1] *The New York Times,* Nov. 26, 2018
[2] Vox, Jan. 22, 2019

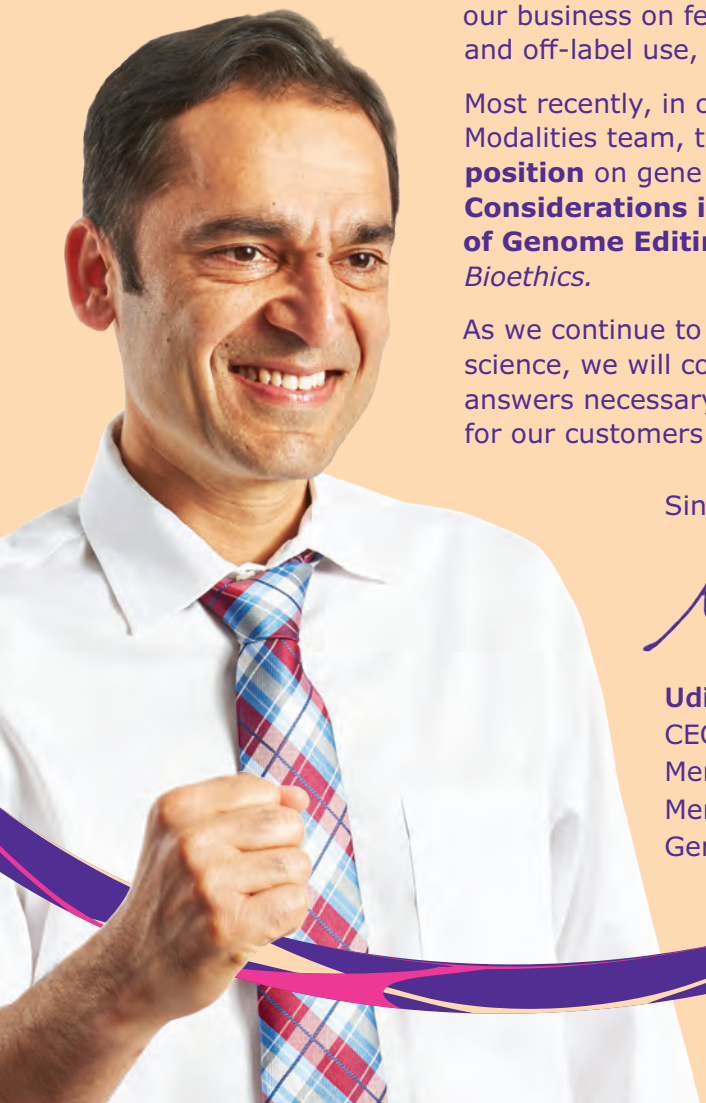

Sincerely yours,

Udit Batra, Ph.D.
CEO, Life Science
Member of the Executive Board,
Merck KGaA, Darmstadt,
Germany

ALDRICHIMICA ACTA
VOL. 52, NO. 2 • 2019

Merck KGaA
Frankfurter Strasse 250
64293 Darmstadt, Germany
Phone +49 6151 72 0

To Place Orders / Customer Service
Contact your local office or visit
SigmaAldrich.com/order

Technical Service
Contact your local office or visit
SigmaAldrich.com/techinfo

General Correspondence
Editor: Sharbil J. Firsan, Ph.D.
Sharbil.Firsan@milliporesigma.com

Subscriptions
Request your FREE subscription to the *Aldrichimica Acta* at **SigmaAldrich.com/acta**

The entire *Aldrichimica Acta* archive is available at **SigmaAldrich.com/acta**

Aldrichimica Acta (ISSN 0002-5100) is a publication of Merck KGaA.

"PLEASE BOTHER US."

Dear Fellow Chemists,

Professor Tomislav Rovis of the Department of Chemistry at Columbia University kindly suggested that we offer dichlorobis(tricyclohexylphosphine)cobalt(II) (**904104**), which, in combination with the photocatalyst $(Ir[dF(CF_3)ppy]_2(dtbpy))PF_6$ (**747793**), enables the facile formation of arenes at room temperature by a spatially and temporally resolved [2 + 2 + 2] alkyne cycloaddition using visible light as an external stimulus.

(1) Ruhl, K. E.; Rovis, T. *J. Am. Chem. Soc.* **2016**, *138*, 15527. (2) Ravetz, B. D.; Ruhl, K. E.; Rovis, T. *ACS Catal.* **2018**, *8*, 5323. (3) Ravetz, B. D.; Wang, J. Y.; Ruhl, K. E.; Rovis, T. *ACS Catal.* **2019**, *9*, 200.

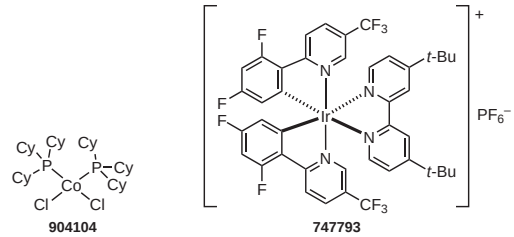

904104 **747793**

904104	Dichlorobis(tricyclohexylphosphine)cobalt(II)	250 mg 100 mg
747793	$(Ir[dF(CF_3)ppy]_2(dtbpy))PF_6$	100 mg 1 g

We welcome your product ideas. Do you need a product that is not featured on our website? Ask us! For more than 60 years, your research needs and suggestions have shaped our product offering. Email your suggestion to **techserv@sial.com**.

Udit Batra, Ph.D.
CEO, Life Science

TABLE OF CONTENTS

ABOUT OUR COVER

The Square of Saint Mark's, Venice (oil on canvas, 114.6 x 153 cm) was painted in 1742/1744 by the renowned Venetian cityscape painter Giovanni Antonio Canal (1697–1768), better known as Canaletto. He apprenticed with his father and brother, painting scenes for the theater and, except for a decade-long stay in England, Canaletto spent all his life in Venice.

In his mid-twenties, Canaletto shifted to painting detailed and accurate scenes of daily life in his native Venice for foreign visitors (mainly English) as mementos of their visit. As a result, Canaletto became widely known and appreciated outside Italy, particularly in England, where many collectors of his paintings lived. While Canaletto also created compositions of scenes in Rome and London, and produced a number of fine etchings, he is best-known for his "vedute" of Venice and surrounding area.*

Detail from ***The Square of Saint Mark's, Venice***. Photo courtesy National Gallery of Art, Washington, DC.

Canaletto's almost photographic rendering of the scene in this painting—with his meticulous depiction of the architecture, light effects, sky and clouds, and realistic colors—beautifully captures the atmosphere and vitality of the square and brings it to life. Were it not for the clothes, hats and sailing ships, one could mistake this scene as one happening now in Venice. Canaletto achieved considerable fame during his lifetime and influenced later generations of landscape artists in England and elsewhere. Of his many pupils, the best-known is his nephew, the accomplished landscape painter Bernardo Belloto.*

A gift of Mrs. Barbara Hutton, National Gallery of Art, Washington, DC.

* *To find out more about Canaletto, his many paintings of Venetian scenes, and his influence, visit* ***SigmaAldrich.com/Acta***

DESIGN THE PERFECT PROTAC

Partial PROTACs are the easiest way to generate libraries of PROTACs that can be screened for effective degradation of your target from cells.

What will be your perfect combination?

See our growing collection at **SigmaAldrich.com/ TargetDegradation**

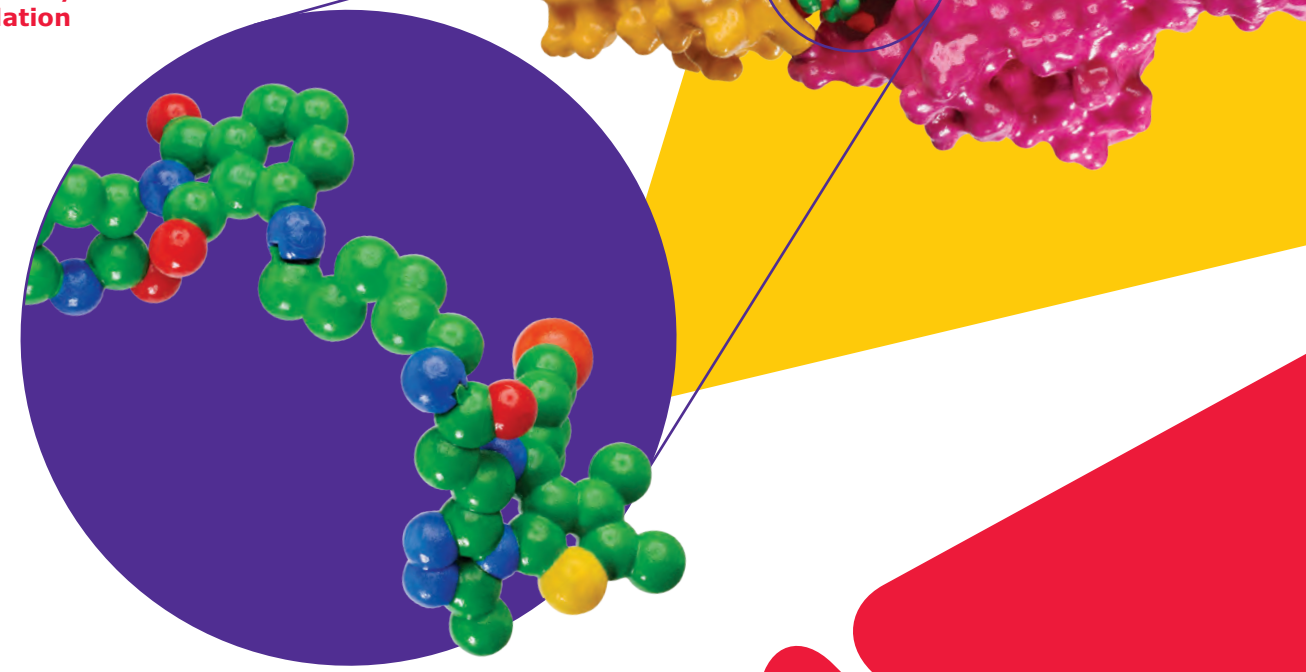

The life science business of Merck operates as MilliporeSigma in the U.S. and Canada.

Sigma-Aldrich®
Lab & Production Materials

Accelerating the Discovery of Next-Generation Small-Molecule Protein Degraders


Dr. S. Schlesiger


Dr. M. Toure


Dr. K. E. Wilke


Dr. B. R. Huck

Sarah Schlesiger,[*,a] Momar Toure,[*,b] Kaelyn E. Wilke,[c] and Bayard R. Huck[b]

[a] Department of Medicinal Chemistry, Merck KGaA, Frankfurter Strasse 250, 64293 Darmstadt, Germany
Email: Sarah.Schlesiger@merckgroup.com
[b] EMD Serono R&D Institute, Inc., 45A Middlesex Turnpike, Billerica, MA 01821, USA
Email: Momar.Toure@emdserono.com
[c] Chemical Synthesis Department, MilliporeSigma, 6000 N. Teutonia Avenue, Milwaukee, WI 53209, USA

Keywords. proteolysis-targeting chimera; degronimid; degron; protein degraders; PROTAC; Partial PROTAC; SNIPER; drug discovery; undruggables.

Abstract. Currently, many pharma and biotech companies as well as academic laboratories are developing PROTAC programs to investigate whether induced protein degradation offers new insights into a protein's pharmacological utility and new treatment opportunities for their high-value therapeutic targets. Within this review, we aim to explain the complexities and empiricism inherent in designing proteolysis-targeting chimeras, which result in the synthesis of compound libraries for the discovery of lead molecules with degrader potential. Due to typically limited resources in exploratory projects or concept space, this required synthesis of large compound libraries to fully explore PROTAC options is a high barrier to overcome. Thus, we also comment on how to strategically choose which molecules to synthesize and how the use of commercial building blocks can accelerate the discovery of degraders. Additionally, we describe the available assays for profiling PROTACs.

Outline

1. Introduction

In the last decade, the development of **pro**teolysis-**ta**rgeting **c**himeras (PROTACs) has emerged as a new therapeutic modality.[1–3] PROTAC compounds are small, hetero-bifunctional molecules that target proteins for degradation by recruiting an E3 ligase in the vicinity of the protein of interest (POI). This proximity enables E3 ligase-mediated ubiquitination of the target protein followed by consecutive recognition and degradation by the proteasome. In this way, the PROTAC hijacks the native cellular degradation mechanism to selectively remove the POI from the cell (**Figure 1**, Part (a)).[4] As a result,

PROTAC technology has a great potential as a new therapeutic approach for the treatment of cancer and other protein-related diseases, for which traditional drug discovery has not led to effective treatments. It is estimated that only a small portion (~10%) of the human proteome is accessible with contemporary inhibitor-based, small-molecule drug programs,[5,6] and targeted protein degradation has the potential to significantly expand the modern medicinal chemistry druggable space.

The limitations of small-molecule, inhibitor-based pharmacology have strongly motivated the development and use of genetic techniques to successfully remove or decrease the expression of disease-causing proteins within the cell (Figure 1, Part (b)). RNAi,[7,8] antisense oligonucleotides,[9,10] and more recently CRISPR[11–13] can be used "on demand" to control protein levels. These genetic strategies, however, suffer from several limitations[14–17]—including the need for genetic manipulation, off-target issues, lack of cell permeability, and poor pharmacokinetics—thus making the translation of these technologies to the clinic highly challenging. Fortunately, PROTAC-mediated targeted protein degradation can overcome these challenges.[18–23] A PROTAC molecule transiently interacts with a POI and E3 ligase prior to POI ubiquitination and degradation by the 26S proteasome, but the PROTAC is not degraded alongside the POI. Consequently, this degradation approach to drug discovery and development differs in two key ways from inhibitor-based pharmacology: (i) The cell needs to resynthesize the POI after treatment before protein function is restored, and (ii) in contrast to the "one drug, one target" model of inhibitor-based pharmacology, a PROTAC compound can be catalytic, with one degrader molecule transiently binding and removing multiple POIs. Thus, this approach offers several advantages over the traditional drug paradigm: (a) Abrogation of protein function can be accomplished at lower drug concentrations due to the catalytic nature of the PROTAC. (b) Modulation of the POI function can be achieved with less exposure time of the drug due to POI removal. (c) Difficult-to-drug targets—such as transcription factors, regulatory/scaffolding proteins, and non-enzymatic proteins—can be targeted since binding at any protein surface is all that is required for modulation. (d) Additional feedback loops or significant scaffolding roles perpetuated by inhibitor-occupied proteins would be lost upon degradation (similarly to genetic knockdowns). (e) Finally, resistance by gene overamplification can be overcome once again due to the catalytic nature of the PROTAC agent.

ARV-110, an oral androgen receptor (AR) degrader, entered clinical trials in the first quarter of 2019 for the treatment of patients with metastatic, castration-resistant prostate cancer (mCRPC), and could demonstrate the technology's therapeutic potential. Nonetheless, this novel technology has proven to be a valuable tool to study target engagement and validation. Moreover, since its discovery, many proteins—ranging from kinases to signaling proteins, cytosolic proteins, and membrane receptors—have been knocked out by degraders.

1.1. State of the Art in Protein Degradation

Almost 20 years ago, Sakamoto et al. reported that an IκBα phosphopeptide inhibitor conjugated with ovalicin was able to recruit the E3 ligase $SCF^{\beta\text{-}TRCP}$ and successfully induce the degradation of the target protein methionine aminopeptidase-2 (MetAP-2).[4b] While being the first PROTAC proof of concept, the peptide ligand used lacked cell permeability, which limited its therapeutic utility. The groups of Crews, Deshaies, and Kim followed this seminal study with extensive research on next-generation PROTAC degraders that possess better physicochemical properties.[24–28] This effort led to the first cell-permeable PROTAC that targets

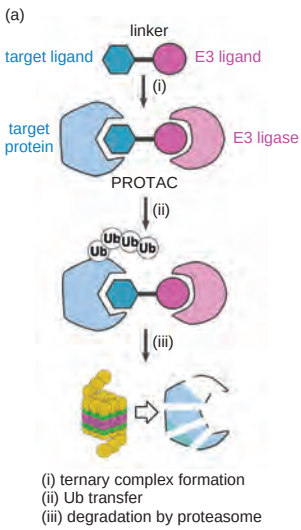

(b)

Abnormal Protein Function	Small-Molecule Inhibitor-Based Pharmacology	Genetic Approaches to Controlling Protein Levels	Small-Molecule Targeted Protein Degradation
Dosage Control	++++	+	+++
Effect on Abundance	—	++++	++++
Reversibility	++++	+	+++
Kinetic Control	++++	+	+++
Selectivity	++++	+++	++++
Permeability	++++	—	++
Target Scope	+	++++	++++

Figure 1. (a) Mechanism of Targeted Protein Degradation Mediated by PROTAC. (b) Comparison of Protein-Centric Drug Discovery Strategies (Small-Molecule Inhibitor-Based Pharmacology, Genetic Approaches to Control Protein Levels, and Small-Molecule Targeted Protein Degradation). *(Ref. 4)*

androgen and estrogen receptors, then the first in vivo PROTAC proof of principle, and ultimately to the future development of all small-molecule degraders.[29]

Despite the impressive progress made beginning with the seminal, impermeable peptidic PROTAC to the subsequent demonstration of phosphoPROTAC-induced targeted protein degradation in vivo, the development of small-molecule degraders remained very limited. This was due to the unavailability of effective small-molecule E3 ligase ligands. The only known example was the nutlin/AR ligand that was reported by Crews and co-workers in 2008 for MDM2-mediated degradation of AR in prostate tumor cells (**Figure 2**).[30] Unfortunately, however, the nutlin/AR PROTAC was less effective than the early peptidic degrader. Two years later, Hashimoto's research team found that bestatin esters can effectively recruit the E3 ligase cIAP1 and successfully knockdown both target proteins and cIAP1 itself through autoubiquitination and degradation, resulting in cell toxicity.[31] To address this challenge and develop small-molecule PROTAC hybrids with desirable physicochemical properties along with better potency, the laboratory of Crews designed and developed small-molecule ligands that potently bind to the primary HIF-binding site on the von Hippel–Lindau (VHL) E3 ubiquitin ligase.[32,33] This ligand was further optimized by Ciulli's group to afford a series of potent VHL ligands.[34,35] Other studies have revealed that thalidomide and its derivatives, lenalidomide and pomalidomide, bind to the E3 ligase complex cereblon (CRBN) and induce proteasomal degradation of the transcription factors Ikaros (IKZF1) and Aiolos (IKZF3)—that being the mechanism of action of these important immunomodulator drugs in multiple myeloma.[36–39] The availability of these ligands (**Figure 3**) for both VHL and CRBN E3 ligases accelerated the discovery—independently, by the research groups of Crews[18], Ciulli,[20] and Bradner[21]—of multiple small-molecule PROTACs, including degraders that target members of the BET family, BRD4/3/2. For example, ARV-825 was found to induce nearly complete degradation of BRD4 at 10 nM.[18] Bradner's team went further and showed that small-molecule PROTAC degraders are effective in vivo.[21] In fact, 50 mg/kg (ip, qd) dBET1 treatment of a mouse model led to an impressive lymphoma tumor regression in 14 days. Interesting additional evidence of PROTAC-induced degradation was revealed with the hook effect, which describes the loss of efficacy at increasing PROTAC concentrations. Further insight about the PROTAC mechanism was gained when Ciulli's group solved the first co-crystal structure of a VHL PROTAC, MZ1, interacting with both the target protein BRD4 and the E3 ubiquitin ligase VHL at their interface.[40] This interaction between target, E3 ligase, and PROTAC is called the "ternary complex." Notably, the protein–protein interaction created by this ternary complex illustrates the complexity of designing a PROTAC. The role of the ternary complex formation and the importance of that protein–protein interaction were investigated by Calabrese

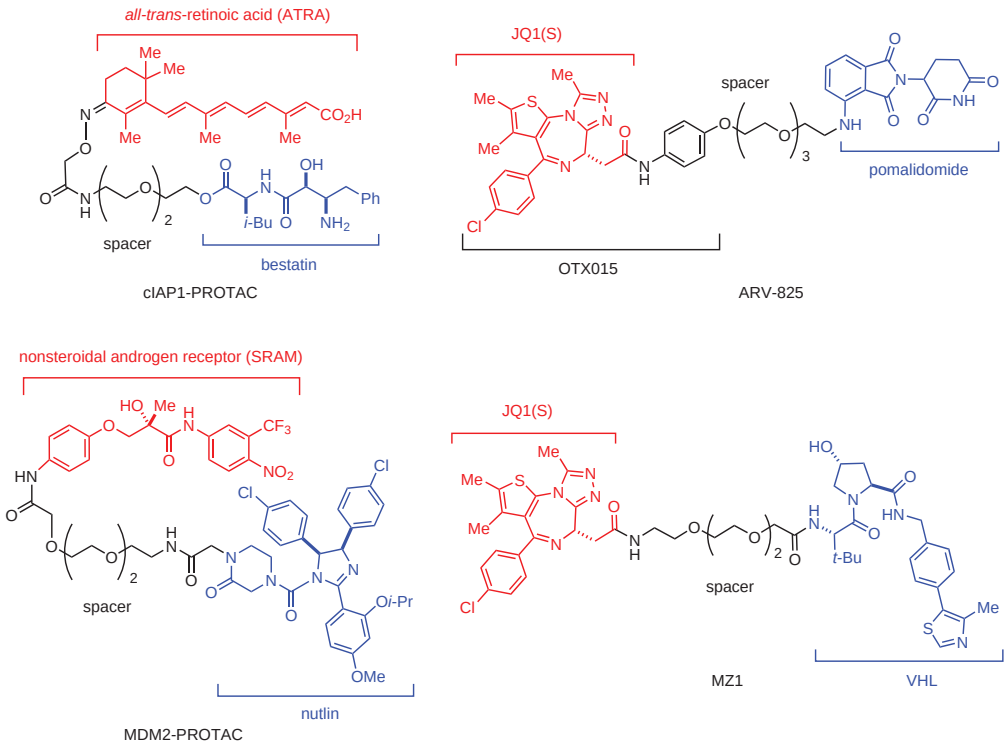

Figure 2. Structures of Selected PROTACs Derived from Popular E3 Ligase Ligands. *(Ref. 18,20,21,30–40,47)*

and co-workers.[41] By developing PROTACs that target BTK, these authors found that the ability of a PROTAC to induce a stable ternary complex is necessary for degradation, but cooperativity was not a key factor. In contrast, thermodynamic entropy/enthalpy was found to be crucial in terms of degradation efficacy. Taken together, the ability of a given PROTAC to form a stable ternary complex might govern potency and selectivity. This hypothesis is in accord with recent work by Crews's group who found that a foretenib-based PROTAC that weakly binds to protein p38α (K_D ~ 11 μM) was able to efficiently degrade p38α with a half maximal degradatory concentration (D_{max}) of 210 nM.[42] This very surprising finding of increased potency could raise questions of potential unexpected off-target degradation. Interestingly, Winter's and Bradner's groups reported that MI-389, a sunitinib-based PROTAC, failed to induce degradation of consensus targets including cKIT plus 40 other kinases.[43] Despite lack of target degradation, an off-target was identified. Comparative profiling via quantitative mass spectrometry of untreated proteomes and those treated with MI-389 demonstrated the sole degradation of the translation termination factor GSPT1 among 6490 proteins quantified, highlighting the power of quantitative proteomics to investigate off-target effects due to unintended E3 ligase modulation. Another very promising characteristic of PROTACs is the fact that they may provide unexpected selectivity. Many such examples are described in the kinase field, where PROTAC derivates of very promiscuous kinase inhibitors such as TL12-186[44] and foretinib[43] yielded more selective kinase degraders. For instance, the promiscuous diaminopyrimidine-based inhibitor TL12-186 binds over 100 known kinases; however, the PROTAC derivate of TL12-186 degraded only 28 kinases. This additional layer of selectivity can be rationalized by the requirement to produce a stable and productive ternary complex for the degradation to happen.[45] More recently, the promiscuous FLT-3 inhibitor quizartinib was conjugated with a VHL ligand, producing a more selective degrader. Additionally, FLT-3 PROTAC had acceptable pharmacokinetics (PK) with half maximal inhibitory concentration (IC_{50}) coverage after 20 hours (10 mg/kg, ip). A further pharmacodynamics (PD) study showed that PROTAC FLT-3 could induce the degradation of FLT-3 in vivo with a 30 mg/kg treatment (ip, qd).[46]

1.2. Recent Progress in the PROTAC Field

A better understanding of the mechanism of action of PROTACs, along with more widely available E3 ligase ligands, accelerated the early proof of concept to a currently viable therapeutic approach with these molecules. Several therapeutically relevant proteins have been successfully degraded this way, either partially or near completely, and most of this work has been extensively reviewed.[47] Notably, a successful use of an MDM2 E3 ligase recruiting PROTAC with dual function (degrader/inhibitor) has been reported.[48] Nutlin-based PROTAC A1874 was able to degrade BRD4 and thus suppress oncogenic protein Myc expression by 85% relative to control. In addition, since nutlin itself is an MDM2 inhibitor, PROTAC A1874 also upregulated p53 via MDM2 inhibition. Furthermore, the loss of cell viability, when

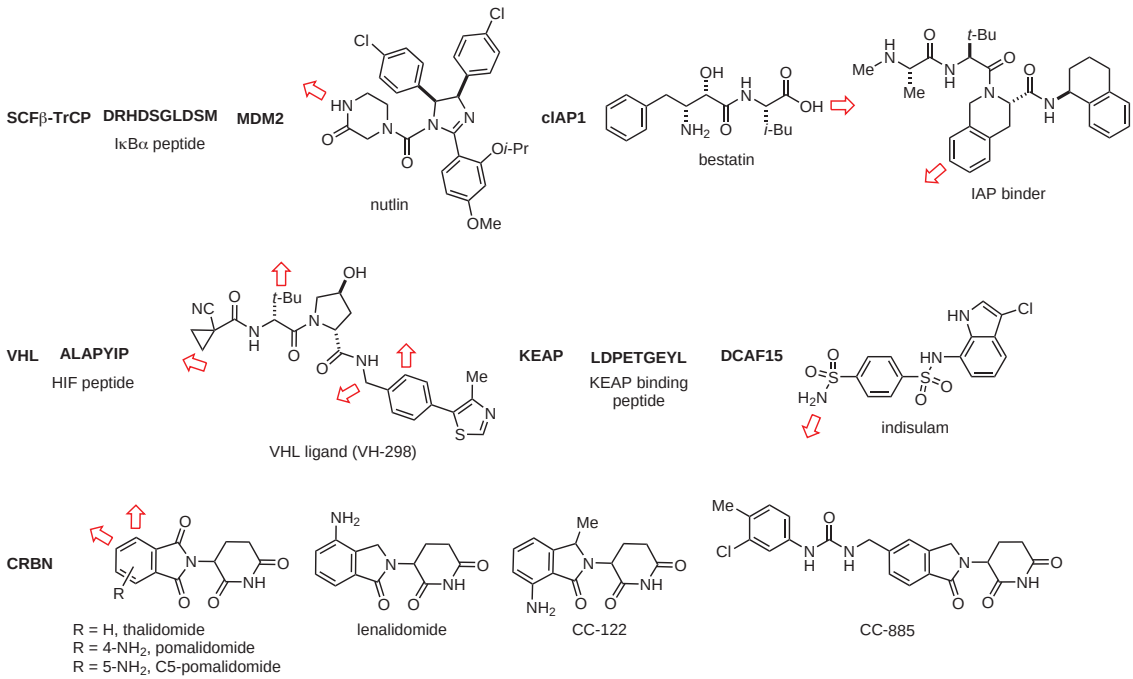

Figure 3. Applied E3 Ligases, Their Binders, and Their Exit Vectors.

different cell lines were treated with A1874, was confirmed to be superior to the sum of the effects of the MDM2 inhibitor idasanutlin alone and JQ1 alone.[48] Given the important roles of Myc and p53 in cancer (tumor suppressor regulation, DNA repair, cell cycle arrest, and apoptosis), this successful PROTAC with a dual function could offer more robust therapeutic effects. Very recently, PROTAC technology has been established as a valuable tool for intracellular target engagement validation in the absence of downstream molecular pharmacodynamic biomarkers in the case of the protein pirin.[49] The authors found that, not only did a pirin ligand based PROTAC degrade the target protein, it also competed with the original ligand to bind to pirin when co-incubated. Similarly, PROTACs were employed as potent and selective tools to study BCL6 biology. Scientists from AstraZeneca found, however, that neither BCL6 inhibitors nor BCL6 degraders could produce the expected phenotypic response when applied in DLBCL, therefore highlighting the challenges associated with small-molecule targeting of BCL6.[50] Targeted protein degradation was elegantly used to address the kinase-independent functions of Focal adhesion kinase (Fak), a protein possessing simultaneous kinase and scaffolding roles for several signaling proteins.[51] In this effort, a defactinib derivative linked to a VHL ligand yielded PROTAC-3, a highly selective, low nanomolar-potency Fak degrader with a DC_{50} value of 3.0 nM as well as an excellent D_{max} of 99%. In addition, PROTAC-3 is five times more selective than the clinical candidate defactinib (Verastem VS-6063) since it binds only 20 kinases at 1 μM. In a direct comparison between PROTAC-3 and defactinib, the authors found that PROTAC-3 outperformed defactinib in reducing Fak downstream target paxillin. Treatment with 50 nM of PROTAC-3 caused over 85% reduction of p-paxillin levels. In comparison, defactinib reduced p-paxillin levels by only 62% at 10 μM. In addition, 50 nM PROTAC-3 treatment was found to impair cell migration and reduce cell wound healing by 53%. As expected, the Fak scaffolding role was overcome by targeting Fak for degradation with PROTAC, while the inhibitor failed. More recently, the oncogenic translation initiation factor protein eIF4E was targeted with a PROTAC. Through an impressive synthetic route, the authors generated a series of GMP lenalidomide-based PROTACs.[52] Unfortunately, these molecules were not able to induce eIF4E proteasomal degradation. Whether this result is due to lack of cell permeability or available lysine for the ubiquitination step remains to be determined.

The first degrader targeting poly(ADP-ribose) polymerase-1 (PARP1), which plays crucial roles in DNA-damage signaling, was successfully developed by Rao's group.[53] Niraparib conjugated to a nutlin derivative yielded a degrader that led to selective and significant reduction in PARP1 levels enough to induce an enhanced apoptotic response in the MDA-MB-231 breast cancer cell line, resulting in the observed caspase-3 cleavage. A control experiment confirmed this hypothesis since niraparib or nutlin-3 alone and in combination failed to cause any detectable caspase-3 cleavage. In a recent study, Focal adhesion tyrosine kinase (PTK2) was degraded by hijacking E3 ligases. Scientists at Boehringer Ingelheim found that even though a series of PROTACs potently and selectively caused PTK2 degradation with an average DC_{50} in the low nanomolar range, these molecules failed to affect proliferation of the tested cell lines in comparison to the PTK2 inhibitor BI-4464 alone.[54] This data suggests that PTK2 might not possess significant scaffolding roles or that its scaffolding function is not required for in vitro cell proliferation. A group of scientists from the University of Calgary reported that the "undruggable" antiapoptotic protein myeloid cell leukemia 1 (MCL1) could also be targeted for PROTAC-mediated degradation.[55] MCL1 is an ideal PROTAC target because it plays a role in complex protein–protein interactions (that promote cell survival) involving the pro-apoptotic factors Bim, Bak, and Bax. MCL1 inhibitor A-1210477 was coupled with thalidomide analogues for CRBN recruitment. After an extensive study with docking and linker exit vector variation, optimized PROTAC dMCL1-2 caused MCL1 reduction at 500 nM in HeLa cells. MCL1 degradation resulted in apoptosis at 250 and 500 nM after 24 hours of treatment, as revealed by Caspase-3 cleavage.[55] Since MCL1 possesses a rapid turnover rate, the authors confirmed that the observed MCL1 level reduction was indeed caused by PROTAC-mediated proteasomal degradation.[55] This innovative work once again highlights the potential of the PROTAC approach as an alternative way to target the so-called "undruggable" proteins. Another property underscoring the novelty of PROTACs is their catalytic, event-driven mechanism. The impact of the catalytic effect on PROTAC degradation profile was investigated by scientists from GSK.[56] From two PROTAC derivatives of ibrutinib/IAP ligand (covalent PROTAC 2) and a reversible BTK inhibitor/IAP ligand (PROTAC 3), the authors found that treatment of THP-1 cells with the covalent PROTAC 2 did not cause any BTK degradation despite confirmed target engagement, and inhibited BTK activity merely to the same extent as non-PROTAC covalent modification of recombinant BTK in vitro. In contrast, reversible PROTAC 3 caused near-complete BTK level reduction with a DC_{50} of 200 nM. Additional investigation with another covalent PROTAC (PROTAC 4) that recruits the E3 ligase CRBN produced a similar degradation profile, thus confirming this finding. Interestingly, covalent PROTAC 4 caused degradation of the Src family kinases CSK and LYN. This is expected since it binds reversibly to these proteins lacking the conserved cysteine present in the BTK kinase domain. Together, these results demonstrate the critical effect of catalysis on PROTAC-induced targeted protein degradation, as well as on an enhanced selectivity profile when converting an inhibitor to a degrader. Using information from high-resolution crystal structures of palbociclib, ribociclib, and abemaciclib with CDK6, researchers at the Dana-Farber Cancer Institute designed a series of PROTACs that degrade both cyclin-dependent kinases 4 and 6 (CDK4/6) or selectively reduce either CDK4 or CDK6 levels.[57] As previously observed, the selected inhibitor, linker length, and linker composition influenced the degradation activity and selectivity. Among these PROTACs, BSJ-02-162 (palbociclib-based) potently degraded CDK4, CDK6, IKZF1, and IKZF3. BSJ-02-162 exhibited an enhanced anti-proliferation effect in MCL cell lines in comparison to BSJ-

03-204 (also palbociclib-based), which only degrades CDK4/6 or the warhead ligands. Independently, Zhao and Burgess reported dual degradation of CDK4/6, resulting in reduced levels of phosphorylated retinoblastoma protein (Rb) and cell cycle arrest, with PROTAC recruiting CRBN.[58]

Since its discovery, impressive progress has been made in advancing the PROTAC technology from an in vitro proof of concept to the first in vivo mice model validation. However, whether the preclinical efficacy of PROTAC drugs will translate into human therapy in the clinic remains to be determined. To assess the potential preclinical efficacy of this class of molecules, a recent study evaluated the ability of PROTACs to induce protein depletion in large animals such as non-human primates (Bama pigs and rhesus monkeys).[59a] A series of PROTACs targeting CRBN and FKBP12 via pomalidomide and rapamycin were synthesized. Among those compounds, RC32 caused FKBP12 degradation with subnanomolar DC_{50} after 12 h in cells. This potent FKBP12 degradation was observed in different cell lines from different species. Further investigation revealed that RC32 treatment of mice twice a day (30 mg/kg, ip) caused complete knockdown of FKBP12 in different organs. The lack of FKBP12 degradation observed in the mice brain was attributed to the inability of RC32 to cross the blood-brain barrier. This finding is not surprising given the physicochemical properties of PROTAC molecules, which often possess a very high surface polar area. The ability of RC32 to induce FKBP12 degradation was further validated in the rhesus monkey model species that is closely related to humans. RC32 caused nearly complete degradation of FKBP12 in different rhesus monkey organs. Moreover, functional heart studies of the monkeys after RC32 administration (8 mg/kg, ip, twice a day) led to reduced ejection fraction (6.7% diminution at day 15) and fractional shortening (13.4% reduction at day 15) in accordance with the reduced systolic blood pressure found in RC32-treated monkeys. This effect was found to be reversible after withdrawal of the treatment. Taken in its entirety, this work demonstrated that PROTACs can indeed produce targeted protein degradation in species closely related to humans, thus strongly demonstrating their clinical potential.[59a] The U.S. Food and Drug Administration (FDA) has recently cleared Arvinas's investigational new drug application (IND) for their oral PROTAC degrader ARV-110 against metastatic castration-resistant prostate cancer (mCRPC).[59b] Thus, this entire research field is eager to learn how PROTACs will behave in these first clinical trials (**Table 1**).[60−104]

1.3. Linkers and Exit Vectors

PROTACs have two recognition elements (heads), one of them specific to the protein of interest and the other to an E3 ligase, and these two heads are separated by a linker. The nature and size of the linker plays an important role in determining the right distance and appropriate physicochemical properties of the entire molecule.[105] The linkers should be long enough to prevent steric clashes between the two proteins. However, if they get too long, the systems would suffer from solubility and physicochemical issues as well as linker folding. The importance of the length and nature of the linker was previously highlighted by the selective degradation of BRD4 over BRD2/BRD3—all members of the BET family of proteins—with a warhead that has nearly equivalent binding to several other BRD subtypes such as BRD2/3/4.[20] Independently, Nowak et al. reported a similar finding, namely that ternary complex conformations are governed by linker length and composition, therefore affecting the degradation selectivity of target proteins.[106] These observations, were further validated by Crews and co-workers who targeted for degradation with a PROTAC a family member of the human epidermal growth factor receptor protein.[82] Using the ligand lapatinib and recruiting the same E3 ligase VHL, but using two different linkers, PROTAC1, with a shorter linker length, efficiently degraded both EGFR *and* HER2, while PROTAC 5, with a longer linker, selectively degraded EGFR over HER2.[82] Thus, varying PROTAC linkers can offer an extra layer of selectivity.

Very recently, Wang's research group reported that the linker could be manipulated to increase solubility and modulate the physicochemical proprieties of the final PROTAC compound, leading to more potent degraders.[66,83] In a recent study, the position of the exit vector was also found to play a critical role in the degradation profile. Using the same BTK-binding ligand, same linker length, and recruiting the same E3 ligase but with different exit vectors, PROTAC MT-797, with attachment points at position 4 of the CRBN ligand pomalidomide, was not able to induce any BTK degradation, while MT-802 was found to be highly potent with D_{max} of 99% at 250 nM along with an impressive DC_{50} of 9.1 nM.[77] Crews and collaborators reported on their progress in compound design and target selection, leading to the preparation of fewer yet more effective molecules, across different classes of proteins.[92] For example, using the same VHL E3-ligase ligand and same p38 ligand (foretinib), but varying the exit vector and/or the linker length, they were able to selectively degrade isoenzymes p38α or p38δ. SJF-8240, having a 12-atom linker, was more selective for p38α (DC_{50} of 7.16 ± 1.03 nM and D_{max} of 97.4%), whereas it had only a D_{max} of 18% and DC_{50} of 299 nM for p38δ. Moreover, it was not able to degrade isoforms β and γ of p38. In contrast, SJFδ, with a shorter linker (10 atoms) and a different VHL ligand, successfully degraded p38δ with a D_{max} of 99.41 ± 3.31% and DC_{50} of 46.17 ± 9.85 nM, but could not degrade the α, β, or γ isoforms of p38. This impressive enzyme isoform degradation selectivity is driven by differential target presentation, leading to one productive ternary complex that is dependent on the exit vector selected and the linker length. Collectively, these studies have demonstrated that linkers and exit vectors can affect the physicochemical properties, selectivity, and even degradation profiles of PROTACs.

2. PROTAC Library Design

After more than 15 years of research, PROTAC design remains a highly complex and mostly empirical task. At present, discovery is centered around known ligands that are utilized as the

handle to recruit the target protein. These ligands are usually well-characterized inhibitors with known structure–activity relationships and/or crystal structures, which helps to identify suitable attachment points for linkers and provides rational starting points for exit vectors. It is important to note that the chosen ligand can severely impact the degradation potential of the PROTAC itself. One study showed that bosutinib- and dasatinib-based PROTACs[22] exhibit different ABL degradation profiles despite possessing similar binding modes and exit vectors. In the case where one has several chemical series to choose the target ligand from, one should be aware that these subtle changes influence the degradation profile. Usually, only few ligands are of interest either due to their physicochemical properties or ADME profile. If possible, one should choose a ligand that has no liabilities here since they could make the optimization of the corresponding PROTAC very challenging.

Table 1. Cellular Protein Degraders

Protein Target	Target Class	Compound	Reference
ABL, BCR-ABL	Tyr Kinase	DAS-6-2-2-6-CRBN	22
Akt	Ser/Thr kinase	Tri_a-PROTAC	60
ALK	Tyr Kinase	TL13-112, MS-4077, MS-4078, TD-004	61–63
α-synuclein	brain protein	TAT-βsynCTM	64
AR	nuclear receptor	IκBα-DHT PROTAC, PROTAC 5, PROTAC A, SARM nutlin, ARCC-4, ARD-69, Compound 42a, SARD279, SNIPER 11	24, 25, 28, 30, 65–69
ARH	transcription factor	Apigenin PROTAC	70
BCL6	transcription factor	Compound 15	50
BET (BRD2, BRD3, BRD4)	bromodomain	ARV-825, MZ1, dBET1, ARV-771, BETd-260/ZBC260, QCA570	18, 20, 21, 23, 71–74
BRD7, BRD9	bromodomain	VZ185	75
BRD9	bromodomain	dBRD9	76
BTK	Tyr kinase	Compound 10, CJH-005-067, DD-04-015, MT-802	41, 44, 77
CAPERα	splicing factor	E7820, Indisulam, CQS	78
CDK6	cyclin-dependent kinase	BSJ-03-123	79
CDK9	cyclin-dependent kinase	Compound 3, Compound 11c	80, 81
cMet	RTK	Compound 7	82
CRABP	nuclear receptor	Compound 4b	31
DAPK1	Ser/Thr kinase	TAT-GluN2BCTM	64
EGFR	RTK	Compound 1 (also 3-5)	82
ER	nuclear receptor	IκBα Phosphopeptide-estradiol PROTAC, E2-SMPI, PROTAC B, SNIPER 9, ERD-308, TD-PROTAC, Compounds 5-7	24, 26, 28, 69, 83, 84, 85
ERK1/2	Ser/Thr kinase	ERK-ClipTac	86
ERRα	nuclear receptor	PROTAC_ERRα	19
Fak	Tyr kinase	PROTAC-3	51
$FKBP12_{F36V}$	prolyl isomerase	PROTAC 4, dTag-13	25, 87
FLT-3	RTK	TL13-117, TL13-149, FLT-3 PROTAC	44, 46
FRS2α	growth receptor	phosphoPROTAC $^{TrkA}PP_{FRS2α}$	29
HaloTag®	fusion tag	HaloPROTAC 3	88
HDAC6	deacetylase	dHDAC6	89
Her2	RTK	Compound 1	82
Huntington	disease protein	60Q-HSC70bm	90
MDM2	E3 ligase	MD-224	91
MetAP2	aminopeptidase	IκBα-OVA PROTAC, Fu-SMPI	4, 26
p38α, p38δ	Ser/Thr kinase	SJFα, SJFδ	92
PARP1	transferase	Compound 3	53
PCAF/GCN5	bromodomain	GSK983	93
PI3K	kinase	phosphoPROTAC $^{ErbB2}PP_{PI3K}$, Compound D	29, 94
Pirin	cupin family	CCT367766	49
Plk1	Ser/Thr kinase	Poloxin-2HT	95
PSD-95	scaffolding protein	TAT-GluN2B9cCTM	64
RAR	nuclear receptor	SNIPER 13	69
RBM39	splicing factor	Indisulam, Tasisulam, CQS	96
RIP2K	Ser/Thr kinase	PROTAC_RIP2k	19
Sirt2	lysine deacetylase	Compound 12	97
Smad3	DNA binding protein	PROTAC	98
TACC3	spindle regulatory protein	SNIPER(TACC3)	99
Tau	microtubuli stabilizing protein	Peptide 1, TH006	100, 101
TBK1	Ser/Thr kinase	Compound 3i	102
VHL	E3 ligase	CM11, Homo-PROTAC	103
X-protein	viral protein		104

Moreover, crystal structures of targets and E3 ligases that have been used to model the ternary complex provide a retrospective justification to degradation and target selectivity.[2] The first effort to use computation to predict the ternary complex[3] and the evolution of this effort will increasingly guide PROTAC design in the future. Until then, researchers must synthesize a permutated library consisting of different E3 ligase binders; linkers with diverse lengths, compositions, and exit vectors; and appropriate protein binders. Coverage of all this synthetic diversity can easily add up to 100+ PROTACs being synthesized for an initial degradation screen to find out if a target is amenable to the approach or not.

Since resources at the proof-of-concept stage or for early projects are usually limited in industry and academia, multistep syntheses and laborious testing of large compound sets to fully explore PROTAC options can set a high barrier to overcome. To help facilitate such efforts, PROTAC building blocks and Partial PROTACs have recently become commercially available. They consist of E3 ligase binders that are connected to linkers of various lengths and with different reactive groups that allow for flexible conjugation chemistry (**Figure 4**). The use of such templates reduces degrader synthesis to a one-step reaction between the building block and the target ligand precursor.

Currently, only binders for CRBN and VHL are available as they are the best studied. For CRBN, pomalidomide-derived building blocks are offered because of their synthetic accessibility. For VHL, modification of the amide group of the VHL ligand leads to accessible derivatives. Linkers are usually based on PEG or alkyl chains, and contain up to 6 ethylene glycol units. Longer linkers have not shown any improvement so far,[4b] and researchers can limit their efforts to utilizing 5–25 atoms. In contrast to PEG chains, which increase the solubility and decrease the lipophilicity of the PROTAC, alkyl chains cause the PROTAC to become more insoluble and lipophilic as the size of the alkyl chain increases. This provides researchers with a first handle to tune PROTAC properties. After examining the published in vivo active compounds, one often finds rigidified linkers possessing piperazine, phenyl, or spirocyclic motifs. Although these linkers have better ADME properties, we do not recommend using them at the degrader discovery stage. Floppy PEG or alkyl chains can adopt multiple conformations, increasing the likelihood of finding a degrader. Once a degrader with an optimal linker length is found, optimization of the linker composition and rigidity can be started.

Moreover, the portfolio of available reactive groups is expanding steadily. Traditionally, first compound design started with amide-bond formation, since carboxylic acid and amide building blocks are readily available. Additionally, click chemistry has proven valuable in PROTAC research,[5–8] and, thus, azide and alkyne building blocks are emerging as good options. Additionally, alkyne derivatives can be employed in Sonogashira couplings with aryl halide containing precursors. This diversity in conjugation reactions increases the applicability of the technology and provides a first tool to tune the angle of

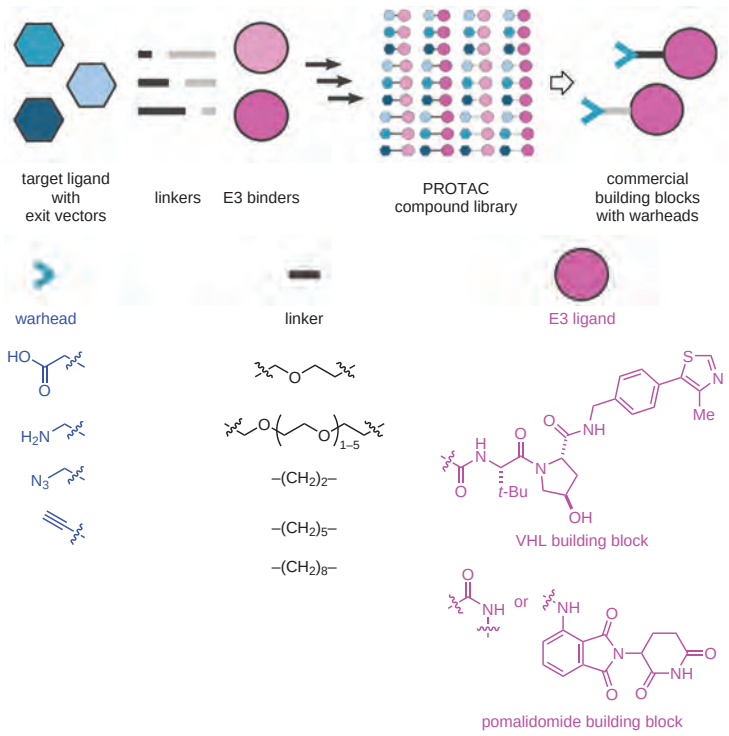

Figure 4. PROTAC Discovery Remains Empirical, and Designed Libraries Rely on Permutations of Target Ligands, Linkers, and E3 Binders.

the PROTAC's exit vector on the target protein side. From a pragmatic point of view, one should start with the conjugation chemistry that is most convenient and gives the fastest results.

Having all these available options, researchers can easily design their first set of PROTAC molecules from their target ligands of choice. The set could consist of a hundred members for an in-depth analysis of the degrader potential or of only a dozen members for a proof-of-concept study. At a minimum, the set should consist of at least five members of different lengths per E3 ligase and target ligand to cover the main aspects of PROTAC design. Such a set would yield well-balanced molecules with sufficient solubility, stability, and permeability to allow initial testing in degradation assays. As demonstrated by recent examples of testing in vivo, compound optimization is also possible, since the "rule-of-5" applies similarly to PROTAC set design[49] and provides chemists with a basis for improving compounds in the set. However, adherence to the "rule-of-5" holistically by all PROTAC degraders in development may vary and should be kept in mind. In addition, further optimization of the set could include using optimized E3 ligands, variation of their exit vectors, linker composition and rigidity with focus on improved ADME profile, as well as target ligand exit vectors, and should be accompanied by straightforward compound profiling.

3. Profiling of PROTAC Compounds

Having the PROTAC library in hand, member compounds can be profiled for target binding and degradation. In addition to state-of-the-art optimization of physicochemical and ADME parameters, in-depth profiling of the degradation process, kinetics, and selectivity can be used to optimize the molecules to create an efficacious in vivo degrader. An example of a screening cascade is depicted in **Figure 5**.

3.1. Binding Confirmation

When the exit vector of the ligand is unknown, the unmodified ligand could be used as a relative baseline for binding. To screen the PROTAC library for target binding, various binding assays, such as the Surface Plasmon Resonance (SPR) assay, may be utilized. For enzyme targets such as kinases, an enzymatic assay can also serve this purpose if an inhibitor is employed as the target handle. Comparing the K_D or IC_{50} of the PROTAC being tested to the unmodified ligand gives a measure of how well the linker position is accepted. If the K_D or IC_{50} is within 20-fold, that can be reasonable evidence that the exit vector on the PROTAC assayed is tolerated. It should be noted, however, that the binding affinity between the PROTAC and target often does not correlate to how effectively the PROTAC will degrade that target; for example, micromolar binding can still yield an active PROTAC.[42]

3.2. Degradation Assay

The most important assay is a degrader assay performed to investigate the ability of a PROTAC compound to induce target degradation by quantifying the changes in intracellular protein levels. Important parameters determined include DC_{50}, the concentration at which half of the protein is degraded; D_{max}, the maximal degradation reported as a percentage level; and t_{max}, the time frame at D_{max} (**Figure 6**, Part (a)). Additionally, a good degradation assay should take into consideration other factors such as cell lines used, concentrations applied, incubation times, control experiments, and method of detection.

3.2.1. Choosing a Cell Line

The cell line chosen should be easy to handle and specific to the phenotype or therapeutic application of the PROTAC target, e.g., cancer cell lines for cancer targets. Moreover, if unknown, the target and E3 expression levels should be sufficiently high or tested beforehand. Ideally, a cell line is chosen that permits further testing, such as proliferation or phenotypic assays, to be performed according to established protocols. However, one can also start with an easy-to-treat cell line such as HEK293, HeLa, or Jurkat and test only optimized compounds in more complex cells such as 3D cultures, co-cultures, or primary cells.

3.2.2. Effect of PROTAC Concentration on Assay

PROTACs should be tested in a concentration range. If concentrations are too low, there may not be enough PROTAC to bring together the ternary complex. If concentrations are too high, elevated levels of PROTAC could preclude complex formation due to saturation of the individual target and E3 ligase binding sites (hook effect; see Figure 6, Part (b).[19] This is drastically different from traditional assay development that usually starts with the highest concentration possible. With PROTACs, the reported DC_{50} values range from sub-nM to 100 μM. For hit discovery, three PROTAC concentrations are recommended: 0.1, 1, and 10 μM. At higher concentrations, small-molecule PROTACs can suffer from solubility issues.

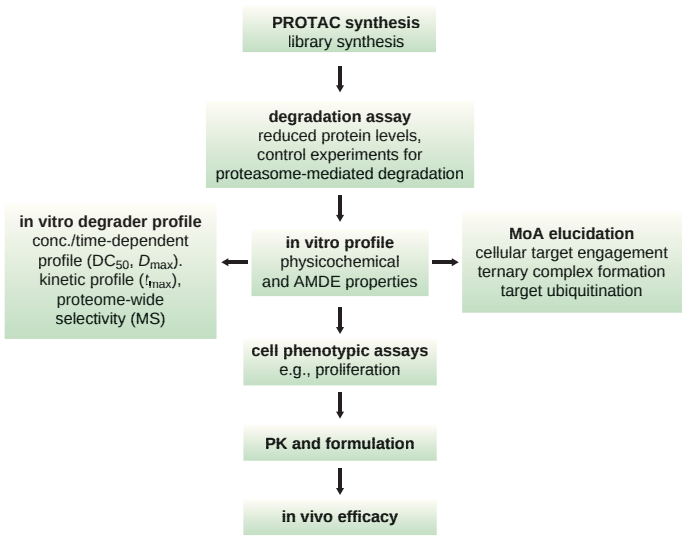

Figure 5. Example of a PROTAC Degrader Screening Cascade.

3.2.3. Assay Time Points

Ideally, assay time points are guided by knowledge about target turnover and re-synthesis rate. It is recommended that different incubation times be investigated during hit discovery for targets with unknown turnover. If the wrong incubation period is chosen, the protein may have already been re-synthesized, and then the PROTAC compound may appear inactive.[107] Moreover, the testing of different incubation times gives preliminary insights into the degradation kinetics, which is helpful for PROTAC optimization.

3.2.4. Assay Controls

Several assay controls have been described in the literature. Frequently, proteasome inhibitors such as carfilzomib,[44] epoxomicin,[77] MG132,[98] and 17-AAG[82] are employed. They prevent target protein degradation by the proteasome, and result in the reconstitution of untreated protein levels. In many cases, the respective E3 ligand[77] is added as a competitor in high concentrations. This suppresses the binding of the PROTAC to its E3 ligase, and thus degradation levels are reduced. Commonly, an inactive PROTAC with similar physicochemical properties is employed, but is unable to bind its E3 ligase. In the case of VHL, this is achieved by incorporating the inactive *S*-enantiomer[65] into the PROTAC. For CRBN, methylated[91] or de-oxygenated[61] thalidomide analogues are used. In the case of cullin RING ligases such as CRBN and VHL, the NEDD8 inhibitor MLN4924[62] can also be utilized since neddylation is essential for the activation of cullin RING ligases (CRLs). If such controls do not reduce the degradation effect, the tested PROTAC is very likely inducing nonspecific degradation effects such as destabilization or autophagy.[108]

Lastly, a few reports have shown that siRNA can also be used as a control. If siRNA is directed against the E3 ligase,[81] degradation is abolished. Similarly, siRNA against the target[100] can be a suitable control for phenotypes with reduced protein levels.

3.2.5. Protein Detection Methods

Western blotting is the current method of choice in the PROTAC field to determine protein levels due to its ease in handling, the availability of established protocols, and its few requirements (i.e., no need for genetic manipulation and expensive instrumentation). The cells are incubated with a PROTAC compound prior to lysis, and the proteome is analyzed by SDS-PAGE and blotted to a membrane. A target-specific antibody and a suitable secondary antibody are chosen that allow for fluorescent or chemiluminescent readout of the target protein. A second, unaffected protein such as GADPH,[83] actin,[53] tubulin,[65] vinculin[87] or histone 3[79] is detected in parallel as a loading control, providing a quantitative readout of the overall protein level in the sample. In this way, degradation effects can be investigated in a concentration and time-

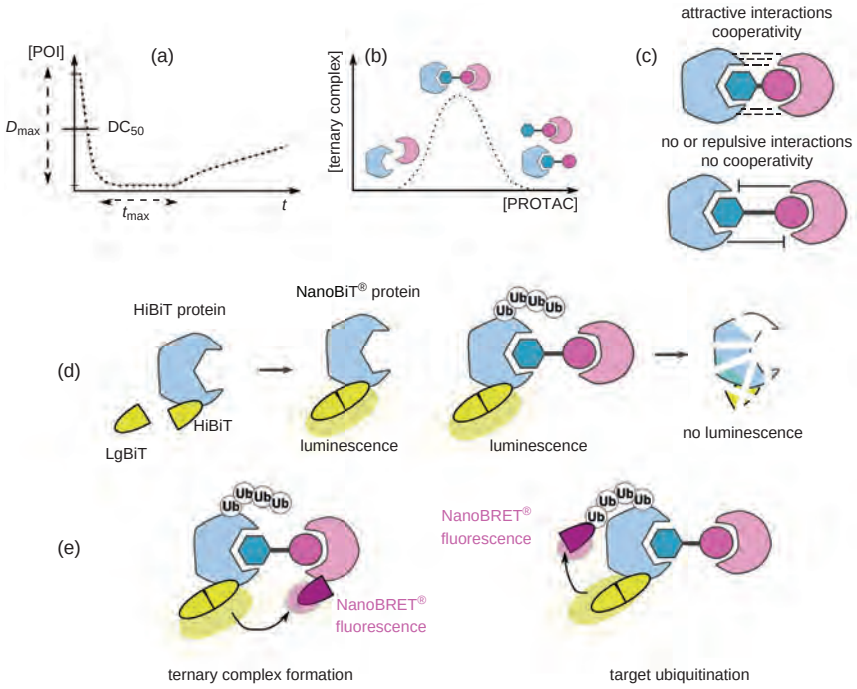

Figure 6. (a) Time-Course of Protein Levels during Induced Degradation. Parameters Measured Are DC_{50}, D_{max}, and t_{max}. (b) Ternary Complex Formation Dependence on PROTAC Concentration. High Concentrations Lead to Unproductive Dimers "Hook-Effect". (c) Cooperativity in Ternary Complexes. (d) NanoBiT® Technology to Quantify Protein Levels. (e) NanoBRET® Technology to Quantify Ternary Complex Formation and Target Ubiquitination.

dependent manner. Likewise, mass spectrometry[42,44,109] has been applied to quantify cellular degradation effects. By combining dynamic-SILAC labeling with isobaric mass tagging, proteome-wide protein levels could be investigated, allowing the additional assessment of PROTAC selectivity and whole proteasome effects.

However, the preparation of cell lysates can be very laborious when performed in high-throughput, e.g., when screening a library of PROTAC compounds. To overcome this, several reports have been published that use fusion proteins to determine protein levels. In some reports, GFP-tagged target proteins are employed,[20,25,64,88] and the relative fluorescence is correlated with protein levels, measurable by flow cytometry[100] or a multiwell-plate reader.[37] Thus, a decrease in fluorescence would indicate a decrease in protein levels. Similarly, a luciferase fusion protein[75,79,96,107] can be employed to detect protein levels by chemiluminescence. Notably, one study[107] compared the PROTAC-induced degradation of transiently expressed fusion proteins with stably expressed fusion proteins and found that parameters measured from ectopic expressions are skewed due to overexpression and missing epigenetic and transcriptional control mechanisms. Consequently, only stably expressed fusion proteins should be utilized for the quantitative interpretation of protein levels and degradation parameters.

3.3. Kinetic Profiling and MoA Studies of Degraders

Targeting a protein for degradation is a highly complex process where the PROTAC molecule can fail in any of several steps. After the degrader molecule enters the cell, it binds to its target and E3 ligase to form a ternary complex that enables the transfer of multiple ubiquitins to the target, thus sending it for lysis by the proteasome. In the case of inactive degraders, or to further optimize PROTACs, it can be beneficial to evaluate the early steps in the degradation process. For instance, a PROTAC might be impermeable[49] or bind more strongly to a second, undesired[43] target. To find out if that is the case, a cellular target engagement assay could be helpful. Another pitfall could be that the PROTAC cannot induce the formation of a ternary complex in cells, or it does so in a geometry that disfavors ubiquitination or selectivity.[40] Here, assays demonstrating ternary complex formation or target ubiquitination could provide further insight.

One particular assay with a potential to greatly contribute to the PROTAC field was recently developed by Daniels and co-workers at Promega.[107] They combined endogenous tagging with NanoBiT® technology to enable the quantitative measurement of protein levels and to investigate the kinetics of target degradation in living cells (Figure 6, Part (d)). The same researchers used CRISPR/Cas9 genome editing[110,111] to insert an 11 amino acid peptide, termed HiBiT, into the protein of interest. Similarly, researchers at Promega and the University of Utah introduced an 18 kDa protein, called LgBiT, that spontaneously assembles with pM affinity to form the functional NanoBiT® luciferase.[112,113] Using bioluminescence imaging, they were able to monitor the degradation profile in real-time with quantitation of degradation parameters such as DC_{50}, D_{max}, and t_{max}. Next, they established a NanoBRET®[114] protocol with ectopically expressed HaloTag® fusion proteins of the E3 ligases[88] and ubiquitin as energy acceptors. When a PROTAC induces proximity between the NanoBiT®-tagged target protein and the HaloTag®-E3 ligase or HaloTag®-ubiquitin, energy transfer occurs and results in a fluorescent signal (Figure 6, Part (e)). Thus, intracellular ternary complex formation and target ubiquitination were investigated in a time-dependent manner.

A few crystal structures[40,50,75,106] have been published that broaden our understanding of the structural features of ternary complexes. It was found that some protein–protein interactions can lead to a cooperative effect[40,41,115] (Figure 6, Part (c)) that turns a PROTAC into an efficient or a particularly selective degrader. Moreover, initial attempts to rationalize PROTAC design and to identify these cooperative interactions by in silico prediction have been published, and will likely evolve with further understanding of the technology.[45,106]

4. Conclusion

Targeted protein degradation is a rapidly growing research area that has evolved within the last decade from a purely academic research tool into a therapeutic modality that is of great interest in industry as well as academia. With the first PROTACs entering clinical trials in 2019, researchers will be keen to find out if PROTACs will keep their promise, and what some of the limitations on their use may be. The list of targets amenable to this approach has been steadily growing, and scientific efforts to expand the scope of suitable E3 ligands, clever assay development, future prediction tools, as well as commercially available building blocks and kits will further advance the technology and facilitate its application to tomorrow's medicines.

5. References

(1) Coleman, K. G.; Crews, C. M. *Annu. Rev. Cancer Biol.* **2018**, *2*, 41.
(2) Lai, A. C.; Crews, C. M. *Nat. Rev. Drug Discovery* **2017**, *16*, 101.
(3) Toure, M.; Crews, C. M. *Angew. Chem., Int. Ed.* **2016**, *55*, 1966.
(4) (a) Mayor-Ruiz, C.; Winter, G. E. *Drug Discovery Today: Technol.* **2019**, *31*, 81. (b) Sakamoto, K. M.; Kim, K. B.; Kumagai, A.; Mercurio, F.; Crews, C. M.; Deshaies, R. J. *Proc. Natl. Acad. Sci. U. S. A.* **2001**, *98*, 8554.
(5) Hopkins, A. L.; Groom, C. R. *Nat. Rev. Drug Discovery* **2002**, *1*, 727.
(6) Clamp, M.; Fry, B.; Kamal, M.; Xie, X.; Cuff, J.; Lin, M. F.; Kellis, M.; Lindblad-Toh, K.; Lander, E. S. *Proc. Natl. Acad. Sci. U. S. A.* **2007**, *104*, 19428.
(7) Burnett, J. C.; Rossi, J. J. *Chem. Biol.* **2012**, *19*, 60.
(8) Wishart, D. S.; Knox, C.; Guo, A. C.; Shrivastava, S.; Hassanali, M.; Stothard, P.; Chang, Z.; Woolsey, J. *Nucleic Acids Res.* **2006**, *34*, D668.
(9) Rinaldi, C.; Wood, M. J. A. *Nat. Rev. Neurol.* **2018**, *14*, 9.
(10) Zamecnik, P. C.; Stephenson, M. L. *Proc. Natl. Acad. Sci. U. S. A.* **1978**, *75*, 280.

(11) Doudna, J. A.; Charpentier, E. *Science* **2014**, *346*, 1077.
(12) Hsu, P. D.; Lander, E. S.; Zhang, F. *Cell* **2014**, *157*, 1262.
(13) Sander, J. D.; Joung, J. K. *Nat. Biotechnol.* **2014**, *32*, 347.
(14) De Smidt, P. C.; Le Doan, T.; de Falco, S.; van Berkel, T. J. C. *Nucleic Acids Res.* **2007**, *19*, 4695.
(15) Jackson, A. L.; Bartz, S. R.; Schelter, J.; Kobayashi, S. V.; Burchard, J.; Mao, M.; Li, B.; Cavet, G.; Linsley, P. S. *Nat. Biotechnol.* **2003**, *21*, 635.
(16) Iyer, V.; Boroviak, K.; Thomas, M.; Doe, B.; Riva, L.; Ryder, E.; Adams, D. J. *PLoS Genet.* **2018**, *14* (7), e1007503 (DOI: 10.1371/journal.pgen.1007503).
(17) Fu, Y.; Foden, J. A.; Khayter, C.; Maeder, M. L.; Reyon, D.; Joung, J. K.; Sander, J. D. *Nat. Biotechnol.* **2013**, *31*, 822.
(18) Lu, J.; Qian, Y.; Altieri, M.; Dong, H.; Wang, J.; Raina, K.; Hines, J.; Winkler, J. D.; Crew, A. P.; Coleman, K. ; Crews, C. M. *Chem. Biol.* **2015**, *22*, 755.
(19) Bondeson, D. P.; Mares, A.; Smith, I. E. D.; Ko, E.; Campos, S.; Miah, A. H.; Mulholland, K. E.; Routly, N.; Buckley, D. L.; Gustafson, J. L.; Zinn, N.; Grandi, P.; Shimamura, S.; Bergamini, G.; Faelth-Savitski, M.; Bantscheff, M.; Cox, C.; Gordon, D. A.; Willard, R. R.; Flanagan, J. J.; Casillas, L. N.; Votta, B. J.; den Besten, W.; Famm, K.; Kruidenier, L.; Carter, P. S.; Harling, J. D.; Churcher, I.; Crews, C. M. *Nat. Chem. Biol.* **2015**, *11*, 611.
(20) Zengerle, M.; Chan, K.-H.; Ciulli, A. *ACS Chem. Biol.* **2015**, *10*, 1770.
(21) Winter, G. E.; Buckley, D. L.; Paulk, J.; Roberts, J. M.; Souza, A.; Dhe-Paganon, S.; Bradner, J. E. *Science* **2015**, *348*, 1376.
(22) Lai, A. C.; Toure, M.; Hellerschmied, D.; Salami, J.; Jaime-Figueroa, S.; Ko, E.; Hines, J.; Crews, C. M. *Angew. Chem., Int. Ed.* **2016**, *55*, 807.
(23) Raina, K.; Lu, J.; Qian, Y.; Altieri, M.; Gordon, D.; Rossi, A. M. K.; Wang, J.; Chen, X.; Dong, H.; Siu, K.; Winkler, J. D.; Crew, A. P.; Crews, C. M.; Coleman, K. G. *Proc. Natl. Acad. Sci. U. S. A.* **2016**, *113*, 7124.
(24) Sakamoto, K. M.; Kim, K. B.; Verma, R.; Ransick, A.; Stein, B.; Crews, C. M.; Deshaies, R. J. *Mol. Cell. Proteomics* **2003**, *2*, 1350.
(25) Schneekloth, J. S., Jr.; Fonseca, F. N.; Koldobskiy, M.; Mandal, A.; Deshaies, R.; Sakamoto, K.; Crews, C. M. *J. Am. Chem. Soc.* **2004**, *126*, 3748.
(26) Zhang, D.; Baek, S.-H.; Ho, A.; Kim, K. *Bioorg. Med. Chem. Lett.* **2004**, *14*, 645.
(27) Lee, H.; Puppala, D.; Choi, E.-Y.; Swanson, H.; Kim, K.-B. *ChemBioChem* **2007**, *8*, 2058.
(28) Rodriguez-Gonzalez, A.; Cyrus, K.; Salcius, M.; Kim, K.; Crews, C. M.; Deshaies, R. J.; Sakamoto, K. M. *Oncogene* **2008**, *27*, 7201.
(29) Hines, J.; Gough, J. D.; Corson, T. W.; Crews, C. M. *Proc. Natl. Acad. Sci. U. S. A.* **2013**, *110*, 8942.
(30) Schneekloth, A. R.; Pucheault, M.; Tae, H. S.; Crews, C. M. *Bioorg. Med. Chem. Lett.* **2008**, *18*, 5904.
(31) Itoh, Y.; Ishikawa, M.; Naito, M.; Hashimoto, Y. *J. Am. Chem. Soc.* **2010**, *132*, 5820.
(32) Buckley, D. L.; van Molle, I.; Gareiss, P. C.; Tae, H. S.; Michel, J.; Noblin, D. J.; Jorgensen, W. L.; Ciulli, A.; Crews, C. M. *J. Am. Chem. Soc.* **2012**, *134*, 4465.
(33) Buckley, D. L.; Gustafson, J. L.; van Molle, I.; Roth, A. G.; Tae, H. S.; Gareiss, P. C.; Jorgensen, W. L.; Ciulli, A.; Crews, C. M. *Angew. Chem., Int. Ed.* **2012**, *51*, 11463.
(34) Van Molle, I.; Thomann, A.; Buckley, D. L.; So, E. C.; Lang, S.; Crews, C. M.; Ciulli, A. *Chem. Biol.* **2012**, *19*, 1300.
(35) Galdeano, C.; Gadd, M. S.; Soares, P.; Scaffidi, S.; van Molle, I.; Birced, I.; Hewitt, S.; Dias, D. M.; Ciulli, A. *J. Med. Chem.* **2014**, *57*, 8657.
(36) Chamberlain, P. P.; Lopez-Girona, A.; Miller, K.; Carmel, G.; Pagarigan, B.; Chie-Leon, B.; Rychak, E.; Corral, L. G.; Ren, Y. J.; Wang, M.; Riley, M.; Delker, S. L.; Ito, T.; Ando, H.; Mori, T.; Hirano, Y.; Handa, H.; Hakoshima, T.; Daniel, T. O.; Cathers, B. E. *Nat. Struct. Mol. Biol.* **2014**, *21*, 803.
(37) Fischer, E. S.; Böhm, K.; Lydeard, J. R.; Yang, H.; Stadler, M. B.; Cavadini, S.; Nagel, J.; Serluca, F.; Acker, V.; Lingaraju, G. M.; Tichkule, R. B.; Schebesta, M.; Forrester, W. C.; Schirle, M.; Hassiepen, U.; Ottl, J.; Hild, M.; Beckwith, R. E. J.; Harper, J. W.; Jenkins, J. L.; Thomä, N. H. *Nature* **2014**, *512*, 49.
(38) Krönke, J.; Udeshi, N. D.; Narla, A.; Grauman, P.; Hurst, S. N.; McConkey, M.; Svinkina, T.; Heckl, D.; Comer, E.; Li, X.; Ciarlo, C.; Hartman, E.; Munshi, N.; Schenone, M.; Schreiber, S. L.; Carr, S. A.; Ebert, B. L. *Science* **2014**, *343*, 301.
(39) Lu, G.; Middleton, R. E.; Sun, H.; Naniong, M.; Ott, C. J.; Mitsiades, C. S.; Wong, K.-K.; Bradner, J. E.; Kaelin, W. G., Jr. *Science* **2014**, *343*, 305.
(40) Gadd, M. S.; Testa, A.; Lucas, X.; Chan, K.-H.; Chen, W.; Lamont, D. J.; Zengerle, M.; Ciulli, A. *Nat. Chem. Biol.* **2017**, *13*, 514.
(41) Zorba, A.; Nguyen, C.; Xu, Y.; Starr, J.; Borzilleri, K.; Smith, J.; Zhu, H.; Farley, K. A.; Ding, W.; Schiemer, J.; Feng, X.; Chang, J. S.; Uccello, D. P.; Young, J. A.; Garcia-Irrizary, C. N.; Czabaniuk, L.; Schuff, B.; Oliver, R.; Montgomery, J.; Hayward, M. M.; Coe, J.; Chen, J.; Niosi, M.; Luthra, S.; Shah, J. C.; El-Kattan, A.; Qiu, X.; West, G. M.; Noe, M. C.; Shanmugasundaram, V.; Gilbert, A. M.; Brown, M. F.; Calabrese, M. F. *Proc. Natl. Acad. Sci. U. S. A.* **2018**, *115*, E7285.
(42) Bondeson, D. P.; Smith, B. E.; Burslem, G. M.; Buhimschi, A. D.; Hines, J.; Jaime-Figueroa, S.; Wang, J.; Hamman, B. D.; Ishchenko, A.; Crews, C. M. *Cell Chem. Biol.* **2018**, *25*, 78.
(43) Ishoey, M.; Chorn, S.; Singh, N.; Jaeger, M. G.; Brand, M.; Paulk, J.; Bauer, S.; Erb, M. A.; Parapatics, K.; Müller, A. C.; Bennett, K. L.; Ecker, G. F.; Bradner, J. E.; Winter, G. E. *ACS Chem. Biol.* **2018**, *13*, 553.
(44) Huang, H.-T.; Dobrovolsky, D.; Paulk, J.; Yang, G.; Weisberg, E. L.; Doctor, Z. M.; Buckley, D. L.; Cho, J.-H.; Ko, E.; Jang, J.; Shi, K.; Choi, H. G.; Griffin, J. D.; Li, Y.; Treon, S. P.; Fischer, E. S.; Bradner, J. E.; Tan, L.; Gray, N. S. *Cell Chem. Biol.* **2018**, *25*, 88
(45) Drummond, M. L.; Williams, C. I. *J. Chem. Inf. Model.* **2019**, *59*, DOI 10.1021/acs.jcim.8b00872.
(46) Burslem, G. M.; Song, J.; Chen, X.; Hines, J.; Crews, C. M. *J. Am. Chem. Soc.* **2018**, *140*, 16428.
(47) Gu, S.; Cui, D.; Chen, X.; Xiong, X.; Zhao, Y. *BioEssays* **2018**, *40*, DOI 10.1002/bies.201700247.
(48) Hines, J.; Lartigue, S.; Dong, H.; Qian, Y.; Crews, C. M. *Cancer*

Res. **2018**, *79*, 251.

(49) Chessum, N. E. A.; Sharp, S. Y.; Caldwell, J. J.; Pasqua, A. E.; Wilding, B.; Colombano, G.; Collins, I.; Ozer, B.; Richards, M.; Rowlands, M.; Stubbs, M.; Burke, R.; McAndrew, P. C.; Clarke, P. A.; Workman, P.; Cheeseman, M. D.; Jones, K. *J. Med. Chem.* **2018**, *61*, 918.

(50) McCoull, W.; Cheung, T.; Anderson, E.; Barton, P.; Burgess, J.; Byth, K.; Cao, Q.; Castaldi, M. P.; Chen, H.; Chiarparin, E.; Carbajo, R. J.; Code, E.; Cowan, S.; Davey, P. R.; Ferguson, A. D.; Fillery, S.; Fuller, N. O.; Gao, N.; Hargreaves, D.; Howard, M. R.; Hu, J.; Kawatkar, A.; Kemmitt, P. D.; Leo, E.; Molina, D. M.; O'Connell, N.; Petteruti, P.; Rasmusson, T.; Raubo, P.; Rawlins, P. B.; Ricchiuto, P.; Robb, G. R.; Schenone, M.; Waring, M. J.; Zinda, M.; Fawell, S.; Wilson, D. M. *ACS Chem. Biol.* **2018**, *13*, 3131.

(51) Cromm, P. M.; Samarasinghe, K. T. G.; Hines, J.; Crews, C. M. *J. Am. Chem. Soc.* **2018**, *140*, 17019.

(52) Kaur, T.; Menon, A.; Garner, A. L. *Eur. J. Med. Chem.* **2019**, *166*, 339.

(53) Zhao, Q.; Lan, T.; Su, S.; Rao, Y. *Chem. Commun.* **2019**, *55*, 369.

(54) Popow, J.; Arnhof, H.; Bader, G.; Berger, H.; Ciulli, A.; Covini, D.; Dank, C.; Gmaschitz, T.; Greb, P.; Karolyi-Oezguer, J.; Koegl, M.; McConnell, D. B.; Pearson, M.; Rieger, M.; Rinnenthal, J.; Roessler, V.; Schrenk, A.; Spina, M.; Steurer, S.; Trainor, N.; Traxler, E.; Wieshofer, C.; Zoephel, A.; Ettmayer, P. *J. Med. Chem.* **2019**, *62*, 2508.

(55) Papatzimas, J. W.; Gorobets, E.; Maity, R.; Muniyat, M. I.; MacCallum, J. L.; Neri, P.; Bahlis, N. J.; Derksen, D. J. *ChemRxiv* **2019**, *1*, 1 (DOI: 10.26434/chemrxiv.7722359.v1).

(56) Tinworth, C. P. ; Lithgow, H.; Dittus, L.; Bassi, Z. I.; Hughes, S. E.; Muelbaier, M.; Dai, H.; Smith, I. E. D.; Kerr, W. J.; Burley, G. A.; Bantscheff, M.; Harling, J. D. *ACS Chem. Biol.* **2019**, *14*, 342.

(57) Jiang, B.; Wang, E. S.; Donovan, K. A.; Liang, Y.; Fischer, E. S.; Zhang, T.; Gray, N. S. *Angew. Chem., Int. Ed.* **2019**, *58*, DOI 10.1002/anie.201901336.

(58) Zhao, B.; Burgess, K. *Chem. Commun.* **2019**, *55*, 2704.

(59) (a) Sun, X.; Wang, J.; Yao, X.; Zheng, W.; Mao, Y.; Lan, T.; Wang, L.; Sun, Y.; Zhang, X.; Zhao, Q.; Zhao, J.; Xiao, R.-P.; Zhang, X.; Ji, G.; Rao, Y. *Cell Discovery* **2019**, *5*, 1. (b) *Globe Newswire* [Online], Jan 4, 2019. https://www.globenewswire.com/news-release/2019/01/04/1680835/0/en/Arvinas-Receives-Authorization-to-Proceed-for-its-IND-Application-for-PROTAC-Therapy-to-Treat-Patients-with-Metastatic-Castration-Resistant-Prostate-Cancer.html.

(60) Henning, R. K.; Varghese, J. O.; Das, S.; Nag, A.; Tang, G.; Tang, K.; Sutherland, A. M.; Heath, J. R. *J. Pept. Sci.* **2016**, *22*, 196.

(61) Powell, C. E.; Gao, Y.; Tan, L.; Donovan, K. A.; Nowak, R. P.; Loehr, A.; Bahcall, M.; Fischer, E. S.; Jänne, P. A.; George, R. E.; Gray, N. S. *J. Med. Chem.* **2018**, *61*, 4249.

(62) Zhang, C.; Han, X.-R.; Yang, X.; Jiang, B.; Liu, J.; Xiong, Y.; Jin, J. *Eur. J. Med. Chem.* **2018**, *151*, 304.

(63) Kang, C. H.; Lee, D. H.; Lee, C. O.; Du Ha, J.; Park, C. H.; Hwang, J. Y. *Biochem. Biophys. Res. Commun.* **2018**, *505*, 542.

(64) Fan, X.; Jin, W. Y.; Lu, J.; Wang, J.; Wang, Y. T. *Nat. Neurosci.* **2014**, *17*, 471.

(65) Salami, J.; Alabi, S.; Willard, R. R.; Vitale, N. J.; Wang, J.; Dong, H.; Jin, M.; McDonnell, D. P.; Crew, A. P.; Neklesa, T. K.; Crews, C. M. *Commun. Biol.* **2018**, *1*, 100.

(66) Han, X.; Wang, C.; Qin, C.; Xiang, W.; Fernandez-Salas, E.; Yang, C.-Y.; Wang, M.; Zhao, L.; Xu, T.; Chinnaswamy, K.; Delproposto, J.; Stuckey, J.; Wang, S. *J. Med. Chem.* **2019**, *62*, 941.

(67) Shibata, N.; Nagai, K.; Morita, Y.; Ujikawa, O.; Ohoka, N.; Hattori, T.; Koyama, R.; Sano, O.; Imaeda, Y.; Nara, H.; Cho, N.; Naito, M. *J. Med. Chem.* **2018**, *61*, 543.

(68) Gustafson, J. L.; Neklesa, T. K.; Cox, C. S.; Roth, A. G.; Buckley, D. L.; Tae, H. S.; Sundberg, T. B.; Stagg, D. B.; Hines, J.; McDonnell, D. P.; Norris, J. D.; Crews, C. M. *Angew. Chem., Int. Ed.* **2015**, *54*, 9659.

(69) Itoh, Y.; Kitaguchi, R.; Ishikawa, M.; Naito, M.; Hashimoto, Y. *Bioorg. Med. Chem.* **2011**, *19*, 6768.

(70) Puppala, D.; Lee, H.; Kim, K. B.; Swanson, H. I. *Mol. Pharmacol.* **2008**, *73*, 1064.

(71) Zhou, B.; Hu, J.; Xu, F.; Chen, Z.; Bai, L.; Fernandez-Salas, E.; Lin, M.; Liu, L.; Yang, C.-Y.; Zhao, Y.; McEachern, D.; Przybranowski, S.; Wen, B.; Sun, D.; Wang, S. *J. Med. Chem.* **2018**, *61*, 462.

(72) Qin, C.; Hu, Y.; Zhou, B.; Fernandez-Salas, E.; Yang, C.-Y.; Liu, L.; McEachern, D.; Przybranowski, S.; Wang, M.; Stuckey, J.; Meagher, J.; Bai, L.; Chen, Z.; Lin, M.; Yang, J.; Ziazadeh, D. N.; Xu, F.; Hu, J.; Xiang, W.; Huang, L.; Li, S.; Wen, B.; Sun, D.; Wang, S. *J. Med. Chem.* **2018**, *61*, 6685.

(73) Sun, B.; Fiskus, W.; Qian, Y.; Rajapakshe, K.; Raina, K.; Coleman, K. G.; Crew, A. P.; Shen, A.; Saenz, D. T.; Mill, C. P.; Nowak, A. J.; Jain, N.; Zhang, L.; Wang, M.; Khoury, J. D.; Coarfa, C.; Crews, C. M.; Bhalla, K. N. *Leukemia* **2018**, *32*, 343.

(74) An, S.; Fu, L. *EBioMedicine* **2018**, *36*, 553.

(75) Zoppi, V.; Hughes, S. J.; Maniaci, C.; Testa, A.; Gmaschitz, T.; Wieshofer, C.; Koegl, M.; Riching, K. M.; Daniels, D. L.; Spallarossa, A.; Ciulli, A. *J. Med. Chem.* **2019**, *62*, 699.

(76) Remillard, D.; Buckley, D. L.; Paulk, J.; Brien, G. L.; Sonnett, M.; Seo, H.-S.; Dastjerdi, S.; Wühr, M.; Dhe-Paganon, S.; Armstrong, S. A.; Bradner, J. E. *Angew. Chem., Int. Ed.* **2017**, *56*, 5738.

(77) Buhimschi, A. D.; Armstrong, H. A.; Toure, M.; Jaime-Figueroa, S.; Chen, T. L.; Lehman, A. M.; Woyach, J. A.; Johnson, A. J.; Byrd, J. C.; Crews, C. M. *Biochemistry* **2018**, *57*, 3564.

(78) Uehara, T.; Minoshima, Y.; Sagane, K.; Sugi, N. H.; Mitsuhashi, K. O.; Yamamoto, N.; Kamiyama, H.; Takahashi, K.; Kotake, Y.; Uesugi, M.; Yokoi, A.; Inoue, A.; Yoshida, T.; Mabuchi, M.; Tanaka, A.; Owa, T. *Nat. Chem. Biol.* **2017**, *13*, 675.

(79) Brand, M.; Jiang, B.; Bauer, S.; Donovan, K. A.; Liang, Y.; Wang, E. S.; Nowak, R. P.; Yuan, J. C.; Zhang, T.; Kwiatkowski, N.; Müller, A. C.; Fischer, E. S.; Gray, N. S.; Winter, G. E. *Cell Chem. Biol.* **2019**, *26*, 300.

(80) Robb, C. M.; Contreras, J. I.; Kour, S.; Taylor, M. A.; Abid, M.; Sonawane, Y. A.; Zahid, M.; Murry, D. J.; Natarajan, A.; Rana, S. *Chem. Commun.* **2017**, *53*, 7577.

(81) Bian, J.; Ren, J.; Li, Y.; Wang, J.; Xu, X.; Feng, Y.; Tang, H.; Wang, Y.; Li, Z. *Bioorg. Chem.* **2018**, *81*, 373.
(82) Burslem, G. M.; Smith, B. E.; Lai, A. C.; Jaime-Figueroa, S.; McQuaid, D. C.; Bondeson, D. P.; Toure, M.; Dong, H.; Qian, Y.; Wang, J.; Crew, A. P.; Hines, J.; Crews, C. M. *Cell Chem. Biol.* **2018**, *25*, 67.
(83) Hu, J.; Hu, B.; Wang, M.; Xu, F.; Miao, B.; Yang, C.-Y.; Wang, M.; Liu, Z.; Hayes, D. F.; Chinnaswamy, K.; Delproposto, J.; Stuckey, J.; Wang, S. *J. Med. Chem.* **2019**, *62*, 1420.
(84) Jiang, Y.; Deng, Q.; Zhao, H.; Xie, M.; Chen, L.; Yin, F.; Qin, X.; Zheng, W.; Zhao, Y.; Li, Z. *ACS Chem. Biol.* **2018**, *13*, 628.
(85) Demizu, Y.; Okuhira, K.; Motoi, H.; Ohno, A.; Shoda, T.; Fukuhara, K.; Okuda, H.; Naito, M.; Kurihara, M. *Bioorg. Med. Chem. Lett.* **2012**, *22*, 1793.
(86) Lebraud, H.; Wright, D. J.; Johnson, C. N.; Heightman, T. D. *ACS Cent. Sci.* **2016**, *2*, 927.
(87) Nabet, B.; Roberts, J. M.; Buckley, D. L.; Paulk, J.; Dastjerdi, S.; Yang, A.; Leggett, A. L.; Erb, M. A.; Lawlor, M. A.; Souza, A.; Scott, T. G.; Vittori, S.; Perry, J. A.; Qi, J.; Winter, G. E.; Wong, K.-K.; Gray, N. S.; Bradner, J. E. *Nat. Chem. Biol.* **2018**, *14*, 431.
(88) Buckley, D. L.; Raina, K.; Darricarrere, N.; Hines, J.; Gustafson, J. L.; Smith, I. E.; Miah, A. H.; Harling, J. D.; Crews, C. M. *ACS Chem. Biol.* **2015**, *10*, 1831.
(89) Yang, K.; Song, Y.; Xie, H.; Wu, H.; Wu, Y.-T.; Leisten, E. D.; Tang, W. *Bioorg. Med. Chem. Lett.* **2018**, *28*, 2493.
(90) Bauer, P. O.; Goswami, A.; Wong, H. K.; Okuno, M.; Kurosawa, M.; Yamada, M.; Miyazaki, H.; Matsumoto, G.; Kino, Y.; Nagai, Y.; Nukina, N. *Nat. Biotechnol.* **2010**, *28*, 256.
(91) Li, Y.; Yang, J.; Aguilar, A.; McEachern, D.; Przybranowski, S.; Liu, L.; Yang, C.-Y.; Wang, M.; Han, X.; Wang, S. *J. Med. Chem.* **2019**, *62*, 448.
(92) Smith, B. E.; Wang, S. L.; Jaime-Figueroa, S.; Harbin, A.; Wang, J.; Hamman, B. D.; Crews, C. M. *Nat. Commun.* **2019**, *10*, 1–13 (Article No. 131 (2019), DOI: 10.1038/s41467-018-08027-7).
(93) Bassi, Z. I.; Fillmore, M. C.; Miah, A. H.; Chapman, T. D.; Maller, C.; Roberts, E. J.; Davis, L. C.; Lewis, D. E.; Galwey, N. W.; Waddington, K. E.; Parravicini, V.; Macmillan-Jones, A. L.; Gongora, C.; Humphreys, P. G.; Churcher, I.; Prinjha, R. K.; Tough, D. F. *ACS Chem. Biol.* **2018**, *13*, 2862.
(94) Li, W.; Gao, C.; Zhao, L.; Yuan, Z.; Chen, Y.; Jiang, Y. *Eur. J. Med. Chem.* **2018**, *151*, 237.
(95) Rubner, S.; Scharow, A.; Schubert, S.; Berg, T. *Angew. Chem., Int. Ed.* **2018**, *57*, 17043.
(96) Han, T.; Goralski, M.; Gaskill, N.; Capota, E.; Kim, J.; Ting, T. C.; Xie, Y.; Williams, N. S.; Nijhawan, D. *Science* **2017**, *356*, eaal3755 (DOI: 10.1126/science.aal3755).
(97) Schiedel, M.; Herp, D.; Hammelmann, S.; Swyter, S.; Lehotzky, A.; Robaa, D.; Oláh, J.; Ovádi, J.; Sippl, W.; Jung, M. *J. Med. Chem.* **2018**, *61*, 482.
(98) Xin, W.; Shaozhen, F.; Jinjin, F.; Xiaoyan, L.; Qiong, W.; Ning, L. *Biochem. Pharmacol.* **2016**, *116*, 200.
(99) Ohoka, N.; Nagai, K.; Hattori, T.; Okuhira, K.; Shibata, N.; Cho, N.; Naito, M. *Cell Death Dis.* **2014**, *5*, e1513 (DOI:10.1038/cddis.2014.471).
(100) Lu, M.; Liu, T.; Jiao, Q.; Ji, J.; Tao, M.; Liu, Y.; You, Q.; Jiang, Z. *Eur. J. Med. Chem.* **2018**, *146*, 251.
(101) Chu, T.-T.; Gao, N.; Li, Q.-Q.; Chen, P.-G.; Yang, X.-F.; Chen, Y.-X.; Zhao, Y.-F.; Li, Y.-M. *Cell Chem. Biol.* **2016**, *23*, 453.
(102) Crew, A. P.; Raina, K.; Dong, H.; Qian, Y.; Wang, J.; Vigil, D.; Serebrenik, Y. V.; Hamman, B. D.; Morgan, A.; Ferraro, C.; Siu, K.; Neklesa, T. K.; Winkler, J. D.; Coleman, K. G.; Crews, C. M. *J. Med. Chem.* **2018**, *61*, 583.
(103) Maniaci, C.; Hughes, S. J.; Testa, A.; Chen, W.; Lamont, D. J.; Rocha, S.; Alessi, D. R.; Romeo, R.; Ciulli, A. *Nat. Commun.* **2017**, *8*, 1 (DOI: 10.1038/s41467-017-00954-1).
(104) Montrose, K.; Krissansen, G. W. *Biochem. Biophys. Res. Commun.* **2014**, *453*, 735.
(105) Cyrus, K.; Wehenkel, M.; Choi, E.-Y.; Han, H.-J.; Lee, H.; Swanson, H.; Kim, K.-B. *Mol. BioSyst.* **2011**, *7*, 359.
(106) Nowak, R. P.; DeAngelo, S. L.; Buckley, D.; He, Z.; Donovan, K. A.; An, J.; Safaee, N.; Jedrychowski, M. P.; Ponthier, C. M.; Ishoey, M.; Zhang, T.; Mancias, J. D.; Gray, N. S.; Bradner, J. E.; Fischer, E. S. *Nat. Chem. Biol.* **2018**, *14*, 706.
(107) Riching, K. M.; Mahan, S.; Corona, C. R.; McDougall, M.; Vasta, J. D.; Robers, M. B.; Urh, M.; Daniels, D. L. *ACS Chem. Biol.* **2018**, *13*, 2758.
(108) Cromm, P. M.; Crews, C. M. *Cell Chem. Biol.* **2017**, *24*, 1181.
(109) Savitski, M. M.; Zinn, N.; Faelth-Savitski, M.; Poeckel, D.; Gade, S.; Becher, I.; Muelbaier, M.; Wagner, A. J.; Strohmer, K.; Werner, T.; Melchert, S.; Petretich, M.; Rutkowska, A.; Vappiani, J.; Franken, H.; Steidel, M.; Sweetman, G. M.; Gilan, O.; Lam, E. Y. N.; Dawson, M. A.; Prinjha, R. K.; Grandi, P.; Bergamini, G.; Bantscheff, M. *Cell* **2018**, *173*, 260.
(110) Cong, L.; Ran, F. A.; Cox, D.; Lin, S.; Barretto, R.; Habib, N.; Hsu, P. D.; Wu, X.; Jiang, W.; Marraffini, L. A.; Zhang, F. *Science* **2013**, *339*, 819.
(111) Jinek, M.; Chylinski, K.; Fonfara, I.; Hauer, M.; Doudna, J. A.; Charpentier, E. *Science* **2012**, *337*, 816.
(112) Hall, M. P.; Unch, J.; Binkowski, B. F.; Valley, M. P.; Butler, B. L.; Wood, M. G.; Otto, P.; Zimmerman, K.; Vidugiris, G.; Machleidt, T.; Robers, M. B.; Benink, H. A.; Eggers, C. T.; Slater, M. R.; Meisenheimer, P. L.; Klaubert, D. H.; Fan, F.; Encell, L. P.; Wood, K. V. *ACS Chem. Biol.* **2012**, *7*, 1848.
(113) Schwinn, M. K.; Machleidt, T.; Zimmerman, K.; Eggers, C. T.; Dixon, A. S.; Hurst, R.; Hall, M. P.; Encell, L. P.; Binkowski, B. F.; Wood, K. V. *ACS Chem. Biol.* **2018**, *13*, 467.
(114) Machleidt, T.; Woodroofe, C. C.; Schwinn, M. K.; Méndez, J.; Robers, M. B.; Zimmerman, K.; Otto, P.; Daniels, D. L.; Kirkland, T. A.; Wood, K. V. *ACS Chem. Biol.* **2015**, *10*, 1797.
(115) Hughes, S. J.; Ciulli, A. *Essays Biochem.* **2017**, *61*, 505.

About the Authors

Sarah Schlesiger studied chemistry in Germany, France, and Australia, earning an M.Sc. degree from Leipzig University (2012). She completed her Ph.D. dissertation (2017) in chemical biology at the University of Konstanz working with Professor Dr. Andreas Marx. Shortly thereafter, Sarah joined

Merck KGaA, Darmstadt, Germany, and is currently working as Laboratory Head in medicinal chemistry seeking to develop tomorrow's medicines.

Momar Toure studied chemistry at ENSCM, France, where he earned his M.Sc. degree in 2010. He then completed the requirements for his Ph.D. degree in 2013 in the research group of Drs. Jean-Luc Parrain and Olivier Chuzel at Aix-Marseille University, France. He then joined Professor Craig Crews's research group at Yale University, where he worked in the PROTAC field. He is currently Senior Research Scientist at EMD Serono.

Kaelyn E. Wilke studied biochemistry at the University of St. Thomas, St. Paul, Minnesota, and completed the requirements for her Ph.D. degree in chemical biology with Professor Erin Carlson at Indiana University. Kaelyn joined the Chemical Synthesis Group at MilliporeSigma in 2015, where she is currently Product Manager developing and commercializing technology within emerging areas of chemical biology and medicinal chemistry.

Bayard R. Huck received his Ph.D. degree in organic chemistry from the University of Wisconsin-Madison under the direction of Professor Samuel H. Gellman. He is currently the Global Head of Medicinal Chemistry at Merck KGaA, Darmstadt, Germany.

Coumarin-Based Hybrids as Fluorescent Probes for Highly Selective Chemosensing and Biological Target Imaging


Dr. C. S. Francisco


Ms. T. C. Valim


Prof. Dr. Á. C. Neto


Prof. Dr. V. Lacerda, Jr.

Carla Santana Francisco, Thays Cardoso Valim, Álvaro Cunha Neto, and Valdemar Lacerda, Jr.*

Department of Chemistry
Center of Exact Sciences
Federal University of Espírito Santo,
Goiabeiras Campus
Fernando Ferrari Avenue, 514
Goiabeiras, Vitória, ES 29075-910, Brazil
Email: vljuniorqui@gmail.com

Keywords. coumarins; coumarin hybrids; chemosensors; fluorescent probes; chromogenic dyes; fluorogenic dyes; biological target imaging; fluorescent sensors; molecular recognition; biological sensors.

Abstract. The coumarins are considered an attractive compound class because the coumarin nucleus is an important, biologically active pharmacophore that plays a significant role in chemical biology and in medical applications. Moreover, due to their excellent photophysical properties, coumarins constitute an important class of chromogenic and fluorogenic dyes. In this article, we review a wide range of very recently reported applications of coumarin hybrids as chemosensors, fluorescent probes, biological markers, and biological trackers.

Outline

1. Introduction

Coumarin is a privileged scaffold, owing to its characteristic structure in which a planar aromatic ring is fused to a lactone functionality and to its conjugated π system, fluorescent properties, and other desirable features. This framework has attracted the attention of several research groups, who incorporated the coumarin scaffold into heterocyclic and non-heterocyclic systems as part of a strategy for obtaining hybrid molecules with potentially versatile biological activities, better selectivity profiles, different or double modes of action, and/or reduced undesirable side effects (**Figure 1**).[1]

Fluorescent probes are considered crucial tools for molecular recognition events in biological systems.[2] In recent years, a number of fluorescent probes have been developed, which possess desirable properties such as high selectivity and sensitivity, straightforward implementation, and noninvasive in situ detection. Among these, coumarin–hybrid probes have been widely utilized in tumor diagnosis or in analyte target detection, enzymes, and organelles. Coumarin dyes are often selected because of their good water solubility, strong fluorescence, relatively high fluorescence quantum yield, and facile synthesis.[3]

In the remainder of this review, we highlight recently reported new molecules that incorporate coumarin rings, with the aim of contributing an understanding that would permit the discovery of novel compounds with improved properties for application as chemosensors and fluorescent probes.

2. Synthetic Methods for the Preparation of Coumarin-Based Hybrids

Generally, molecular systems incorporating a coumarin moiety and intended for biological, pharmaceutical, and biomedical applications have been assembled using traditional synthetic chemistry. This includes classical transformations such as the Perkin, Wittig, and Reformatsky reactions; the Pechmann and Knoevenagel condensations; and the Claisen rearrangement. An example of such methods is the use of the Pechmann condensation in the straightforward synthesis of the new fluorescent chemodosimeter **1**, incorporating a coumarin fluorophore and a carbonothiolate functionality as the recognition unit (Scheme 1).[4] Compound **1** was then used for the detection of Hg^{2+} concentrations in real water samples by fluorescence turn-on response. The Pechman condensation, however, suffers in general from a number of drawbacks such as the need for excess acid and the production under some circumstances of byproducts such as chromone.[5]

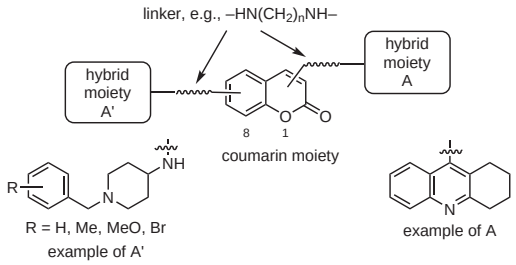

Figure 1. General Structure of a Coumarin–Hybrid Pharmacophore. *(Ref. 1)*

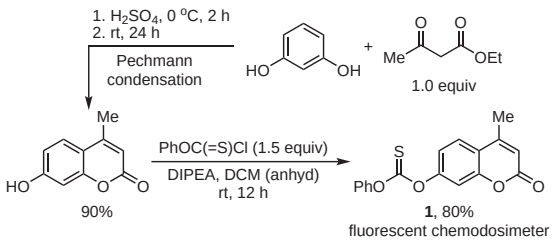

Scheme 1. An Example of the Use of the Pechmann Condensation as a Key Step in the Synthesis of the New Fluorescent Chemodosimeter **1**. *(Ref. 4)*

The Knoevenagel condensation is also extensively used for the synthesis of coumarin scaffolds, which are later incorporated into other small molecules of interest in chemistry and biology.[6–17] This reaction can be catalyzed by piperidine, piperazine, 1,1′-carbonyldiimidazole (CDI), 1,8-diazabicyclo[5.4.0]undec-7-ene (DBU), or an ionic liquid, among others.[18] An example of its utilization in the synthesis of a dual-emission ratiometric fluorescent chemosensor, **2**, with applications in cellular imaging is depicted in Scheme 2.[6]

In addition to these popular traditional methods, other approaches have been explored for the purpose of enhancing yields, reducing reaction times, and improving product recovery.[19] These include reactions that use microwave irradiation, sonication, transition-metal catalysis, heterogeneous catalysis, or ionic liquids.

3. Applications of Coumarin Hybrids as Fluorescent Probes for Chemosensing and Target Imaging

Because of their easy operating techniques, real-time response, and high selectivity and sensitivity, fluorescent chemical sensors have been developed in recent years as powerful tools for monitoring levels of ions, molecules, and other chemical entities. In particular, coumarin-based compounds are attractive as fluorescent sensors because of their excellent chromogenic and fluorogenic properties, associated high quantum yields, excellent water solubility, large Stokes relative displacement, and good cell permeability.[20] Moreover, and owing to their highly variable size, hydrophobicity, and chelation capabilities, coumarin-based hybrids have found specific applications as highly selective fluorescent probes for detecting metal ions.[21]

3.1. Detection of Mercury(II)

Because of the serious risk that mercury in the environment poses to human health and biological reproduction, the development of mercury detection probes has gained in prominence in recent

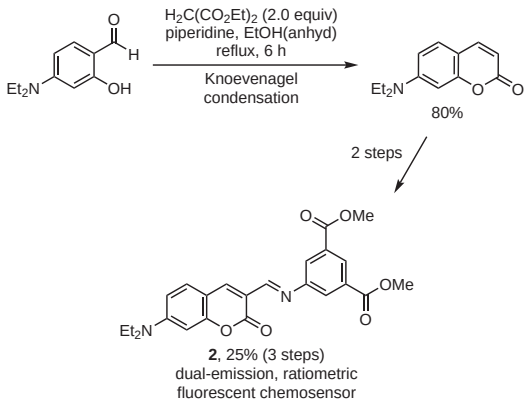

Scheme 2. An Example of the Use of the Knoevenagel Condensation as a Key Step in the Synthesis of the Dual-Emission Ratiometric Fluorescent Chemosensor **2**. *(Ref. 6)*

years.[22] Relevant studies can be performed in water, in another solvent when water solubility is low, and even in a range of pH values for those probes that are not sensitive to pH.

7-Vinyloxy-4-methylcoumarin (**3**), a hybrid comprising methylcoumarin as a fluorophore and a vinyl ether group as a recognition unit, was shown to be highly selective and sensitive to Hg^{2+} in aqueous solutions (**Scheme 3**).[23] Wang, Zhou, and co-workers pointed out that, when compared to other systems, the protocol they developed using **3** is a low cost, simple, and highly sensitive Hg^{2+} detection method. Similarly, coumarin dye hybrid **2** (see Scheme 2) was employed by Jiao et al. as a highly selective, ratiometric fluorescent chemosensor to detect nanomolar levels of Hg^{2+} at physiological pH.[6] Interestingly, the novel, rectilinear, and π-extended rhodol–coumarin hybrid dye **4** was shown to possess high selectivity for Hg^{2+} ions on a nanomolar scale, even in the presence of biologically or environmentally relevant alkali, alkaline earth, and transition metal ions (**Scheme 4**).[24] The detection mechanism is believed to involve an Hg^{2+} promoted reaction cascade consisting of ring-opening and desulfurization. Moreover, incubation of **4** with HeLa cells [37 °C, 1.5 h, CO_2 atmosphere (5%)] with and without Hg^{2+} suggested that **4** is living-cell-membrane permeable, making it suitable for practical in vitro applications.

Cheng and co-workers have recently reported the synthesis of a pair of novel and water-soluble thioacetalized coumarin hybrids and their application as ratiometric fluorescent probes that are highly selective for Hg^{2+} ions. The chemosensing ability was attributed to the mercury(II)-promoted conversion reaction of the dithioacetal functional group into the corresponding aldehyde with a corresponding shift in fluorescence from blue to green visible with the naked eye (**Scheme 5**).[22] The authors also showed that coumarin–hybrid probe **5** penetrates the membrane of HeLa cells and could potentially be used for the fluorescent imaging of mercury(II) in living cells.

3.2. Detection of Copper(II)

Cupric ion plays a key role in several basic physiological processes, and is the third most abundant heavy metal in humans. However, high levels of copper(II) in the human body can cause oxidative stress and disorders associated with neurodegenerative diseases, as well as rheumatoid arthritis, gastrointestinal disturbances, and Wilson's disease; in the environment, Cu^{2+} is considered a pollutant that is potentially very harmful to organisms.[7,21] A novel, highly selective, and highly sensitive method for detecting Cu^{2+} in acetonitrile in the presence of other metal ions has been reported by Mei, Zhou, and co-workers. This approach relies on colorimetric and fluorescence changes that result from a Cu^{2+}-induced intramolecular nucleophilic addition in coumarin–hybrid **6**, leading to a substituted imidazole ring (**Scheme 6**).[7] The changes, which are complete in less than 3

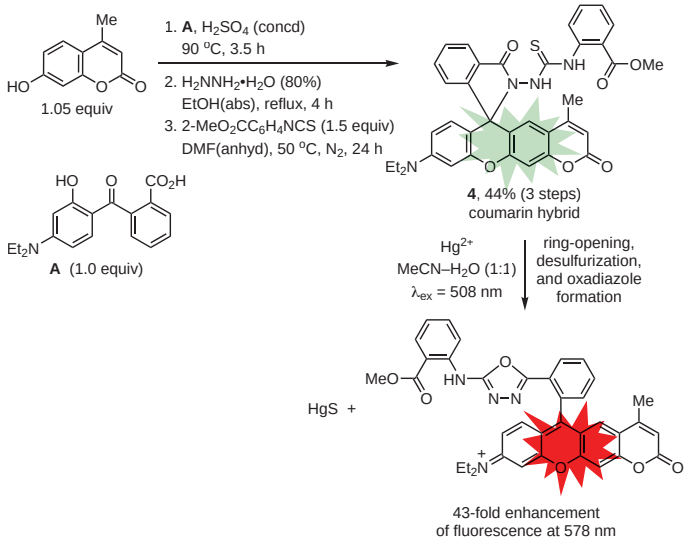

Scheme 4. Novel and Living-Cell-Membrane Permeable Rhodol–Coumarin Hybrid Dye **4** with Potential in Vitro Applications. *(Ref. 24)*

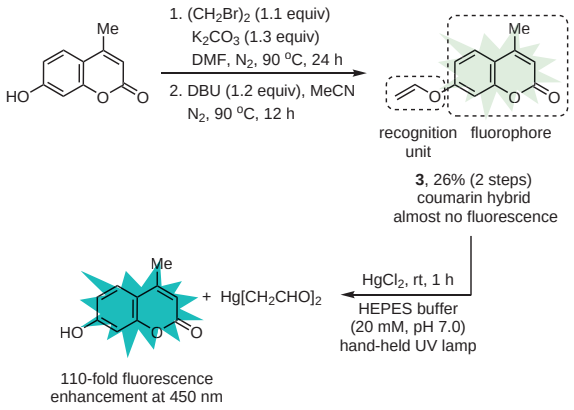

Scheme 3. Synthesis and Testing of 7-Vinyloxy-4-methylcoumarin (**3**) as a Coumarin-Hybrid Fluorescent Probe with High Selectivity for Mercuric Ion. *(Ref. 23)*

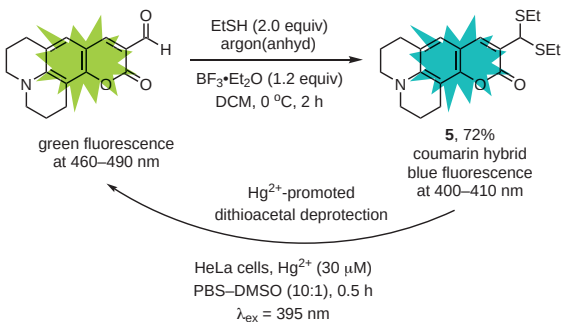

Scheme 5. Dithioacetal-Functionalized Coumarin-Based Probe for the Bioimaging of Mercury(II) in HeLa Cells. *(Ref. 22)*

minutes, would allow this process to be utilized for the real-time tracking of copper(II). The authors were also able to extend this methodology to detecting intracellular copper(II) in HepG2 cells, thus demonstrating that compound **6** could be employed as a practical and reliable probe for imaging Cu^{2+} in living cells.

The monitoring of Hg^{2+} and Cu^{2+} in the mitochondria of HeLa cells and mouse kidney tissues using the two new, structurally related, coumarin-based, and biocompatible fluorescent sensors **7** and **8** has been described by Zhou and co-workers (**Scheme 7**).[25] The authors carried out bioimaging experiments, fluorescence co-localization studies, and time effects studies in vitro to evaluate the ligands' response to metal ions. Both probes exhibited excellent selectivity for mercury(II) and copper(II) even in the presence of other ions. Probe **7** exhibited an excellent selective fluorescence response to Hg^{2+} in MeOH–H_2O, whereby its fluorescence intensity increased significantly for Hg^{2+} but changed only slightly in the presence of Cu^{2+}. In contrast, probe **8** exhibited significantly increased fluorescence intensity upon addition of Hg^{2+} but complete attenuation of fluorescence upon addition of Cu^{2+} in H_2O.

A number of other novel, coumarin-based fluorescent probes have also been developed and successfully tested for the selective detection of copper(II) under a variety of experimental conditions and in living cells (**Figure 2**).[8,9,21,26] In these cases, Cu^{2+} induces fluorescence enhancement or quenching either through complexation with the probe or through initial complexation followed by hydrolysis of an imino group to generate the fluorescent species.

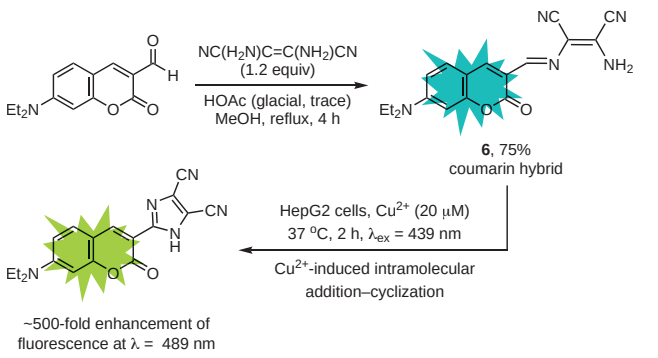

Scheme 6. Coumarin-Based Fluorescence Off-On Probe for Detecting Intra- and Extracellular Copper(II). *(Ref. 7)*

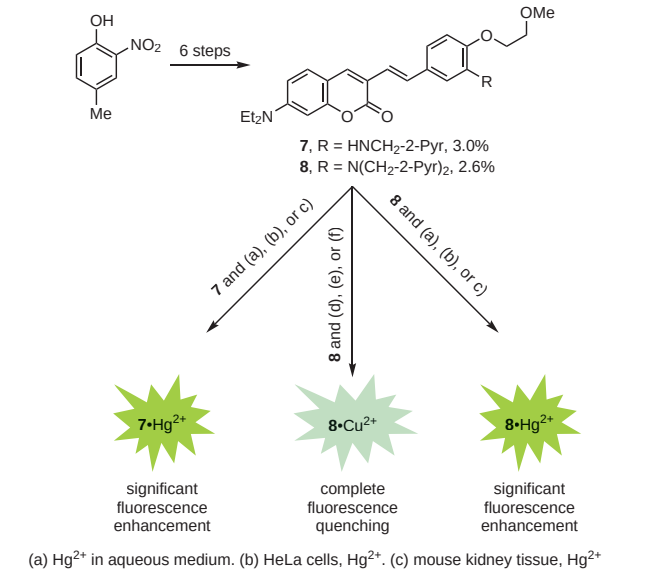

(a) Hg^{2+} in aqueous medium. (b) HeLa cells, Hg^{2+}. (c) mouse kidney tissue, Hg^{2+}
(d) Cu^{2+} in aqueous medium. (e) HeLa cells, Cu^{2+}. (f) mouse kidney tissue, Cu^{2+}

Scheme 7. New, Structurally Related Fluorescent Probes That Are Highly Selective for Hg^{2+} and Cu^{2+} in Vitro, in HeLa Cells, and in Mouse Kidney Tissues. *(Ref. 25)*

3.3. Ratiometric Sensing of Zinc(II)

Zinc is one of the most important transition metals. It is present in the human body in nanomolar (nM) to millimolar (mM) concentrations, and is involved in a variety of biological processes. Genetic abnormalities and environmental factors may lead to disturbances in the metabolism of zinc, resulting in a variety of diseases such as Alzheimer's disease, Parkinson's disease, epilepsy, cerebral ischemia, amyotrophic lateral sclerosis (ALS), diabetes, and childhood diarrhea. As a consequence, there is keen interest in developing suitable fluorescent probes for detecting Zn^{2+} in order to help maintain its physiological concentrations at suitable levels.

To this end, two new, coumarin-based ligands, **9a** and **9b**, have been synthesized and evaluated as ratiometric fluorescent

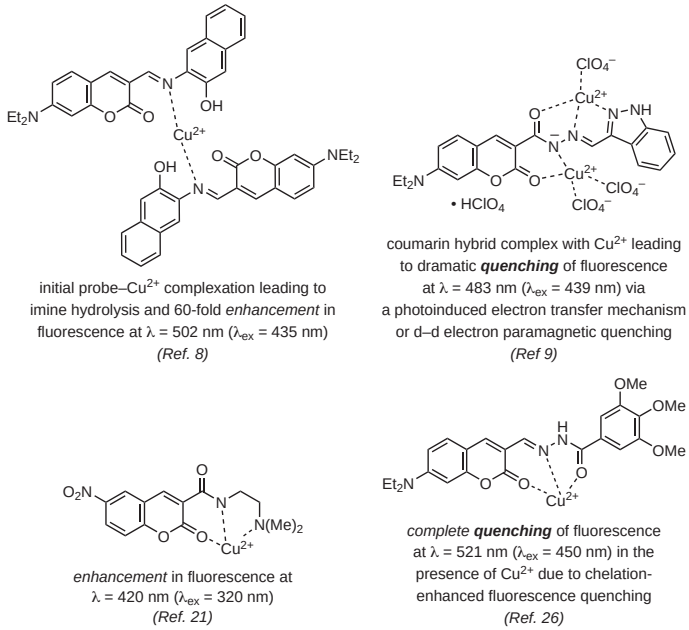

Figure 2. Novel Coumarin–Hybrid Chemosensors of Copper(II) Either via Enhancement or Quenching of Fluorescence.

probes for detecting and quantifying Zn^{2+} in aqueous media and in living cells (**Figure 3**).[10,11] Both displayed good selectivity and high sensitivity toward Zn^{2+} without interference by other metal ions, especially by Cd^{2+}, which is in the same periodic table group as Zn^{2+}. For both **9a** and **9b**, the ratiometric fluorescence response was ascribed to enhanced intramolecular charge-transfer upon binding of the ligand to Zn^{2+}. In ethanol–water (9:1), coumarin–furan hybrid, **9a**, exhibited a fast (0.5 min) and reversible ratiometric fluorescence response, suggesting that **9a** could be employed as a ratiometric fluorescent sensor for the detection and monitoring of Zn^{2+} in environmental and biological systems in real time and under physiological conditions.[10] Similarly, coumarin–quinoline hybrid **9b** showed significant colorimetric and ratiometric responses to Zn^{2+}, exhibited low toxicity, and had good cell-membrane permeability at physiological temperature in MCF-7 cells.[11] It was also suggested that **9b** could be utilized for the qualitative determination of Zn^{2+} in living cells and its quantitative detection in environmental water samples.

3.4. Chemosensing of Aluminum(III), Phosphate, and Pyrophospate

Two modes of fluorescence enhancement have been employed for the selective and highly sensitive detection of aluminum(III) in aqueous buffers at neutral pH values in the presence of other metal ions and its bioimaging in living cells (HeLa or PC3). The first mode relies on an Al^{3+}-triggered fluorescence resonance energy transfer (FRET) from quinoline to coumarin in the ratiometric fluorescent small-molecule probe **10** (**Scheme 8**).[27] This chemosensor had a very low detection limit for Al^{3+} (1×10^{-6} M) and passed through HeLa or PC3 cell membranes in a short period of time, making it suitable for monitoring intracellular aluminum(III) in vitro and potentially in vivo.

In the second mode, chelation-enhanced fluorescence (CHEF) was taken advantage of in developing a highly sensitive and selective coumarin–Schiff base sensor, **11**, for detecting Al^{3+} in 90% aqueous methanol at pH 7.4 (HEPES buffer) and in living HeLa cells (**Scheme 9**).[28] The 1:1 complex resulting from the binding of Al^{3+} to **11** was found to act by the reverse process, fluorescence attenuation, as a highly selective probe for detecting pyrophosphate ($HP_2O_7^-$) and phosphate ($H_2PO_4^-$) anions, such as found in calf thymus DNA (ctDNA), in the presence of 20 equivalents of other competitive anions such as acetate and nitrate.

3.5. Ratiometric Fluorescence Detection of Fluoride

A new, silyl-protected fluorescein-coumarin hybrid, **12**, has been reported by Ma, Song, and co-workers as a highly selective and sensitive probe for the ratiometric fluorescence detection of fluoride ion in the presence of other competing anions, reactive oxygen species (e.g., H_2O_2, ClO^-, $ONOO^-$), and sulfur-containing organics (e.g., GSH, Cys).[12] Upon addition of F^-,

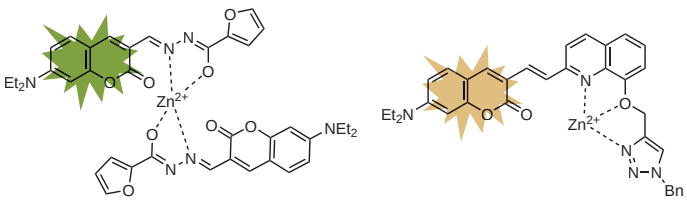

Figure 3. Ratiometric Fluorescent Sensors Suitable for the Detection and Monitoring of Zinc(II) in Environmental and Biological Systems.

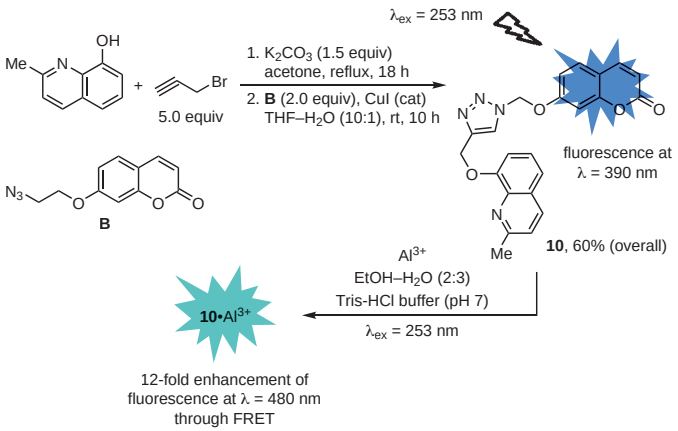

Scheme 8. Chemosensing of Al^{3+} via a Fluorescence Resonance Energy Transfer (FRET) Mechanism. *(Ref. 27)*

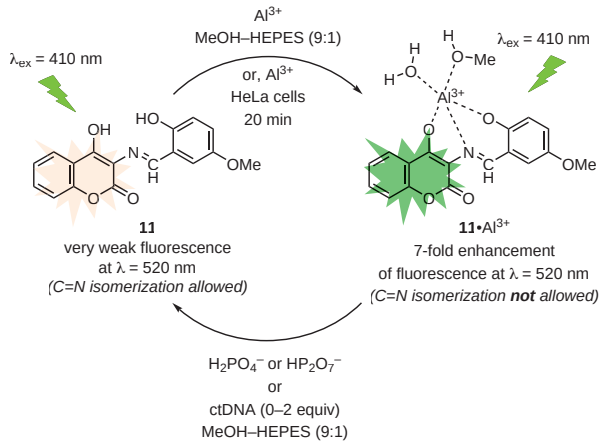

Scheme 9. Coumarin–Schiff Base Probe for the Highly Selective Detection of Aluminum(III) as Well as Pyrophosphate and Phosphate Anions in the Presence of Competing Ions. *(Ref. 28)*

desilylation of the phenolic oxygen occurs by rapid reaction of fluoride with the *tert*-butyldiphenylsilyl (TBDPS) protecting group leading to fluorescein–coumarin hybrid **13**, and a change of fluorescence from blue to green (**Scheme 10**). The limit of detection (LOD) for fluoride was calculated to be 0.025 μM, and the process was successfully applied to the bioimaging of fluoride in living HeLa cells and 5-day-old zebrafish larvae, hinting at the potential application of this process in clinical diagnosis. Another coumarin-based, ratiometric fluorescent probe that relies on a desilylation of a triisopropylsilyl group by fluoride ion was reported by Shen et al., and successfully applied to the detection of fluoride in mitochondria of living HepG2 cells by ratiometric fluorescence imaging.[29]

Two other effective and highly selective sensors for fluoride ion have also been reported. These rely on fast colorimetric changes or fluorescence quenching to selectively detect and determine fluoride ion concentration (**Figure 4**).[13,14] They also proved to have high response rates and very low fluoride detection limits (e.g., LOD = 2.16 x 10^{-7} M).

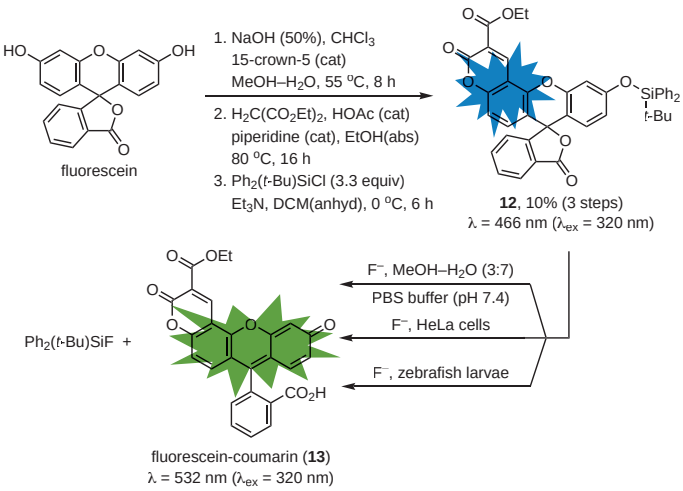

Scheme 10. Highly Selective and Sensitive Ratiometric Fluorescence Detection and Quantification of Fluoride Ion Based on Its Well-Known Affinity for the *tert*-Butyldiphenylsilyl Group. *(Ref. 12)*

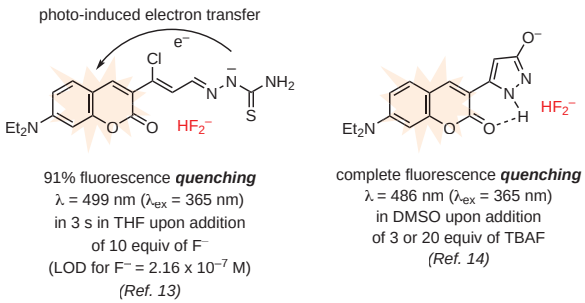

Figure 4. Other Effective and Highly Selective Coumarin-Based Sensors for Fluoride Ion.

3.6. Sensing of Hypochlorite (ClO^-) in Aqueous Media and Living Cells

Hypochlorous acid and its conjugated base (HClO/ClO^-) play an important role in biological systems; however, excessive production of HClO/ClO^- could lead to several types of disorders, such as Parkinson's disease, rheumatism, lung injury, arthritis, degeneration of neurons, and even certain cancers. Hence, the monitoring of hypochlorite anion (ClO^-) in a sensitive and selective manner in aqueous media and living cells is of great interest.

To this end, a number of research groups have reported highly sensitive and selective coumarin-based hybrids for the ratiometric fluorescence detection of hypochlorite in water samples and in mitochondria of living cells (**Scheme 11**).[3,30,31] Rapid response times (e.g., 20–30 s) and low detection limits (e.g., 8.3–22 nM) were observed with these probes, without interference by other anions or reactive oxygen or nitrogen species (e.g., HO•, H_2O_2, $O_2^{\bullet-}$, $^1O_2$, *t*-BuO•, $ONOO^-$, NO•,NO_2^-) over a range of pH values. The hypochlorite-recognition mechanism of these probes relied in each case on a unique chemical reaction triggered by ClO^-—such as oxime oxidation to an aldehyde, δ-lactone ring-opening,

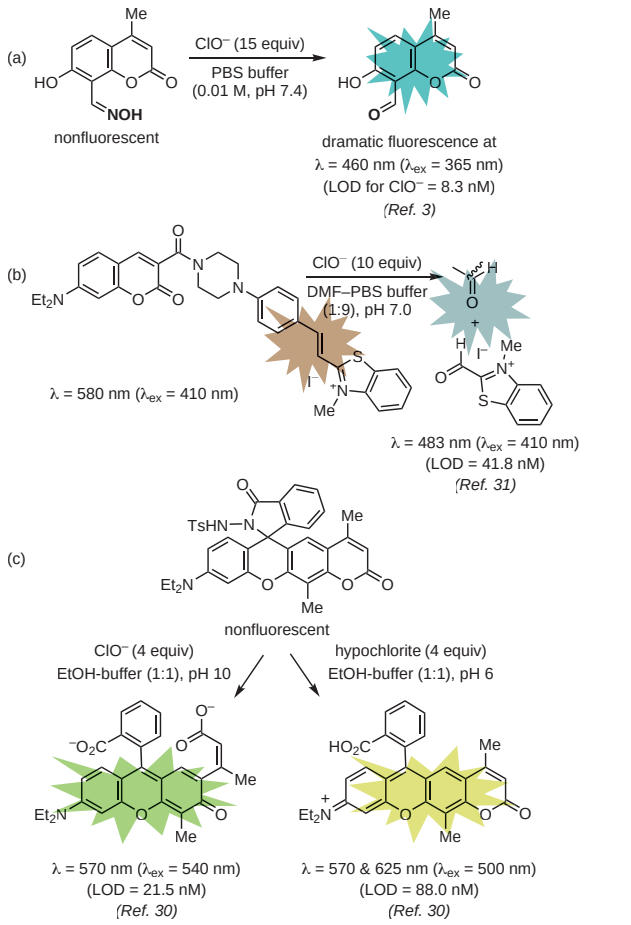

Scheme 11. Selective ClO^- Detection by Hypochlorite-Triggered Unique Reactivity of Coumarin-Based Fluorescent Probes.

or oxidative cleavage of a carbon–carbon double into two formyl groups—and resulting in an intense fluorescence response. The probes were successfully applied to the determination of ClO^- in real water samples (tap, river, and lake water, as well as diluted commercial disinfectant) and to the bioimaging of hypochlorite in RAW264.7 and SW480 cells.

3.7. Colorimetric and Ratiometric Detection of Sulfite

Endogenous sulfur dioxide (SO_2) is present in mammalian cells in the form of its aqueous derivatives (HO_3S^- and SO_3^{2-}), which are generated in biosynthetic pathways from sulfur-containing amino acids through the action of enzymes such as thiosulfate sulfurtransferase. While low concentrations of sulfites can be beneficial, abnormally high concentrations are associated with a number of health disorders such as respiratory and cardiovascular diseases.[15,32] Moreover, sulfur dioxide is a recognized air pollutant generated by the burning of fossil fuels. The detection, determination, and monitoring of the levels of SO_2 and its derivatives in the environment and in biological systems is therefore of great interest.

The research groups of Qian,[15] Zhao,[32] and Wang[33] have independently developed coumarin hybrids for sensing sulfites in aqueous media and living cells, such as human colon cancer cells SW480 as well as HeLa, HepG2, L-02, and L929 cells (**Figure 5**). Highly selective, sensitive, and rapid colorimetric, ratiometric, or turn-on fluorescence sensing was achieved in each case with sulfite detection limits in the nano- to micromolar range. The sensing mechanisms consisted of either a disruption of π conjugation via bisulfite addition to a double bond,[15] SO_3^{2-} addition to a hemicyanine moiety that interrupts an ICT/FRET process,[32] or the liberation of 6-hydroxycoumarin from its levulinate ester precursor.[33]

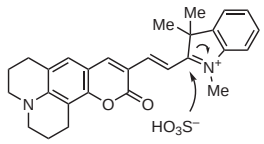

addition of HO_3S^- to C=N, followed by rearrangement, significantly enhances fluorescence at λ = 516 nm (λ_{ex} = 470 nm) in 10 min in PBS buffer (pH 7.4)–DMSO (trace) (LOD for HSO_3^- = 0.53 μM)
(Ref. 15)

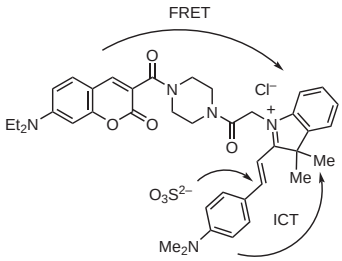

SO_3^{2-}	FRET	ICT	λ_{ex}	λ_{em}	Fl. Color
absent	on	on	430 nm	589 nm	red
present	off	off	430 nm	476 nm	blue

(a) In DMF–PBS buffer (4:6), pH 7.4. (b) LOD for SO_3^{2-} = 12.9 nM. (c) 32.3-fold enhancement of fluorescence observed within 3 min. (d) ICT = intramolecular charge transfer. (e) FRET = fluorescence resonance energy transfer.
(Ref. 32)

Figure 5. Rapid, Selective, and Sensitive Detection of Sulfur Dioxide Derivatives.

3.8. Hydrogen Peroxide Detection

The known reactivity of hydrogen peroxide toward boronates has been taken advantage of in the design and testing of new coumarin-based probes for the detection of hydrogen peroxide in aqueous buffer and in mitochondria of living cells.[34,35] In one instance, Shen et al. have demonstrated that coumarin–pyridinium hybrid **14** can be utilized as a highly sensitive and selective colorimetric and ratiometric fluorescent sensor for H_2O_2 with an LOD of 10 nM (**eq 1**).[35] They also showed that this probe is not responsive to other biologically relevant reactive oxygen species (ROS), reactive nitrogen species (RNS), or metal ions, as these did not cause any significant change in the I_{535}/I_{640} emission ratio under the same conditions. Additionally, the authors reported the successful application of this probe to the bioimaging of hydrogen peroxide in mitochondria of NRK cells with a response time of 5 minutes. Investigation of the sensing mechanism by ^{1}H NMR and HRMS as well as by density functional theory (DFT) calculations revealed that it takes place through oxidation of the boronate with hydrogen peroxide followed by hydrolysis and 1,6-elimination to form coumarin-pyridine **15**.

3.9. Biothiol Detection and Imaging

Thiol-containing biomolecules, known collectively as biothiols, include cysteine (Cys) and homocysteine (Hcy) amino acids and the low-molecular-weight antioxidant peptide glutathione (GSH). Biothiols play important roles in biological systems, and their levels within cells or in human plasma are indicative of underlying disorders and risk factors for a broad range of conditions and diseases.[36] It is thus not surprising that the development of effective fluorescent probes for the selective detection of specific biothiols has been an active area of research aiming to provide tools and methods for the early diagnosis of these conditions, risk factors, and disorders.[37–43]

Among the effective biothiol sensors developed, coumarin derivative **16** proved to be a highly sensitive colorimetric and fluorescent probe not only for the imaging of cysteine and

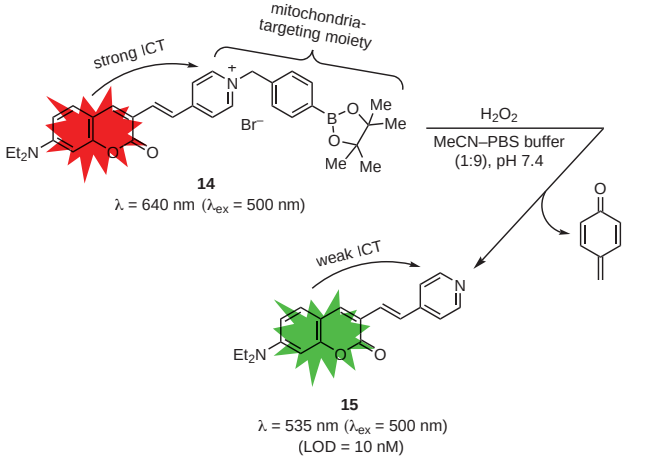

eq 1 *(Ref. 35)*

homocysteine over GSH in living HeLa cells and mouse liver tissue, but also for their detection in five types of animal serum from chicken, horse, sheep, cattle, and goat. This rapid and biocompatible probe works by fluorescence turn-on following suppression of a photoinduced electron transfer (PET) as a result of a cyclization reaction between the thiol group and the aldehyde functional group in the probe, and was not responsive to 19 other amino acids tested (**Scheme 12**, Part (a)).[36]

Meng et al. reported another new and effective coumarin-based chemosensor, **17**, for cysteine in buffer solution, in the endoplasmic reticulum of live U-343 MGa and MDA-MB-231 cells, and in real urine samples. Probe **17** achieves the highly selective and sensitive detection of Cys (LOD for Cys = 0.72 μM) through an "ON-OFF-ON" fluorescence process (Scheme 12, Part (b)).[38] In the absence of copper(II), **17** is highly fluorescent; this fluorescence is significantly reduced (98.4% quenching) after addition of Cu^{2+}, which forms a complex with **17**. However, upon incubation with Cys, complex **17**•Cu^{2+} is decomposed, and highly fluorescent **17** is released with 43.4-fold enhancement in fluorescence that is not affected by the presence of competing biomolecules and physiologically important anions.

Yin, Huo, and co-workers reported the first recyclable coumarin-based sensor, **18**, for the rapid turn-on fluorescence detection of Cys in aqueous buffer and exogenous Cys in living A549 and Hela cells (Scheme 12, Part (c)).[42] Probe **18** showed a 78-fold fluorescence enhancement upon addition of Cys—by forming the cysteine thiol 1,4-addition product, **19**—and could detect Cys even in the presence of biothiols Hcy and GSH, common amino acids, metal ions, physiologically relevant anions, *N*-acetylcysteine, and H_2O_2. The specificity of the response of **18** toward Cys was demonstrated in an "ON-OFF-ON" fluorescence sequence, whereby the quenching effects of *N*-ethylmaleimide (NEM) or H_2O_2 on the fluorescence of **19** were reversed by re-introducing Cys. The authors subjected probe **18** to five such "ON-OFF-ON" cycles and observed no noticeable attenuation in the fluorescence of **19**, providing evidence for the recyclability of **18**.

A number of other, novel, and coumarin-based probes have been synthesized and successfully utilized for the highly selective fluorescent sensing of biothiols such as cysteine, homocysteine, and glutathione in aqueous buffer and in living cells without interference by other physiologically relevant molecular species or anions (**Figure 6**).[16,37,39–41,43] However, the limits of detection of these probes for biothiols varied widely from 0.46 nM to 657 nM (Cys), 0.86 to 79 nM (HCy), and 0.73 nM to 1.07 μM (GSH). In one case, the coumarin-based probe proved effective also for detecting cyanide ion (LOD for CN^- = 0.32 nM).[40]

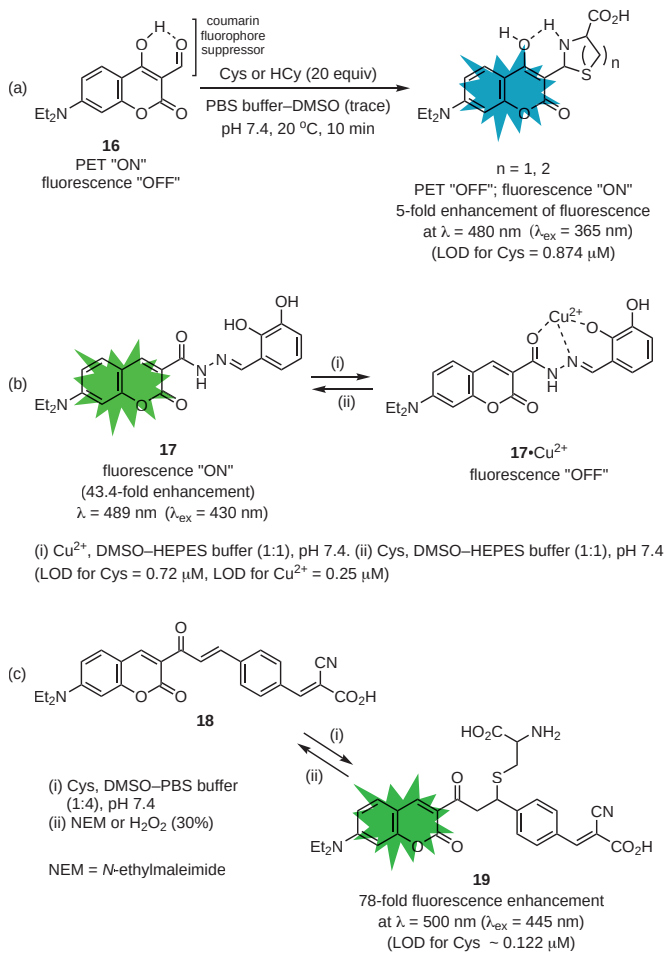

Scheme 12. Examples of Highly Selective and Sensitive Fluorescent Probes for the Determination of Biothiols. *(Ref. 36,38,42)*

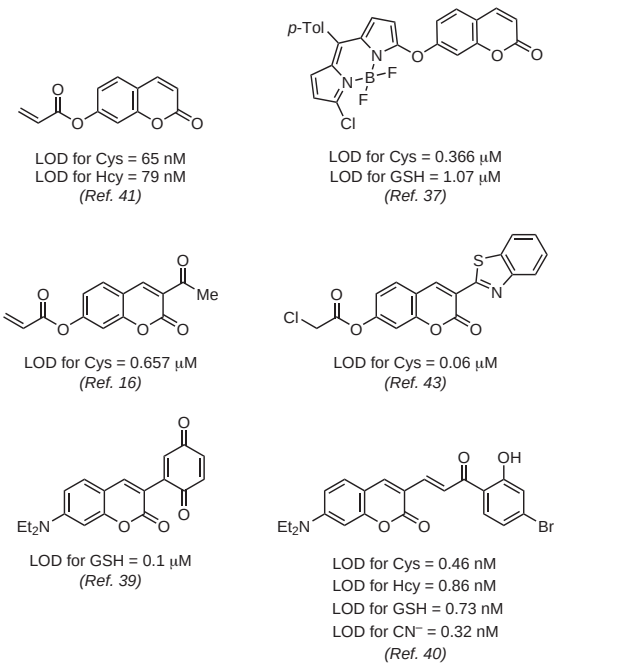

Figure 6. Additional, Selective, and Sensitive Coumarin-Based Sensors for the Detection and Imaging of Biothiols.

4. Conclusion

We have highlighted in this review the rapidly growing applications of coumarin–small-molecule hybrids as fast and highly selective and sensitive fluorescent probes for detecting, quantifying, and bioimaging of a wide variety of physiologically relevant metal ions, anions, molecules, reactive oxygen species, and reactive nitrogen species. It is our sincere hope that the review will prove of great benefit to a wide range of researchers looking to capitalize on ever more sensitive and selective tools for the assay of analytes of interest in biological systems.

5. Acknowledgments

The authors thank the National Council for Scientific and Technological Development (CNPq), the Coordination Bureau for the Improvement of Higher Education Personnel (CAPES), and the Espírito Santo Research Foundation (FAPES) for financial support and fellowships.

6. References

(1) Ibrar, A.; Shehzadi, S. A.; Saeed, F.; Khan, I. *Bioorg. Med. Chem.* **2018**, *26*, 3731.
(2) Fu, Y.-J.; Yao, H.-W.; Zhu, X.-Y.; Guo, X.-F.; Wang, H. *Anal. Chim. Acta* **2017**, *994*, 1.
(3) Han, J.; Li, Y.; Wang, Y.; Bao, X.; Wang, L.; Ren, L.; Ni, L.; Li, C. *Sens. Actuators, B* **2018**, *273*, 778.
(4) Li, Q.; Hu, Y.; Hou, H.-N.; Yang, W.-N.; Hu, S.-L. *Inorg. Chim. Acta* **2018**, *471*, 705, and reference 24 therein.
(5) Choi, H.; Kim, J.; Lee, K. *Tetrahedron Lett*. **2016**, *57*, 3600.
(6) Jiao, Y.; Liu, X.; Zhou, L.; He, H.; Zhou, P.; Duan, C. *Sens. Actuators, B* **2017**, *247*, 950.
(7) Yang, M.; Wang, H.; Huang, J.; Fang, M.; Mei, B.; Zhou, H.; Wu, J.; Tian, Y. *Sens. Actuators, B* **2014**, *204*, 710.
(8) Wang, S.; Wang, Z.; Yin, Y.; Luo, J.; Kong, L. *J. Photochem. Photobiol., A* **2017**, *333*, 213.
(9) He, G.; Liu, X.; Xu, J.; Ji, L.; Yang, L.; Fan, A.; Wang, S.; Wang, Q. *Spectrochim. Acta, Part A* **2018**, *190*, 116.
(10) Li, C.; Li, S.; Yang, Z. *Spectrochim. Acta, Part A* **2017**, *174*, 214.
(11) Wu, G.; Gao, Q.; Li, M.; Tang, X.; Lai, K. W. C.; Tong, Q. *J. Photochem. Photobiol., A* **2018**, *355*, 487.
(12) Jiao, S.; Wang, X.; Sun, Y.; Zhang, L.; Sun, W.; Sun, Y.; Wang, X.; Ma, P.; Song, D. *Sens. Actuators, B* **2018**, *262*, 188.
(13) Ma, L.; Leng, T.; Wang, K.; Wang, C.; Shen, Y.; Zhu, W. *Tetrahedron* **2017**, *73*, 1306.
(14) Babür, B.; Seferoğlu, N.; Seferoğlu, Z. *J. Mol. Struct.* **2018**, *1161*, 218.
(15) Yao, Y.; Sun, Q.; Chen, Z.; Huang, R.; Zhang, W.; Qian, J. *Talanta* **2018**, *189*, 429.
(16) Dai, X.; Wu, Q.-H.; Wang, P.-C.; Tian, J.; Xu, Y.; Wang, S.-Q.; Miao, J.-Y.; Zhao, B.-X. *Biosens. Bioelectron.* **2014**, *59*, 35.
(17) Liao, Y.-C.; Venkatesan, P.; Wei, L.-F.; Wu, S.-P. *Sens. Actuators, B* **2016**, *232*, 732.
(18) Vekariya, R. H.; Patel, H. D. *Synth. Commun*. **2014**, *44*, 2756.
(19) Priyanka; Sharma, R. K.; Katiyar, D. *Synthesis* **2016**, *48*, 2303.
(20) Li, J.; Zhang, C.; Wu, S.; Wen, X.; Xi, Z.; Yi, L. *Dyes Pigm*. **2018**, *151*, 303.
(21) Bekhradnia, A.; Domehri, E.; Khosravi, M. *Spectrochim. Acta, Part A* **2016**, *152*, 18.
(22) Cheng, X.; Qu, S.; Xiao, L.; Li, W.; He, P. *J. Photochem. Photobiol., A* **2018**, *364*, 503.
(23) Wu, C.; Wang, J.; Shen, J.; Bi, C.; Zhou, H. *Sens. Actuators, B* **2017**, *243*, 678.
(24) Huang, K.; Jiao, X.; Liu, C.; Wang, Q.; Qiu, X.; Zheng, D.; He, S.; Zhao, L.; Zeng, X. *Dyes Pigm*. **2017**, *142*, 437.
(25) Yao, S.; Zhang, G.; Wang, H.; Song, J.; Liu, T.; Yanga, M.; Yu, J.; Yang, X.; Tian, Y.; Zhang, X.; Zhou, H. *Sens. Actuators, B* **2018**, *272*, 574.
(26) Mergu, N.; Kim, M.; Son, Y.-A. *Spectrochim. Acta, Part A* **2018**, *188*, 571.
(27) Zhu, Q.; Li, L.; Mu, L.; Zeng, X.; Redshaw, C.; Wei, G. *J. Photochem. Photobiol., A* **2016**, *328*, 217.
(28) Sheet, S. K.; Sen, B.; Thounaojam, R.; Aguan, K.; Khatua, S. *J. Photochem. Photobiol., A* **2017**, *332*, 101.
(29) Shen, Y.; Zhang, X.; Zhang, Y.; Li, H.; Chen, Y. *Sens. Actuators, B* **2018**, *258*, 544.
(30) Zhu, J.-H.; Wong, K. M.-C. *Sens. Actuators, B* **2018**, *267*, 208.
(31) Wu, W.-L.; Zhao, X.; Xi, L.-L.; Huang, M.-F.; Zeng, W.-H.; Miao, J.-Y; Zhao, B.-X. *Anal. Chim. Acta* **2017**, *950,* 178.
(32) Zhang, L.-J.; Wang, Z.-Y.; Liu, J.-T.; Miao, J.-Y.; Zhao, B.-X. *Sens. Actuators, B* **2017**, *253*, 19.
(33) Wang, L.; Li, W.; Zhi, W.; Ye, D.; Wang, Y.; Ni, L.; Bao, X. *Dyes Pigm.* **2017**, *147*, 357.
(34) Kalyanaraman, B.; Hardy, M.; Podsiadly, R.; Cheng, G.; Zielonka, J. *Arch. Biochem. Biophys*. **2017**, *617*, 38.
(35) Shen, Y.; Zhang, X.; Zhang, Y.; Wu, Y.; Zhang, C.; Chen, Y.; Jin, J.; Li, H. *Sens. Actuators, B* **2018**, *255*, 42.
(36) Chen, C.; Liu, W.; Xu, C.; Liu, W. *Biosens. Bioelectron.* **2016**, *85*, 46.
(37) Liu, X.-L.; Niu, L.-Y.; Chen, Y.-Z.; Yang, Y.; Yang, Q.-Z. *Biosens. Bioelectron.* **2017**, *90*, 403.
(38) Meng, Q.; Ji, H.; Succar, P.; Zhao, L.; Zhang, R.; Duan, C.; Zhang, Z. *Biosens. Bioelectron.* **2015**, *74*, 461.
(39) Dai, X.; Du, Z.-F.; Wang, L.-H.; Miao, J.-Y.; Zhao, B.-X. *Anal. Chim. Acta* **2016**, *922*, 64.
(40) Sun, Y.; Shan, Y.; Sun, N.; Li, Z.; Wu, X.; Guan, R.; Cao, D.; Zhao, S.; Zhao, X. *Spectrochim. Acta, Part A* **2018**, *205*, 514.
(41) Wei, L.-F.; Thirumalaivasan, N.; Liao, Y.-C.; Wu, S.-P. *Spectrochim. Acta, Part A* **2017**, *183*, 204.
(42) Xie, X.; Yin, C.; Yue, Y.; Huo, F. *Sens. Actuators, B* **2018**, *267*, 76.
(43) Yang, J.; Yu, Y.; Wang, B.; Jiang, Y. *J. Photochem. Photobiol., A* **2017**, *338*, 178.

About the Authors

Carla Santana Francisco received her bachelor's degree in chemistry in 2006 from Paulista State University, São Paulo, Brazil. She then obtained her master's degree in medicinal chemistry (2009) and her doctorate degree in chemistry (2013) from Minho University, Portugal. Since 2018, she has been a postdoctoral researcher at the Federal University of Espírito Santo (UFES), working first with Professor Dr. Valdemar Lacerda, Jr., and presently with Professor Dr. Álvaro Cunha Neto. Carla's research experience covers a wide range from natural product

chemistry to synthetic and medicinal chemistry, biological assays, molecular modeling, and coumarin synthesis.

Thays Cardoso Valim obtained a B.Sc. degree in forensic investigation and analysis (2013) from the Institute of Technology Sligo, Ireland, and a B.Sc. degree in chemistry (2015) from the Federal University of Espirito Santo (UFES). She received her master's degree in chemistry (2019) from UFES under the supervision of Professor Dr. Alvaro Cunha Neto. Thays has carried out research in analytical chemistry, NMR spectroscopy, food chemistry, forensic science, and environmental chemistry.

Álvaro Cunha Neto received his B.Sc. (1999), M.Sc. (2002), and Ph.D. (2006, with Professor Dr. Gil Valdo José da Silva) degrees in chemistry from the University of São Paulo. He then did postdoctoral research at the State University of Campinas (2007–2009) under the supervision of Professor Dr. Roberto Rittner Neto. Álvaro is currently Associate Professor at UFES, conducting research in NMR spectroscopy, organic synthesis, and petroleum science.

Valdemar Lacerda, Jr., obtained his B.Sc. degree in chemistry in 1997 from the Federal University of Goiás, and received his M.Sc. (2000) and Ph.D. (2004) degrees from the University of São Paulo (USP), conducting research in organic synthesis and NMR spectroscopy. After two years of postdoctoral research at USP, he joined the department of chemistry at the Federal University of Espírito Santo as Associate Professor. His current research interests focus on organic synthesis, NMR studies, theoretical calculations, and petroleum studies. Valdemar is CNPq level 2 researcher, and has published about 80 articles in different high-impact journals.

MERCK

Find your Lead

Leverage DNA-encoded library technology for drug discovery

Accelerate your drug discovery with the DNA-encoded library (DEL) technology, an alternative approach to high-throughput screening (HTS) compound libraries for effective hit and lead discovery.

Learn more about the DyNAbind off-the-shelf DNA-encoded library, visit **SigmaAldrich.com/DEL**

Sigma-Aldrich®
Lab & Production Materials

Page intentially blank

Page intentially blank

VOLUME 52, NO. 3 | **2019**
SPECIAL ISSUE: DNA-ENCODED LIBRARIES (DELs)

MERCK

ALDRICHIMICA ACTA

DNA-Encoded Libraries—*Finding the Needle in the Haystack*

DNA-Encoded Fragment Libraries: Dynamic Assembly, Single-Molecule Detection, and High-Throughput Hit Validation

DNA-Encoded Library Chemistry: Amplification of Chemical Reaction Diversity for the Exploration of Chemical Space

DEAR READER:

We, at Merck, value the spirit of discovery. Since 2006, the Bader Award in Synthetic Organic Chemistry has recognized outstanding research from graduate students all over the world. This year, four eminently deserving young scientists were selected to receive the award and were invited to present their winning research at the 2019 Bader Student Chemistry Symposium in Milwaukee, WI, on September 12, 2019.

Michael Crocker, of Vanderbilt University, gave a presentation on "The Halo-Amino-Nitro Alkane Functional Group: A Platform for Reaction Discovery". He explained, "From an organic chemistry perspective, the next advancement I expect to fundamentally impact the way we put molecules together is C–H activation. Just as cross-coupling revolutionized synthetic planning, C–H activation will give access to more complex and difficult chemical space with implications in the particularly exciting areas of sustainable energy materials and personalized medicine."

Lucas Hernandez, of the University of Illinois at Urbana-Champaign, stated, "With the advent of machine learning in chemistry, the discovery of novel reactions will become more rapid over the next 100 years." His research on the "Synthesis of Isocarbostyril Alkaloids from Benzene" demonstrated how new compounds can be synthetically discovered and tested, providing molecular solutions to pressing challenges in oncology.

For **Joseph Dennis Jr**, of Massachusetts Institute of Technology, the need to mitigate the adverse environmental and economic effects of climate change on oceans should be paramount in order to protect the livelihood and food supply of millions of people that rely on fisheries. His research on "Breaking the Base Barrier: An Electron-Deficient Catalyst Enables the Use of Common, Soluble Bases in Pd-Catalyzed C–N Coupling" explores possible ways to reverse carbon dioxide absorption that is causing the current acidification of oceans while the world continues to work on eliminating the root causes.

Samantha Green, of Scripps Research, speculated that other variations of dual catalysis would significantly impact chemistry in the next 100 years. Her research on "Quaternary Centers via Dual-Catalytic Alkene Hydroarylation" identified the biocompatibility of MHAT catalysts, which could lead to the development of new synergistic methods for metal–enzyme dual catalysis or artificial metalloenzymes.

In addition to the graduate students, Dr. Joseph R. Clark, of Marquette University, gave the keynote presentation on his research on "Site-Selective Copper-Catalyzed Deuterium Incorporation into Small Molecules".

For more information on this year's event, visit **SigmaAldrich.com/BaderAward.**

ALDRICHIMICA ACTA
VOL. 52, NO. 3 • 2019

Merck KGaA
Frankfurter Strasse 250
64293 Darmstadt, Germany
Phone +49 6151 72 0

To Place Orders / Customer Service
Contact your local office or visit
SigmaAldrich.com/order

Technical Service
Contact your local office or visit
SigmaAldrich.com/techinfo

General Correspondence
Editor: Sharbil J. Firsan, Ph.D.
Sharbil.Firsan@milliporesigma.com

Subscriptions
Request your FREE subscription to the *Aldrichimica Acta* at **SigmaAldrich.com/acta**

The entire *Aldrichimica Acta* archive is available at **SigmaAldrich.com/acta**

Aldrichimica Acta (ISSN 0002-5100) is a publication of Merck KGaA.

"PLEASE BOTHER US."

Dear Fellow Chemists,

Professor Donald A. Watson of the Department of Chemistry and Biochemistry at the University of Delaware kindly suggested that we offer (bathocuproine)$NiBr_2$ (**902985**), which is used as part of a novel and general catalytic system for the C-alkylation of nitroalkanes with unactivated alkyl iodides at 40 °C under mild reaction conditions. The system exhibits excellent functional-group tolerance; works with primary, secondary, and tertiary alkyl iodides; and offers easy access to a diversity of complex nitroalkanes in moderate-to-good yields. The system's effectiveness was demonstrated in a two-step synthesis of the antiviral drug adapromine in 52% yield.

Rezazadeh, S.; Devannah, V.; Watson, D. A. *J. Am. Chem. Soc.* **2017**, *139*, 8110.

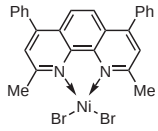

902985

902985	(Bathocuproine)$NiBr_2$	250 mg

We welcome your product ideas. Do you need a product that is not featured on our website? Ask us! For more than 60 years, your research needs and suggestions have shaped our product offering. Email your suggestion to **techserv@sial.com**.

Udit Batra, Ph.D.
CEO, Life Science

TABLE OF CONTENTS

ABOUT OUR COVER

Perhaps it is auspicious to be featuring a field with huge haystacks on the cover of this issue of the *Acta*, which is shining light on the rapidly evolving research field of DNA-Encoded Chemical Libraries (DECLs). Until recently, the search for "hits" in DECLs has seemed like looking for the proverbial needle in the haystack. But, today, researchers, armed with more effective and selective synthetic methods and more sensitive analytical tools, have become more adept at finding promising leads in their DECLs—to the benefit of all.


Detail from ***Haystacks: Autumn***. Photo courtesy The Metropolitan Museum of Art, New York, NY.

Jean-François Millet (1814–1875), a member of the Barbizon School of nature painters, finished ***Haystacks: Autumn*** (oil on canvas, 85.1 x 110.2 cm) ca. 1874. Believed to be one of his last paintings, it was commissioned by a patron as part of a series depicting the four seasons.* The painting depicts an end-of-harvest scene most likely painted in Millet's workshop based on sketches he made outdoors of fields near Barbizon where he was living. The autumnal colors, the impending storm, and the afternoon sun perhaps foreshadow Millet's death less than a year later. Millet's work was a significant influence on later 19-century European painters such as van Gogh and Seurat.

This painting is a bequest of Lillian S. Timken to the Metropolitan Museum of Art, New York, NY.

** To find out about the other three paintings in the series, visit **SigmaAldrich.com/Acta***

MERCK

Find your Lead

Leverage DNA-encoded library technology for drug discovery

Accelerate your drug discovery with the DNA-encoded library (DEL) technology, an alternative approach to high-throughput screening (HTS) compound libraries for effective hit and lead discovery.

Learn more about the DyNAbind off-the-shelf DNA-encoded library, visit **SigmaAldrich.com/DEL**

Sigma-Aldrich®
Lab & Production Materials

DNA-Encoded Fragment Libraries: Dynamic Assembly, Single-Molecule Detection, and High-Throughput Hit Validation

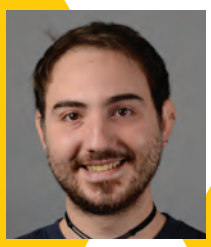
Dr. F. V. Reddavide


Dr. M. Thompson


Dr. L. Mannocci


Prof. Y. Zhang

Francesco V. Reddavide,[a] Michael Thompson,[a] Luca Mannocci,[b] and Yixin Zhang*[,c]

[a] DyNAbind GmbH, Tatzberg 47, 01307 Dresden, Germany
[b] DECLTech Consulting, Birkenweg 13, 5074 Eiken, Switzerland
[c] B CUBE - Center for Molecular Bioengineering, Technische Universität Dresden, Tatzberg 41, 01307 Dresden, Germany
Email: yixin.zhang1@tu-dresden.de

Keywords. DNA-encoded chemical library (DECL); self-assembly; screening; selection; fragment-based drug discovery; bidentate; protein; inhibitor; drug discovery; sequencing; DNA origami.

Abstract. An urgent challenge in chemistry and biotechnology is to develop a routine, robust, and cost-effective method for the identification of molecules that specifically bind to a large variety of protein targets. In recent years, an elegant selection method for small-molecule drug discovery, DNA-encoded chemical library (DECL) technology, has been receiving much attention from the pharmaceutical and biotechnology industries. Here, we review the major recent developments in DECL technology, with a focus on the self-assembling dual-display format, which aims to combine the bio-inspired selection process with a fragment-based approach to discover potent binders to protein targets.

Outline

1. Introduction

1.1. Challenges in Drug Discovery

Cancer is not one disease; rather, it is many different diseases that develop in various organs and are associated with a myriad of genes and their mutations, as well as numerous environmental factors. The same is also true for many other diseases such as autoimmune disease or dementia. Specific diagnoses and treatments have been developed for specific diseases, and those have become not only increasingly more efficient, but also more sophisticated, with the ultimate goal of developing truly personalized medicine. Target complexity combined with an ageing population and the looming expiration of blockbuster patents have driven an unprecedented development effort for novel drug discovery technologies to complement existing high-throughput screening (HTS) platforms.[1-2] One such technology is DNA-Encoded Chemical Library (DECL) synthesis and selection technology. Originally proposed by Brenner and Lerner in 1992,[3]

the last 27 years have seen this idea grow from a "back-of-the-envelope scribble" into an increasingly mature and robust tool for hit discovery.[4a]

A DECL is a pooled collection of up to billions of different molecules, each of which is tagged with a unique DNA strand that functions primarily as an identifying barcode. In a standard DECL compound selection, a target protein is immobilized on a solid support and treated with the library, followed by washing to remove non-binding library members. This is followed by elution of binding moieties, which are then amplified via a Polymerase Chain Reaction (PCR) and sequenced by Next Generation Sequencing (NGS) to reveal the identities of the binding compounds by ranking the sequences according to their frequency. The identified hits are then quantitatively validated in follow-up experiments using an orthogonal technology—e.g., enzyme inhibition assay, isothermal titration calorimetry, fluorescence polarization, or surface plasmon resonance—to determine binding affinity and/or biological potency (e.g., K_d, IC_{50}, EC_{50}) and thus prioritize the further development of the hits (**Figure 1**).[4b,c]

Over the past years, advances in DECL technologies have rendered the field too broad for a thorough treatment in only one review article. Therefore, we will focus our discussion in this paper on fragment-based DECL approaches. Generally speaking, fragment-based discovery has become increasingly popular because of the belief that the small size and the potential high ligand efficiency of the molecular fragments can offer advantageous starting points for drugging traditionally difficult pharmaceutical targets, such as protein–protein interactions. Bringing a fragment-based approach to DECL technology can help minimize the potential weaknesses of fragment screening (e.g., solubility), while the use of dual-DNA-display approaches allows the mimicking of evolutionary principles, such as dynamics[5] and recombination principles.[6]

1.2. A Brief History of DECL

The original design of DECL was largely inspired by phage display technology.[3] The first proof-of-principle library was generated through parallel synthesis of peptide and DNA on polystyrene resin in a one-bead one-compound format.[7] While this experiment was crucial to DECL development, the beads utilized were much larger than bacteriophages (up to 10^5–10^6-fold; >1000-fold larger than M13 bacteriophage), setting a practical limit on potential library size, as well as precluding selection experiments with the bio-panning protocol employed in phage display technology. With the bead library, the first proof-of-concept affinity-based selection was performed using a peptide-DNA conjugate library and a fluorescently labelled target protein, and identification of the interaction between the peptide and its antibody was accomplished by Fluorescence Activated Cell Sorting (FACS).[7] Until the beginning of the new millennium, the development and application of DECL technology proceeded very slowly, limited mainly by the lack of sufficiently robust auxiliary technologies. Then, supported by improvements in DNA microarray, DNA conjugation chemistry,[8–12] DNA-templated chemical reactions,[8,13–15] and especially by the introduction of DNA NGS,[16,17] DECL technology experienced a rapid and impressive growth in both academic and industrial settings.[4,18] The introduction of split-and-pool synthesis and enzymatic tag-encoding ushered in the use of a combinatorial assembly approach to quickly prepare libraries of massive sizes, currently on the order of billions or trillions of compounds.[19,20] When DECLs became comparable with phage display libraries in terms of size and biopanning protocol compatibility, their advantages

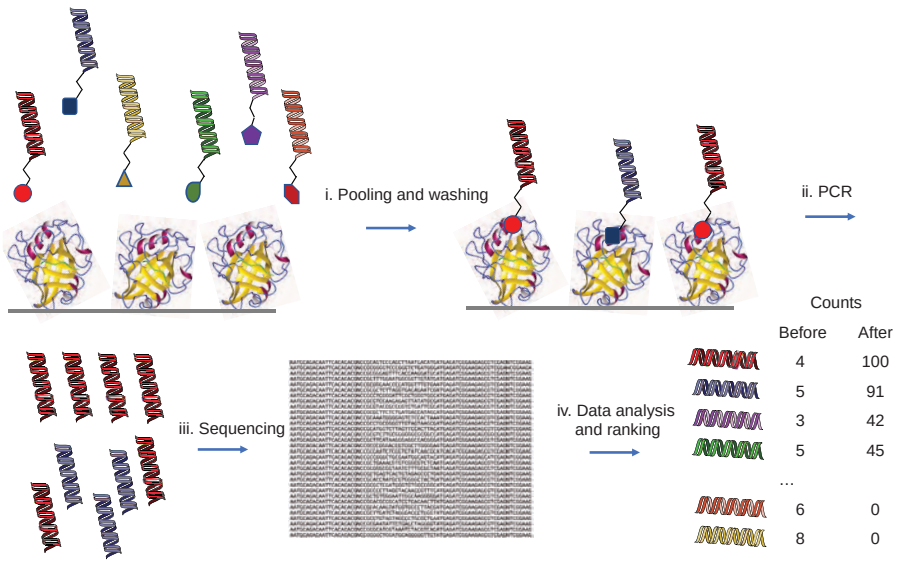

Figure 1. Common Protocol for DECL Compound Selection Experiments. *(Ref. 4b,c)*

became obvious: the run time for a DECL experiment is largely independent of library size, making the process significantly faster than a traditional HTS campaign. Indeed, DECL-based drug discovery methodologies continue to mature and have, in recent years, proven their worth by discovering new drug candidates for a number of diverse targets.[21–24]

2. Selection vs Screening

Four major methods are employed in chemical genomics and drug discovery to identify new pharmaceutically relevant molecular entities (**Figure 2**): (i) *High-throughput screening (HTS)*: This is currently the dominant method for the discovery of small-molecule drug compounds, whereby each chemical compound is assayed one-by-one in well-plate formats.[25–27] (ii) *Array-based method*: In this complementary method to high-throughput screening, chemical compounds are spotted on a planar surface as an addressable library, while the binding of the target protein can be directly detected by using labeled proteins or antibodies.[28,29] (iii) *Selection*: In nature, high-affinity binders, such as antibodies, are generated through selection processes, wherein a number of potential binders are competing simultaneously. The same principle is also used in bioengineering (e.g., protein/peptide display, aptamer technology) to develop macromolecule-based therapeutics.[30,31] (iv) *Structure-based design*: This is a rational approach that commonly focuses on developing potent binders by combining information from fragment screening with protein structural information and structure–activity relationships in multivalent protein–ligand interactions.[32–34]

Each method has its advantages and disadvantages. For example, drug screening can make use of a great variety of chemical structures, but it is expensive and requires assay development for each protein target. Conversely, the array-based method does not need any particular activity-based assay development, but library size is a limitation. Selection technologies allow for the use of larger libraries and can be routinely applied to polypeptides and nucleic acids (e.g., antibodies and aptamers). Therefore, DECL has expanded the scope of the selection approach to small-molecule chemical libraries. However, although the affinity-based assay can lead to high-affinity binders, the hit compounds may not have the desired biological properties or functions. The fragment-based approach is the most rational, but it is also the most time- and labor-intensive method.

HTS, array-based screening, and fragment-based approaches test chemical compounds one-by-one, causing campaign costs to scale with library size. Selection approaches offer the advantage of being relatively independent of library size. Moreover, all compounds compete with each other under the selection conditions, thus reflecting their thermodynamic differences in binding to the target protein. While DECL can be thought of as primarily a selection technology, it borrows concepts from most of the other approaches.[12,35] Similar to screening, the focus in the selection approach is traditionally on small organic molecules or fragments, while recent new developments have also incorporated elements of array technology or structure-based design, as will be discussed in later parts of this review.

The use of selection-based methodologies in the discovery of small-molecule binders was traditionally constrained by the sensitivity of the analytical tools available to identify the selected compounds. Prior to the widespread use of DECL, the best known approach was Novartis's SpeedScreen,[36] which selects binders for a protein target from a mixture of 100–600 compounds using mass spectrometry for the screening

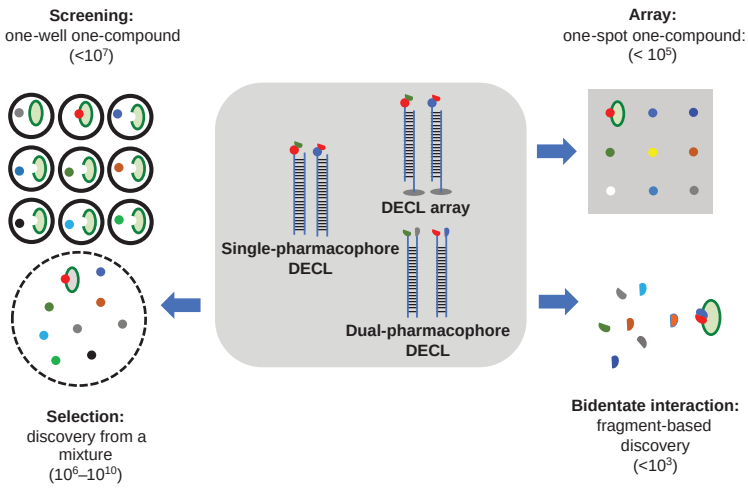

Figure 2. DNA Sequences as Barcodes for Small-Molecule Compounds. DECLs Can Be Designed and Synthesized in Various Forms to Mimic Different Drug Discovery Technologies (Middle). By Conjugating DNA Sequences as Barcodes to Small Organic Molecules, This Technology Allows the Application of Selection Methods to Small-Molecule Ligand Discovery, Which Is Traditionally Done by HTS (Left). DECLs Can Also Be Generated as an Array, and Displayed as Fragment Pairs, Mimicking Small-Molecule Array and Fragment-Based Drug Discovery, Respectively (Right). DECL Selection and DECL-Derived Technology Represent Attractive Alternatives to HTS Technology. *(Ref. 25–34)*

read-out. Libraries of up to 600,000 compounds (in 96-well plate format, with 400 compounds in each well) have been successfully investigated by SpeedScreen.

Since then, DECLs have been a revolutionary selection technology for small-molecule compounds. Because DNA offers a reasonably broad information space and can be PCR-amplified, the detection limit issues of other analytical chemical methods (e.g., the 600 compounds limit for SpeedScreen using mass spectrometry) can be largely overcome. Today, DECLs of billions of compounds are routinely screened in selection experiments.

2.1. Main Challenges in DECL

With the reports of ever-growing DECL sizes, drug discovery researchers have realized that the major challenges are not only about the number of library members.[37] For example, in order to generate large libraries, increasing the number of synthetic cycles (i.e., the number of combinatorial split-and-pool steps) increases the mass and lipophilicity of the member compound. Even three cycles of combinatorial synthesis with fragment-like building blocks can result in library members moving well outside the bounds of traditional drug-likeness (e.g., Lipinski's rules).[38]

A potentially greater problem, however, is that combinatorial synthesis prevents meaningful quality control or assessment of library contents. While chromatography can be used to clean up the coupling of stage 1 building blocks to DNA, this is no longer feasible once the initial reaction products are pooled. Over additional synthetic cycles, this increases the possible presence of side products or unreacted precursors, resulting in a single DNA tag encoding a number of different compounds and complicating the effort to identify and validate hits.[39] This issue can snowball in very large libraries and manifest itself as false negative results, as the individual copy number of a given molecule can dip below detectable levels.[40] Another limitation of DECL is that many common chemical reactions in the medicinal chemist's toolbox are not compatible with DNA. While progress has recently been made in broadening the synthetic methodology for preparing DECLs[41–43]—especially with the DNA-templated synthesis of small-molecule macrocycles pioneered in the lab of David Liu[8,44]—amide-bond formation nevertheless remains one of the most reliable reactions for DECL construction. Through repetition of coupling steps, relatively high yields with small variations among the building blocks can be achieved.[45]

In contrast to the high-fidelity DNA synthesis by DNA polymerase in the replication process, both the chemical synthesis and sequencing of DNA are error-prone. For the construction of DECL, in addition to chemical library synthesis errors caused by the previously discussed side reactions and low reactivity of some of the building blocks, errors in the coding sequence may also be introduced during the DNA-tagging step. The affinity-based selection protocols with immobilized target proteins on polymer matrices can likewise cause artifacts such as promiscuous interactions and protein misfolding. Eventually, the PCR and NGS decoding steps can similarly introduce further biases.

Data analysis by ranking the detected sequence counts is largely based on the assumption that the binding affinity to a native protein—the amount of DNA-conjugate small molecule captured, the PCR amplification, and the NGS reads—are linearly correlated and mostly error-free. Unfortunately, errors and biases accumulate over the whole DECL workflow, resulting in reduced correlations between the measured binding affinities of the selected compounds and the NGS-decoding counts. While DECLs with more sophisticated structures have been constructed in recent years, this has exacerbated the problem by adding more synthetic and encoding steps. Moreover, another undesired consequence of increasing library size is the inability of NGS to provide sufficient sequencing depth for comprehensive statistical analysis. Together with the challenges associated with individual synthetic and biochemical reactions, statistical requirements must also be taken into consideration in the analysis of the NGS-decoding results in order to statistically identify significantly enriched hit compounds.[46]

Despite the significant progress made in DECL technology in recent years, the main challenges have remained mostly unchanged, and researchers are still working toward two common goals: (i) adding new chemical reactions to the DECL synthesis tool box, not only for increasing library purity and size, but also for generating pools of compounds with higher structural diversity and drug likeness; and (ii) improving library design and selection protocol in order to achieve a superior correlation between the sequence counts and the subsequently measured affinities, thus reducing the occurrence of false positives, and, more importantly, false negatives.

2.2. Optimizing the Selection Conditions, from Surface to Solution

The standard DECL selection protocol uses immobilized target proteins on polymer matrices;[47] this protocol can cause artifacts such as promiscuous interaction and protein misfolding. Most commonly, a protein of interest is either immobilized on cyanogen bromide (CNBr)-activated Sepharose® beads or captured on streptavidin-Sepharose® after protein biotinylation. The use of magnetic beads has enabled automated selections, while non-covalent immobilization allows researchers to evaluate the effect of protein modification on protein activity prior to immobilization.[22] Alternative strategies such as His-tag, FLAG-tag, STREP-TAG®, and GST-fusion can also be employed for immobilization, but biotinylation remains the most favorable method because of the strong and reliable immobilization through streptavidin–biotin interaction which prevents protein dissociation.

In order to minimize the artifacts caused by polymer matrices, a two-step selection protocol has been developed.[48] A DECL is first incubated with the target protein in solution. After the system reaches equilibrium, resin is added to capture the protein and the DECL compounds bound to it. Eventually, the resin is washed and the binding library is recovered either by heat-induced denaturation of the protein or chemical elution. To completely remove the effect associated with the protein immobilization process, Li's group has reported a DECL design

which allows selection against unmodified protein targets in solution.[49] A library of single-strand DECL was hybridized to a DNA carrying a photo-crosslinking group. After target-protein binding and irradiation, the protein–ligand–DNA complex was isolated and submitted to decoding by NGS sequencing.

A number of valuable drug targets are membrane-bound proteins that don't lend themselves to convenient solid-support immobilization. To access this target space, GlaxoSmithKline developed and reported a cell-based selection approach using DECL.[50] Tachykinin receptor neurokinin-3 (NK3), a G-protein coupled receptor, was expressed on HEK293 cells. After optimizing the expression condition, cells expressing approximately 5 x 10^5 receptors per cell (the highest level that could be achieved with this expression system for NK3) were utilized in the subsequent selection experiments. Remarkably, several hits identified in this study have potency, specificity, and ligand efficiency properties comparable to talnetant and osanetant, two antagonists developed for the same membrane protein through classical screening and medicinal chemistry approaches.[50]

3. Conventional Chemical Library vs Fragment-Based Approach

Similarly to the one-well one-compound format in HTS, most DECLs are in the form of one-DNA one-compound (1_d–1_c), constructed as combinatorial chemical libraries conjugated to a single DNA strand. An alternative approach is to take advantage of DNA hybridization in dual-display technology, where annealed DNA strands are used to present two moieties simultaneously. The two-DNA two-compound (2_d–2_c) approach resembles another drug discovery method: the fragment-based one.[12,35] The (2_d–2_c)-DECL approach was pioneered by Neri's group at ETH Zürich by using a straightforward setup of two DNA strands containing a universally complementary annealing region.[12] After synthesis, the two sub-libraries are mixed, resulting in the random and stable pairing of the molecules. The 2_d–2_c format has an obvious advantage for the construction of large but high-purity libraries: Whereas it is practically impossible to purify every compound in a 1_d-1_c library with 1 million members, it is possible to assemble a 10^6-member library by the pairing of two 10^3-member, DNA-encoded sub-libraries that have been individually HPLC purified and characterized by mass spectrometry.

The majority of existing DECL platforms, however, are still based on a 1_d–1_c architecture. This is at least partially due to the relatively recent development of 2_d–2_c libraries, but one cannot ignore the fact that the two DNA-conjugated moieties must at some point in the process be taken off the DNA and resynthesized as a single compound, which is not a trivial undertaking. On the other hand, the 2_d–2_c format offers a significant, "hidden" increase in library diversity: the fragments in this format possess larger rotational and translational freedoms to interact with a protein, as opposed to the rigidly assembled compounds present in 1_d–1_c DECL or HTS collections. The chemical structures in 2_d–2_c libraries are linked to DNA strands at either the 3′ or 5′ terminus through flexible linkers, typically composed of C_3–C_{12} aliphatic chains or short PEGs (polyethylene glycols). This puts fewer restrictions on structure-based drug design and medicinal chemistry to explore different spatial arrangements and conformational spaces. While a systematic test of different linking systems can then be pursued in later stages of hit development, this is also where fragment-based DECLs can fit together nicely with a structure-based design approach by taking advantage of crystallographic information about the target. For the design of a fragment library—provided that binding enthalpy can offset the loss of rigid-body entropy—chemical building blocks are chosen, privileging structures that can form thermodynamically favorable interactions with the target protein.[32,51] Future developments in fragment-based DECLs could also provide additional context for fragment interactions. For example, if different linkers could be employed in generating 2_d–2_c libraries with the structural information of the linkers also encoded in the DNA sequences, it would be possible to get simultaneously both more reliable selection results (e.g., whether same pair of fragments are selected with different linkers) and complementary information regarding the preferred distance between the binding fragments.

The inhibition of protein–protein interactions (PPIs) represents an increasingly prominent goal for drug developers, but also one where traditional methods such as HTS have had only limited success. Fragment-based drug discovery (FBDD) has in the past two decades emerged as an alternative to HTS and, after 20 years of gradual improvement, it is now accepted as a part of mainstream drug discovery. As of 2016, more than 30 drug candidates derived from fragments have entered the clinical phase, with two approved and several more in advanced trials.[51] Research from multiple groups is supporting the idea that the combination of DECL and FBDD approaches is a logical next step for both of these technologies. For example, while weakly binding fragments can be missed in classical fragment screening experiments due to assay sensitivity, their chances of successful detection are improved in 2_d–2_c DECLs. This is due to the bidentate interaction in which a pair of weak binders assembled by a DNA duplex will exhibit a higher cooperative affinity than when displayed as individual fragments.[22] Furthermore, a common problem with FBDD—the often limited solubility—is overcome by conjugation with highly soluble DNA.

3.1. Developments in Fragment-Based DECL

As discussed in the previous section, some challenges with 2_d–2_c libraries arise because multiple moieties are presented for target binding. Selection with a 2_d–2_c fragment library does not *directly* lead to a list of fragment pairs revealed by their corresponding DNA codes, because in a 2_d–2_c library both chemical fragments and their corresponding DNA codes are separated on two different DNA strands. Therefore, in the early days of fragment DEL development, the fragments identified from sequencing had to then be combinatorially assembled and tested to reveal ideal pairings.[52] To circumvent such a cumbersome workflow, most 2_d–2_c fragment libraries were designed in an affinity-maturation format,[12,22] in which one

of the two displayed strands was exclusively conjugated to a known but relatively weak binder to the target protein. In 2015, Neri, Scheuermann, and co-workers disclosed an elegant inter-strand code-transfer method that results in a 2_d–2_c library in which one of the two DNA strands is able to host the coding information of both pairing fragments (**Figure 3**).[53]

As shown in Figure 3, sub-library B was constructed in a way that allowed hybridization with sub-library A and, at the same time, the transfer of B coding sequences onto the corresponding A strand by means of a fill-in reaction. With this strategy, the A strand for each library member would contain sequence information that would unambiguously identify the A–B fragment pair, while the B strand would not be amplifiable by PCR. Using this approach, the authors have reported the identification of a low-micromolar binder to alpha-1-acid glycoprotein (AGP) and the affinity maturation of a ligand to carbonic anhydrase IX, a well-known marker of carcinoma of kidney cells.[53]

4. Self-Assembled Dynamic DECL

A particularly clever innovation in drug discovery screening is Dynamic Combinatorial Chemistry (DCC). A library using the DCC approach consists of a pool of small-molecule building blocks that can interconnect via reversible reactions that form transient adducts in a thermodynamic equilibrium (e.g., disulfide bond and Schiff base). Each building block possesses one or more functional groups that allow dynamic combinatorial interactions with other members of the library. In this pool, new chemical species are continuously formed and dissociated following the reversible equilibrium of the DCC reaction. When a target protein is introduced into the system, the equilibrium can be shifted toward the formation of higher-affinity binders. The protein thus acts as a template for the synthesis in situ of the binders through thermodynamic stabilization of the otherwise unstable adducts.

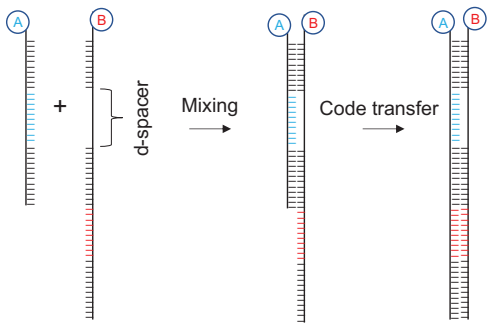

Figure 3. Library Construction with Code-Transferring Mechanism. The Syntheses of Sub-Libraries A (Light Blue) and B (Red) Were Carried Out Separately. A DNA Polymerase Assisted Fill-in Reaction Allowed the B Code to Be Transferred onto the Sub-Library A Strand. The Final Library Was Used for Selection Experiments against Target Proteins of Choice. Subsequent PCR Amplified Only the A Strand, and High-Throughput DNA Sequencing Simultaneously Revealed Binding Fragment Pairs. *(Ref. 53)*

The development of DCC technology was limited by the available analytical tools, such as mass spectrometry and NMR, which can analyze only mixtures of compounds with very low complexity. In contrast, techniques capable of analyzing complex mixtures of oligonucleotides, like microarray technologies and the more recent NGS, are much more powerful. These novel analytical technologies can in principle resolve a complex mix of thousands or millions of different oligonucleotide sequences in a single analysis in a few hours.[18,54,55] We thus saw an opportunity to fuse the efficient and simple self-assembling and "self-screening" features of DCC with the extremely sensitive hit-identification methods of DECL, allowing the generation of very large dynamic libraries.

As the utility of DCC in drug discovery also represents a fragment-based approach, it was relatively straightforward to design a DCC-based DECL in the 2_d–2_c format.[53] The first "DNA-Encoded Dynamic Combinatorial Chemical Library" (EDCCL) was constructed in a dynamic 2_d–2_c format including a hybridization domain of 4 to 8 nucleotides. These short domains are naturally unstable, driving only transient pairing of the chemical moieties conjugated to the DNA construct, in analogy to the reverse reactions in DCC. All the chemical moieties from one sub-library are free to pair with all the other members of the other sub-library. Fragment-pair binding to a target protein can overcome the weak pairing of the hybridization domain, stabilizing higher affinity pairs and shifting the binding equilibrium. One of the advantages of a dynamic library over its static counterpart is that different chemical species are continuously synthesized in the selection mixture, while only high-affinity binders are "locked" on the protein. If we think of a pair of high-affinity fragments as the "right combination" of the "right fragments", then most "right fragments" in a static library are in the "wrong combinations", i.e., paired with nonbinding fragments. In a dynamic library, the right fragments in wrong combinations can always be unpaired and thus free to search for another fragment for pairing, and so on until stabilized by the protein after forming the "right combination". In this way, a high signal-to-noise ratio can be achieved by sorting out a number of nonbinding fragments. EDCCL can also be deployed for ligand optimization (similarly to the previously discussed "affinity maturation"). In this approach, one of the sub-libraries is composed by a single member, a known binder. When the known binder is in low amounts with respect to the pairing (sub)-library, it is "forced" to form the "right combination" with the "right partner", thus enhancing the signal-to-noise ratio of the "right" to "wrong" partner. While this has obvious applications for improving binding strength, it can just as effectively be employed for improving target specificity.

The 2_d-2_c dynamic format pays an energy cost for de-stabilizing the tertiary complex of two DNA strands and one protein, as the weak interaction between the two strands can weaken the chelation effect. Among the different hybridization domains tested, the 4 and 5 base-pair (bp) domains are not sufficiently stable to guarantee the enrichment of high-affinity binders, while the 6 and 8 bp domains show a much higher enrichment of the high-affinity pairs compared to a static counterpart (e.g., 18 bp

hybridization domain, with no compound reshuffling possible). To reduce the energy barrier associated with short dynamic hybridization domains, "Heat Induced-EDCCL" technology (hi-EDCCL) has been developed.[56] Here, the dynamic equilibrium is established by exposing the unbound library fraction to a temperature higher than the hybridization domain melting point, while the protein-loaded matrix is kept at relatively low temperature (achieved via physical separation) to prevent unfolding of the protein. Heat denaturation followed by a DNA re-annealing step cause pair reshuffling and the rearrangement of the library into a collection of new pairs, some of which are high-affinity binders. The reshuffled library is then reapplied onto the immobilized protein to allow the newly generated pairs to bind to the target. Shuffling and selection can be repeated several times to increase the signal-to-noise ratio and stringency of selection. In order to overcome reproducibility issues and the critical loss of material during the manual handling of liquids at the microliter scale, a dedicated hi-EDCCL automated microfluidic device has been developed. This device is capable of controlling the continuous liquid transfer and the temperature in different sections of the pathway.[57]

More recently, we have developed a second-generation EDCCL, which utilizes a Y-shaped DNA construct for the creation of a third DNA strand—at the end of the selection process—containing the codes of both binding fragments to reveal binder-pairing information (**Figure 4**).[58] A challenge in developing this technology was that Y-shaped constructs exhibit different melting behavior than linear duplexes. Linear constructs begin to melt from the extremities, while Y-shaped constructs have the tri-junction as the point of instability. For this reason, larger hybridization domains, 11 and 13 bp, were optimal for building a Y-shaped EDCCL. At the end of the selection process, the two coding regions of the binding fragments captured on the immobilized protein were linked by means of DNA ligation. Second-generation Y-shaped EDCCL are also capable of minimizing the signal noise caused by unpaired single-fragment binding. Indeed, when a fragment binds to the target protein without previously forming a pair, it can neither be ligated to a partner fragment nor PCR-amplified later, thus becoming "invisible" to the NGS decoding.

Li and co-workers have developed another format of EDCCL that featues two hybridization domains of 6 and 7 base pairs, one of which also carries a psoralen photo-crosslinker.[59] Following incubation of the dynamic library with a soluble target protein, UV irradiation triggers the photo-crosslinking of the two DNA strands, thus "freezing" the dynamic exchange at the binding

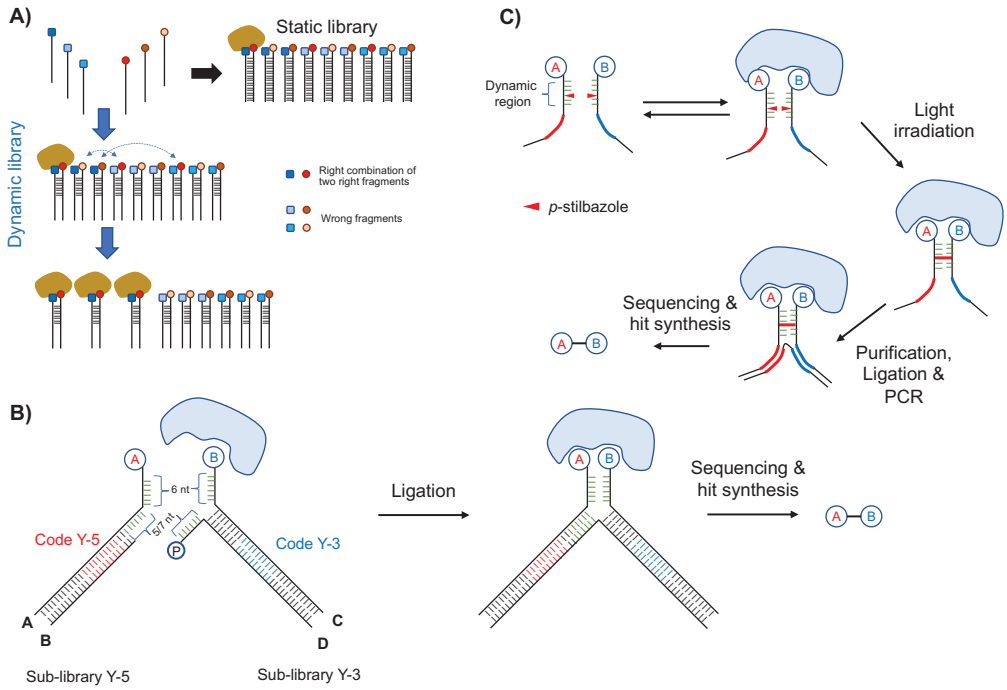

Figure 4. (A) Principle of Dynamic DECL. For 2d-2c Fragment Libraries with n x n Combinations, When the Library Is in a Static Form, a Certain "Right Combination" of Two "Right Fragments" Is of $1/n^2$ of the Entire Library, Independently of the Presence or Absence of a Protein Target. When the Library Is in a Dynamic Form, the Thermodynamic Equilibrium Will Shift the "Right Combination" from $1/n^2$ to 1/n of the Entire Library in the Presence of the Target Protein, through Shuffling Between the Different Combinations. **(B) Construction of Dynamic DECL with Code Ligation Mechanism.** Strands A and B Are Assembled to Form Sub-Library Y-5. Strands C and D Make Up Sub-Library Y-3. Upon Binding to the Target Protein, Phosphorylated Strand D Can Be Ligated to Strand B. **(C) Dynamic DECL with Photo-Crosslinking.** Two Sets of DNA-Encoded Small Molecules with a Short Complementary Dynamic Region Form the DNA-Encoded Dynamic Library. Target Addition Shifts the Equilibrium, Promoting the Formation of High-Affinity Duplexes. UV Irradiation Locks the Shifted Equilibrium through *p*-Stilbazole (B-Base)-Mediated Photo-Crosslinking. Crosslinked Duplexes Are Isolated, and the Sequences at the Encoding Sites Are Decoded for Hit Identification. *(Ref. 58).*

equilibrium. Finally, the photo-crosslinked oligonucleotides are purified via gel electrophoresis, and then sequenced. In 2018, the same laboratory reported further development of this concept.[60] To improve the photo-crosslinking efficacy, the psoralen photo-crosslinker was substituted by two facing *p*-stilbazoles photo-crosslinkers in the center of the dynamic hybridization domain. *p*-Stilbazole does not disturb the DNA base pairing when located in the middle of the oligonucleotide sequence. Moreover, the ability to crosslink the oligonucleotide in the center of the sequence permitted the joining of the two codes of the binding fragments into one sequence. Since a DNA polymerase cannot go through the unnatural linkage of the oligonucleotides, a relay-primer bypass strategy was adopted. This strategy features the use of a primer to mask the unnatural linking region, while a DNA polymerase and ligase assemble the final amplicon, which eventually can be PCR-amplified and subjected to NGS.

5. Hit Validation

While a number of research groups have made significant advances in areas related to library architecture and DNA-compatible chemistry, relatively little progress has been achieved in downstream hit validation. The most common hit-validation approach has been to immediately resynthesize the compounds off-DNA for follow-up testing. It is worth noting however, that modern DECL's increasing library sizes and potentially large hit lists would require a substantial synthetic effort and cause this step to be a bottleneck in the discovery process.

Hit validation can be carried out with a conventional protein-activity assay in solution. However, since DECL discovery works well even for targets where only limited knowledge is available, a functional assay (e.g., enzyme inhibition) may not be available. In this case, a number of kinetic or thermodynamic binding assays can be utilized. For example, a fluorescently labelled off-DNA compound can be synthesized, and the binding constant can be measured with such techniques as fluorescence polarization or microscale thermophoresis.[61] While microcalorimetry offers thermodynamic characterization of protein–ligand interactions, avoiding artifacts associated with labeling and surface immobilization, the consumption of materials and the labor effort involved are high compared to other methods.[62]

One of the most appealing methods for characterizing protein-ligand interactions is biosensor-based technology, which is able to simultaneously provide thermodynamic information about the dissociation constants (K_d) as well as the characteristic kinetic parameter values K_{on} and K_{off} that are associated with the binding process. Unfortunately, this approach is challenging for high-throughput hit validation of small-molecule compounds, since small-molecule covalent immobilization on solid support is time-consuming and cost-inefficient. Moreover, utilizing small molecules as binders in the mobile phase frequently leads to very weak signals and poor data quality. Neri, Scheuermann, and co-workers have reported the validation of on-DNA resynthesized hits by fluorescence polarization, Alphascreen® technology, and microscale thermophoresis.[61] For dual-display approaches, hit validation is doubly problematic. To prevent false negatives from incorrect linker selection, off-DNA synthetic efforts need to include a number of different linking groups, again presenting an intimidating synthetic task for any hit list containing more than a small number of molecular structures.[22,52,58]

To increase the throughput of hit validation, Lin et al. have described the use of a regenerable biosensor chip for characterizing on-DNA small-molecule compounds (**Figure 5**).[63] The concept is simple: A DNA handle for binding library members is covalently attached to the biosensor surface. On-DNA hit compounds are then loaded by annealing onto this handle, subjected to protein binding measurement, and then chemically stripped to regenerate the DNA handle for characterizing the next round of hit compounds. The loading and regeneration procedure can be reiterated over 20 cycles without losing the signal intensity. This permits the automated measurement of kinetic profiles of protein–ligand interactions for DECL hits. Moreover, this method can be adapted to characterize pairs of compounds, greatly alleviating the concerns over the synthetic effort required for dual-fragment hit validation. While the most promising hit pairs must still be resynthesized and linked off-DNA, this approach allows an initial triage in the same chemical context in which the hits were originally registered, reducing the risk of false negative results.[63]

6. Application of Nanotechnology in DECL

As discussed previously, the synthesis of structurally diversified high–purity, drug-like libraries and the development of new selection procedures with superior signal-to-noise ratios that minimize the rates of false positives or false negatives represent the two major challenges for DECL. While library size is currently not considered as the limiting factor for DECLs, the development of new chemical and biochemical methods for DECL will inevitably lead to the production of larger libraries. Indeed, NGS has revolutionized the field of DECL. However, to cope with libraries of growing sizes, sequencing depth (i.e., the ratio between the number of reads and library size) must be similarly improved. Therefore, sequencing power may become soon a new bottleneck. Because of the resolution limitation associated with the fluorescence-based detection mechanism, as well as the need to prevent over-clustering,[64] NGS will soon meet its limitation of 1 sequence/μm^2 (or $10^8/cm^2$). Therefore, the ultimate limitation of DECL in the current setup is neither the chemical space nor the DNA sequences, but rather the optical resolution.

As many modern imaging techniques (e.g., atomic force microscopy (AFM), super-resolution fluorescence microscopy, and scanning tunneling microscopy) are not limited by optical resolution, Kielar et al. made use of the available DNA nanotechnology tool box to construct nanoscale pharmacophore arrays (**Figure 6**).[65] Several different pharmacophores were displayed with nanometer precision on DNA origami substrates either as individual ligands or as fragment pairs, and their binding to different model proteins was evaluated by AFM as a

single-molecule detection method. This work demonstrated the successful detection of several different binding events including strong binding, weak binding, symmetric bidentate binding, and asymmetric bidentate binding. This method was further applied to the discovery of bidentate trypsin binders based on the pairing of the weak trypsin inhibitor benzamidine with different aromatic fragments.[65] The combination of benzamidine with the fluorescent dye carboxytetramethylrhodamine (TAMRA) results in about a 10-fold enhancement of the trypsin binding yield compared to that from benzamidine alone. Since AFM can

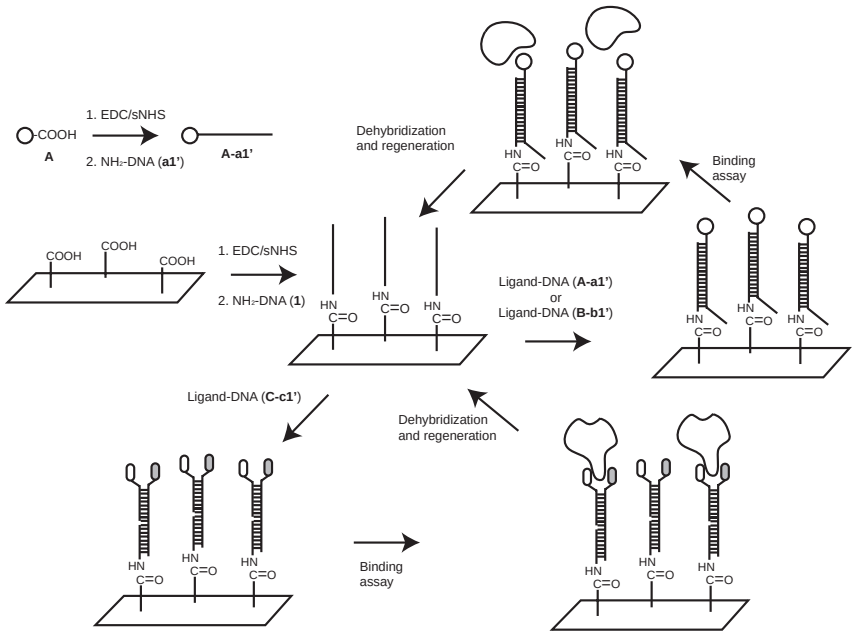

Figure 5. Principle of Affinity Measurement on a Regenerable Biosensor Chip. The Carboxylic Acid Groups on the Chip Were Coupled with the Amino Groups of 5′-Amino-DNA (1) (Middle Cycle). A Small-Molecule Ligand (A) Was Conjugated to the Amino Group of 5′-Amino-DNA (a1′) That Is Complementary to Sequence 1. After Annealing A-a1′ to 1 on the Chip, the Target Protein Is Injected at Different Concentrations to Assess the Binding Affinity. A-a1′ Can Be Washed off the Chip under Dehybridization/Regeneration Conditions. Another DNA-Ligand Conjugate, B-b1′, Can Then Be Immobilized on the Regenerated Chip, and Its Binding Affinity to the Same or a Different Protein Can Be Evaluated (Upper Cycle). This Method Can Also Be Applied to a Double-Strand DNA, C-c1′, Displaying Two Ligands (Lower Cycle). *(Ref. 63)*

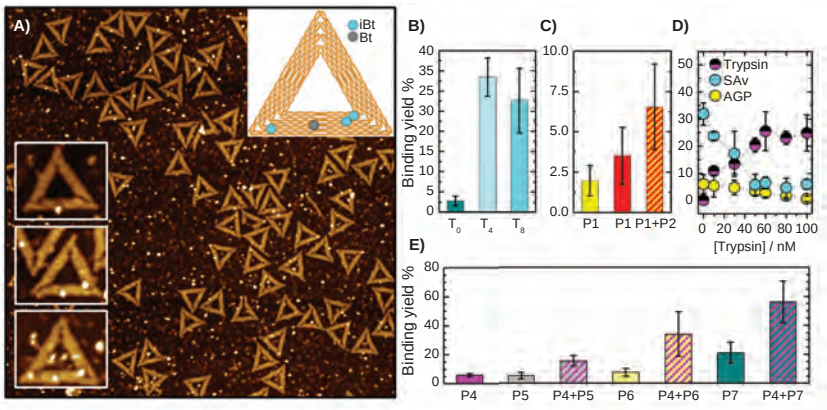

Figure 6. DNA-Origami-Based Nanoarrays for Studying Protein–Ligand Interactions. (A) Representative AFM Image of Iminobiotin (Ibt) Nanoarrays Taken after Incubation with Streptavidin (SAv). The Image Size and Height Scale Are 2 x 2 μm^2 and 4.2 nm, Respectively. The Upper Right Inset Depicts the Positions of the Modified Staple Strands. A Single Biotin (Bt) Modification Is Used to Distinguish Between the Two Different iBt Sites. The Insets on the Left Are Zoom-ins of Single DNA-Origami Substrates Exhibiting (i) No SAv Bound to iBt, (ii) Bidentate Binding of SAv to iBt, and (iii) Monodentate and Bidentate Binding of SAv to iBt. **(B)** Bidentate SAv-iBt Binding Yields for Different Thymine Spacer Lengths. **(C)** Binding Yields for Mono- and Bidentate Binding of AGP to Pharmacophore Ligands P1 (Propenamide Derivative) and P2 (Acetamide Derivative). **(D)** Binding Yields for Bidentate SAv-iBt Binding, Monodentate AGP-P1 Binding, and Bidentate Trypsin Binding to Ligands P3 (3-Iodophenyl Isothiocyanate) + P4 (4-Aminobenzamidine) in a Single Nanoarray as a Function of Trypsin Concentration. **(E)** Binding Yields for Mono- and Bidentate Trypsin Binding to Fragments P4 to P7 (TAMRA). *(Ref. 65)*

distinguish two DNA-origami-bound proteins with a distance of about 10 nm, these pharmacophore nanoarrays could achieve spatial resolutions 5–7 orders of magnitude higher than the conventional microarray technologies on glass slides, which have feature sizes of 10–100 μm. Given that no modifications or immobilization of the target proteins is required, the method can detect the binding of pharmacophores in their native forms. Moreover, the DNA-origami substrates provide a platform to display DNA-modified ligands with variable spatial arrangements, and thus represent a versatile tool for fragment-based lead discovery research.

The chemical library on DNA origami has only been demonstrated in proof-of-principle experiments, while many challenges still remain for its real application in drug discovery. However, with the ever-increasing library sizes, single-molecule-based detection methods will inevitably be needed in the future. In addition to ultra-high-resolution imaging techniques such as AFM,[66] the emerging nanopore sequencing[67] is a very attractive technology: Using nanopore sequencing, a single molecule of DNA or RNA can be sequenced without PCR amplification in a label-free fashion. Although nanopore sequencing has higher error rates than NGS based on chromatin immunoprecipitation sequencing (ChIP-seq) technology, DNA codes can be designed to possess high error tolerance,[68] which would make nanopore sequencing particularly suitable for large DECLs.

7. Conclusion and Outlook

The continued, rapid advances in library synthesis methodology and library size beg the question: Is there a limit to how large a library can be? Answering this question literally, one could calculate that, in a 1 mL DECL solution with a total compound concentration of 1 μM, there would be room for more than 10^{15} individual molecules—a number that our current synthetic methods won't get us anywhere close to. A more prudent question might be: Is there a limit to how large a useful library can be? To answer these questions, Samain and co-workers have recently reported the quantitative evaluation of affinity selection performance using both quantitative PCR (qPCR) and NGS techniques.[40] Interestingly, for compounds with sub-μM dissociation constants, selection performance drops if 10^4 copies per library member are used as the input. This result implies a size limit of DECL in the range of 10 to 100 billion different molecules, to ensure that each potential hit has more than 10^4 copies. Whether the limit of 10^4 copies can be circumvented remains to be tested in the future, probably through implementation of single-molecule techniques to assess the interactions at a single-molecule level, or by employing new generations of sequencing methods with higher sequencing depth, or by applying advanced statistical tools in data analysis.[37,46,69–71]

Dynamic DECL technology represents another possibility to circumvent the size limit. In a 1 mL solution of dynamic DECL with two sub-libraries, each with a total compound concentration of 0.5 μM, there exist about 10^{29} different possible combinations. When the 10^4-copies rule is applied to both sub-libraries, the theoretical size limit for a dynamic DECL is 10^{21}-member compound pairs. While in the absence of protein, each of these pairs has a near-zero representation, the presence of a protein will shift the thermal dynamic equilibrium, generating these high-affinity pairs on demand. The triplex library with three pharmacophores (3_d–3_c) that was suggested by Neri and co-workers during the early development of self-assembled DECL has so far not been practically implemented.[12] Although such a library would present challenges in later hit linkage and re-synthesis, if the 3_d–3_c library could be realized in a dynamic format, the number of possible structure combinations would be astronomical.

As we've aimed to convey in this review, DECL research also focuses on questions more complex than just library size. For standard libraries in the 1_d–1_c format, improving the library quality, as well as developing new DNA-compatible chemical reactions for library synthesis, represent two major challenges for chemistry. In combination with novel biochemical assays, e.g., in-solution or on-cell selection, the goal has been to achieve a good correlation between the sequencing outcome and the measured binding affinity of different hit compounds. For fragment libraries in the 2_d–2_c format, DECL can become a very powerful tool for fragment-based drug discovery, which has a great potential to overcome the shortage of screening-based methods for tackling difficult drug targets such as protein–protein interactions. However, similarly to all fragment-based approaches, the question of how to link the fragments and generate high-affinity binders remains the most daunting challenge. Because of the large size of the compound library, DECL technology allows us to collect unprecedented amounts of information. When the binding of fragments presented on a DNA duplex to target a protein can be elucidated in crystallographic analysis, valuable information can be provided for structure-based drug design. Our ability to effectively use this information, to obtain new insights into the structure–activity relationship, and design potent drug compounds will benefit from new technologies and concepts such as structural biology and artificial intelligence.

8. References

(1) Paul, S. M.; Mytelka, D. S.; Dunwiddie, C. T.; Persinger, C. C.; Munos, B. H.; Lindborg, S. R.; Schacht, A. L. *Nat. Rev. Drug Discovery* **2010**, *9*, 203.

(2) Khanna, I. *Drug Discovery Today* **2012**, *17*, 1088.

(3) Brenner, S.; Lerner, R. A. *Proc. Natl. Acad. Sci. U. S. A.* **1992**, *89*, 5381.

(4) (a) Goodnow, R. A., Jr.; Dumelin, C. E.; Keefe, A. D. *Nat. Rev. Drug Discovery* **2017**, *16*, 131. (b) Zhang, Y. Hit Identification and Hit Follow-Up. In *A Handbook for DNA-Encoded Chemistry: Theory and Applications for Exploring Chemical Space and Drug Discovery;* Goodnow, R. A., Jr., Ed.; Wiley: Hoboken, NJ, 2014; pp 357-376. (c) Goodnow, R. A., Jr., Ed. *A Handbook for DNA-Encoded Chemistry: Theory and Applications for Exploring Chemical Space and Drug Discovery*; Wiley: Hoboken, NJ, 2014.

(5) Otto, S.; Furlan, R. L. E.; Sanders, J. K. M. *Drug Discovery Today* **2002**, 7, 117.

(6) Market, E.; Papavasiliou, F. N. *PLoS Biol.* **2003**, *1*, 24.
(7) Needels, M. C.; Jones, D. G.; Tate, E. H.; Heinkel, G. L.; Kochersperger, L. M.; Dower, W. J.; Barrett, R. W.; Gallop, M. A. *Proc. Nat. Acad. Sci. U. S. A.* **1993**, *90*, 10700.
(8) Gartner, Z. J.; Tse, B. N.; Grubina, R.; Doyon, J. B.; Snyder, T. M.; Liu, D. R. *Science* **2004**, *305*, 1601.
(9) Halpin, D. R.; Harbury, P. B. *PLoS Biol.* **2004**, *2*, 1015.
(10) Halpin, D. R.; Harbury, P. B. *PLoS Biol.* **2004**, *2*, 1022.
(11) Halpin, D. R.; Lee, J. A.; Wrenn, S. J.; Harbury, P. B. *PLoS Biol.* **2004**, *2*, 1031.
(12) Melkko, S.; Scheuermann, J.; Dumelin, C. E.; Neri, D. *Nat. Biotech.* **2004**, *22*, 568.
(13) Gartner, Z. J.; Liu, D. R. *J. Am. Chem. Soc.* **2001**, *123*, 6961.
(14) Calderone, C. T.; Puckett, J. W.; Gartner, Z. J.; Liu, D. R. *Angew. Chem., Int. Ed.* **2002**, *41*, 4104.
(15) Gartner, Z. J.; Kanan, M. W.; Liu, D. R. *Angew. Chem., Int. Ed.* **2002**, *41*, 1796.
(16) Margulies, M.; Egholm, M.; Altman, W. E.; Attiya, S.; Bader, J. S.; Bemben, L. A.; Berka, J.; Braverman, M. S.; Chen, Y.-J.; Chen, Z.; Dewell, S. B.; Du, L.; Fierro, J. M.; Gomes, X. V.; Godwin, B. C.; He, W.; Helgesen, S.; Ho, C. H.; Irzyk, G. P.; Jando, S. C.; Alenquer, M. L. I.; Jarvie, T. P.; Jirage, K. B.; Kim, J.-B.; Knight, J. R.; Lanza, J. R.; Leamon, J. H.; Lefkowitz, S. M.; Lei, M.; Li, J.; Lohman, K. L.; Lu, H.; Makhijani, V. B.; McDade, K. E.; McKenna, M. P.; Myers, E. W.; Nickerson, E.; Nobile, J. R.; Plant, R.; Puc, B. P.; Ronan, M. T.; Roth, G. T.; Sarkis, G. J.; Simons, J. F.; Simpson, J. W.; Srinivasan, M.; Tartaro, K. R.; Tomasz, A.; Vogt, K. A.; Volkmer, G. A.; Wang, S. H.; Wang, Y.; Weiner, M. P.; Yu, P.; Begley, R. F.; Rothberg, J. M. *Nature* **2005**, *437*, 376.
(17) Mannocci, L.; Zhang, Y.; Scheuermann, J.; Leimbacher, M.; De Bellis, G.; Rizzi, E.; Dumelin, C.; Melkko, S.; Neri, D. *Proc. Nat. Acad. Sci. U. S. A.* **2008**, *105*, 17670.
(18) Neri, D.; Lerner, R. A. *Annu. Rev. Biochem.* **2018**, *87*, 479.
(19) Kinoshita, Y.; Nishigaki, K. *Nucleic Acids Symp. Ser.* **1995**, *34*, 201
(20) Buller, F.; Mannocci, L.; Zhang, Y.; Dumelin, C. E.; Scheuermann, J.; Neri, D. *Bioorg. Med. Chem. Lett.* **2008**, *18*, 5926.
(21) Clark, M. A.; Acharya, R. A.; Arico-Muendel, C. C.; Belyanskaya, S. L.; Benjamin, D. R.; Carlson, N. R.; Centrella, P. A.; Chiu, C. H.; Creaser, S. P.; Cuozzo, J. W.; Davie, C. P.; Ding, Y.; Franklin, G. J.; Franzen, K. D.; Gefter, M. L.; Hale, S. P.; Hansen, N. J. V.; Israel, D. I.; Jiang, J.; Kavarana, M. J.; Kelley, M. S.; Kollmann, C. S.; Li, F.; Lind, K.; Mataruse, S.; Medeiros, P. F.; Messer, J. A.; Myers, P.; O'Keefe, H.; Oliff, M. C.; Rise, C. E.; Satz, A. L.; Skinner, S. R.; Svendsen, J. L.; Tang, L.; van Vloten, K.; Wagner, R. W.; Yao, G.; Zhao, B.; Morgan, B. A. *Nat. Chem. Biol.* **2009**, *5*, 647.
(22) Melkko, S.; Zhang, Y.; Dumelin, C. E.; Scheuermann, J.; Neri, D. *Angew. Chem., Int. Ed.* **2007**, *46*, 4671.
(23) Buller, F.; Steiner, M.; Frey, K.; Mircsof, D.; Scheuermann, J.; Kalisch, M.; Bühlmann, P.; Supuran, C. T.; Neri, D. *ACS Chem. Biol.* **2011**, *6*, 336.
(24) Clark, M. A. *Curr. Opin. Chem. Biol.* **2010**, *14*, 396.
(25) Hann, M. M.; Oprea, T. I. *Curr. Opin. Chem. Biol.* **2004**, *8*, 255.
(26) Inglese, J.; Johnson, R. L.; Simeonov, A.; Xia, M.; Zheng, W.; Austin, C. P.; Auld, D. S. *Nat. Chem. Biol.* **2007**, *3*, 466.
(27) Macarron, R.; Banks, M. N.; Bojanic, D.; Burns, D. J.; Cirovic, D. A.; Garyantes, T.; Green, D. V. S.; Hertzberg, R. P.; Janzen, W. P.; Paslay, J. W.; Schopfer, U.; Sittampalam, G. S. *Nat. Rev. Drug Discovery* **2011**, *10*, 188.
(28) Novoa, A.; Machida, T.; Barluenga, S.; Imberty, A.; Winssinger, N. *ChemBioChem* **2014**, *15*, 2058.
(29) Winkler, D. F.; Campbell, W. D. *Methods. Mol. Biol.* **2008**, *494*, 47.
(30) Smith, G. P.; Petrenko, V. A. *Chem. Rev.* **1997**, *97*, 391.
(31) Ellington, A. D.; Szostak, J. W. *Nature* **1990**, *346*, 818.
(32) Congreve, M.; Carr, R.; Murray, C.; Jhoti, H. *Drug Discovery Today* **2003**, *8*, 876.
(33) Hajduk, P. J.; Greer, J. *Nat. Rev. Drug Discovery* **2007**, *6*, 211.
(34) Joseph-McCarthy, D.; Campbell, A. J.; Kern, G.; Moustakas, D. *J. Chem. Inf. Model.* **2014**, *54*, 693.
(35) Daguer, J.-P.; Zambaldo, C.; Ciobanu, M.; Morieux, P.; Barluenga, S.; Winssinger, N. *Chem. Sci.* **2015**, *6*, 739.
(36) Muckenschnabel, I.; Falchetto, R.; Mayr, L. M.; Filipuzzi, I. *Anal. Biochem.* **2004**, *324*, 241.
(37) Satz, A. L.; Hochstrasser, R.; Petersen, A. C. *ACS Comb. Sci.* **2017**, *19*, 234.
(38) Lipinski, C. A.; Lombardo, F.; Dominy, B. W.; Feeney, P. J. *Adv. Drug Delivery Rev.* **2001**, *46*, 3.
(39) Eidam, O.; Satz, A. L. *MedChemComm* **2016**, *7*, 1323.
(40) Sannino, A.; Gabriele, E.; Bigatti, M.; Mulatto, S.; Piazzi, J.; Scheuermann, J.; Neri, D.; Donckele, E. J.; Samain, F. *ChemBioChem* **2019**, *20*, 955.
(41) Škopić, M. K.; Willems, S.; Wagner, B.; Schieven, J.; Krause, N.; Brunschweiger, A. *Org. Biomol. Chem.* **2017**, *15*, 8648.
(42) Ding, Y.; Franklin, G. J.; DeLorey, J. L.; Centrella, P. A.; Mataruse, S.; Clark, M. A.; Skinner, S. R.; Belyanskaya, S. *ACS Comb. Sci.* **2016**, *18*, 625.
(43) Satz, A. L.; Cai, J.; Chen, Y.; Goodnow, R. A., Jr.; Gruber, F.; Kowalczyk, A.; Petersen, A.; Naderi-Oboodi, G.; Orzechowski, L.; Strebel, Q. *Bioconjugate Chem.* **2015**, *26*, 1623.
(44) Usanov, D. L.; Chan, A. I.; Maianti, J. P.; Liu, D. R. *Nat. Chem.* **2018**, *10*, 704.
(45) Leimbacher, M.; Zhang, Y.; Mannocci, L.; Stravs, M.; Geppert, T.; Scheuermann, J.; Schneider, G.; Neri, D. *Chem.—Eur. J.* **2012**, *18*, 7729.
(46) Buller, F.; Zhang, Y.; Scheuermann, J.; Schäfer, J.; Bühlmann, P.; Neri, D. *Chem. Biol.* **2009**, *16*, 1075.
(47) Decurtins, W.; Wichert, M.; Franzini, R. M.; Buller, F.; Stravs, M. A.; Zhang, Y.; Neri, D.; Scheuermann, J. *Nat. Protoc.* **2016**, *11*, 764.
(48) Cuozzo, J. W.; Centrella, P. A.; Gikunju, D.; Habeshian, S.; Hupp, C. D.; Keefe, A. D.; Sigel, E. A.; Soutter, H. H.; Thomson, H. A.; Zhang, Y.; Clark, M. A. *ChemBioChem* **2017**, *18*, 864.
(49) Zhao, P.; Chen, Z.; Li, Y.; Sun, D.; Gao, Y.; Huang, Y.; Li, X. *Angew. Chem., Int. Ed.* **2014**, *53*, 10056.
(50) Wu, Z.; Graybill, T. L.; Zeng, X.; Platchek, M.; Zhang, J.; Bodmer, V. Q.; Wisnoski, D. D.; Deng, J.; Coppo, F. T.; Yao, G.; Tamburino, A.; Scavello, G.; Franklin, G. J.; Mataruse, S.; Bedard, K. L.; Ding, Y.; Chai, J.; Summerfield, J.; Centrella, P. A.; Messer, J. A.; Pope, A. J.; Israel, D. I. *ACS Comb. Sci.* **2015**, *17*, 722.
(51) Erlanson, D. A.; Fesik, S. W.; Hubbard, R. E.; Jahnke, W.; Jhoti,

H. *Nat. Rev. Drug Discovery* **2016**, *15*, 605.
(52) Scheuermann, J.; Dumelin, C. E.; Melkko, S.; Zhang, Y.; Mannocci, L.; Jaggi, M.; Sobek, J.; Neri, D. *Bioconjugate Chem.* **2008**, *19*, 778.
(53) Wichert, M.; Krall, N.; Decurtins, W.; Franzini, R. M.; Pretto, F.; Schneider, P.; Neri, D.; Scheuermann, J. *Nat. Chem.* **2015**, *7*, 241.
(54) Goodnow, R. A., Jr. *SLAS Discovery* **2018**, *23*, 385.
(55) Ottl, J.; Leder, L.; Schaefer, J. V.; Dumelin, C. E. *Molecules* **2019**, *24*, 1629.
(56) Reddavide, F. V.; Lin, W.; Lehnert, S.; Zhang, Y. *Angew. Chem., Int. Ed.* **2015**, *54*, 7924.
(57) Grünzner, S.; Reddavide, F. V.; Steinfelder, C.; Cui, M.; Busek, M.; Klotzbach, U.; Zhang, Y.; Sonntag, F. Lab-on-a-Chip Platform for High Throughput Drug Discovery with DNA-Encoded Chemical Libraries. In *Microfluidics, BioMEMS, and Medical Microsystems XV*, Proceedings of the SPIE BiOS Conference, San Francisco, CA, January 28–February 2, 2017; Gray, B. L., Becker, H., Eds.; Society of Photo-Optical Instrumentation Engineers (SPIE), February 28, 2017; Volume 10061, Paper 1006111 (https://doi.org/10.1117/12.2253840).
(58) Reddavide, F. V.; Cui, M.; Lin, W.; Fu, N.; Heiden, S.; Andrade, H.; Thompson, M.; Zhang, Y. *Chem. Commun*. **2019**, *55*, 3753.
(59) Li, G.; Zheng, W.; Chen, Z.; Zhou, Y.; Liu, Y.; Yang, J.; Huang, Y.; Li, X. *Chem. Sci.* **2015**, *6*, 7097.
(60) Zhou, Y.; Li, C.; Peng, J.; Xie, L.; Meng, L.; Li, Q.; Zhang, J.; Li, X. D.; Li, X.; Huang, X.; Li, X. *J. Am. Chem. Soc.* **2018**, *140*, 15859.
(61) Zimmermann, G.; Li, Y.; Rieder, U.; Mattarella, M.; Neri, D.; Scheuermann, J. *ChemBioChem* **2017**, *18*, 853.
(62) Freyer, M. W.; Lewis, E. A. *Methods Cell Biol.* **2008**, *84*, 79.
(63) Lin, W.; Reddavide, F. V.; Uzunova, V.; Gur, F. N.; Zhang, Y. *Anal. Chem.* **2015**, *87*, 864.
(64) Ma, Z.; Lee, R. W.; Li, B.; Kenney, P.; Wang, Y.; Erikson, J.; Goyal, S.; Lao, K. *Proc. Natl. Acad. Sci. U. S. A.* **2013**, *110*, 14320.
(65) Kielar, C.; Reddavide, F. V.; Tubbenhauer, S.; Cui, M.; Xu, X.; Grundmeier, G.; Zhang, Y.; Keller, A. *Angew. Chem., Int. Ed.* **2018**, *57*, 14873.
(66) Piontek, M. C.; Roos, W. H. *Methods Mol. Biol.* **2018**, *1665*, 243.
(67) Van Dijk, E. L.; Jaszczyszyn, Y.; Naquin, D.; Thermes, C. *Trends Genet.* **2018**, *34*, 666.
(68) Zhang, Y.; Herrmann, J.; Wieduwild, R.; Boden, A. Method for the Deconvolution of Nucleic Acid Containing Substance Mixtures. World Patent WO2015/104411A1, July 16, 2015.
(69) Satz, A. L. *ACS Chem. Biol.* **2015**, *10*, 2237.
(70) Satz, A. L. *ACS Comb. Sci.* **2016**, *18*, 415.
(71) Kuai, L.; O'Keeffe, T.; Arico-Muendel, C. *SLAS Discovery* **2018**, *23*, 405.

About the Authors

Francesco Reddavide is the Director of R&D at DyNAbind GmbH. He graduated in 2011 from the University of Bari (Italy) with an M.Sc. degree in Medical and Pharmaceutical Biotechnology. From 2012 to 2016, Francesco pursued his doctoral studies in the lab of Professor Yixin Zhang at TU Dresden, where he participated in the development of a regenerable chip for kinetic hit validation of DNA-encoded compounds. He is co-author of multiple patents and peer-reviewed publications about novel designs and applications of DELs and auxiliary technologies. In 2015, he joined DyNAbind's EXIST-Forschungstransfer development team to lead development efforts aimed at taking DyNAbind's technology from proof-of-principle to market-ready status.

Mike Thompson grew up in Florida and studied biochemistry at the University of Florida, where he worked on organic ligand synthesis for organometallic clusters in the laboratory of Professor George Christou. In 2011, he moved to Germany for his doctoral work in the lab of Professor Yixin Zhang. After completing his Ph.D. degree in 2015, Mike led a team to secure EXIST-Forschungstransfer funding and scale their DECL technology for industrial applications, leading to the founding of DyNAbind GmbH in 2017, where he now serves as CEO.

Luca Mannocci was born in 1979 in Pisa, Italy, and received his B.S. degree in chemistry from the University of Pisa. In 2008, Luca earned his Ph.D. degree in chemistry under the supervision of Professor Dario Neri at the Institute of Pharmaceutical Sciences of ETH Zürich (Switzerland). After leading a drug discovery unit at Philochem AG, Luca has worked as independent consultant on the development and use of DECLs for drug and ligand discovery applications for major pharmaceutical, life science, and biotech companies as well as academic groups. In addition to over 15 years of experience in DECL technologies, Luca has co-founded DyNAbind GmbH and authored several key publications on DECL-technology in peer-reviewed journals and in drug discovery and DECL-dedicated books.

Yixin Zhang is a professor at Technische Universität Dresden (TU Dresden), Germany. He studied organic chemistry in Shanghai, China, and did his doctorate studies on immunosuppressive drugs and cis–trans isomerase with Gunter Fischer in Halle, Germany. After postdoctoral work with Professor Dario Neri in ETH Zürich, he joined B CUBE, Center for Molecular Bioengineering, in 2009 as group leader, and became a professor of biomolecular interaction at TU Dresden in 2016. His research interests include (i) self-assembled biomaterials, (ii) drug screening with DELs, (iii) drug design, and (iv) peptide bond cis–trans isomerase.

DNA-Encoded Library Chemistry: Amplification of Chemical Reaction Diversity for the Exploration of Chemical Space


Ms. Y. Huang


Ms. O. Savych


Dr. Y. Moroz


Prof. Y. Chen


Dr. R. A. Goodnow, Jr.

Ying Huang,[a] Olena Savych,[b] Yuii Moroz,[b,c] Yiyun Chen,[*,a] and Robert A. Goodnow, Jr.[*,d]

[a] Shanghai Institute of Organic Chemistry, University of Chinese Academy of Sciences, 200032 Shanghai, China, Email: yiyunchen@sioc.ac.cn
[b] Chemspace, ilukstes iela 38-5, Riga, LV-1082, Latvia
[c] National Taras Shevchenko University of Kyiv, 61 Volodymyrska Street, 01601 Kyiv, Ukraine
[d] Pharmaron USA Inc., Boston, MA 02451, USA, Email: robert.goodnow@pharmaron.com

Keywords. DNA-encoding; DNA-compatible chemistry; chemical diversity; hit generation; affinity selection; building blocks; commercial availability; drug-like properties; library design.

Abstract. The use of DNA for encoding and decoding in small-molecule synthesis for lead identification continues to gain widespread attention and application—more than a quarter century after its first disclosure. Successful execution of a diverse, drug-like library usually requires hundreds to thousands of commonly functionalized building blocks of relatively similar reactivity profiles. Aqueous and DNA-compatible organic reactions that utilize a large number of functionalized building blocks are perhaps among the most obvious and often discussed aspects of the successful application of this chemistry. This review highlights recent (since ~2015), relevant, new, and potentially highly useful such chemical transformations. Thereafter follows a discussion of the properties, requirements, costs, and diversity of building blocks that are currently available and may be useful for the construction of DNA-encoded libraries.

Outline

1. What Is DELT and Why Does It Continue to Be Important?

DNA-Encoded Library Technology (DELT) is a combination of several technologies for the creation of large mixtures of small molecules that are then used in affinity selection methods for the identification of small molecules having high binding affinity for a particular biological target, usually proteinaceous. In a DEL, each small molecule is covalently attached to a strand

of single- or double-strand DNA as a means of encoding its synthetic history. Population enrichment of high affinity binders, followed by amplification of the encoding DNA with a polymerase chain reaction (PCR) and subsequent sequencing of the resulting amplicons by next generation sequencing (NGS) make possible the identification of such higher affinity hit molecules. The chemistry for creating DELs has been useful for developing mixtures of hundreds of millions to billions of small molecules on a small scale. The concept for this innovation was first proposed in 1992 by Brenner and Lerner,[1] and was promptly followed by its exemplification.[2] During the intervening quarter century, DELT has grown from an interesting concept for the encoding of short peptides synthesized on a solid phase, to a well-established method for small-molecule hit identification, increasingly commonplace in pharma, biotech, and academic drug discovery research. This approach has been thoroughly reviewed.[3] It has also been described in multiple publications that are focused on synthetic chemistry as applied to this technology and hit identification[4] for biological targets of interest as well as clinical drug candidates.[5] Innovation in DELT is appealing to many scientists given its multidisciplinary nature that includes small-molecule organic chemistry, oligonucleotide chemistry, affinity chromatography, informatics, high-throughput (HT) DNA sequencing, and process design.

This review highlights newly disclosed DNA-compatible synthetic organic reactions that have been employed in the preparation of DELs or have the potential of being used for this purpose. Since a critical component for success in DELT is ready access to hundreds to thousands of building blocks (BBs), their availability, cost, chemical classification, and properties may seem obvious and simplistic. However, upon further examination, and given the number of BBs in question, it becomes clear that rigorous attention to these BB aspects is critical for implementing a successful DELT process. To this end, key BB aspects are explored in this review, thereby providing readers with, not only an update of the latest organic chemistry that might be applied in a DELT, but also an understanding of the general availability of BBs needed to demonstrate new molecular designs.

2. General DEL Design Principles: Balancing Diversity, Size, and Drug-Like Properties against the Requirements of DNA-Compatible Reactions

Whereas aspects of cost and feasibility of HTS decks limit screening campaigns to 10^6–10^7 compounds,[6,7] the advent of DELT now allows libraries to comprise typically 10^7–10^{10} compounds.[8,9] While this remains a tiny sampling of the theoretically accessible chemical space (10^{18}–10^{200} molecules, depending on the method of calculation),[10] DELT remains an attractive choice for hit generation. This is because DEL compound libraries result from split-and-pool synthesis, which has been known for many years,[11] even though the details of encoding and decoding millions of small molecules have come about only with the advent of NGS and the perfection of DELT.[1] The power of DELT's combinatorial synthesis to produce large numbers of compounds is strikingly demonstrated in Table 1.

However, well known to drug discovery scientists is Lipinski's "rule of 5"[12] that guides the design of small molecules with respect to oral bioavailability according to upper limits on molecular weight (MW), CLogP, and the count of hydrogen bond donors and acceptors (i.e., 500 Da, 5, 5, and 10, respectively). Without proper and rigorous attention to building block selection, multicycle combinatorial libraries often create molecules that surpass these limits. High affinity hits may be found, but their transformations to useful, orally bioavailable, drug-like substances may be challenging or impossible. Vividly illustrating this obvious point, is a seminal DELT paper by Clark et al. which describes the synthesis of 3- and 4-cycle DELs that are based on the triazine scaffold.[13] The DELs were then probed by affinity selection against p38α, resulting in the identification of high-affinity, off-DNA inhibitors of p38 MAP kinase (Figure 1).[13] In Table 2, entries 2 and 5 show the final molecular weights that would result from fairly low-molecular-weight building blocks, whereas entries 3 and 6 show the same from heavier building blocks. The highest molecular weight building blocks in these libraries are in excess of 275 Da for several of the inputs. It thus becomes clear that for 3-cycle DEL-A, the building block and core MWs cannot exceed 125 Da in order to produce molecules of less than 500 Da; for DEL-B the limit is 105 Da. Based on this simple analysis, it should be obvious that building block selection for DELs is quite constrained by molecular weight. As a rule of thumb, DEL building blocks and cores of molecular weights of 125 Da or less are generally the most useful if one expects all members of a DEL library to have less than 500 Da molecular weights. Often DELT chemists design libraries with building blocks that are available to them at the time and thus can end up with final compounds having MWs far in excess of 500 Da. The thinking then is that the DEL library will have some representation of molecular weights less than 500 Da, while larger MWs can be useful for structure–activity relationship (SAR) studies. Indeed, while diversity exploration of higher-molecular-weight products is useful for selection, their potential utility as starting points for small-molecule hit-to-lead drug discovery is invariably negatively assessed against these stringent, hard-wrought design criteria.

Before optimizing the drug-like properties of a DEL for use in hit generation, two key aspects need to be considered: (i) a good understanding of new and established chemical reactions that are compatible with a DNA encoding format, and (ii) the

Table 1. The Number of Compounds That May Result from 3- and 4-Cycle Combinatorial Libraries

No. of Cycles	Input Count for				No. of Library Members
	Cycle I	Cycle II	Cycle III	Cycle IV	
3	96	96	96	–	884,736
3	96	96	96	96	84,934,656
4	1,000	1,000	1,000	–	1×10^9
4	1,000	1,000	1,000	1,000	1×10^{12}

availability of suitable building blocks for the modeling of such reactions. Large pharmaceutical companies, having thousands of small-molecule building blocks in their compound inventories, have a significant advantage in terms of availability of small, diverse, and novel molecular inputs at already sunk costs. For DELT chemists who do not have access to such "hidden treasure", commercially available BBs are the next best option. To this end, the analysis in Section 5 of commercially available BB sets is presented as a means to understand the numbers of commonly used building blocks that are readily commercially available. Whereas an exhaustive analysis of relevant BBs may be more meaningful to a particular design and the preforming organization, it is still useful to the practicing DELT chemist to have an overview of what is available.

3. Recently Developed Reactions That Have Been Applied on DNA or Have the Potential to Be Applied on DNA

3.1. Photochemical and Radical Reactions

Liu and co-workers reported in 2011 the first visible-light-induced photoredox reaction performed on DNA, which was run in pH 7.4 aqueous buffer without precautions against air or oxygen (**eq 1**).[14] The substrate scope expansion and functional group compatibility of the azide reduction reaction were demonstrated with small molecules in organic solvents. A variety of protic functional groups; including free indoles, acids, and alcohols; were compatible with the reaction. Functional groups that are sensitive to hydrogenation; including alkenes, alkynes, and aryl halides; were not affected. In addition, functional groups that are sensitive to nucleophiles; including alkyl halides, alkyl mesylates, and aldehydes; were stable under the reaction conditions. An alkyl azide was also reduced in 24 hours under modified conditions, giving rise to the corresponding amine in 72% yield.

A "photoclick" cycloaddition between a diaryltetrazole tethered to a single-strand or a double-strand DNA, **3**, and the electron-deficient maleimide double bond in sulfo-Cy3 dye **4** was induced by UV irradiation at 365 nm in a temperature-controlled device (**eq 2**).[15] It was observed that the yield of the purified product DNA, **5**, was higher (34%) on the double-strand DNA relative to the single-strand one (8%). Remarkably, the measured rate constant was found to be high relative to those of other copper-free bioorthogonal transformations and was similar to those of the traditional copper-catalyzed "click" reaction. Two other alkene dipolarophiles, *N*-methylmaleimide and methylmethacrylate, were also reacted with **3** to evaluate the scope of the reaction and they led to 42% and 23% yield, respectively, of the corresponding product DNA.

The first visible-light-induced oxidative coupling reaction with the potential for DNA modification and DNA-encoded library synthesis was disclosed by Chen and co-workers (**eq 3**).[16] The reaction worked well with readily available primary, secondary, and tertiary alkylboronic acids or trifluoroborates to generate aryl-, silyl-, and alkyl-substituted alkynes. Various functional groups including alkenes, alkynes, aldehydes, ketones, esters, nitriles, azides, aryl halides, alkyl halides, alcohols, and indoles were tolerated in this deboronative alkynylation in organic solvents. In addition, compatibility of the reaction with amino acids, oligosaccharides, proteins, and cell lysates was demonstrated. The reaction could be run in pH 7.4 aqueous buffer without excluding air or oxygen.

The same laboratory has also reported the first visible-light-induced reductive coupling reactions with DNA-compatibility, and the reaction conditions did not affect the enzyme activity of a protein enzyme (**eq 4**).[17] This C_{sp3}–C_{sp} bond coupling reaction worked with primary, secondary, tertiary, and α-heteroatom-substituted alkyl *N*-acyloxyphthalimides to construct aryl-, alkyl-,

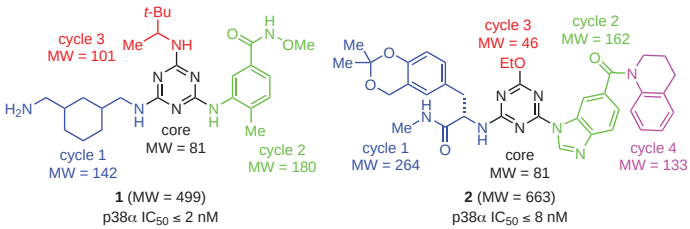

Figure 1. DEL-A and DEL-B, 3- and 4-Cycle DNA-Encoded Libraries Were Employed to Identify High-Affinity Hits against p38α. *(Ref. 13)*

Table 2. Final Product Molecular Weight (MW) That Results from Building Block Inputs for 3- and 4-Cycle DELs[a]

Entry	Building Block MW Input for				Final Product	MW of Final Product
	Cycle I	Cycle II	Cycle III	Cycle IV		
1	142	180	101	–	DEL-A hit **1**	499
2	75	75	75	–	DEL-A low	301
3	200	200	200	–	DEL-A high	676
4	264	162	46	133	DEL-B hit **2**	663
5	75	75	75	75	DEL-B low	357
6	200	200	200	200	DEL-B high	875

[a] Core MW = 81

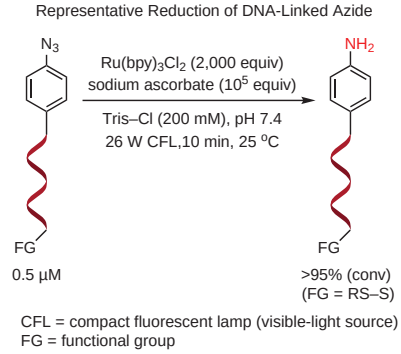

eq 1 *(Ref. 14)*

and silyl-substituted alkynes. The reaction was chemoselective when substrates were used that contained sensitive functional groups such as alkenes, alkynes, aldehydes, ketones, esters, amides, azides, aryl/alkyl halides, alcohols, phenols, carboxylic acids, and indoles. This rapid and mild reaction is compatible with biomolecules and thus has the potential to be applied to DNA modification and DNA-encoded library synthesis.

Flanagan and co-workers have reported a first proof of concept that a photoredox-mediated, 1,4-radical-addition reaction can take place under mild, aqueous conditions that are suitable for the preparation of DELs of around 75 million compounds (**eq 5**).[18] This C_{sp3}–C_{sp3} coupling reaction is compatible with a range of structurally diverse radical precursors a well as Michael acceptors and styrene derivatives. Moreover, to achieve high coupling yields, 1,000 equivalents of the protected α-amino acids need to be used. Alcohol, carboxylic acid, carboxamide, and guanidine functional groups are tolerated; however, unprotected aliphatic α-amines, such as H-Pro-OH, afford the coupling product in significantly diminished yield. Unlike the other transformations presented thus far in this review, oxygen has a detrimental effect on the reaction necessitating that the glass reaction vial be degassed with nitrogen for 5 minutes before irradiation with blue LED light.

A fast, chemoselective, and general *anti*-Markovnikov hydrothiolation of alkenes and alkynes under mild conditions has been disclosed by Glorius, Guldi, and co-workers (**eq 6**).[19] The transformation relies on a biocompatible disulfide–ene reaction that proceeds by triplet–triplet energy transfer (TTEnT) sensitization of disulfides by the visible-light photocatalyst, and tolerates a wide range of functional groups including amides, sulfonamides, nitriles, alcohols, epoxides, aldehydes, ketones, esters, and heterocycles. The electron-rich, sterically

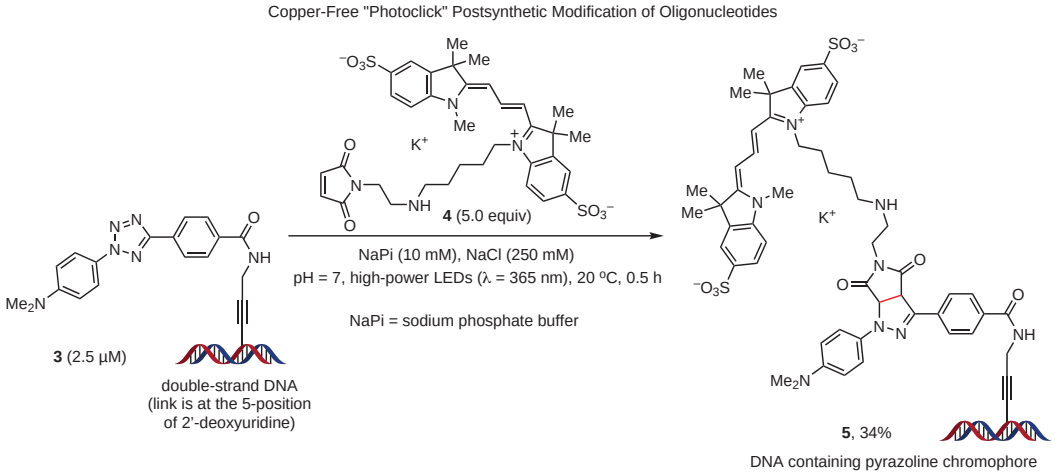

eq 2 *(Ref. 15)*

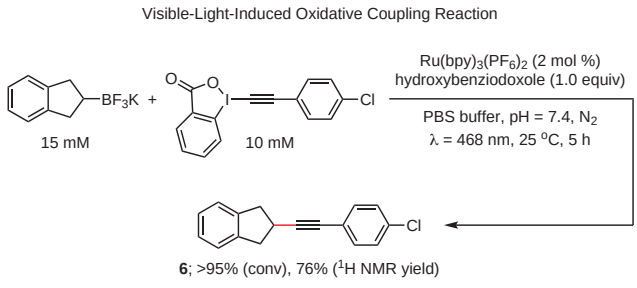

In the presence of L-tyrosine, L-cysteine, L-methionine, guanosine, naringin, ssDNA, bovine serum albumin, and bacterial cell lysates: >95% (conv) and 68–86% (^{1}H NMR) yield of **6** in 5–12 h

eq 3 *(Ref. 16)*

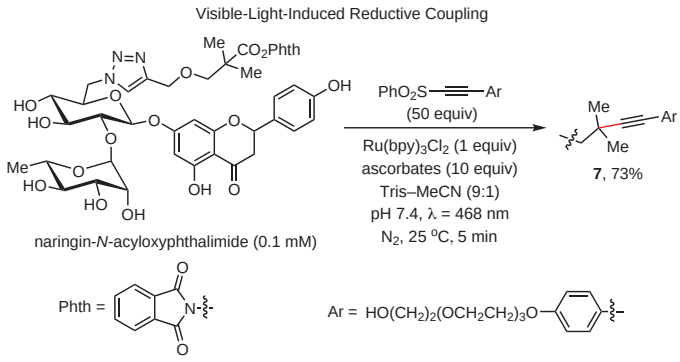

The reaction was compatible with stoichiometric amounts of amines, amino acids, proteins, oligosaccharides, nucleic acids, nucleosides, and cell lysates: Yield of **7**: 73–84%

The enzymatic activity of Human Carbonic Anhydrase II (HCA II) was unaffected by the reaction conditions

eq 4 *(Ref. 17)*

accessible alkene functionality reacts exclusively, while sterically demanding disulfides such as *tert*-butyl disulfide are unreactive. In aqueous buffer (pH 7.4), the yield of the reaction of carvone with dimethyl disulfide was not affected by the presence of 20 biomolecules such as saccharides, amino acids, nucleosides, nucleic acids, and human cell lysates. A minor modification of the reaction conditions permitted diaryl disulfides to be utilized for the synthesis of arylthioethers.

A team of researchers from Scripps, Pfizer, and Asymchem led by Baran and Blackmond have reported the first decarboxylative one-electron alkylation of a DNA-bound molecule using zinc nanopowder as the reductant (**eq 7**).[20] The reaction works with amino-containing alkyl carboxylic acids and even a dipeptide, and tolerates functional groups, such as thioethers and aryl iodides, that are potentially sensitive to reductive conditions or nonphysiological pH. Highly hindered C_{sp3}–C_{sp3} bond linkages, such as those forming quaternary carbons, could also be constructed on DNA through this cross-coupling reaction with electron-deficient alkenes.

The direct, visible-light photoredox-catalyzed deoxygenative ketone synthesis has also been achieved under mild conditions in aqueous medium.[21] This formal hydroacylation of alkenes is compatible with a broad range of alkenes and para-substituted aromatic carboxylic acids and is achieved in moderate-to-good yields. It is proposed to occur via an acyl radical species [RC(O)•] that adds to the alkene with Ph_3P acting as an oxygen-transfer agent and water supplying a proton in the final step of the reaction. Both pyridyl-substituted alkenes and styrene derivatives were good alkene partners, and the reaction was not affected by the presence of biomolecules such as amino acids, oligosaccharides, nucleosides, nucleic acids, and proteins.

Very recently, two open-air, on-DNA synthetic protocols have been developed by Molander and co-workers (**Scheme 1**).[22] The first involves a Ni/photoredox dual catalytic C_{sp2}–C_{sp3} cross-coupling between a halogenated arene and an alkane. The

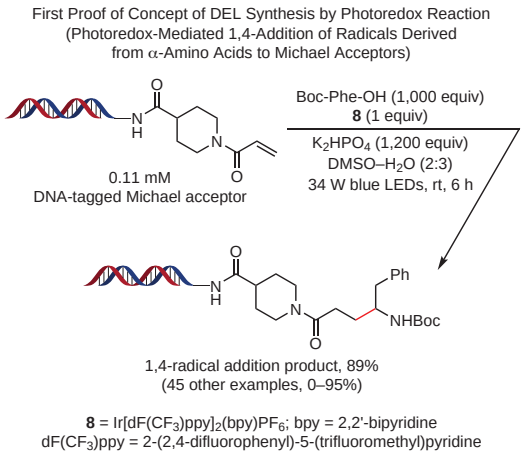

eq 5 *(Ref. 18)*

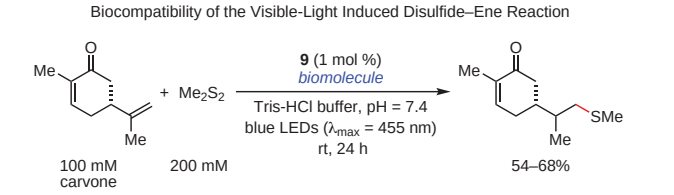

eq 6 *(Ref. 19)*

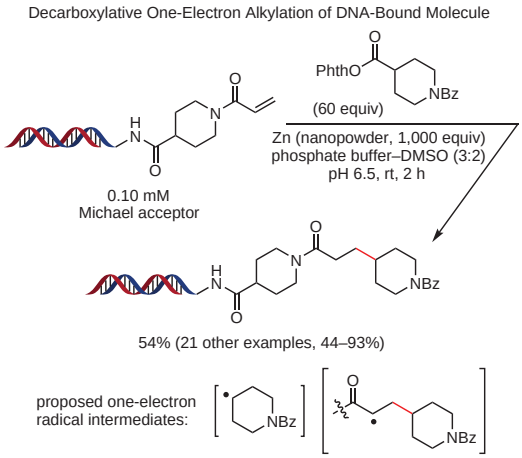

eq 7 *(Ref. 20)*

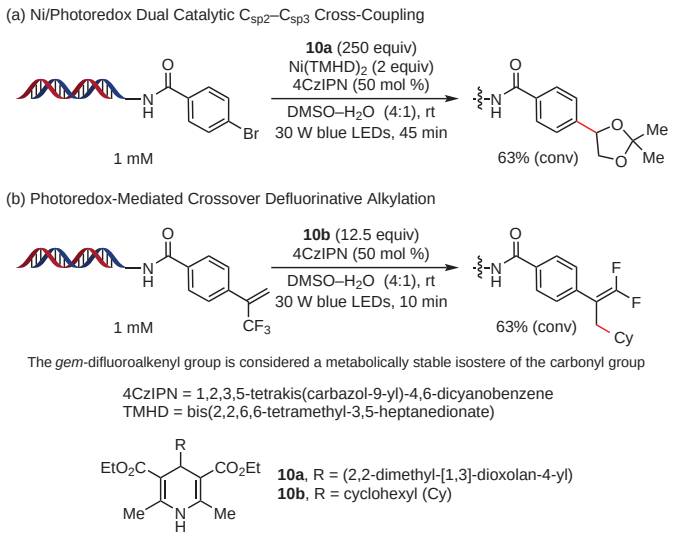

Scheme 1. Photoredox-Mediated, on-DNA Alkylations in Ambient Air and Aqueous Media under Mild Conditions. *(Ref. 22)*

second is the first example of a photoredox-mediated crossover defluorinative alkylation of a trifluoromethylalkene to generate a *gem*-difluoroalkene, which is proposed as a metabolically stable isostere of the carbonyl group. In the dual catalytic process, the water-compatible alkyl radical precursors included alkyl silicates, alkyl dihydropyridines, and amino acids which reacted well with variously substituted aryl iodides and with heteroaryl bromides bearing electron-deficient substituents. Functional groups that could be further elaborated in later cycles of DEL synthesis—e.g., epoxides, esters, alkenes, and *N*-Boc amines—were compatible with the reaction conditions. In the second protocol, the defluoroalkylation of trifluoromethyl alkenes, a DNA compatibility test was done by DNA misreads frequency sequencing, which was meaningful for the DEL synthesis, and such assessment of DNA integrity had often been overlooked before.

3.2. Transition-Metal-Catalyzed Reactions

The first on-DNA ring-closing metathesis (RCM) and cross-metathesis (CM) were achieved on a double-strand DNA in water–*tert*-butyl alcohol solvent system by Lu et al. (**eq 8**).[23] The unoptimized RCM was promoted by Grubbs third-generation ruthenium complex **11** (150 equivalents), and required a large excess of $MgCl_2$ (8,000 equivalents) to be utilized to protect the DNA backbone from ruthenium-induced decomposition. The substrate scope for the on-DNA RCM was investigated with the purpose of forming saturated small (5-, 6-, 7-, and 8-membered) and large (14- and 16-membered) rings in synthetically useful conversions. The on-DNA CM was tested with a representative on-DNA alkene and allyl alcohol as the other olefin under similar reaction conditions; here, too, $MgCl_2$ was required to achieve a 50% conversion.

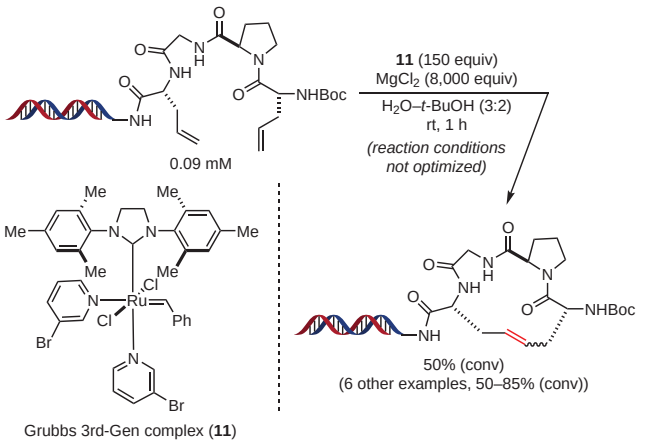

eq 8 *(Ref. 23)*

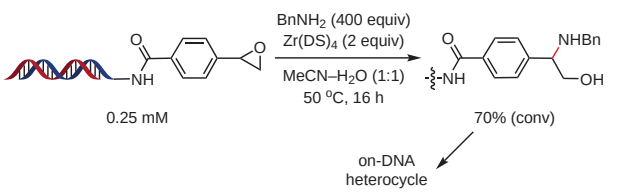

(DEL library of 136.6 million compounds prepared)

eq 9 *(Ref. 24)*

Fan and Davie reported in 2017 the first water-compatible, Zr(IV)-catalyzed aminolysis of epoxides on DNA to afford β-amino alcohols (**eq 9**).[24] Both aliphatic and aromatic primary amines gave moderate-to-excellent yields of the amino alcohols, while sterically hindered amines reacted more sluggishly to form mostly diols. The researchers took advantage of this protocol to build a library of 136.6 million on-DNA β-amino alcohols and their cyclization products, which led to the identification of multiple hits for a number of targets.

The acid- and gold-mediated on-DNA syntheses of hexathymidine-DNA-heterocycle chimeras have been disclosed by a team of researchers from Dortmund University (**Scheme 2**).[25] Diversely substituted β-carbolines—core scaffolds of drugs and pharmacologically active natural products—were accessed by a Brønsted acid catalyzed Pictet–Spengler reaction, while hexathymidine-DNA (hexT) conjugates of highly substituted pyrazolines and pyrazoles were prepared by a Au(I)-mediated cascade reaction. The hexT-heterocycle conjugates could then be ligated to the coding DNA sequences by T4 DNA ligation to produce encoded screening libraries that were informed by drug structures.

The same laboratory has also reported a similar Au(I)-mediated three-component reaction between alternately DNA-tethered aldehydes, hydrazides, and alkynols.[26] The reaction was compatible with thymine-, cytosine-, and adenine-

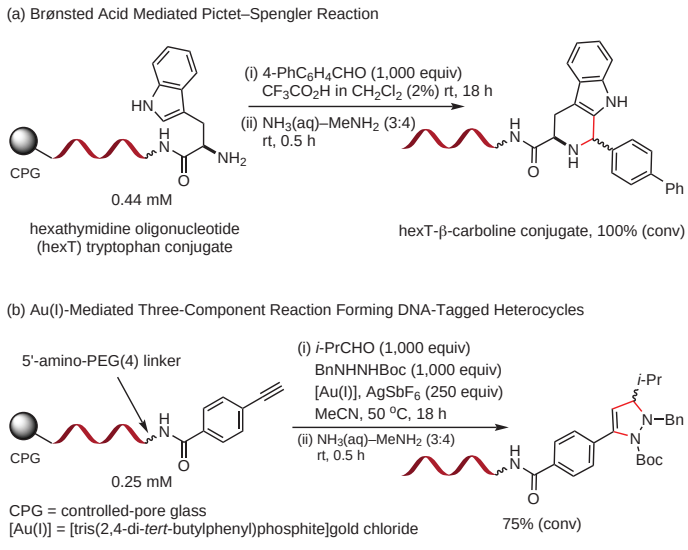

Scheme 2. TFA- and Au(I)-Mediated on-DNA Syntheses of Substituted β-Carbolines, Pyrazolines, and Pyrazoles. *(Ref. 25)*

containing DNA, while guanine-containing DNA strands were degraded under the reaction conditions. The DNA-coupled aldehyde starting material resulted in the best yields of DNA-tagged substituted spiroheterocycles, whereas the alkynol- and hydrazide DNA-conjugates gave complex product mixtures, which precludes their use for parallel synthesis.

The first Pd- or Cu-promoted C–N cross-coupling between DNA-conjugated aryl iodides and primary amines has been achieved (**Scheme 3**).[27] The reaction works well for primary aromatic amines, aliphatic amines, and amino acids, which included over five hundred amino acids. The amino acids not only serve as Cu(I) ligands to promote the C–N coupling, but also prevent DNA decomposition as a result of DNA coordination to Cu(I). Using this technology, the authors succeeded in generating DNA-encoded libraries of 30.4 and 177 million compounds, of which a number of small-molecule hits were identified for biological targets of interest. An analogous copper-promoted amination of DNA-conjugated aryl iodides was reported by Ruff and Berst.[28] In this variant, the novel ligand 2-((2,6-dimethoxyphenyl)amino)-2-oxoacetic acid was found to improve conversions, and both primary and secondary amines—even some sterically congested secondary amines—were competent coupling partners. It is worth noting that this protocol could be carried out in air at low temperature, worked well for a large number of amine building blocks, and was compatible with DMSO as a water-miscible organic cosolvent.

More recently, a palladium-mediated C–N cross-coupling between DNA-conjugated aryl bromides and aromatic amines was disclosed by Torrado and collaborators.[29] The reaction worked for diverse heteroaromatic amines such as thiazoles, pyrazoles, pyrazines, pyridines, benzoxazoles, benzimidazoles, and oxadiazoles as well as anilines containing aliphatic alcohols, sulfonamides, and ester functional groups. Not surprisingly, the coupling of the aryl bromides required a higher temperature (60 °C) to achieve useful conversions than the coupling of the aryl iodides (30 °C).

Lu, Zhong, and co-workers have disclosed the first ruthenium-promoted, on-DNA C_{sp2}–C_{sp2} coupling between acrylamides and aromatic carboxylic acids via a C–H activation reaction (**eq 10**).[30] Under the optimized conditions, good-to-excellent conversions were obtained regardless of whether the acrylamide or the carboxylic acid was conjugated to the DNA. Because aromatic carboxylic acids are more readily commercially available, the reaction scope was investigated with respect to the acid partner. The reaction tolerated bromo, iodo, chloro, amino, hydroxyl, and carboxyl substituents in the carboxylic acid partner, whereas aldehydo, vinyl, and alkoxycarbonyl substituents resulted in low conversions. The value of this approach is that the aromatic carboxylic acid partner serves as a bifunctional building block, whereby the carboxylic acid group can, after the coupling step, be further elaborated to introduce more diversity in a DEL that could range in size from millions to billions after three cycles.

The palladium-promoted Heck coupling has been successfully extended to the reaction of double-strand and single-strand DNA-conjugated acrylamides, styrenes, and aryl iodides with aryl iodides and bromides, aromatic borates, and styrenes (**Scheme 4**).[31] Moderate-to-excellent conversions were observed, and the reaction was compatible with cyano, hydroxyl, amino, and halide functional groups, which could conceivably be elaborated further. The applicability of this method to library diversification was demonstrated with the on-DNA Heck reaction as the cycle 2 step in a three-cycle DEL synthesis.

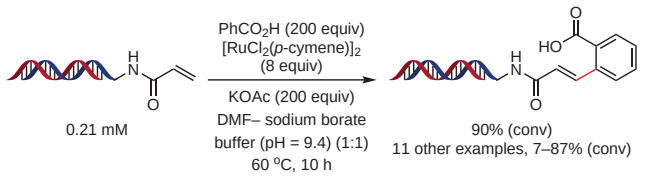

eq 10 *(Ref. 30)*

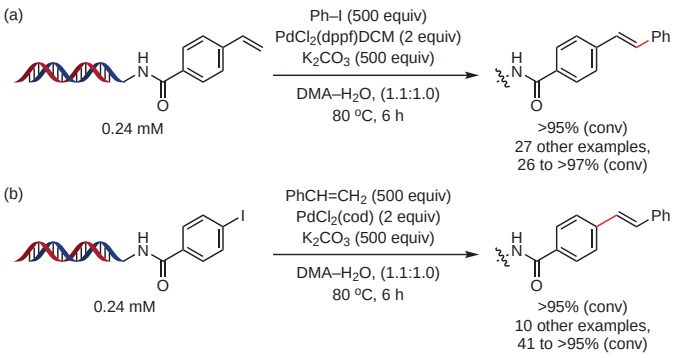

Scheme 4. Palladium-Promoted Heck Reaction on the DNA. *(Ref. 31)*

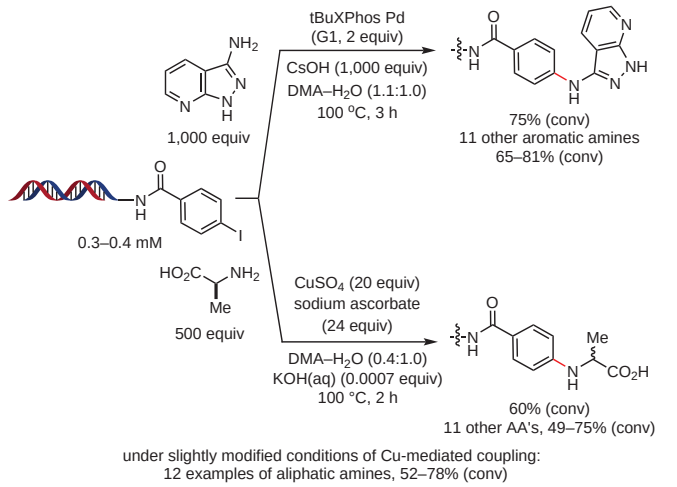

Scheme 3. Pd- or Cu-Promoted C–N Cross-Coupling between DNA-Conjugated Aryl Iodides and Primary Amines or Amino Acids. *(Ref. 27)*

3.3. Nucleophilic Reactions

One of very few examples of an on-DNA reaction sequence that forms two carbon–carbon bonds was reported by Tian et al. (**eq 11**).[32] In this process, termed "T-reaction" for "tertiary amino effect reaction", *ortho*-dialkylaminoaryl aldehydes undergo a reaction cascade consisting of a Knoevenagel condensation, a 1,5-hydride shift, and a Mannich cyclization to form diversely substituted spirocycles. Various benzylic amines were applicable, less activated alkyl amines were tolerated, and differentially substituted secondary amines were also tolerated. Heterocyclic and structurally complex substrates performed equally well as simple piperidines and pyrrolidines. The reaction worked for activated cyclic ketones, amides and esters, which gave higher yields than their acyclic counterparts. Various remote functional groups such as thiocarbonyls and esters did not hinder the reaction.

Neri and co-workers employed an on-DNA Diels–Alder cycloaddition protocol to generate a 4,000-compound DEL in good purities and yields. The DNA fragments functioned as amplifiable bar codes for identification purposes, and the DEL was compatible with decoding strategies that are based on ultra-HTS techniques,[33] In a similar vein, Dai and co-workers demonstrated the utility and versatility of the inverse-electron-demand Diels–Alder reaction for the synthesis of DNA-tagged pyridazines (**eq 12**).[34] The authors reported two complementary protocols for reacting DNA-conjugated 1,2,4,5-tetrazines with olefins and alkene surrogates such as cyclic ketones to yield the desired pyridazines with moderate-to-excellent conversions. Select functionalized pyridazines were shown to undergo Suzuki–Miyaura coupling, acylation, and S_NAr substitution, respectively, underscoring the potential utility of the pyridine scaffold for future DEL syntheses.

In a series of papers,[35–37] Kodadek and his research teams have reported the development of DNA-compatible variants of the asymmetric aldol reaction (**Scheme 5**, Part (a)), the asymmetric Mannich reaction, and the Knoevenagel condensation (Scheme 5, Part (b)) all on solid support. In the aldol variant, proline promoted the asymmetric synthesis of β-hydroxy ketones from immobilized aldehydes and soluble ketones. Heteroaromatic aldehydes were compatible with the reaction and the reaction conditions did not adversely affect the polymerase chain amplification of DNA; however, the enantioselectivities observed were generally modest (ee = 54%−79%). Similarly, the same laboratory disclosed a DNA-compatible, solid-phase synthesis of β-amino ketones through a proline-mediated asymmetric Mannich reaction, again between immobilized aldehydes and soluble ketones.[36] Anilines substituted at the meta or para position worked well, in contrast to ortho-substituted anilines which did not form the desired products. Moreover, the syn product was favored, and the ee of the syn product varied from 54% to 96%. Extending the applicability of the DNA-compatible, combinatorial synthesis on solid support approach, another of Kodadek's teams reported the synthesis of β-cyanoacrylamides by a Knoevenagel condensation between immobilized α-cyano amides and soluble aldehydes.[37] The cyanoacrylamides underwent Michael additions with thiol and phosphine nucleophiles, and thus could serve as a source of reversibly covalent protein ligands that are cysteine-reactive. The Knoevenagel reaction worked well for aliphatic and aromatic aldehydes including those with branched alkyl groups; however ketones were unreactive.

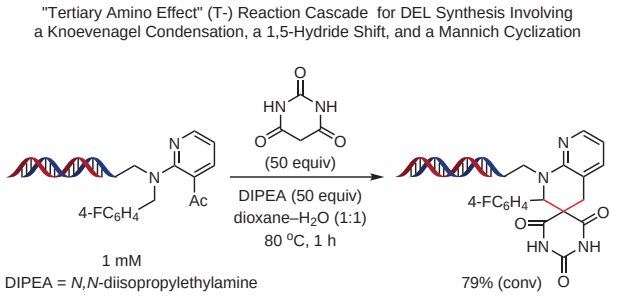

eq 11 *(Ref. 32)*

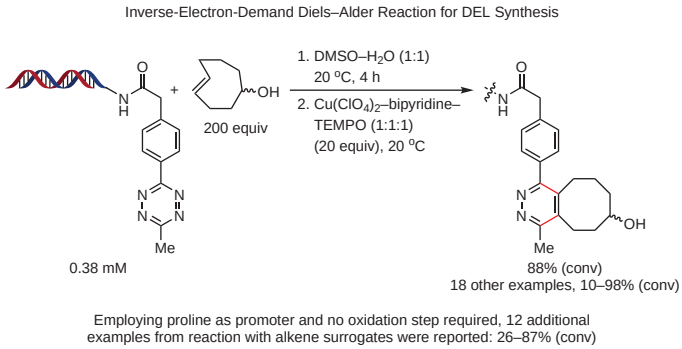

eq 12 *(Ref. 34)*

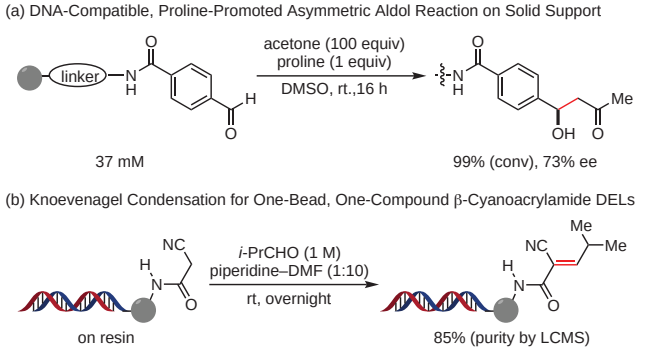

Scheme 5. DNA-Compatible Aldol Reaction and Knoevenagel Condensation on Solid Support. *(Ref. 35,37)*

A method for synthesizing DELs that contain members possessing the less well studied polycyclic isoxazolidine moiety was developed by a team led by Schreiber.[38] The method relies on an intramolecular and DNA-compatible nitrone–alkene [3 + 2] cycloaddition that forms the DNA-linked isoxazolidine, a structural feature found in a number of alkaloids and bioactive compounds (**eq 13**). The nitrone is formed in situ from reaction of the corresponding *N*-alkylhydroxylamine with the carbonyl group of the substrate, and the subsequent intramolecular cycloaddition generates a minimum of two stereogenic centers. The method allows for appendage diversification and does not cause DNA damage or preclude subsequent amplification and ligation steps.

Very recently, Sharpless and co-workers reported the first iminosulfur oxydifluoride ($R–N=SOF_2$) reaction with primary amines and phenols on single-strand DNA with the aim of demonstrating the usefulness of the SuFEx click chemistry for bioconjugation applications (**Scheme 6**).[39] The off-DNA model reactions took place under mild conditions in aqueous buffer to give sulfamides (from primary amines), sulfuramidimidoyl fluorides (from secondary amines), and sulfurofluoridoimidates (from phenols) in up to 99% isolated yields (29 examples).

3.4. Enzymatic Reactions

The first on-DNA chemo-enzymatic synthesis of a small, carbohydrate-based library was reported by Thomas et al. (**Scheme 7**).[40] This approach relied on either an enzymatic galactosylation or an enzymatic and site-specific oxidation to generate the DNA-glycoconjugate library members. In the galactosylation protocol, bovine β1,4-galactosyltransferase (β1,4-GalT) catalyzed the selective transfer of Gal-β1,4 from uridine diphosphate galactose (UDP-Gal) to an acceptor GlcNAc in the presence of $MnCl_2$ under mild conditions and leading to excellent conversions. In the site-specific oxidation protocol, galactose oxidase (GOase) variants M_1 and F_2 generated aldehydes from hexoses by a highly selective oxidation of the C6 hydroxyl group in the galactose moiety. The aldehydes were then elaborated further by hydrazone/oxime ligation or reductive amination.

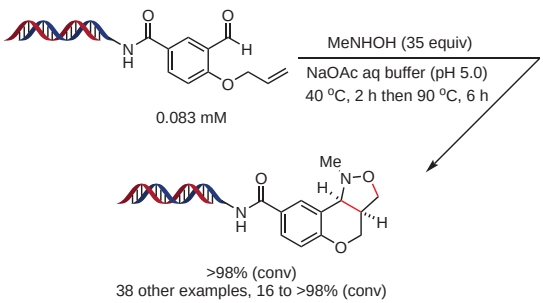

eq 13 *(Ref. 38)*

4. Commonly Employed Reactions in DELT

DEL chemistry is at its core combinatorial chemistry. Accordingly, it should not be a surprise that its practice has evolved to date using chemical transformations that are robust, high yielding, and for which the necessary building blocks are readily available. DELT-compatible chemistries must not only satisfy the three criteria just listed, but must also operate under DNA-compatible conditions: dilute (0.1–1 mM) aqueous media at pH between 4 and 14 and at temperatures between 25 and 90 °C, and the reactions must not alter or degrade the DNA encoding tags. In Section 3, we have presented "recently developed reactions", which we arbitrarily define as those

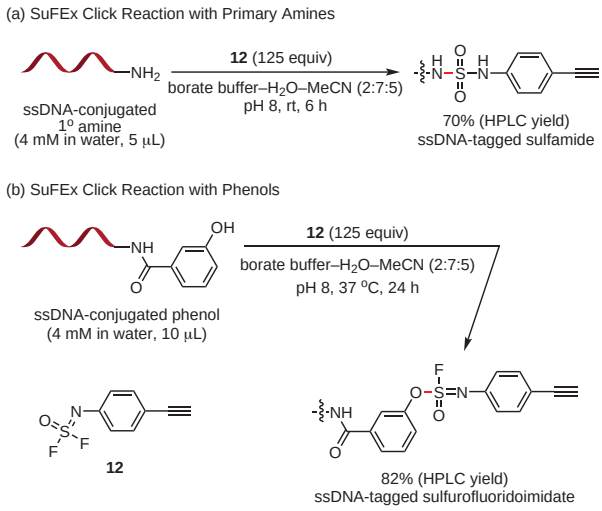

Scheme 6. First Iminosulfur Oxydifluoride on-DNA Reaction with Primary Amines and Phenols. *(Ref. 39)*

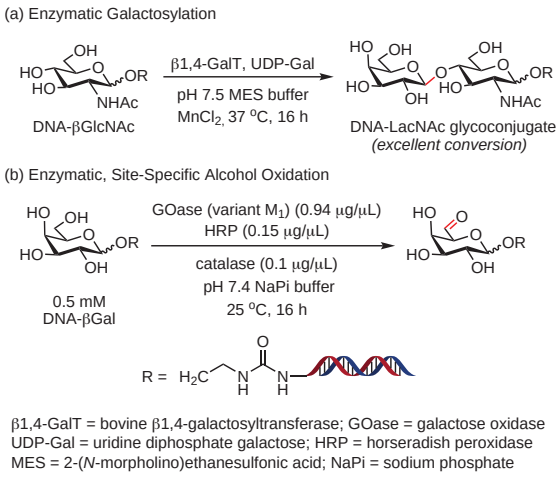

Scheme 7. Carbohydrate DEL Synthesis via Enzymatic Catalysis. *(Ref. 40)*

having been reported since 2015, and which have included many interesting and potentially very useful transformations. For the purposes of this review, we term "commonly employed reactions" in DELT as those already reported and tabulated in various reviews and communications.[41,42] Such reactions include amide formation, reductive aminations, amine capping reactions, Suzuki and Sonogashira couplings, some condensations and some heterocycle-forming cyclizations.

5. Analysis of Commonly Used, Commercially Available Building Block Sets

Presently, published reports of methods developed specifically for assembling DEL libraries are growing rapidly. However, many newly described DELT-applied reactions are often exotic and lacking sufficient validation with a wide variety of reagents. For some of these reactions, reagents are simply not available in any practical numbers (hundreds) to create a DEL. At the same time, large and diverse DELs reported to date have been synthesized using what one would mostly call classical combinatorial chemistry transformations and producing libraries that have been used in affinity selection campaigns to identify useful hits for drug discovery. While such classical and well-known reactions are modest in number compared to standard organic chemistry in solution, an abundance of building blocks for these reactions (e.g., amines, carboxylic acids, and aryl halides) has enabled the creation of DELs of sufficient size, quantity, and diversity. Therefore, while more advanced approaches will continue to be reported and building blocks for them will become available, the use of commonly applied reactions will likely remain the mainstay of DEL production for the time being. Thus, an understanding of the availability and diversity of building blocks commercially available and applicable to DELT becomes critical to creating the most economical, diverse, drug-like, and ultimately the most useful DELs for drug discovery.

The number of modifiable functional groups in the DELT cores is also limited because of the necessity of orthogonal reactivity. For this analysis, we selected several functional groups that have many readily available reaction partners in well-established and DELT-compatible protocols. The list includes classical functional groups such as amines, aldehydes, and carboxylic acids, as well as more recently introduced ones such as terminal alkynes, azides, aryl halides, and boronic acids/esters.

We have grouped the modifiers in three categories: (1) *Amine Modifiers* (aldehydes, aryl halides, carboxylic acids, and sulfonyl halides but not alkyl halides due to concerns about reaction selectivity); (2) *Carbo Modifiers (*primary and secondary amines), and (3) *Couplers* (alkynes, aryl halides, azides, and boronic acids or esters). Indeed, depending on the library chemistry in question, one might require a different classification of functional groups. Furthermore, the exclusion of various chemical substituents will likely reduce these numbers. Nevertheless, the intent of this analysis is to give an understanding of building blocks that exist physically and fall into acceptable categories of cost and molecular weight.

To analyze the availability of the modifiers, we selected 12 vendors with more than 8,000 "off-the-shelf" compounds.[43] This cut-off identifies vendors that could immediately ship large numbers of building blocks as a single source. As such, this helps to reduce costs, logistical complexity, and lead time, as special formatting is typically required. The distribution of the modifiers from each supplier is shown in Figure 2, and the percentages among them of so-called *small* compounds and *inexpensive* compounds are shown in Table 3. The criteria used for selecting *small* and *inexpensive* are: (i) A *small* modifier for two-cycle libraries should have a molecular weight (MW) ≤150 Da, while a *small* core building block's MW should not exceed 200 Da. (ii) An *inexpensive* compound is one costing not more

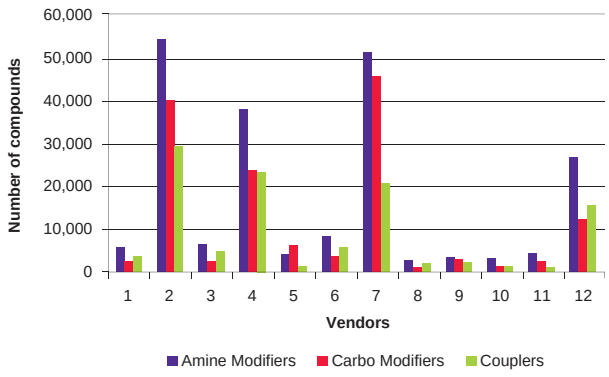

Figure 2. Distribution of Modifiers from the Ten Vendors Selected. *(Ref. 43)*

Table 3. Commercially Available Modifier Compounds: Count and % Small / % Inexpensive. *(Ref. 43)*

Vendor No	1	2	3	4	5	6	7	8	9	10	11	12
Amine Modifiers[a]	**5,665**	**54,083**	**6,328**	**37,892**	**4,169**	**8,200**	**51,163**	**2,476**	**3,409**	**2,897**	**4,300**	**26,571**
	65/42	24/24	60/40	22/29	46/25	60/42	15/22	64/53	32/42	0/22	21/14	34/30
Carbo Modifiers[b]	**2,400**	**40,342**	**2,338**	**23,575**	**5,891**	**3,528**	**45,602**	**1,047**	**2,856**	**1,241**	**2,202**	**12,124**
	55/26	15/14	59/25	14/16	48/14	51/22	10/13	57/34	20/25	0/14	20/11	27/19
Couplers[c]	**3,608**	**29,323**	**4,590**	**23,497**	**1,396**	**5,757**	**20,516**	**1,752**	**2,354**	**1,161**	**1,282**	**15,408**
	67/57	25/37	58/52	22/42	50/46	60/55	18/37	66/67	32/51	0/37	25/25	33/46

[a] Aldehydes, aryl halides, carboxylic acids, and sulfonyl halides. [b] Primary and secondary amines. [c] Alkynes, aryl halides, azides, and boronics.

than US $100 per gram. To add flavor to these numbers, we estimate the size of a possible 2-cycle DEL assembled from each vendor's collection. For this simulation, we selected an alkyne-containing N-protected amino acid as the core molecule (**Scheme 8**). The chemistry for decorating these cores appears classical from one side while challenging from the other: *amine modifiers* being the largest group of decorators, while *azides* being the smallest.

The sizes of the resultant libraries are obtained by multiplying the number of decorators by the number of cores (**Table 4**). As the number of cores, we took all available from selected 12 vendors core compounds. Column "All" shows the libraries assembled with all decorators and cores; columns "*Small*" and "*Inexpensive*" show the libraries assembled with small or inexpensive modifiers, respectively. For the "*Inexpensive*" libraries, we took all available numbers of cores, while for "*Small*" libraries, the cores had MW ≤ 200 Da. The number of cores is indicated in the header.

In some cases, modifiers that meet the small or inexpensive criteria do not exist and, thus, the library size is zero. Clearly, it is generally possible to enumerate many compounds. This is a good start from which to exclude compounds according to various design criteria (e.g., size, molecular diversity, undesired functional groups, predicted target affinity, etc.). This simulation also illustrates the numbers of building blocks that will have to be available in order for recently reported DNA-compatible reactions to have the impact for hit identification as the more classical reactions have already had.

6. Conclusion and Outlook

The past decades have witnessed excellent and widely used applications of transition-metal catalysis and nucleophilic addition reactions in the synthesis of DNA-encoded libraries. In the years to come, it is expected that the recently disclosed photochemical, radical, and enzymatic reactions—with their excellent chemoselectivity, functional group compatibility, and mild reaction conditions—will have a profound impact on DNA-encoded library chemistry by enabling greater chemical reaction diversity amplification and more extensive chemical space exploration. At the same time, business drivers will make available ever larger numbers of building blocks to create large DEL sets based on these reactions.

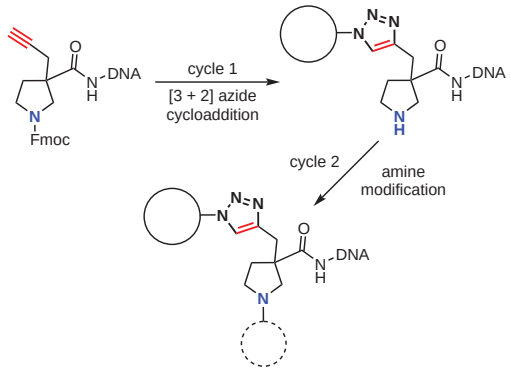

Scheme 8. Decoration of Alkyne-Containing N-Protected Amino Acid for a Simulated DEL.

7. Acknowledgments

Y. H. and Y. C. contributed to the DNA-compatible reaction analysis. O. S. and Y. M. contributed to the building block analysis. R. A. G. developed the manuscript concept and contributed to the introduction, design principle, and final editing. Financial support to Y. C. was provided by the National Natural Science Foundation of China 91765126, 21622207, 21602242, and the Strategic Priority Research Program of the Chinese Academy of Sciences XDB20020200.

8. References and Notes

(1) Brenner, S.; Lerner, R. A. *Proc. Natl. Acad. Sci. U. S. A.* **1992**, *89*, 5381.
(2) Nielsen, J.; Brenner, S.; Janda, K. D. *J. Am. Chem. Soc.* **1993**, *115*, 9812.
(3) Goodnow, R. A., Jr.; Dumelin, C. E.; Keefe, A. D. *Nat. Rev. Drug Discovery* **2017**, *16*, 131.
(4) Franzini, R. M.; Randolph, C. *J. Med. Chem.* **2016**, *59*, 6629.
(5) Harris, P. A.; Berger S. B.; Jeong, J. U.; Nagilla, R.; Bandyopadhyay, D.; Campobasso, N.; Capriotti, C. A.; Cox, J. A.; Dare, L.; Dong, X.; Eidam, P. M; Finger, J. N.; Hoffman, S. J.; Kang, J.; Kasparcova, V.; King, B. W.; Lehr, R.; Lan, Y.; Leister, L. K.; Lich, J. D.; MacDonald, T. T.; Miller, N. A.; Ouellette, M. T.; Pao, C. S.; Rahman, A.; Reilly, M. A.; Rendina, A. R.; Rivera, E. J.; Schaeffer, M. C.; Sehon, C. A.; Singhaus, R. R.; Sun, H. H.; Swift, B. A.; Totoritis, R. D.; Vossenkämper, A.; Ward, P.; Wisnoski, D. D.; Zhang, D.; Marquis, R. W.; Gough, P. J.; Bertin,

Table 4. Estimated Size of a Possible 2-Cycle DEL Assembled from each Vendor's Collection.[a]

Vendor No	All Cores & Modifiers	"Small" Cores & Modifiers	All Cores & "Inexpensive" Modifiers
1	291,195	0	0
2	169,523,700	1,789,452	5,453,700
3	1,635,300	732,144	0
4	34,957,725	917,084	836,925
5	908,460	141,470	95,130
6	1,688,400	394,730	52,575
7	715,456,170	2,085,552	35,033,625
8	42,810	0	0
9	17,902,500	1,382,346	4,120,830
10	524,205	0	19,650
11	7,628,310	93,296	54,540
12	31,920,480	2,971,458	854,595

[a] Cores: 15 total, 14 "small".

J. *J. Med. Chem.* **2017**, *60*, 1247.
(6) Mayr, L. M.; Bojanic, D. *Curr. Opin. Pharmacol*. **2009**, *9*, 580.
(7) Gong, Z.; Hu, G.; Liu, Z.; Wang, F.; Zhang, X.; Xiong, J.; Li, P.; Xu, Y.; Ma, R.; Chen, S.; Li, J. *Curr. Drug Discovery Technol.* **2017**, *14*, 216.
(8) Dickson, P.; Kodadek, T. *Org. Biomol. Chem.* **2019**, *17*, 4676.
(9) Favalli, N.; Bassi, G.; Scheuermann, J.; Neri, D. *FEBS Lett.* **2018**, *592*, 2168.
(10) Follmann, M.; Briem, H.; Steinmeyer, A.; Hillisch, A.; Schmitt, M. H.; Haning, H.; Meier, H. *Drug Discovery Today* **2019**, *24*, 668.
(11) Furka, Á.; Sebestyén, F.; Asgedom, M.; Dibó, G. *Abstracts of Papers, 10th International Symposium on Medicinal Chemistry*, Budapest, Hungary, 1988; p 288.
(12) Lipinski, C. A.; Lombardo, F.; Dominy, B. W.; Feeney, P. J. *Adv. Drug Delivery Rev.* **1997**, *23*, 3.
(13) Clark, M. A.; Acharya, R. A.; Arico-Muendel, C. C.; Belyanskaya, S. L.; Benjamin, D. R.; Carlson, N. R.; Centrella, P. A.; Chiu, C. H.; Creaser, S. P.; Cuozzo, J. W.; Davie, C. P.; Ding, Y.; Franklin, G. J.; Franzen, K. D.; Gefter, M. L.; Hale, S. P.; Hansen, N. J. V.; Israel, D. I.; Jiang, J.; Kavarana, M. J.; Kelley, M. S.; Kollmann, C. S.; Li, F.; Lind, K.; Mataruse, S.; Medeiros, P. F.; Messer, J. A.; Myers, P.; O'Keefe, H.; Oliff, M. C.; Rise, C. E.; Satz, A. L.; Skinner, S. R.; Svendsen, J. L.; Tang, L.; van Vloten, K.; Wagner, R. W.; Yao, G.; Zhao, B.; Morgan, B. A. *Nat. Chem. Biol.* **2009**, *5*, 647.
(14) Chen, Y.; Kamlet, A. S.; Steinman, J. B.; Liu, D. R. *Nat. Chem.* **2011**, *3*, 146.
(15) Arndt, S.; Wagenknecht, H. A. *Angew. Chem., Int. Ed.* **2014,** *53*, 14580.
(16) Huang, H.; Zhang, G.; Gong, L.; Zhang, S.; Chen, Y. *J. Am. Chem. Soc.* **2014,** *136*, 2280.
(17) Yang, J.; Zhang, J.; Qi, L.; Hu, C.; Chen, Y. *Chem. Commun.* **2015**, *51*, 5275.
(18) Kölmel, D. K.; Loach, R. P.; Knauber, T.; Flanagan, M. E. *ChemMedChem* **2018,** *13*, 2159.
(19) Teders, M.; Henkel, C.; Anhäuser, L.; Strieth-Kalthoff, F.; Gomez-Suarez, A.; Kleinmans, R.; Kahnt, A.; Rentmeister, A.; Guldi, D.; Glorius, F. *Nat. Chem.* **2018,** *10*, 981.
(20) Wang, J.; Lundberg, H.; Asai, S.; Martin-Acosta, P.; Chen, J. S.; Brown, S.; Farrell, W.; Dushin, R. G.; O'Donnell, C. J.; Ratnayake, A. S.; Richardson, P.; Liu, Z.; Qin, T.; Blackmond, D. G.; Baran, P. S. *Proc. Natl. Acad. Sci. U. S. A.* **2018,** *115*, E6404.
(21) Zhang, M.; Xie, J.; Zhu, C. *Nat. Commun.* **2018,** *9*, 3517.
(22) Phelan, J. P.; Lang, S. B.; Sim, J.; Berritt, S.; Peat, A. J.; Billings, K.; Fan, L.; Molander, G. A. *J. Am. Chem. Soc.* **2019,** *141*, 3723.
(23) Lu, X.; Fan, L.; Phelps, C. B.; Davie, C. P.; Donahue, C. P. *Bioconjugate Chem.* **2017,** *28*, 1625.
(24) Fan, L.; Davie, C. P. *ChemBioChem* **2017**, *18*, 843.
(25) Škopić, M. K.; Salamon, H.; Bugain, O.; Jung, K.; Gohla, A.; Doetsch, L. J.; dos Santos, D.; Bhat, A.; Wagner, B.; Brunschweiger, A. *Chem. Sci.* **2017,** *8*, 3356.
(26) Škopić, M. K.; Willems, S.; Wagner, B.; Schieven, J.; Krause, N.; Brunschweiger, A. *Org. Biomol. Chem.* **2017**, *15*, 8648.
(27) Lu, X.; Roberts, S. E.; Franklin, G. J.; Davie, C. P. *MedChemComm* **2017,** *8*, 1614.
(28) Ruff, Y.; Berst, F. *MedChemComm* **2018**, *9*, 1188.
(29) De Pedro Beato, E.; Priego, J.; Gironda-Martinez, A.; González, F.; Benavides, J.; Blas, J.; Martin-Ortega, M. D.; Toledo, M. Á.; Ezquerra, J.; Torrado, A. *ACS Comb. Sci.* **2019,** *21*, 69.
(30) Wang, X.; Sun, H.; Liu, J.; Dai, D.; Zhang, M.; Zhou, H.; Zhong, W.; Lu, X. *Org. Lett.* **2018**, *20*, 4764.
(31) Wang, X.; Sun, H.; Liu, J.; Zhong, W.; Zhang, M.; Zhou, H.; Dai, D.; Lu, X. *Org. Lett.* **2019,** *21*, 719.
(32) Tian, X.; Basarab, G. S.; Selmi, N.; Kogej, T.; Zhang, Y.; Clark, M.; Goodnow, R. A., Jr. *Med. Chem. Commun.* **2016**, *7*, 1316.
(33) Buller, F.; Mannocci, L.; Zhang, Y.; Dumelin, C. E.; Scheuermann, J.; Neri, D. *Bioorg. Med. Chem. Lett.* **2008**, *18*, 5926.
(34) Li, H.; Sun, Z.; Wu, W.; Wang, X.; Zhang, M.; Lu, X.; Zhong, W.; Dai, D. *Org. Lett.* **2018**, *20*, 7186.
(35) Shu, K.; Kodadek, T. *ACS Comb. Sci.* **2018**, *20*, 277.
(36) Tran-Hoang, N.; Kodadek, T. *ACS Comb. Sci.* **2018**, *20*, 55.
(37) Pels, K.; Dickson, P.; An, H.; Kodadek, T. *ACS Comb. Sci.* **2018**, *20*, 61.
(38) Gerry, C. J.; Yang, Z.; Stasi, M.; Schreiber, S. L. *Org. Lett.* **2019**, *21*, 1325.
(39) Liu, F.; Wang, H.; Li, S.; Bare, G. A. L.; Chen, X.; Wang, C.; Moses, J. E.; Wu, P.; Sharpless, K. B. *Angew. Chem., Int. Ed.* **2019**, *58*, 8029.
(40) Thomas, B.; Lu, X.; Birmingham, W. R.; Huang, K.; Both, P.; Reyes Martinez, J. E.; Young, R. J.; Davie, C. P.; Flitsch, S. L. *ChemBioChem* **2017**, *18*, 858.
(41) Satz, A. L.; Cai, J.; Chen, Y.; Goodnow, R.; Gruber, F.; Kowalczyk, A.; Petersen, A.; Naderi-Oboodi, G.; Orzechowski, L.; Strebel, Q. *Bioconjugate Chem.* **2015**, *26*, 1623.
(42) Luk, K.-C.; Satz, A. L. DNA-Compatible Chemistry. In *A Handbook for DNA-Encoded Chemistry: Theory and Applications for Exploring Chemical Space and Drug Discovery;* Goodnow, R. A., Jr., Ed.; Wiley: Hoboken, NJ, 2014; pp 67–98.
(43) (a) Vendor: Accela ChemBio (1), Angene Chemical (2), Apollo Scientific (3), AstaTech (4), ChemBridge (5), ChemScene (6), Enamine (7), Manchester Organics (8), Pharmablock (9), Specs (10), Toronto Research Chemicals (11), and WuXi LabNetwork (12). (b) Analysis of the vendors' catalogs and pricing as well as the classification of compounds and calculation of molecular weights (using RDKit software tools) were performed by Chemspace (chem-space.com).

About the Authors

Ying Huang received her B.S. degree in chemistry in 2015 from Central China Normal University. The same year, she moved to the Shanghai Institute of Organic Chemistry, University of Chinese Academy of Sciences, to pursue a master's degree under the direction of Professor Yiyun Chen. She is currently a doctorate student in Professor Yiyun Chen's group, and is focusing on developing novel and biocompatible light-induced chemical reactions for the post-synthetic modification of nucleic acids.

Olena Savych received her M.Sci. degree in organic chemistry in 2017 from the National Taras Shevchenko University of Kyiv. Her thesis research project focused on developing new

technologies for parallel chemistry applications. She is currently a data curation specialist at Chemspace.

Yurii Moroz received his Ph.D. degree in inorganic chemistry in 2010 from the National Taras Shevchenko University of Kyiv. His doctoral dissertation was on the topic of polymetal coordination compounds. Yurii then did postdoctoral research at Tufts University, working with organometallic compounds, and at Syracuse University, working with peptides and proteins. After returning to the Ukraine, Yurii has focused on approaches to generate synthetically feasible small molecules. He joined Chemspace as CEO in 2017.

Yiyun Chen is a professor at the Shanghai Institute of Organic Chemistry and a joint professor at ShanghaiTech University. Yiyun received his B.S. degree in chemistry with honors in 2002 from Peking University, and earned his Ph.D. degree in organic chemistry in 2007 with Professor Chulbom Lee at Princeton University. During his postdoctoral studies with Professor David R. Liu at Harvard University and Howard Hughes Medical Institute, Yiyun used the DNA-encoded reaction-discovery system to discover a new biocompatible visible-light-induced azide reduction reaction. In 2011, Yiyun was appointed Principal Investigator at the Shanghai Institute of Organic Chemistry, where he is developing novel biocompatible light-induced chemical reactions and new optochemical tools for studying biological systems.

Robert A. Goodnow, Jr. obtained his B.S. degree in chemistry from Georgetown University and his Ph.D. degree (in natural products organic and bioorganic chemistry) from Columbia University. He then carried out research on oligosaccharide synthesis at Princeton University as an NIH Postdoctoral Fellow. Rob began his industrial career at Hoffmann-La Roche, and his research interest has since focused on medicinal chemistry and the implementation of several chemistry platform technologies such as small-molecule targeted delivery of siRNA, analytical chemistry, and DNA-encoded chemistry. In 2013, he joined AstraZeneca as Executive Director of the Discovery Sciences Chemistry Innovation Centre, where he led research projects in chemical biology, fragment-based lead generation, and computational chemistry. Since October 2016, Rob has been Vice President of Chemistry Innovation at Pharmaron, Inc. (Boston, MA), and is responsible for shared risk research programs. He has edited the book, *A Handbook for DNA-Encoded Chemistry: Theory and Applications for Exploring Chemical Space and Drug Discovery* (Wiley, 2014).

product highlight

Enrich Your Chemical Toolbox

The fluoroalkylation toolbox has now been expanded beyond the standard Togni Reagents to include novel hypervalent iodine perfluoroalkylation reagents as well as fluoroalkyl bromides, silanes, carboxylates, and sulfonyl fluorides.

The installation of highly fluorinated groups into drug and pesticide candidates is a powerful strategy to modulate their properties. An incorporated fluorinated sidechain can tune the acidobasic behavior and lipophilicity, impart a dipole moment, lock a favorable conformation, and mitigate undesirable metabolic degradation of the parent compound. Fluorinated groups have been typically limited to a single fluorine or trifluoromethyl groups because they are easier to access through synthesis. More elaborate fluoroalkylation is now possible with the development of a new suite of reagents—including hypervalent iodine perfluoroalkylation reagents as well as fluoroalkyl bromides, silanes, carboxylates, and sulfonyl fluorides—that allow late-stage fluoroalkylation of a variety of functional groups through different reactivities.

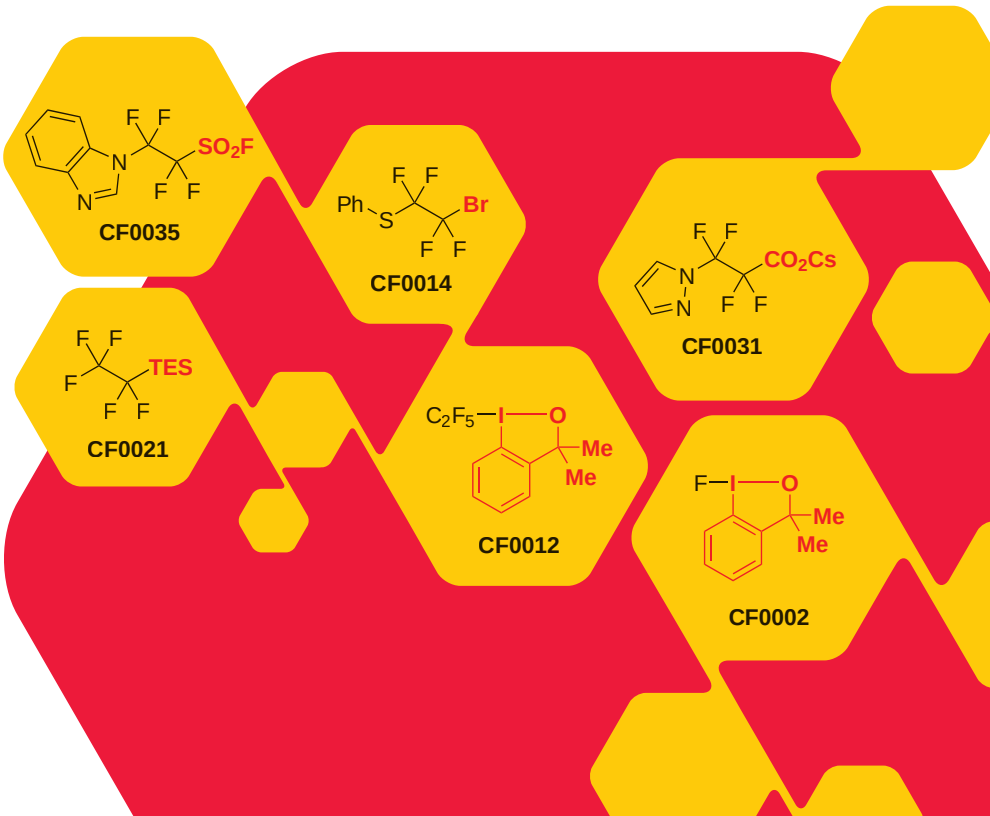

To learn about the entire fluoroalkylation toolbox, visit
SigmaAldrich.com/fluoroalkylation

DESIGN THE PERFECT PROTAC

Partial PROTACs are the easiest way to generate libraries of PROTACs that can be screened for effective degradation of your target from cells.

What will be your perfect combination?

See our growing collection at **SigmaAldrich.com/ TargetDegradation**

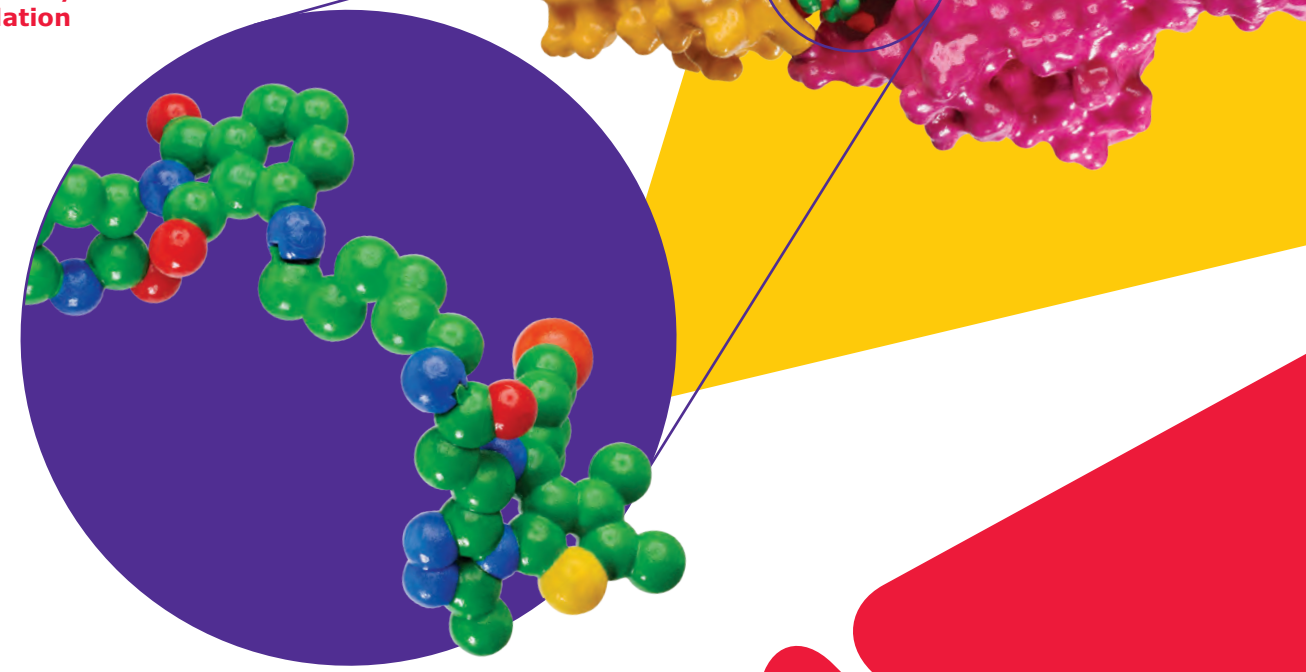

The life science business of Merck operates as MilliporeSigma in the U.S. and Canada.

Sigma-Aldrich®
Lab & Production Materials

MERCK

Join the tradition

Subscribe to the *Aldrichimica Acta*, an open access publication for over 50 years.

In print and digital versions, the *Aldrichimica Acta* offers:

- Insightful reviews written by prominent chemists from around the world
- Focused issues ranging from organic synthesis to chemical biology
- International forum for the frontiers of chemical research

To subscribe or view the library of past issues, visit
SigmaAldrich.com/Acta

MK_BR4714EN
2019 – 25032
11/2019

The life science business of Merck operates as MilliporeSigma in the U.S. and Canada.

Acta Archive Indexes

The Acta Archive Indexes document provides easy searching of all of the Acta content; 1968 to the present.

The volumes, issues, and content are sorted as follows:

- Chronological
- Authors
- Titles
- Affiliations
- Painting Clues (by volume)

Using the sorted sections, you can locate reviews by various authors or author affiliation. Additionally, the content is fully searchable, allowing you to look for a particular key word from the various data available. Once you identify a topic and which volume/issue it is in, you can access it via the archive table.

To access the index, **click here**.

2017-02521
11/2018